TESIS DE LA UNIVERSIDAD DE ZARAGOZA
2021
263

Lidia García Quiles

Desarrollo e implementación de estrategias de mejora de las propiedades estéticas de biopolímeros.

Director/es
Castell Muixi, Pere
Fernández Cuello, Ángel

ISSN 2254-7606

Prensas de la Universidad
Universidad Zaragoza

ISSN 2254-7606

Universidad Zaragoza
1542

Tesis Doctoral

DESARROLLO E IMPLEMENTACIÓN DE ESTRATEGIAS DE MEJORA DE LAS PROPIEDADES ESTÉTICAS DE BIOPOLÍMEROS.

Autor

Lidia García Quiles

Director/es

Castell Muixi, Pere
Fernández Cuello, Ángel

UNIVERSIDAD DE ZARAGOZA
Escuela de Doctorado

Programa de Doctorado en Ingeniería Mecánica

2021

Universidad Zaragoza
1542

Tesis Doctoral

Desarrollo e implementación de estrategias de mejora de las propiedades estéticas de biopolímeros

Autor

Lidia García Quiles

Director/es

Pere Castell Muixí
Ángel Fernández Cuello

Universidad de Zaragoza
Programa de Doctorado en Ingeniería Mecánica

Abril, 2021

GRACIAS…

A Candela y Óscar porque os quiero y por darme ese empujoncito hacia adelante en los momentos más difíciles. Me habéis dado luz cuando más lo necesitaba.

A mis padres y hermanas por ser un pilar en mi formación a nivel intelectual y personal. También os quiero.

A Pere y Ángel por su sabiduría, enseñanzas y paciencia.

Al equipo de Tecnopackaging y Aitiip por darme la oportunidad de emprender este apasionante camino en el mundo de los bioplásticos.

RESUMEN EJECUTIVO

Los bioplásticos (plástico de origen renovable o biológico) han supuesto una revolución tanto en la gestión del fin de vida como en la limitación en cuanto al uso de recursos fósiles finitos. Gracias a los avances en I+D+i enfocados a mejorar las propiedades de estos materiales se comienzan a sustituir los plásticos convencionales ("commodities") tanto en nuevas aplicaciones y sectores como en mercados más tradicionales.

Los bioplásticos tienen una serie de limitaciones en cuanto a sus propiedades funcionales se refiere que son ampliamente conocidas por la comunidad científica y a la que se les viene dando solución en la última década, como por ejemplo: mejora de propiedades mecánicas, estabilidad química, estabilidad térmica e incremento de propiedades barrera a gases, etc. Sin embargo, los bioplásticos presentan otras carencias como son sus pobres propiedades estéticas a las que hasta el momento no se les había prestado tanto interés dado que era más relevante resolver las debilidades del material y el producto en cuanto a su propiedad funcional.

La motivación para el desarrollo de esta tesis surge de la necesidad para garantizar una mayor aceptación de los bioplásticos por mercados en los que las propiedades estéticas son un requerimiento valorado. El objetivo general se centra en el estudio y desarrollo de nuevos biopolímeros con propiedades estéticas mejoradas que supongan una alternativa en aplicaciones plásticas típicamente cubiertas con poliolefinas derivadas del petróleo, en concreto como sustitutas potenciales del polipropileno.

En el marco de la tesis se llevan a cabo dos estrategias principales con propuestas para mejorar las propiedades estéticas sobre dos tipologías diferentes de matrices poliméricas de origen renovable: la eliminación de olores indeseados propios de algunos de estos bioplásticos obtenidos a partir de bacterias y microorganismos (como los polihidroxialkanoatos); y la fijación de color (realizada en sustratos de polibutileno-succinato biobasado). Para ello ha sido necesario revisar el estado actual de la técnica en cuanto a estrategias de mejora de los bioplásticos mediante mezclas en masa con aditivos, nanoaditivos y otros polímeros orgánicos a través de tecnologías de mezclado industriales como es el proceso de extrusión-compounding y la extrusión reactiva.

La presente memoria expone en detalle la problemática medioambiental así como el estado del arte en cuanto a los materiales seleccionados. Además, se concretan los objetivos, se explica el proceso de diseño y desarrollo de las muestras de material a estudiar; una breve descripción de las técnicas de caracterización seleccionas; la metodología desarrollada para cada una de las líneas y se exponen los resultados obtenidos que han sido publicados en cuatro artículos científicos siguiendo la unidad temática objetivo de la tesis. Finalmente, la memoria cierra con unas conclusiones y líneas de continuación de la investigación realizada.

EXECUTIVE SUMMARY

Bioplastics (plastic of renewable or bio-based origin) are a revolution because of their sustainable end-of-life management and because they limit the use of finite fossil resources. Thanks to advances in R&D&I focused on improving the properties of these materials, they are now starting to replace conventional plastics ("commodities") in new applications and in more traditional markets.

Bioplastics have a series of limitations in terms of their functional properties such as poor mechanical properties, low chemical stability, low thermal stability, unsatisfactory barrier properties to gases, etc. that are widely known by the scientific community and to which solutions have been found over the last decade. However, bioplastics have other shortcomings like poor aesthetic properties, which until now have been of less interest because it was more important to solve the weaknesses of the material and the product in terms of its functional properties.

The motivation for the development of this thesis arises from the need to ensure greater acceptance of bioplastics by markets where aesthetic properties are a critical requirement. The general objective focuses on the study and development of new biopolymers with improved aesthetic properties as an alternative in plastic applications typically obtained with petroleum-derived polyolefins, in particular as potential substitutes for polypropylene.

In the framework of the thesis, two main strategies have been carried out with the aim to improve the aesthetic properties of two different types of biopolymeric matrices: the elimination of undesired odours typical of some of these bioplastics obtained from bacteria and microorganisms (such as polyhydroxyalkanoates); and enhance the colour fixation (carried out on biobased polybutylene-succinate substrates). For this purpose, it has been necessary to review the current state of the art in terms of finding and selecting the best strategies to improve bioplastics by mass blending with additives, nanoadditives and other organic polymers through industrial blending technologies such as extrusion-compounding and reactive extrusion.

This thesis explains in detail the environmental problems as well as the state of the art of the selected materials. It also describes the objectives, explains the

design and development process of the material samples to be studied; a brief description of the characterisation techniques selected; the methodology developed for each of the lines and the results obtained, which have been published in four scientific articles following the thematic unit of the thesis. Finally, the thesis closes with some conclusions and continuation routes of the research carried out.

INDICE

INDICE DE FIGURAS

GLOSARIO

PHA: Polihidroxialkanoatos
PBS: Polibutileno succinato o succinato de polibutileno
PP: Polipropileno
IA: Ácido Itacónico
ZrO_2: Óxido de Zirconio
PLA: ácido poliláctico o poliácido láctico
PBAT: Poli(Butilén Adipato-co-Tereftalato)
TPS: *Thermoplastic starch* – Almidón Plastificado
PCL: Policaprolactona
PUR: Poliuretano
PET: Tereftalato de polietileno, Polietileno tereftalato
PS: Poliestireno
EPS: Poliestireno expandido
PVC: Cloruro de polivinilo, Policloruro de vinilo
PE: Polietileno
PELD: Polietileno de baja densidad
PELLD: Polietileno de muy baja densidad
PEHD: Polietileno de alta densidad
PEMD: Polietileno de densidad media
PA: Poliamida
N: Nitrógeno
S: Azufre
O: Oxígeno
Mg: Magnesio
DVB/CAR/PDMS: Divinilbenceno/Carboxeno/Polidimetilsiloxano
CAGR: Tasa compuesta anual
REX: Extrusión Reactiva

BLOQUE 1

INTRODUCCIÓN

MOTIVACIÓN

OBJETIVO

ESTADO DEL ARTE

APORTACIONES ORIGINALES / INNOVACIONES TÉCNICO-CIENTÍFICAS

INTRODUCCIÓN

LA "EDAD DEL PLÁSTICO"

Los materiales plásticos están presentes en todos los ámbitos de la sociedad y han vivido una gran evolución en los últimos años. Su descubrimiento ha supuesto un hito en la sociedad moderna tan trascendente que puede compararse al descubrimiento del hierro y el bronce y se conoce como *"la edad del plástico";* cuyo impacto social y medioambiental supone para muchos antropólogos y geólogos el fin de la era actual, Holoceno, y la entrada a una nueva era: el Antropoceno[1].

El plástico es una de las invenciones modernas de mayor éxito debido a una combinación de características que difícilmente se encuentran en otros materiales: resistente a la corrosión, buenas propiedades mecánicas, alta durabilidad, baja conductividad eléctrica y térmica, ligero, moldeable, con bajo coste económico y capaz de aportar un gran atractivo visual. Por todo ello, los productos realizados con plásticos tienen multitud de aplicaciones en diversidad de sectores.

A pesar de ser unos de los materiales que más utilizamos en nuestra vida cotidiana los plásticos convencionales cuentan con dos grandes inconvenientes: el primer problema es que provienen del **petróleo**, un recurso no renovable y limitado; el segundo gran problema reside en los **residuos** que generan. Para contrarrestar estos inconvenientes, en los últimos años la comunidad científica ha puesto un especial énfasis en el desarrollo de lo que se conoce como **biopolímeros o bioplásticos**.

[1] *Zalasiewicz, J., et al., (2016). The geological cycle of plastics and their use as a stratigraphic indicator of the Anthropocene. Anthropocene, 13, 4–17.*

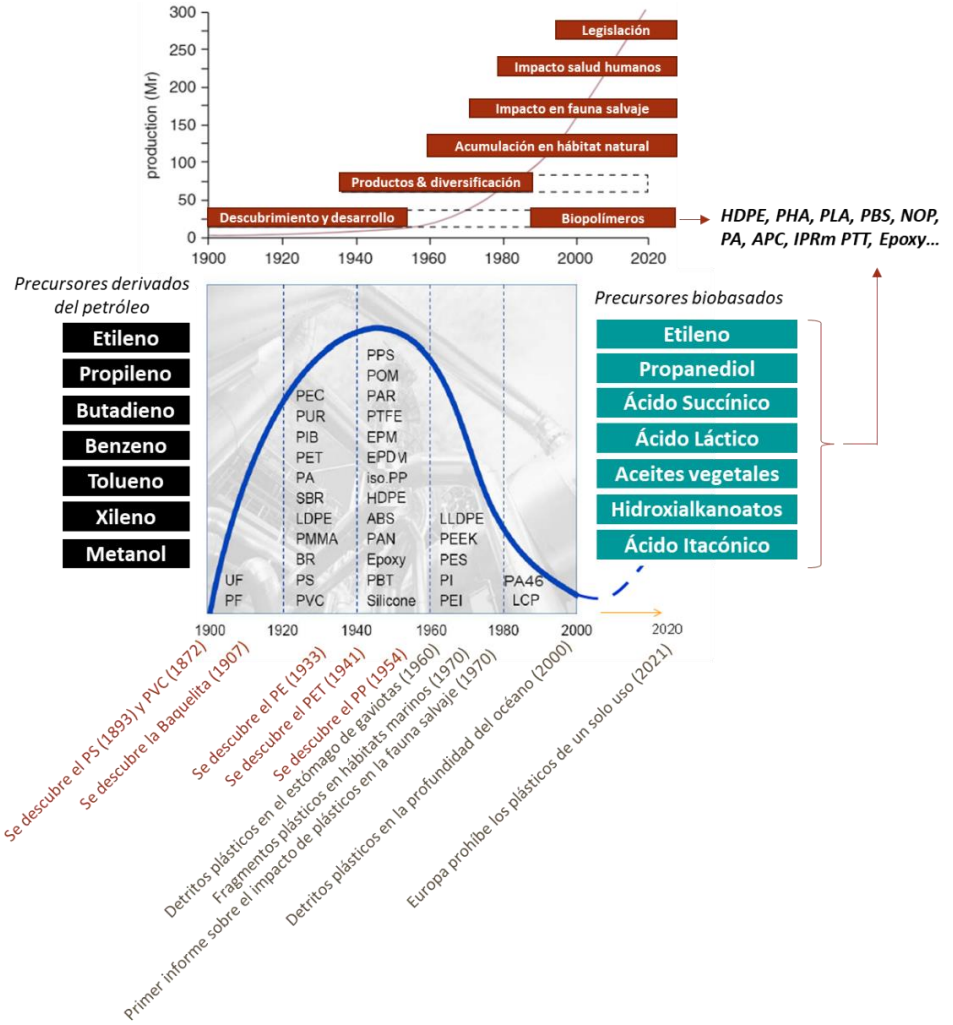

Figura 1: Producción mundial de plásticos con las etapas históricas del desarrollo, impacto ambiental y legislación. Figura adaptada de M. Lackner [2] & J. Ravenstijn[3]

[2] *Lackner, M. (2017). Handbook of Climate Change Mitigation and Adaptation. Biopolymers. Springer International Publishing. ISBN - 978-3-319-14408-5*

[3] *Ravenstijn, J. (2014). PHA. Is it here to stay?. Presentation online. [http://www.kcpk.nl/algemeen/bijeenkomsten/presentaties/20140508-jan-ravenstijn-pha-is-it-here-to-stay].*

¿QUÉ SON LOS BIOPLÁSTICOS / BIOPOLÍMEROS?

El prefijo **"bio"** referido a plásticos o polímeros, es un término que se aplica para describir varias clases diferentes de materiales dependiendo principalmente de su origen, función o fin de vida. La norma europea *CEN/TR 15932:2010 - Plásticos. Recomendación para la terminología y la caracterización de biopolímeros y bioplásticos* pretende abordar la ambigüedad de las definiciones en este campo. Los tres usos aceptados se dividen en:

- **Biobasado**: atiende al origen del material. Son polímeros con unidades constitutivas que provienen total o parcialmente de la biomasa. Pueden provenir directamente de fuentes vegetales y animales, o ser sintetizados mediante organismos vivos.
- **Biocompatible**: atiende a una función específica del material. Son polímeros compatibles con los tejidos humanos o animales y adecuados para la terapia médica.
- **Biodegradable**: atiende al fin de vida. Es la capacidad que tiene el material de descomponerse en sustancias más sencillas (metano, nutrientes, dióxido de carbono, agua, biomasa,…) al aplicar un proceso biológico en el que intervienen enzimas y microorganismos. Además pueden actuar otros agentes físicos del entorno como el sol o el agua en condiciones ambientales. Ahondando en el concepto de biodegradabilidad, ha de resaltarse el término **compostabilidad**. La principal diferencia es que un material compostable se descompondrá en elementos simples carentes de toxicidad y efectos negativos para el medio ambiente aportando nutrientes que añadan valor añadido al ecosistema (calidad de compost). Por tanto, todos los plásticos compostables son biodegradables pero no todos los biodegradables son compostables. La norma europea EN 13432 de 2002 describe las características que un material debe poseer para poder ser definido biodegradable o compostable.

En el marco medioambiental, cuando nos referimos a biopolímeros o bioplásticos, comúnmente estaremos hablando de materiales que pueden ser biobasados o biodegradables o ambos. La biodegradabilidad está vinculada a la estructura de la cadena del polímero; no depende del origen de las materias

primas. Es por ello conveniente detallar para cada caso el término al que nos referimos dado que pueden darse multitud de combinaciones.

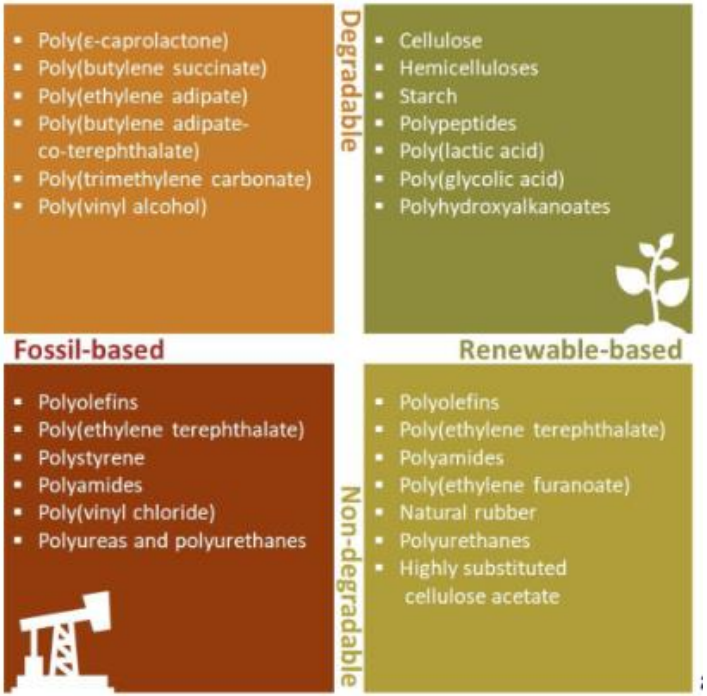

Figura 2: Ejemplos de polímeros y biopolímeros según origen y fin de vida (fuente ARTICULO 4[4], adaptado de European Bioplastics – 2017)

[4] *Imre,B., et al (2019). Reactive Compatibilization of Plant Polysaccharides and Biobased Polymers: Review on Current Strategies, Expectations and Reality. Carbohydrate Polymers 209,20–37*

ORIGEN

La biomasa se puede clasificar en función de su procedencia en: forestal, agrícola, derivada de procesos industriales y procedente de la gestión de residuos como por ejemplo los urbanos[5]. Sin embargo, existe una clasificación que tiene en cuenta el impacto del origen de la biomasa en la sociedad y en el medio ambiente. Es la que habitualmente se usa cuando se habla en bioeconomía de la sostenibilidad de la cadena de valor:

- **Biomasa de primera generación:** la fuente de carbono para producir bioplásticos es el azúcar, los lípidos o el almidón extraídos directamente de un cultivo que es también apto para la alimentación humana y animal. Ejemplos de estas plantas serían la caña de azúcar, la remolacha, la patata o el maíz. En este sentido hay abierta una discusión ética sobre la posible sobre-explotación de tierras aptas para cultivos alimentarios en otros usos como es la industria del plástico y en qué países se produce dicha explotación, cuando el hambre en el mundo afecta a 690 millones de personas (según datos de la FAO – año 2020[6])
- **Biomasa de segunda generación:** se refiere tanto a cultivos no aptos para la producción de alimentos o piensos (por ejemplo, árboles para extraer celulosa) como al desecho de materias primas de primera generación (por ejemplo, residuos de aceite vegetal o derivados de procesos de la industrial de la alimentación).
- **Biomasa de tercera generación:** es un término que se usa describir aquella biomasa derivada de las algas (incluyendo las microalgas), la cual tiene un mayor rendimiento de crecimiento que las materias primas de 1ª y 2ª generación, por lo que se les ha asignado su propia categoría.
- **Biomasa de cuarta generación:** se refiere a materiales que conforman una biomasa la cual ha absorbido CO_2 durante su crecimiento. La diferenciación radica en la captación y almacenamiento de carbono tanto a nivel de materia prima como de la tecnología del proceso.

[5] *EUBIA: European Biomass Industry Association. https://www.eubia.org/cms/wiki-biomass/biomass-resources/*
[6] *http://www.fao.org/hunger/es/*

La biomasa es la materia prima de las biorefinerías. Una **biorrefinería** es una instalación, en cierto modo análoga a la refinería de petróleo, que integra procesos y tecnologías de conversión de biomasa para producir combustibles, energía, y un amplio espectro de bioproductos: productos químicos, materiales, alimentos y piensos[7]. Los productos químicos suelen ser productos intermedios, precursores o componentes esenciales que tienen la capacidad de generar una amplia variedad de productos finales o de consumo[8].

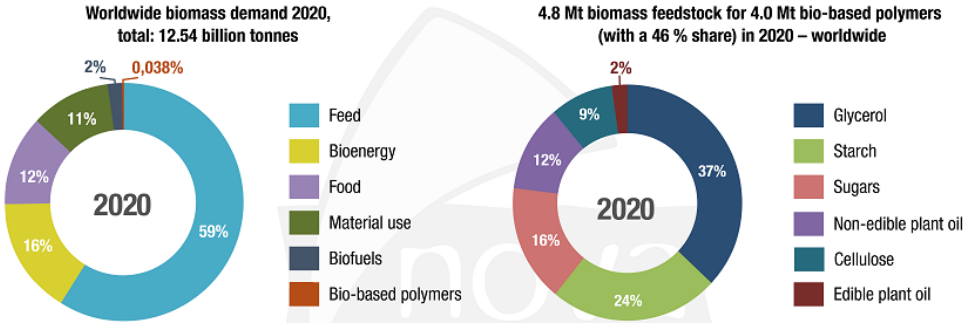

Figura 3: Principales usos y tipos de biomasa, año 2020 (imagen de Nova-Institut[9])

En el caso particular de los biopolímeros existen multitud de clasificaciones atendiendo a su origen. Una clasificación genérica agrupa las principales familias según se trate de biopolímeros que se encuentran de manera natural en el medio, biopolímeros que son producidos directamente por microorganismos o biopolímeros que son sintetizados a partir de otros monómeros biobasados[10].

---

[7] *Suschem & BioPlat. (2017). Manual sobre las Biorrefinerías en España. [https://www.suschem-es.org/docum/pb/2017/publicaciones/Manual_de_Biorrefinerias_en_Espana_feb_2017.pdf]*

[8] *Aristizábal-Marulanda, V., et al., (2018). Methods for designing and assessing biorefineries: Review. Biofuels, Bioproducts and Biorefining*

[9] *Nova Institut (2021). Report on the global bio-based polymer market 2020 – A deep and comprehensive insight into this dynamic market*

[10] *Lalit, R. et al (2018). Natural Fibers and Biopolymers Characterization: A Future Potential Composite Material. Strojnícky Casopis – Journal of Mechanical Engineering, 68(1), 33–50*

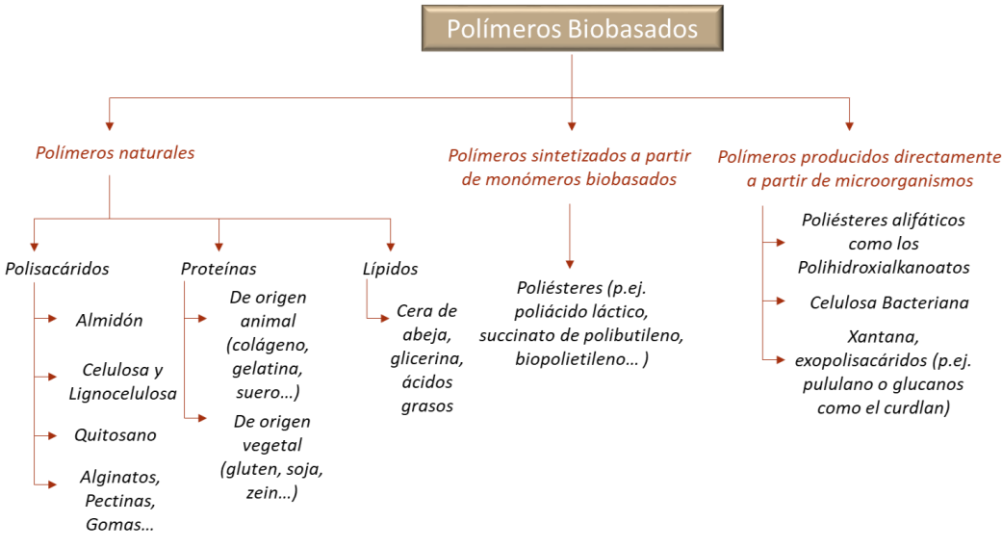

Figura 4: Clasificación general de los Polímeros Biobasados (diagrama adaptado de Lalit R. et al[10])

Durante el desarrollo de la tesis se procesan y mejoran con dos matrices poliméricas: 1) polihidroxialkanatos – *PHA* que son tanto biobasados como biodegradables y 2) polibutileno succinato – *PBS* que originalmente es un polímero sintetizado a partir del petróleo, pero biodegradable. Sin embargo, en la tesis trabajamos con una variante biobasada obtenida a partir de ácido succínico procedente de glucosa y 1,4-butanodiol procedente de almidón, por lo que se matiza como bioPBS.

Para conseguir esta extensa gama de productos se requiere la integración de diferentes procesos y tecnologías en una misma instalación. El concepto de biorrefinería debe llevar implícita una clara componente de utilización eficiente de los recursos, asegurando la sostenibilidad global del proceso.

Las biorrefinerías son por tanto el corazón de la **bioeconomía**[11]**,** motor de la economía "verde" y sostenible europea.

Figura 5: Imágenes de biorrefinerías en España: a) Algaenergy (Cádiz), b) Cener (Navarra), c) Clamber (Ciudad Real) y d) Urbaser (Zaragoza)

[11] *Bio-based Industries Consortium. Strategic Innovation & Research Agenda (SIRA - 2017). Bio-Based Industries for Development & Growth in Europe*

FIN DE VIDA

Hasta la fecha, solo el 14% de los residuos plásticos del mundo se han recuperado de manera adecuada para su reciclaje, lo que significa que la mayoría de nuestros productos con componente plástica van a parar a los vertederos, se incineran o se pierden en nuestro hábitat natural. Además, en la actualidad, solo el 2% de los plásticos recuperados se reciclan en un circuito cerrado[12].

En 2018 sólo en la UE se recogieron 29,1 millones de toneladas de residuos plásticos para ser tratados y unos 9,4 millones de toneladas de residuos de plástico postconsumo fueron reciclados, lo que representa el 32.5% del total. Sobre el resto del plástico recuperado por los canales de gestión habilitados, el 24.9% terminó en vertedero y el 42.6% restante incinerado[13]. Para el caso particular de España, el volumen de residuos plásticos de postconsumo recuperados fue de 2.5 millones de toneladas a través de los canales oficiales de recogida, de los cuales el 41.9% fue reciclado, el 19.3% incinerado y el 38.8% acabó en vertedero. No obstante, los índices de vertido son muy desiguales en Europa; por ejemplo, en los países en los que está prohibida la descarga en vertederos, presentan una tasa inferior al 10% (Bélgica, Luxemburgo, Países Bajos, Alemania, Dinamarca, Suiza, Austria, Noruega y Suecia)[14].

Además de la gestión de residuos que se realiza a nivel interno dentro de los países de la UE, la opción de exportar residuos de plástico entre países de la UE o incluso fuera de ella está permitida por la legislación comunitaria vigente, siempre y cuando la recuperación de materiales se realice en condiciones equivalentes a las de la legislación de la UE[15]. Esta situación está empezando a cambiar. Durante décadas, China fue el mayor importador de residuos del

---

[12] https://newsroom.tomra.com/only-2-plastic-packaging-closed-loop/

[13] Plastics Europe, Plastics – the Facts 2020. An analysis of European plastics: production, demand and waste data [https://www.plasticseurope.org/en/resources/publications/4312-plastics-facts-2020]

[14]Plastics Europe, Plastics—the Facts 2018. An analysis of European plastics production, demand and waste data. [https://www.plasticseurope.org/es/resources/publications/619-plastics-facts-2018]

[15] Available online: https://www.cnbc.com/2018/04/16/climate-change-china-bans-import-of-foreign-wasteto-stop-pollution.html.

mundo, pero desde Enero de 2018 Pekín prohibió la entrada de 24 tipos de residuos. Esta decisión ha obligado a otros países, como Europa, Estados Unidos y Japón, a mejorar la gestión de los suyos propios[16]; lo que se ha visto reflejado en la UE habiendo disminuido la exportación de residuos plásticos entre 2016 y 2018 en un 39%[13].

Al inicio de esta introducción se ha mencionado el impacto social y ambiental del plástico, llegando a ser tan importante como para inducir un cambio de era geológica, el Antropoceno. Recientemente, se ha identificado un nuevo tipo de roca que surge de la combinación de minerales, coral, arena y plástico. Son los denominados **plastiglomerados[17]** (del inglés "*plastiglomerate*" y en referencia a los conglomerados naturales). El problema se acentúa aún más cuando se habla de **microplásticos**[14]**.** A pesar de las medidas de control para la adecuada gestión del fin de vida de los residuos plásticos, unos 8 millones de toneladas se extravían de estos canales de recogida y terminan en los océanos cada año, donde forman grandes acumulaciones en toda la superficie oceánica y generan microplásticos, diminutas partículas de menos de 0,5 centímetros de largo, que están pasando a la cadena trófica causando problemas irreversibles en el ecosistema y la salud pública. Según el Parlamento Europeo, en 2018 los océanos albergaban ya más de 150 millones de toneladas de residuos plásticos y si no se revierte la situación se estima que para el año 2050 los océanos podrían albergar más plásticos que peces[18].

Los plásticos se están depositando en el fondo del océano y son ahora parte de los sedimentos de las grandes cuencas sedimentarias que ahí se forman. En algunas zonas cercanas a los continentes, se ha documentado que hasta el 33% de todos los sedimentos acumulados en los últimos 20 años son plásticos[17].

---

[16] Available online: https://www.reuters.com/article/us-eu-environment/eu-targets-recycling-as-china-bansplastic-waste-imports-idUSKBN1F51SP

[17] Corcoran P.L., et al (2014). An anthropogenic marker horizon in the future rock record. GSA Today, 24, 6 (Estudios realizados en costa EEUU e islas de Hawai)

[18] Ellen MacArthur Foundation and McKinsey & Company, (2016). The New Plastics Economy: Rethinking the future of plastics. World Economic Forum.

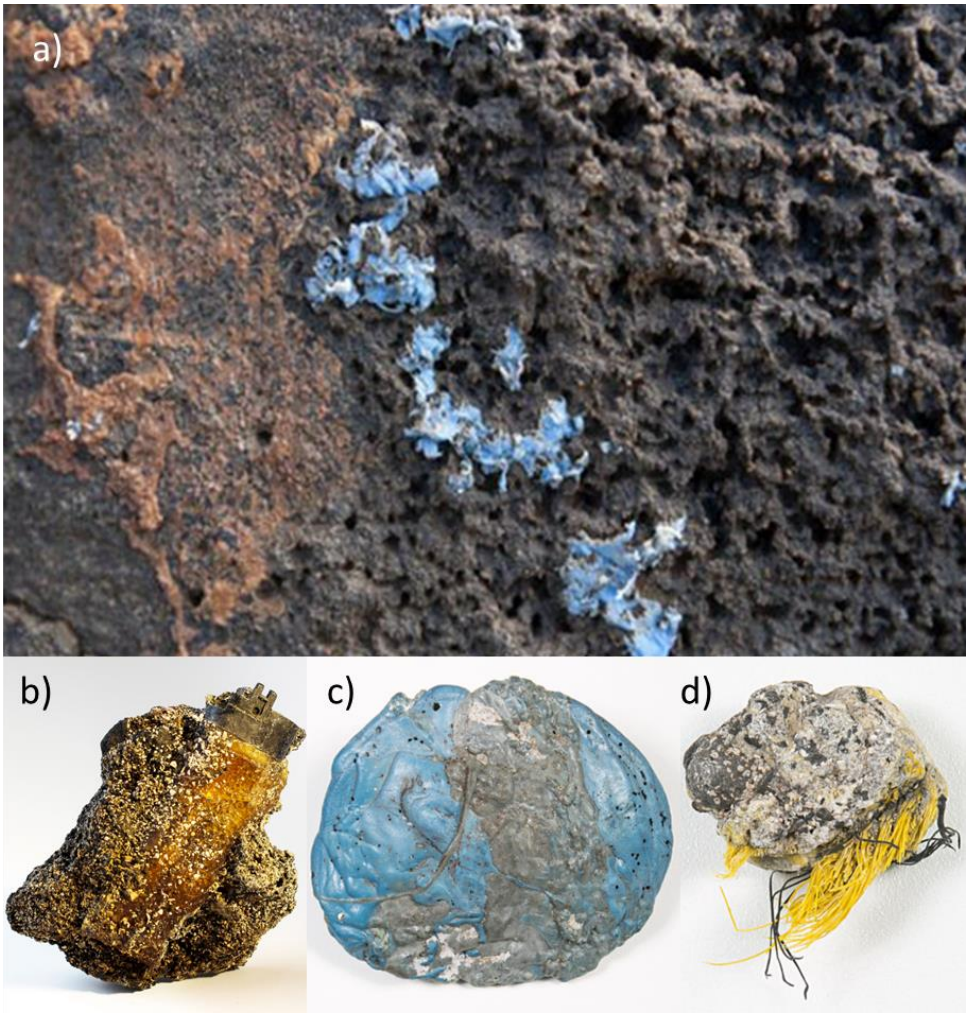

Figura 6: Imagen a) Descubren plástico incrustado en rocas de isla portuguesa de Madeira[19]; Imágenes b), c) y d) muestras de plastiglomerados hallados en playa Kamilo - Hawái por la geóloga Patricia Corconan y la escultora Kelly Jazvac[17].

[19] *Gestoso, I., et al (2019). Plasticrusts: A new potential threat in the Anthropocene's rocky shores. Science of The Total Environment. Science of The Total Environment 687:413-415.*

Figura 7: a) Larva de perca europea afectada por la ingestión de microplásticos[20]; b) Microplásticos en la coste de Fuerteventura[21]; c) Contaminación por plástico en las playas de Isla Henderson[22]; d) Procedencia de los microplásticos en los océanos (Infografía publicada por Iberdrola[23], adaptado de Unión Internacional para la Conservación de la Naturaleza (UICN, 2019)

[20] *https://www.lavanguardia.com/ciencia/planeta-tierra/20161202/412342764181/desaparecen-datos-estudio-microplasticos-resultados-cuestionados.html*

[21] *https://www.diariodefuerteventura.com/noticia/micropl%C3%A1sticos-y-pesticidas-la-combinaci%C3%B3n-letal-que-amenaza-las-playas-de-fuerteventura*

[22] *https://www.nationalgeographic.com.es/naturaleza/actualidad/millones-plasticos-los-confines-tierra_11511*

[23] *https://www.iberdrola.com/medio-ambiente/microplasticos-amenaza-para-la-salud*

Actualmente, siempre y cuando un plástico no pueda reciclarse de forma efectiva, la compostabilidad del plástico es la única estrategia que puede reducir el problema de los microplásticos[24]. Por ello, se está trabajando cada vez más en estudiar las propiedades de biodegradación y compostabilidad de los biopolímeros en distintos entornos: 1) compostaje industrial, 2) compostaje doméstico, 3) compostaje obtenido del proceso de digestión anaerobia (típicamente utilizado para la producción de biogás), 4) biodegradación en suelo y 5) biodegradación en medio marino. Se están desarrollando normas y estándares de calidad que dichos materiales deben cumplir para poder ser etiquetados y gestionados consecuentemente.

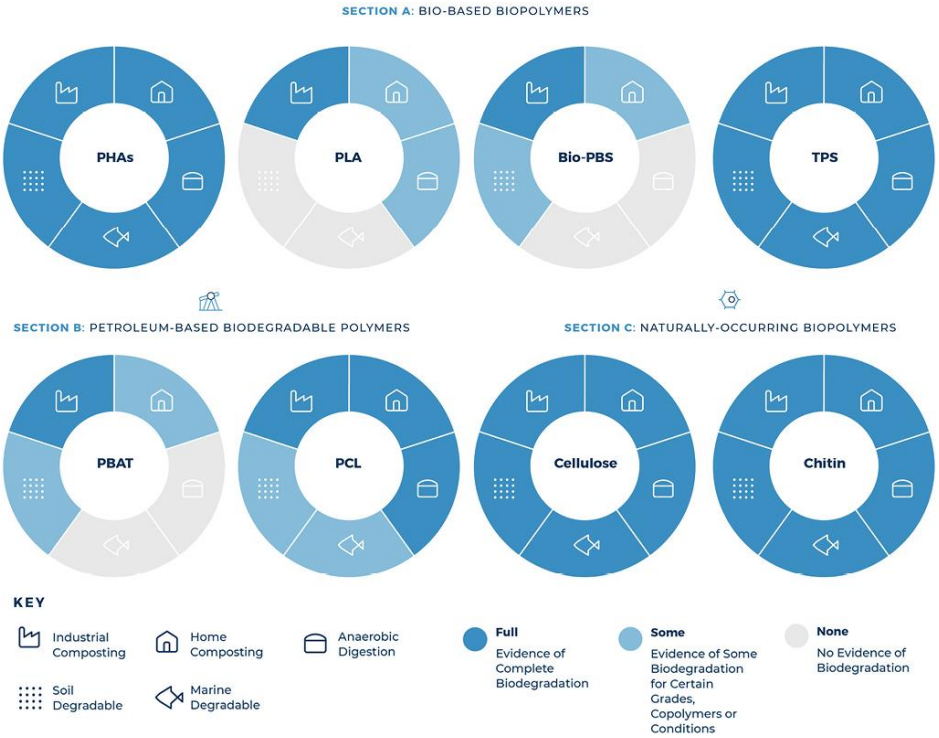

Figura 8: Alternativas del fin de vida de biopolímeros (fuente: revista Biocyle[25])

[24] *Meereboer K.W., et al (2020). Review of recent advances in the biodegradability of polyhydroxyalkanoate (PHA) bioplastics and their composites. Green Chem., 22, 5519–5558*

[25] *https://www.biocycle.net/demystifying-biopolymers-and-compostable-packaging/*

La

Figura 8 muestra la versatilidad de los PHAs en cuanto a su potencial para descomponerse en distintos entornos sin generar un impacto negativo al medio ambiente. Esta es una de las principales razones por las que se lleva realizando en los últimos años un esfuerzo considerable en inversiones para aumentar la capacidad de producción de esta familia de biopolímeros y sus aplicaciones en productos cotidianos como por ejemplo los envases.

Por su parte el bioPBS, es un ejemplo de biopolímero que muestra buenas condiciones de biodegradación en entornos controlados como son el industrial y la digestión anaeróbea, aunque también parece ser adecuado para aplicaciones en campo (por ejemplo productos para la agricultura como acolchados. Un ejemplo de ello es el proyecto Life Multibiosol[26]).

[26] *https://multibiosol.eu/*

SOLUCIÓN: PLAN DE ACCIÓN HACIA UNA BIOECONOMÍA CIRCULAR

Todas éstas, son las principales razones por las que los reguladores de la UE quieren garantizar que el plástico sea totalmente reciclable o biodegradable. En diciembre de 2015, la Comisión Europea adoptó un Plan de Acción de la UE para una economía circular, y en enero de 2018 publicó su comunicado *"Una estrategia europea para los plásticos en una economía circular"* como un paso ambicioso para hacer que el sistema europeo de plásticos sea más eficiente en cuanto a recursos y para impulsar el cambio de un sistema lineal a uno circular[27]. Todo ello, ha culminado en una hoja ruta presentada en el marco del "Pacto Verde Europeo" (*the European Green Deal*); un plan con acciones concretas dirigidas a que Europa tenga una economía limpia, con cero emisiones, y proteger nuestro hábitat natural. Entre esas acciones, se resalta el eliminar la dependencia de los recursos finitos (como por ejemplo los derivados del petróleo) e incrementar la economía circular[28]. Una economía circular tiene como objetivo mantener los productos, componentes y materiales en su máxima utilidad y valor en todo momento, haciendo hincapié en los beneficios del reciclaje[29]. La Nueva Economía de los Plásticos (*New Plastics Economy*) tiene tres objetivos principales:

1. Crear una economía eficaz de los plásticos después de su uso, mejorando la economía y la aceptación del **reciclaje, la reutilización y la biodegradación controlada** para aplicaciones específicas;
2. Reducir drásticamente las fugas o vertidos no controlados de plásticos en los sistemas naturales (en particular, en el océano);
3. **Desvincular los plásticos de las materias primas fósiles**, explorando y adoptando materias primas de **origen renovable**.

Además, para alcanzar los objetivos marcados en el año 2050 por el Pacto Verde Europeo, se han tomado algunas medidas drásticas dentro de esta Nueva Economía

[27] European Commission (2018). Communication from the Commission to the European Parliament, the Council, the European Economic and Social Committee and the Committee of the Regions; A European Strategy for Plastics in a Circular Economy; European Commission: Brussels, Belgium.
[28] https://ec.europa.eu/spain/news/20191212_Europe-climate-neutral-2050_es
[29] European Commision (2015). A European Strategy for Plastics in a Circular Economy, 2015. Available online: [http://ec.europa.eu/environment/circular-economy/pdf/plastics-strategy-brochure.pdf]

de los Plásticos, como ha sido la prohibición de plástico de un solo uso en la UE, aprobada en 2019 y que entró en vigor en verano del año 2020. Ni siquiera en el marco de esta ley los bioplásticos (biobasados y biodegradables) quedan exentos de la prohibición.

Por ello, es urgente y necesario encontrar nuevas soluciones sostenibles para el sector del plástico, las cuales deben abordarse teniendo en cuenta tres pilares fundamentales: el eco-diseño, la funcionalidad y el fin de la vida útil del producto. En este sentido, diversas investigaciones, como la presente tesis, se dirigen a incrementar el uso de materias primas de origen renovables y a eliminar el residuo en función de la aplicación final, para fabricar productos con menor impacto ambiental a través de promover tanto nuevas tecnologías de reciclaje (e.g. mecánico, térmico, químico o enzimático) o mediante el uso de materiales biodegradables. La tesis, busca mediante la mejora de las propiedades estéticas de los biopolímeros, lograr una mayor aceptación de los mismos por el mercado.

MOTIVACIÓN

La motivación de la tesis resulta de la oportunidad de **aumentar o generar mercado para incrementar la aceptación y el uso de los bioplásticos por la industria y la sociedad**. Desde Tecnopackaging, empresa en la cual se realiza la presente tesis en colaboración con el centro tecnológico Aitiip y la Universidad de Zaragoza, se ha detectado la necesidad de mejorar las propiedades estéticas de los biopolímeros dada la multitud de componentes de plástico visibles (por ejemplo, en piezas de automoción de interior de cabina, carcasas de electrodomésticos, mueble de decoración, envases etc) donde el aspecto estético y superficial tiene una extraordinaria importancia.

Hasta el momento, se han focalizado esfuerzos mayoritariamente en mejorar las propiedades funcionales de los biopolímeros (mecánicas, térmicas, barrera etc) y apenas se han centrado en mejorar dichas propiedades estéticas, como potenciales sustitutos de los polímeros convencionales en muchas aplicaciones industriales. Estas mejoras son necesarias para satisfacer los requerimientos de las aplicaciones finales, ya que sin ellas será difícil **lograr una sustitución completa de los plásticos derivados del petróleo**. Por esta razón, con la realización de esta tesis doctoral, **se inicia una nueva línea de investigación en la empresa, de carácter estratégico, que permitirá aumentar la aceptación** de estos materiales por el consumidor a medio plazo favoreciendo la ampliación de productos y el crecimiento de la empresa.

OBJETIVO

El objetivo general de la tesis se centra en **mejorar las propiedades estéticas de biopolímeros para incrementar su uso y aplicaciones** como materiales más sostenibles. En particular se proponen alternativas a las poliolefinas convencionales como el polipropileno (PP). Por ello se partirá de aquellos se consideran sus principales sustitutos biobasados con mayor potencial como son los PHAs y el bioPBS, conforme al estado actual de la técnica.

Se valoran dos enfoques distintos para alcanzar dichas mejoras: el primero basado en mejorar la **coloración** de los biopolímeros y el segundo enfocado en disminuir **olores** desagradables derivados de la oxidación de biopolímeros producidos a partir de fermentación bacteriana. Para ello, se trabaja en la **formulación y procesado** del propio material mediante mezclas de las matrices ("blendas") y la integración de los diferentes aditivos (principalmente basados en ácidos orgánicos y nanopartículas) así como estrategias de funcionalización y **escalado industrial** para mejorar la compatibilidad (procesado por extrusión-*compounding* y extrusión reactiva).

OBJETIVOS ESPECÍFICOS

- Contribuir a la ampliación del conocimiento propio sobre los polímeros biobasados y biodegradables como sustitutos de polímeros convencionales (al menos en dos familias de biopolímeros, como son los PHAs y bioPBS).
- Contribuir a incrementar el conocimiento propio en estrategias de mejora en funciones específicas como son las propiedades estéticas, mediante la incorporación de aditivos (como las nanopartículas, colorantes y ácidos orgánicos) así como sus técnicas de integración.
- Aprender a desarrollar métodos experimentales que permitan obtener un número suficiente de formulaciones como para ser capaz de testear y validar variaciones en las propiedades objetivo a estudiar; en base a criterios propios y consultados en el estado del arte de otros científicos en la temática (definir nº de muestras, necesidades y definición del ensayo y proceso, % de cada aditivo, etc)
- Aprender y entender nuevas técnicas de caracterización de materiales aplicadas a biopolímeros para ser capaz de definir métodos aplicados que

permitan valorar cambios en las propiedades objetivo a estudiar (cuantificar, cualificar).

- Incrementar el conocimiento propio en técnicas físico-químicas que permitan mejorar la compatibilidad entre materiales, así como mejorar la integración y dispersión de aditivos en matrices poliméricas.
- Aprender fases de escalado del conocimiento adquirido de nivel laboratorio a nivel piloto para ser capaz de proponer procesos de industrialización de los materiales desarrollados, así como productos y aplicaciones industriales concretas.
- Ser capaz de discutir los resultados obtenidos y cotejarlos con los de otros expertos en el tema, así como elaborar conclusiones finales del trabajo realizado
- Transferencia tecnológica a la empresa en cuanto al diseño, procesado y aplicaciones de biopolímeros, así como estrategias para mejorar las propiedades estéticas de los mismos.
- Crear relaciones y grupos de trabajo con expertos internacionales en el área temática.
- Aprender a divulgar ciencia a distintos niveles, desde foros especialistas y científico-técnicos expertos en biopolímeros, foros industriales y foros abiertos a la sociedad.

ESTADO DEL ARTE

LAS POLIOLEFINAS (PP)

Las poliolefinas son polímeros producidos por la polimerización de olefinas o alquenos, hidrocarburos con enlaces dobles carbono-hidrógeno. Son duras, ligeras y rígidas, tenaces y con buena resistencia al impacto, a la humedad y los ataques químicos; por lo que se utilizan en multitud de aplicaciones industriales como por ejemplo el sector de la automoción, construcción e infraestructuras como tuberías, electrónica y bienes de consumo o envases. Las poliolefinas más comunes son el polipropileno (PP), el polietileno (PE) que habitualmente se diferencia entre polietileno de baja densidad (LDPE) y de alta densidad (HDPE); y el caucho de etileno-propileno-dieno (EPDM).

El Polipropileno es un polímero lineal que presenta en su cadena principal hidrocarburos saturados y cada dos átomos de carbono se encuentra ramificado un grupo metilo $(C_3H_6)_n$. La posición de ese grupo metilo permite la formación de tres isómeros: isotáctico, sindiotáctico y atáctico. Los procesos industriales más empleados (polimerización por polimerización Ziegler-Natta o por catálisis de metaloceno) están dirigidos hacia la fabricación de polipropileno isotáctico y sindiotáctico, los cuales producen un polímero semicristalino que despierta mayor interés comercial. Desde el inicio de su producción comercial en 1958, ha aumentado su presencia en el mercado hasta posicionarse como la poliolefina por excelencia junto con el Polietileno (PE).

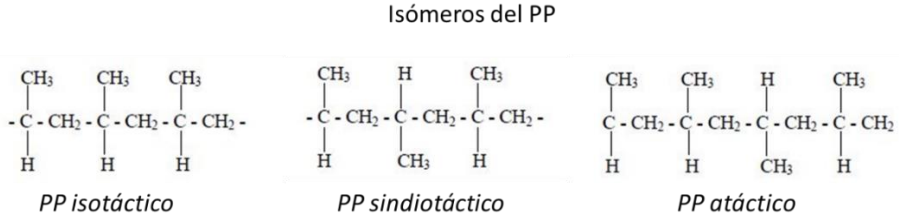

Figura 9: Isómeros del PP según la posición del grupo metilo. (Adaptado de Z.M.Ariff et al[30])

[30] *Z.M.Ariff, et al. (2012). Rheological Behaviour of Polypropylene Through Extrusion and Capillary Rheometry. Polypropylene. InTech ISBN 978-953-51-0636-4*

Entre el periodo 2021-2026, se espera que el mercado de poliolefinas crezca a una tasa compuesta anual (CAGR) del 8%[31]. En particular, el mercado mundial del PP alcanzó un valor de $ 126.03 mil millones en 2019 y se espera que crezca un CAGR del 12% hasta el año 2023 alcanzando los $ 192.33 mil millones. Según el último informe publicado por *Plastics Europe - 2020*, es el polímero más consumido en EU con una tasa del 19,4%. (Se disputa el ranking con el PE, solo que este se subdivide en función de su peso molecular en diversas aplicaciones: baja densidad 17,4% y media y alta densidad: 12,4%).

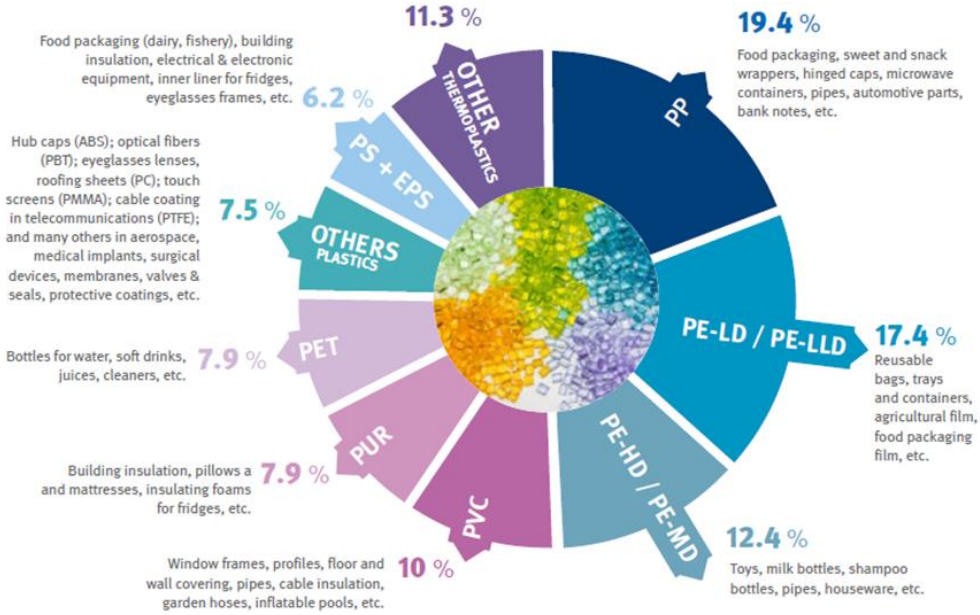

Figura 10: Distribución de la demanda de plásticos por tipología de resina en EU – 2019 (Imagen de Plastics Europe[13])

La causa de su elevado consumo es su versatilidad en los procesos de transformación, sus costes competitivos y su facilidad de reciclado. A esto se unen otras propiedades como su rigidez y capacidad de coloración; y un alto aguante a la temperatura y al impacto. Es también muy valorado, por su elevada resistencia a la abrasión, a la deformación y al rayado. Incluso por la buena absorción acústica,

[31] *https://www.mordorintelligence.com/industry-reports/polyolefin-market*

que hacen del PP un elemento esencial para su uso en una amplia variedad de aplicaciones. Por ejemplo, es uno de los plásticos más utilizados en la industria del automóvil, donde el 36% de las piezas plásticas de un coche se fabrican con este polímero. Sirve para la fabricación de algunos de los componentes del interior del vehículo, como salpicaderos o revestimientos de puertas; también de otros que se encuentran en la parte exterior, como parachoques; y de elementos bajo capó, como carcasas de faros, embellecedores, filtros de aire o calefactores…El PP también se utiliza en la fabricación de carcasas y piezas técnicas de pequeños electrodomésticos como cafeteras, planchas, freidoras o cilindros para lavadoras. También es apto para muebles de jardín, como tumbonas, sillas y mesas que, además, ofrecen una amplia gama de colores[32].

Figura 11: Ejemplos de productos elaborados en base PP

Por lo tanto, los mercados de sus alternativas biobasadas como el PHA y el bioPBS son potencialmente igual de grandes; aunque es cierto que en el corto plazo, mientras que el coste de producción siga siendo significativamente más alto, el mercado de estos biopolímeros estará más enfocado en nichos de producto de alto valor añadido.

[32] *http://www.mundoplast.com/noticia/el-consumo-mundial-polipropileno-alcanzara-los-624-millones-toneladas-2020/71607*

BIOPOLÍMEROS SUSTITUTOS DE LAS POLIOLEFINAS: LOS POLIÉSTERES ALIFÁTICOS

En 2019, el volumen de producción total de polímeros de base biológica (biobasados) fue de 3,8 millones de toneladas, que es el 1% del volumen de producción de polímeros de base fósil y aproximadamente un 3% más que en 2018; se espera que esta CAGR continúe así hasta 2024[33]. Hoy en día, los polímeros biobasados se pueden utilizar en casi todos los sectores y multitud de aplicaciones. Según datos del 2020 publicados por Nova-Institut, al sector fibras cuenta con un 24% de cuota de mercado del cual aproximadamente el 20% pertenece al textil; le sigue el sector de la automoción y transporte con 16%, edificación y construcción con 13% (ambas principalmente resinas epoxi, PA y PUR), bienes de consumo con 9% (principalmente resinas epoxi, PA y PUR), envases flexibles 13 % (principalmente compuestos poliméricos que contienen almidón, PBAT y PE) y envases rígidos 11% (mayoritariamente PET, PLA y PBAT). Los sectores eléctrico y electrónico, agrícola y hortícola entre otros presentan una cuota de mercado en torno al 3%.

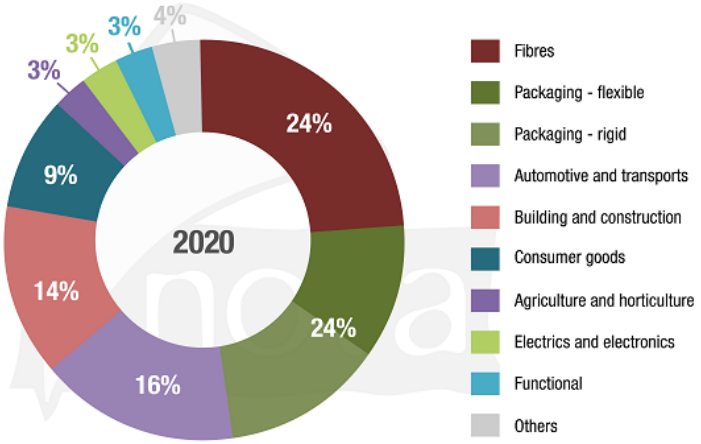

Figura 12: Cuota de mercado de los polímeros biobasados producidos – 2020 (imagen de Nova-Institut[9])

[33] *Nova-Institute (2019). "Bio-based Building Blocks and Polymers – Global Capacities, Production and Trends 2019-2024"*

De entre todos ellos, los poliésteres alifáticos son probablemente la familia de biopolímeros más estudiada dentro de los biopolímeros biodegradables debido a su variedad y versatilidad. Éstos contienen enlaces de tipo "éster" que se hidrolizan al entrar en contacto con un medio acuoso. Los poliésteres alifáticos pueden derivar de un único monómero con grupos funcionales distintos (como por ejemplo los PHAs) o de dos monómeros en los que en cada uno de ellos existen dos grupos funcionales de la misma naturaleza (como por ejemplo el PBS: 1,4- butanodiol & ácido succínico).

Recientemente (en Diciembre del 2019) se comenzó la primera producción industrial del bioPP o PP de origen renovable en cooperación entre las empresas Boeralis y Neste, y comercializada bajo el nombre de Everminds™. Neste ha sido capaz de producir propano de origen renovable y Borealis en su planta de dehydrogenación está siendo capaz de producir PP[34].

De cualquier modo, el desarrollo de nuevos materiales plásticos biobasados requerirá de una disponibilidad sostenible de la materia prima (de segunda y tercera generación)[35], además de ser competitivo no solo económicamente sino en funcionalidad superando las barreras tecnológicas que están típicamente relacionadas con estos materiales: escasa resistencia al calor, necesidad de estabilización UV, pobres propiedades barrera al vapor de agua y a los gases, y deficientes propiedades mecánicas para muchas aplicaciones.

La mezcla entre biopolímeros (también conocido como "blendas") así como el refuerzo mediante la incorporación de fibras o nanopartículas es una estrategia útil para modificar las propiedades de la matriz polimérica principal en aplicaciones específicas. También pueden mejorarse mediante reticulación química y física, o incluso con el uso de tratamientos superficiales como es la activación por medios físico-químicos o el uso de recubrimientos. Se espera que la barrera económica se compense una vez que se tengan en cuenta los costes de fin de vida y/o se aumenten los volúmenes de producción[36].

---

[34] https://news.bio-based.eu/borealis-producing-certified-renewable-polypropylene-at-own-facilities-in-belgium/

[35] https://bioplasticsnews.com/2018/09/12/bioplastic-feedstock-1st-2nd-and-3rd-generations/

[36] La Rosa, A.D. (2016). Biopolymers and Biotech Admixtures for Eco-Efficient Construction Materials, 1st ed.; Woodhead Publishing: Cambridge, UK; ISBN -9780081002148.

LOS PHAs

Los polihidroxialcanoatos o PHAs son una clase de poliésteres lineales producidos por la fermentación bacteriana directa de azúcares o lípidos. Son producidos por las propias bacterias para almacenar carbono y energía en forma de inclusiones orgánicas intracelulares[37], generalmente al someterlas bajo condiciones de estrés fisiológico (exceso en la fuente de carbono y limitación en elementos esenciales como N, S, O, P o Mg). Los gránulos formados tienen un tamaño de unas 0,2-0,5 micras y contienen al polímero en estado amorfo. A su vez, están recubiertos por una membrana monocapa de fosfolípidos y proteínas de unos 3-4 nm de grosor[38].

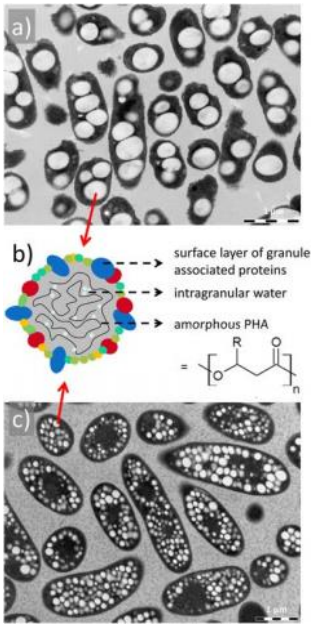

Figura 13: Morfología de los gránulos de PHA generados por bacterias[39]

[37] *Koller, M.; et al., (2018). Advanced approaches to produce polyhydroxyalkanoate (PHA) biopolyesters in a sustainable and economic fashion. EuroBiotech J., 2, 89–103.*
[38] *Kabasci, S. (2014). Bio-Based Plastics: Materials and Applications; JohnWiley & Sons Ltd.: Hoboken, NJ, USA; Chapter 7.3.2, ISBN - 9781119994008.*
[39] *Obruca, S., et al., (2020). Novel unexpected functions of PHA granules. Applied Microbiology and Biotechnology, 104:4795–4810*

Los PHAs, se forman principalmente a partir de ácidos hidroxialcanoicos saturados e insaturados. Cada unidad de monómero alberga un grupo R de cadena lateral, que suele ser un grupo alquilo saturado. Según el número de átomos de carbono en la cadena principal se clasifican en tres sub-categorías: 1) de cadena corta (scl – "*short-chain-length*") cuando las unidades monoméricas contienen de tres a cinco átomos de carbono, 2) de cadena media (mcl - "*medium-chain-length*") con unidades monoméricas que poseen de seis a catorce átomos de carbono y 3) de cadena larga (lcl - "*long-chain-length*") con más de 14 átomos de carbono[40],[41].

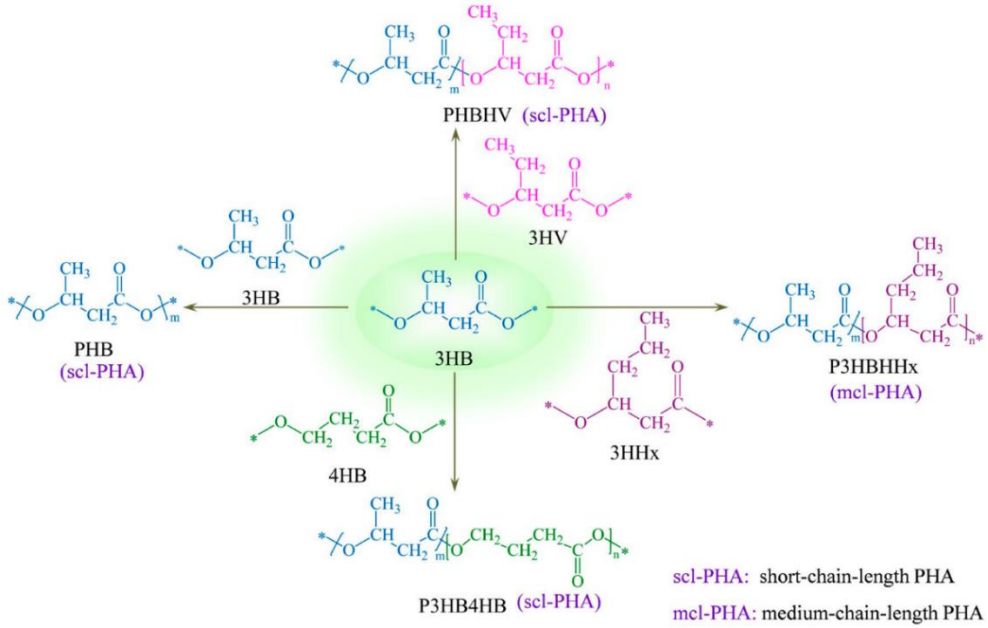

Figura 14: Estructura general de varios copolímeros de PHA. (Figura de S. Wang et al[42])

[40] *Pramanik, K.; et al., (2014). Polyhydroxyalkanoates: Biodegradable Plastics for Environmental Conservation In Industrial & Environmental Biotechnology; Studium Press: N. Delhi, India; Chapter 1.*
[41] *Rehm, B.H.A. (2003). Polyester synthases: Natural catalysts for plastics. Biochem. J., 376, 15–33.*
[42] *Wang, S., et al., (2016). Modification and Potential Application of Short-Chain-Length Polyhydroxyalkanoate (SCL-PHA). Polymers, 8(8), 273.*

Estas características dan lugar a diversas combinaciones de PHA. Dentro de esta familia se pueden combinar más de 150 monómeros para obtener polímeros específicos con propiedades muy diferentes: desde los termoplásticos frágiles a elastómeros gomosos[43]. Propiedades que puede controlarse mediante la elección del sustrato, las bacterias y las condiciones de fermentación. El resultado son estructuras de copolímeros semicristalinas diseñadas para tener un punto de fusión adaptado habitualmente entre 80 °C y 150 °C (pero puede variarse entre 40 °C y 180 °C) y que son menos susceptibles a la degradación térmica durante su procesado. Los ejemplos más representativos son la familia de los polihidroxibutiratos-*PHBs,* destacando el *poli(3- hidroxibutirato) P3HB,* con un alto punto de fusión, siendo muy cristalino y frágil*;* y los polihidroxivaleratos-*PHVs como el poli(3-hidroxibutirato-co-valerato) PHBV,* con una menor cristalinidad y un punto de fusión más bajo. Más recientemente, se han desarrollado nuevos copolímeros personalizados mediante la incorporación aleatoria de cantidades controladas de espaciadores alifáticos lineales flexibles a lo largo de la cadena principal; por ejemplo, el 3-hidroxipropionato (3HP), 3-hidroxioctanoato (3HO), o el 4-hidroxibutirato (4HB)[44,43].

En particular los usados por la doctoranda para la ejecución práctica de experimentos han sido tres tipos de matrices comerciales basadas en dos estructuras: un poli(3-hidroxibutirato) lineal (P3HB) y dos copolímeros basados en poli(3-hidroxibutirato)-co-poli(4-hidroxibutirato) (P3HB-co-P4HB) con diferente cantidad de P4HB en su estructura; tal y como se explica en el ARTICULO 1[45].

Aunque se desarrollaron en la década de 1990, los PHAs aún permanecen actualmente como materiales sólo aptos para nichos de mercado de alto valor añadido. El coste de producción de los biopolímeros de PHA ha disminuyendo en los últimos años y se espera que disminuya aún más gracias al uso de materias primas más baratas con las que alimentar a las bacterias (como por ejemplo mediante el uso de residuos agrícolas). Sin embargo, el mayor reto en cuanto a la

[43] Wang, S.; et al., (2016). Modification and Potential Application of Short-Chain-Length Polyhydroxyalkanoate (SCL-PHA). Polymers, 8, 273.

[44] Sudesh, K.; et al., (2008). Sustainability of Biobased and Biodegradable Plastics. Clean, 36, 433–442

[45] García-Quiles L. et al (2019). Sustainable Materials with Enhanced Mechanical Properties Based on Industrial Polyhydroxyalkanoates Reinforced with Organomodified Sepiolite and Montmorillonite. Polymers, 11(4), 696.

industrialización de este material reside en su etapa de purificación y en la robustez del proceso entre lotes para garantizar siempre las mismas propiedades (estándares de calidad).

Para recuperar los gránulos de PHA es necesario romper las células bacterianas y eliminar la membrana para aislar las cadenas del polímero. Para ello, se utiliza una combinación de disolventes, normalmente orgánicos y/o clorados que modifican la permeabilidad de la membrana celular y disuelven el PHA, siendo capaz de escapar a través de la membrana y la pared celular[46-48]. Con frecuencia lípidos de la membrana y endotoxinas quedan adheridas a los gránulos de PHA permaneciendo unidos al biopolímero después de la extracción[49] siendo la causa del olor a rancio. Los lípidos al oxidarse (en presencia de luz, calor, humedad…), pueden romperse en moléculas más pequeñas que generan radicales libres[50].

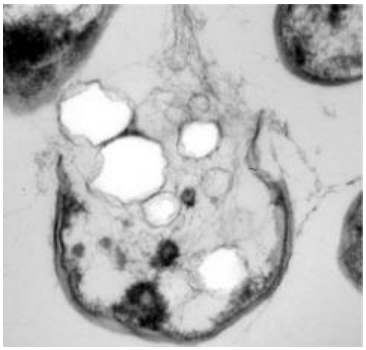

Figura 15: Extracción del PHA celular (Fuente de M.J. Marconi et al[51]; CBIB – universidad Andrés Bello, Chile)

[46] Koller, M. el at (2017). Producing microbial polyhydroxyalkanoate (PHA) biopolyesters in a sustainable manner. New Biotechnol., 37, 24–38.

[47] Ong, S.Y.; et al (2018). An integrative study on biologically recovered polyhydroxyalkanoates (PHAs) and simultaneous assessment of gut microbiome in yellow mealworm. J. Biotechnol., 265, 31–39.

[48] Choi JI, et al., (1999). Efficient and economical recovery of poly (3-hydroxybutyrate) from recombinant Escherichia coli by simple digestion with chemicals. Biotechnol Bioeng.; 62: 546-553

[49] Fung, F.M. et al (2017). Extraction, separation and characterization of endotoxins in water samples using solid phase extraction and capillary electrophoresis-laser induced fluorescence. Sci.Rep. 7,10774.

[50] Koller, M. et al (2013). Extraction of short-chain-length poly-[(R)-hydroxyalkanoates], (scl-PHA) by the antisolvent acetone under elevated temperature and pressure. Biotechnol. Lett. 35, 1023–1028.

[51] https://ciencia.unab.cl/cientificos-unab-crean-sistema-para-obtener-bioplastico-partir-de-bacterias/

La oxidación de los dobles enlaces de los ácidos grasos insaturados con formación de peróxidos o hidro-peróxidos, que posteriormente se polimerizan y descomponen dando origen a la formación de aldehídos, cetonas y ácidos de menor peso molecular causantes del olor característico de estos materiales. Otros métodos de extracción más "limpios" que intentan minimizar los lípidos adheridos utilizan antisolventes[50], alta presión y fluidos supercríticos[52]. Algunos estudios achacan también que el uso de disolventes orgánicos durante la extracción del polímero podría favorecer la liberación de volátiles causantes de mal olor[53].

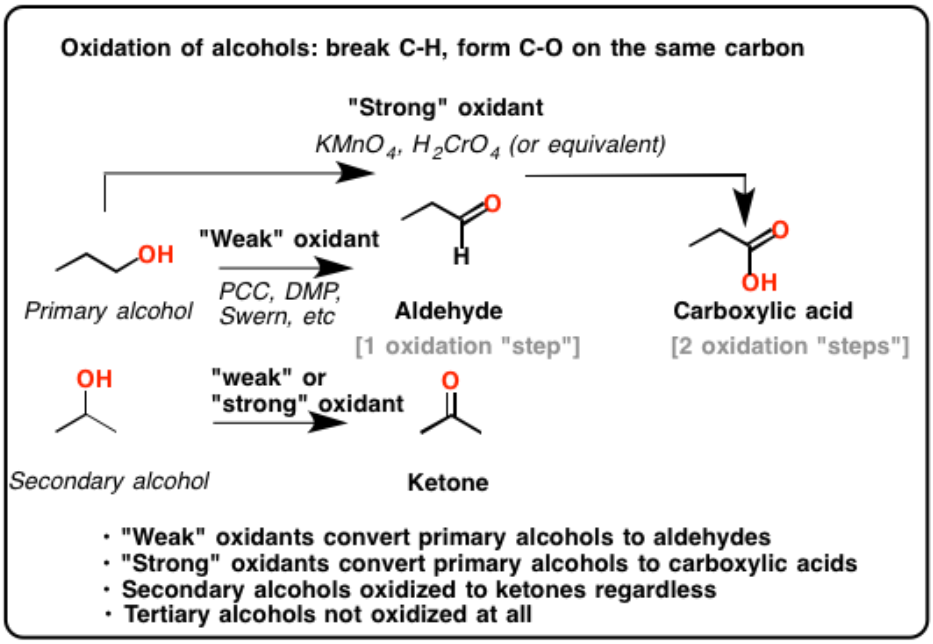

Figura 16: Oxidación de los grupos Alcohol: Oxidantes "Fuerte" y "Débil"[54]

[52] *Khosravi-Darani K, et al., (2005). Application of supercritical fluid extraction in biotechnology. Critic Rev Biotechnol; 25: 1-12*

[53] *Brigham, C.J.; et al., (2018). The Potential of Polyhydroxyalkanoate Production from Food Wastes. Appl. Food Biotechnol, 6, 7–18.*

[54] *Ashenhurst. J., (2015). Master Organic Chemistry. Alcohols, Epoxides and Ethers: Alcohol Oxidation: "Strong" and "Weak" Oxidants.*

La solución propuesta en la presente tesis se aborda desde la etapa de composición de mezclas personalizadas, un desarrollo de materiales desde el punto de vista del productor de granzas, cuya labor se centra en mitigar el efecto del olor a rancio. Como solución se propone el uso de nanoarcillas con propiedades de alta adsorción como son la Sepiolita y la Montmorillonita capaces de capturar o secuestrar ciertos compuestos volátiles responsables del desagradable olor. En el ARTICULO 2[55] se ha desarrollado una metodología que permite por un lado identificar cuáles son los volátiles principales derivados de los PHAs seleccionados, así como comparar cuánto se reduce la emisión de dichos volátiles una vez se introducen las nanoarcillas. Se comparan tanto nanoarcillas de distinta naturaleza, funcionalización superficial y % en masa de la mezcla.

EL bioPBS

El Poli (succinato de butileno) o PBS es uno de los poliésteres biodegradables con mayor potencial de aplicación. Es un termoplástico sintetizado primero por la esterificación de sus dos oligómeros: 1,4- butanodiol con ácido succínico; y después a través de su policondensación a altas temperaturas (220ºC-240ºC) y usando varios catalizadores[56] como por ejemplo titanato de tetraisopropilo, triflatos de lantánidos y $SnCl_2$.

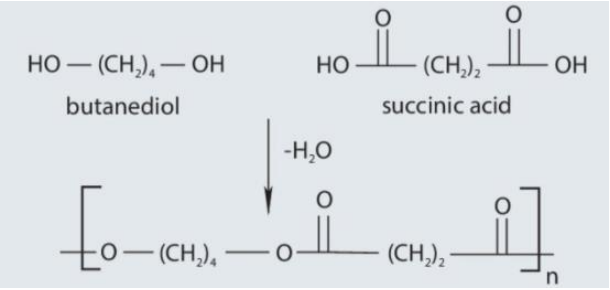

Figura 17: BioPBS monómero [57]

[55] *García-Quiles L. et al (2019). Reducing off-Flavour in Commercially Available Polyhydroxyalkanoate Materials by Autooxidation through Compounding with Organoclays. Polymers, 11, 945.*
[56] *Adriaan S., et al., (2019). Plastics to Energy. Fuel, Chemicals, and Sustainability Implications. Chapter 16 - Can Biodegradable Plastics Solve Plastic Solid Waste Accumulation?. 403-423*
[57] *Storz, H., et al (2013). Biobased plastics: status, challenges & trends. Appl Agric Forestry Res,4 (63), 321-332*

Sus precursores pueden sintetizarse con origen a partir del petróleo o de biomasa. El ácido succínico (ácido butanodioico) es un ácido dicarboxílico cuya fórmula química es $C_4H_6O_4$. Las rutas industriales más comunes incluyen la hidrogenación del ácido maleico, la oxidación del 1,4-butanodiol y la carbonilación del etilenglicol. Más recientemente, se ha obtenido a través de la fermentación de glucosa procedente de materias primas renovables y de la purificación del ácido biosuccínico. Por su parte el 1,4-butanodiol (BDO) es un dialcohol con fórmula molecular $C_4H_{10}O_2$. Es un compuesto orgánico comúnmente utilizado como disolvente en la industria de limpieza y como precursor de polímeros (no sólo PBS, sino también poliuretanos o elastanos)[58] y su origen biobasado proviene de la hidrólisis del almidón. El crecimiento en el uso de este precursor en Europa está sin duda vinculado a la historia de éxito de la industria Novamont[59] (Genomática).

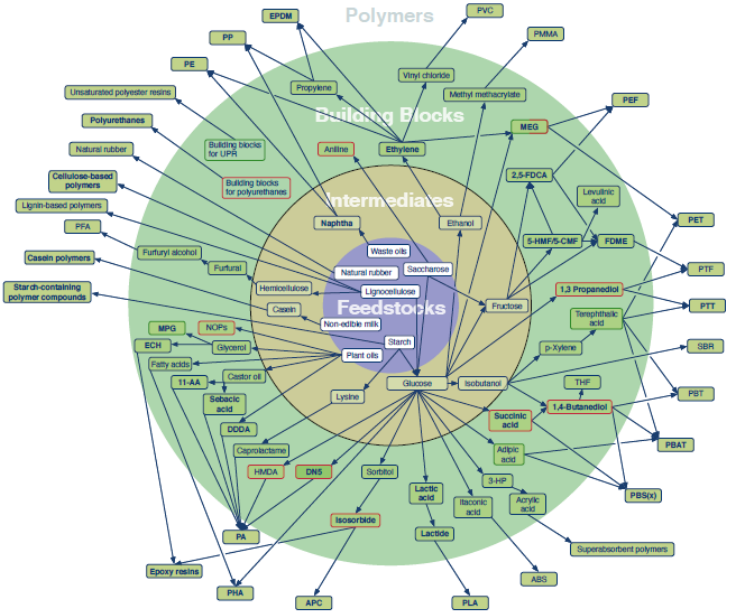

Figura 18: Rutas hacia los polímeros biobasados[60]

[58] *Jamaluddin N., (2016). Mechanical and Morphology Behaviours of Polybutylene (succinate)/Thermoplastic Polyurethaneblend. Procedia Chemistry 19, 426 – 432*

[59] *https://bioplasticsnews.com/bio-bdo-bio-butanediol-novamont/*

[60] *Nova-Institut (2021). Bio-based Building Blocks and Polymers – Global Capacities, Production and Trends 2020 – 2025*

Este polímero tiene una gran flexibilidad, excelente resistencia al impacto y propiedades térmicas, así como presenta alta resistencia a ataques con químicos[61]. Prueba de ello, en 2018 Starbucks y McDonald's lanzaron una campaña para sustituir vasos de bebida por nuevos materiales biobasados y biodegradables entre los que se incluyen materiales compuestos de cartón con recubrimientos de bioPBS[62]. Sin embargo, otras propiedades tales como la rugosidad superficial, barrera a gases, viscosidad en estado fundido durante su procesado (comportamiento reológico) etc, son con frecuencia insuficientes para diversas aplicaciones[58]. Por lo tanto, el PBS se mezcla a menudo con otros compuestos, tales como cargas y blendas o mezclas de copolímeros para mejorarlas.

[61] *Kennouche S., et al., (2016). Morphological characterization and thermal properties of compatibilized poly(3-hydroxybutyrate-co-3-hydroxyvalerate) (PHBV)/poly(butylene succinate) (PBS)/halloysite ternary nanocomposites. European Polymer Journal, 75, 142–162*

[62] *https://stories.starbucks.com/press/2020/update-on-starbucks-journey-to-find-a-more-sustainable-cup/*

NANOPARTÍCULAS PARA MEJORAR LAS PROPIEDADES OBJETIVO

Los nanocompuestos basados en polímeros han ganado mucho interés en las últimas décadas debido a los grandes avances que se han realizado en este campo con el objetivo de mejorar diversas propiedades del material, entre las principales: mecánicas, térmicas, solubilidad, permeabilidad o biodegradabilidad. Se consideran nanocompuestos aquellos cuyo refuerzo tiene un tamaño nanométrico. Por convenio de la comunidad científica se admiten como partículas nanométricas aquellas en las que al menos una de sus dimensiones es de tamaño inferior a los 100 nm. Existen multitud de nanoaditivos, principalmente se subdividen en función de su geometría predominante:

- Una dirección principal o eje, con forma de aguja como la Sepiolita, o de tubo como en el caso de los nanotubos de carbono, o Haloisitas.
- Dos direcciones principales o estructuras planas con forma de plaquetas o capas planas o láminas, como el grafeno o las que presentan la mayoría se silicatos como por ejemplo la Montmorillonita.
- Tridimensionales o esféricas como el óxido de zinc, el fullereno o los silsesquioxanos poliédricos oligoméricos (POSS).

Las nanopartículas tienen una gran variedad de aplicaciones en múltiples campos. En la siguiente tabla se recogen algunas de las aplicaciones más significativas y la naturaleza de las mismas:

APLICACIÓN	TIPO DE NANOPARTÍCULAS
POTENCIA/ENERGÍA[63,64]	
Células solares sensibilizadas por colorante	*TiO_2, ZnO y Au*
Almacenamiento de hidrógeno	*Nanopartículas híbridas metálicas*
Mejora de los materiales para ánodo y cátodo para pilas de combustible	*Nanoarcillas, Nanotubos de Carbono*
Catalizadores ambientales	*TiO_2, cerio*

[63] *Shanmugam, N., et al. (2020). Anti-Reflective Coating Materials: A Holistic Review from PV Perspective. Energies, 13, 2631.*

[64] *Singh R., et al. (2020). Nanomaterials in the advancement of hydrogen energy storage. Heliyon, 6(7): e04487*

Catalizadores para automoción	*Nanopartículas cerámicas óxidos metálicos (cerio, zirconio) y metales (Pt, Rh, Pd y Ru)*
SALUD/MEDICINA[65-67]	
Promotores de crecimiento óseo	*Hidroxiapatita (HAp) cerámica*
Cremas con protección solar	*ZnO y TiO_2*
Apósitos para heridas antibacterianos	*Ag*
Fungicidas	*Cu_2O*
Etiquetado y detección	*Ag y coloides de Au*
Agentes de contraste de MRI (imagen por resonancia magnética)	*Magnetita - Fe_3O_4; maghemita - γ-Fe_2O_3 y óxidos de hierro dopados con otros metales como Mn, Co o Ni*
INGENIERÍA[68-70]	
Herramientas de corte	*ZrO_2 y Al_2O_3, cerámicos no-óxidos (WC, TaC, TlC) y Co*
Sensores químicos	*Diversas nanopartículas válidas, depende de la aplicación*
Resistentes al desgaste / recubrimientos resistentes a la abrasión	*Nanopartículas de alumina y Y-Zr_2O_3*
Nanoarcilla polímero reforzado con composites	Organoarcillas (*sepiolita*, *laponita* y *montmorilonita),* silicageles y *POSS*
Pigmentos	Pb, Zn, Mg y Ag. Otras Nanopartículas metálicas incluyendo ViO, AlO, CdO y otras
Tintas: conductores, magnéticos, etc (utilizando polvos de metal)	Ag

[65] *Mitchell, M.J., et al.(2021). Engineering precision nanoparticles for drug delivery. Nat Rev Drug Discov 20, 101–124.*

[66] *Su S., et al. (2020). Systemic Review of Biodegradable Nanomaterials in Nanomedicine. Nanomaterials, 10, 656.*

[67] *Tuukkanen J, et al., (2017). Hydroxyapatite as a Nanomaterial for Advanced Tissue Engineering and Drug Therapy. Curr Pharm Des.;23(26):3786-3793.*

[68] *Jeevanandam J., et al., (2018). Review on nanoparticles and nanostructured materials: history, sources, toxicity and regulations. Beilstein J Nanotechnol, 9: 1050–1074.*

[69] *Nayak L., (2019). A review on inkjet printing of nanoparticle inks for flexible electronics. J. Mater. Chem. C, 7, 8771-8795*

[70] *Wanasinghe, D., (2020). Review of Polymer Composites with Diverse Nanofillers for Electromagnetic Interference Shielding. Nanomaterials, 10, 541.*

Mejora estructural y física de polímeros y materiales compuestos	Nanoarcillas, nanoóxidos y nanohidróxidos de metals. Montmorillonita modificada orgánicamente, TiO_2, Y_2O_3 o SiO_2.
UTENSILIOS DE CONSUMO[71]	
Barrera de embalaje utilizando silicatos *Vidrio autolimpiable*	Nanoarcillas, en particular bentonita y kaolinita TiO_2
MEDIO AMBIENTE[72]	
Tratamientos de agua (foto-catalisis)	Cerámicas óxidos metálicos, TiO_2
ELECTRÓNICA[73,74]	
Nanoescala partículas magnéticas para la alta densidad de almacenamiento de datos *Circuitos electrónicos* *Ferro-líquido (utilizando materiales magnéticos)* *Optoelectrónica dispositivos tales como interruptores (por ejemplo, usando las tierras raras dopadas cerámica)* *Química mecánica planarización – CMP*	Fe solo o en combinación con otros metales (o no metales), CoPt o FePt Plata, cobre y nanopartículas de Aluminio Fe (posiblemente recubiertas con una capa de carbono), Co, FeCo y Fe_3O_4 Gd_2O_3 o Y_2O_3 dopados con Eu, Tb, Er, Ce Alúmina, sílice y cerio

Tabla resumen que relaciona el tipo de nanopartícula con principal aplicación

La motivación detrás de la preparación de materiales nanocompuestos es la de conseguir la mayor mejora posible de propiedades introduciendo la menor cantidad posible de carga. Para maximizar la interacción entre ambos componentes, habitualmente se aplican estrategias de funcionalización de las nanopartículas con el objeto de obtener una máxima transferencia de propiedades eléctricas, mecánicas, térmicas… de la carga a la matriz. Dichas estrategias mejoran

[71] *Emamhadi, M. et al. (2020). Nanomaterials for food packaging applications: A systematic review. Food and Chemical Toxicology, 146, 111825.*

[72] *Taghipour S. et al. (2019). Engineering nanomaterials for water and wastewater treatment: review of classifications, properties and applications. New J. Chem., 43, 7902-7927.*

[73] *Shrivas K., et al. (2020). Advances in flexible electronics and electrochemical sensors using conducting nanomaterials: A review. Microchemical Journal, 156, 104944.*

[74] *Cardoso, C.E.D. et al. (2019). Recovery of Rare Earth Elements by Carbon-Based Nanomaterials—A Review. Nanomaterials, 9, 814.*

la compatibilidad entre ambos componentes, ayudan a obtener una mayor dispersión del nanomaterial y homogeneidad del compuesto.

En función de cómo es esa interacción, la **funcionalización** puede clasificarse como **covalente** o **no covalente**. Existen multitud de reacciones químicas para obtener funcionalizaciones de ambos tipos[75-79]: intercambio de ligando, introducción de grupos funcionales, formación de micelas, encapsulación, envoltura mediante polímeros anfifílicos, modificación química del surfactante…

En el primer caso se aumenta la afinidad del nanoaditivo por la matriz mediante la introducción de grupos funcionales en la estructura del nanoaditivo. Esta introducción de defectos estructurales causa una merma en las propiedades eléctricas, mecánicas, térmicas, etc. Por esta razón, el grado de funcionalización covalente constituye un compromiso entre la mejora del procesado, dispersión y la pérdida de propiedades intrínsecas del aditivo. Sin embargo es una funcionalización robusta y que evita problemas de agregación. En el segundo caso se necesita una especie que actúe de intermediaria estableciendo interacciones por una parte sobre la superficie del nanoaditivo y por otra parte con las moléculas de la matriz, de manera que no se altera la estructura del nanoaditivo. Sin embargo, el débil carácter de las interacciones no covalentes pueden desestabilizarse fácilmente, por cambios en la concentración, fuerza iónica o temperatura, rompiendo estas interacciones y provocando la agregación de las nanopartículas.

[75] *Subbiah, R., et al., (2010). Nanoparticles: Functionalization and Multifunctional Applications in Biomedical Sciences. Current Medicinal Chemistry, 17(36), 4559–4577*

[76] *Amina, S.J., et al., (2020). A Review on the Synthesis and Functionalization of Gold Nanoparticles as a Drug Delivery Vehicle. International Journal of Nanomedicine, 15, 9823—9857*

[77] *Xuqiang Ji, et al., (2016). Review of functionalization, structure and properties of graphene/polymer composite fibers. Composites Part A: Applied Science and Manufacturing 87, 29-45*

[78] *Guo F., et al., (2018). A Review of the Synthesis and Applications of Polymer–Nanoclay Composites. Applied Science, 8, 1696*

[79] *BY R. A. et al., (2010). Surface modification, functionalization and bioconjugation of colloidal inorganic nanoparticles. Phil. Trans. R. Soc. A 368, 1333–1383*

En el marco de la tesis se ha preseleccionado el uso de dos nanoarcillas. A continuación, se presenta una breve descripción para información del lector. Se puede encontrar más detalle en el ARTICULO 1[45] y en literatura[80-82]

Sepiolita

La sepiolita pertenece a los silicatos del grupo de las cloritas. Es un silicato hidratado de magnesio. Está formada por bloques estructurales tipo "*Sandwich*" y compuesta por enlaces tetraédricos de Silicio en las capas más externas y una capa central de enlaces octaédricos que contienen el Magnesio. Se estructura en forma de agujas o cintas con canales interiores llamados túneles zeolíticos que ofrecen microporosidad y una gran superficie específica (red capilar). Las dimensiones de las agujas varían entre las 0.2-4 µm de largo, 10-30 nm de ancho y 5-10 nm de grueso.

Debido a su morfología natural, se considera un buen agente de refuerzo además de presentar una destacada capacidad de sorción (absorción y adsorción). Es la arcilla que más área superficial tiene de entre las arcillas minerales conocidas. Además, existe literatura que demuestra que su funcionalización superficial también ayuda a mejorar la transferencia de propiedades a la matriz polimérica[83]. La arcilla original usualmente contiene cationes inorgánicos hidratados (por ejemplo: Na^+, K^+, Ca_2^+). Cuando los cationes inorgánicos son intercambiados por cationes orgánicos, e.g. surfactantes, la superficie de la arcilla cambia de hidrofílica a hidrofóbica u organofílica. Dichos cationes bajan la energía superficial y disminuyen la energía cohesiva facilitando así la intercalación del polímero. Además, pueden contener grupos funcionales que reaccionan con el polímero para mejorar la adhesión interfacial entre ambos.

En la presente tesis se utilizan dos sepiolitas para el desarrollo experimental:

---

[80] *Wang, S.; et al., (2005).Characteristics and biodegradation properties of poly(3-hydroxybutyrate-co-3-hydroxyvalerate)/organophilic montmorillonite (PHBV/OMMT) nanocomposite. Polym. Degrad. Stab., 87, 69–76*

[81] *Peinado, V. et al., (2014). Novel lightweight foamed poly(lactic acid) reinforced with different loadings of functionalised sepiolite. Compos. Sci. Technol., 101, 17–23*

[82] *Khandal, D., et al., (2016). Elaboration and behavior of poly(3-hydroxybutyrate-co-4-hydroxybutyrate)- nano-biocomposites based on montmorillonite or sepiolite nanoclays. Eur. Polym. J., 81, 64–76*

[83] *Falco, G., et al., (2019). Self-organization of sepiolite fibbers in a biobased thermoset. Compos. Sci. Technol., 171, 226–233*

- *T1: Sepiolita modificada orgánicamente mediante grupos aminosilanos en la superficie;*
- *T2: Sepiolita natural sin modificaciones en su superficie (contiene naturalmente grupos silanol, comercializada como Pangel 9);*

Montmorillonita

La montmorillonita pertenece al grupo de las esmectitas, dentro de las pirofilitas. Consiste en capas formadas por una hoja de alúmina octaédrica entre dos hojas de sílice tetraédrica. Se utiliza principalmente por sus propiedades de hinchamiento (relacionado con las propiedades reológicas) y adsorción[84]. Las capas de aluminosilicato ~ 1 nm de espesor con cationes metálicos se apilan en capas de unas 10 µm. Estas capas tienen una alta relación de aspecto por lo que una baja carga de nanoarcilla altera dramáticamente las propiedades de un polímero.
En la presente tesis se utiliza una montmorillonita para el desarrollo experimental:

- *T3: Montmorillonita sódica natural (Na-MMT) modificada con una sal de amonio cuaternario es una organoarcilla aniónica (altamente compatible con polímeros no polares).*

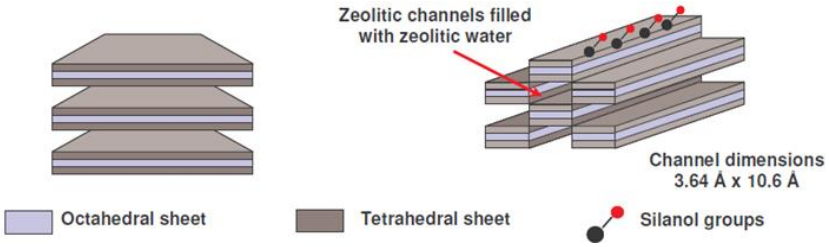

Figura 19: Estructura de la Montmorillonita (capas octaédricas) y la Sepiolita (tipo aguja)[85]

[84] *Zheng,Y., et al., (2018). Mechanical behavior in hydrated Na-montmorillonite clay.Phys.A,505,582–590*
[85] *Franchini E. (2008). Structuration of Nano-Objects in Epoxy-based Polymer Systems: Nanoparticles & Nanoclusters for improved fire retardant properties. Institut National des Sciences Appliquées de Lyon, Lyon, PhD Thesis.*

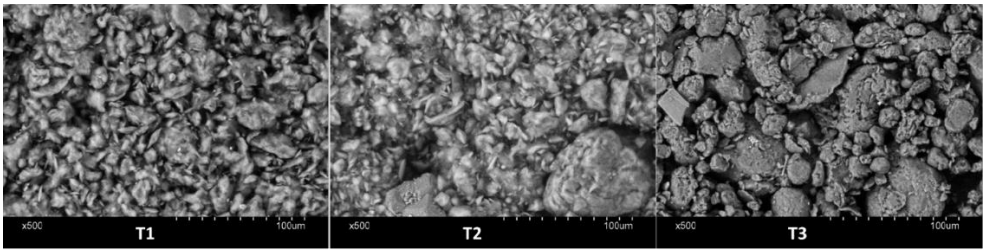

Figura 20: Micrografías SEM de las Nanoarcillas utilizadas en la tesis: T1 – Sepiolita modificada con grupos aminosilano; T2 – Sepiolita, T3 - Montmorillonita

Otro tipo de nanopartículas utilizadas en el marco de la presente tesis (ARTICULO 3[86]) para mejorar la dureza del material fueron las nanopartículas de zircona (ZrO_2).

Dióxido de circonio (ZrO_2) o circona

Es una cerámica cuyas propiedades mecánicas son muy similares a las de los metales (de hecho se le denomina como "acero cerámico"[87]). Los cristales de circonio pueden organizarse en tres patrones diferentes: monoclínico (que se encuentra a temperatura ambiente, bajo presión ambiental y al calentarse hasta 1170^{o}C), tetragonal (entre 1170^{o}C y 2370^{o}C) y cúbico (por encima de 2370^{o}C y hasta el punto de fusión)[88].

Su color blanquecino natural y su excelente estabilidad dimensional, así como sus propiedades mecánicas y químicas, han hecho de la circonia un material cerámico muy atractivo en aplicaciones médicas[89] como la sustitución de la cabeza femoral en prótesis en lugar titanio o alúmina y, en particular, para la prostodoncia[90] (donde suele alearse con el óxido de Itrio Y_2O_3). La circonia también se ha utilizado para

[86] *G. Quiles, L. et al. (2021). Color Fixation Strategies on Sustainable Poly-Butylene Succinate Using Biobased Itaconic Acid. Polymers, 13, 79*

[87] *Garvie, R.C.; et al., (1975). Ceramic steel? Nature, 258, 703*

[88] *Manicone, P.et al., (2007). An overview of zirconia ceramics: Basic properties and clinical applications. J. Dent., 35, 819–826.*

[89] *Rahaman, M.N. et al (2008). Functionally graded bioactive glass coating on magnesia partially stabilized zirconia (Mg-PSZ) for enhanced biocompatibility. J. Mater. Sci. Mater. Med. 19, 2325–2333.*

[90] *Kim, D.J. et al (2000). Mechanical properties, phase stability, and biocompatibility of (Y, Nb)-TZP/Al(2)O(3) composite abutments for dental implant. J. Biomed. Mater. Res., 53, 438–443.*

producir revestimientos duros para superficies de plástico con propiedades antiniebla, antihumectantes y antiestáticas[91].

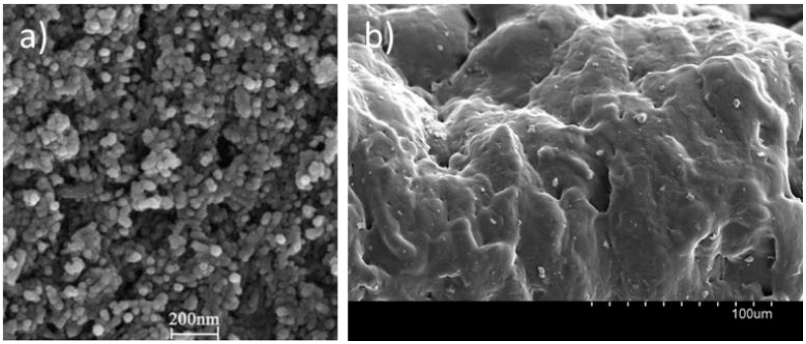

Figura 21: Micrografías SEM: a) nanopartículas ZrO_2 muestra su forma esférica. Fuente Ali Majedi et al[92]; b) nanopartículas ZrO_2 dispersas en bioPBS.

[91] Chang, C.-C. et al (2015). Preparation of zirconia loaded poly(acrylate) antistatic hard coatings on PMMA substrates. J. Appl. Polym. Sci., 132, 42411.

[92] Majedi, A. et al (2016). Green synthesis of zirconia nanoparticles using the modified Pechini method and characterization of its optical and electrical properties. J Sol-Gel Sci Technol 77, 542–552.

Modificación de polímeros mediante anclaje utilizando ácido orgánicos

Un ácido orgánico es un ácido carboxílico que incluye un ácido graso de fórmula R-COOH con propiedades ácidas. Los ácidos orgánicos se denominan alifáticos, si R es una cadena lineal de carbonos y aromáticos si R es un anillo de carbonos. También se denominarán "di, "tri", etc... "policarboxílicos", si contienen más de un grupo carboxilo. Son sustancias polares, que pueden formar puentes de hidrógeno entre sí o con las moléculas de otra especie.

En los apartados anteriores se han descrito brevemente las propiedades y usos principales del PHA y el bioPBS. Estos polímeros se constituyen a partir de ácidos orgánicos como son los ácidos carboxílicos. Estos ácidos actúan como "building-blocks" o moléculas precursoras que una vez combinadas y polimerizadas dan lugar diferentes biopolímeros que pueden constituir una matriz polimérica pero también pueden dar lugar a distintos aditivos como por ejemplo plastificantes.

Durante la tesis se ha considerado el uso de otros **ácidos orgánicos** para que actúen como tercer agente en mezclas complejas (injertos en blendas ternarias y cuaternarias) **entre la matriz y el aditivo principal con el fin de favorecer la afinidad entre ambos**. En particular se eligió el ácido itacónico como potencial agente fijador de color (pigmento diazo rojo) en el bioPBS. A continuación se describen brevemente sus principales características por las que se considera un elemento tan versátil en la industria química:

El **ácido itacónico** (IA) es un monómero que se usa como precursor de varios polímeros[93,94] y se obtiene o bien mediante la conversión térmica del ácido cítrico o bien como producto de fermentación del hongo *Aspergillus terreus* en presencia de materia con contenido en carbohidratos (patata, jatrofa, maíz…)[95]. También hay

[93] *Van Beilen JB, et al., (2008). Production of renewable polymers from crop plants. Plant J;54:684-701.*
[94] *Marvel CS, et al.,(1959). Polymerization reactions of itaconic acid and some of its derivatives. J Org Chem;24:599-605*
[95] *Mralidharao D., et al., (2007). Fermentatative production of itaconic acid by aspergillus terreus using Jatropha seed cake. Afr J Biotechnol;18:2140-2*

levaduras que lo producen como la familia de las *Ustilaginaceae*[96]. Es un ácido dicarboxílico ramificado y diprótico no saturado. La presencia del **doble enlace le aporta características químicas activas**, como por ejemplo polimerizar. Es soluble en agua, etanol y otros disolventes[97].

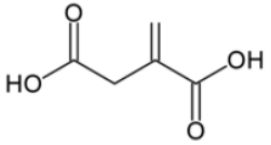

Figura 22: molécula elemental de IA

El IA biobasado tiene gran potencial para reemplazar a otros monómeros derivados del petróleo; en particular, alternativas al ácido poli(meta)acrílico[98]. Por lo tanto, el campo de productos y aplicaciones es amplio, como por ejemplo, el látex sintético, el caucho de estireno-butadieno, los polímeros superabsorbentes o las resinas de poliéster insaturadas[99]. Además, se considera uno de los principales precursores de las incipientes biopoliamidas[100], polímeros técnicos que están marcando fuertemente el crecimiento del IA en los próximos años (se espera que el mercado del IA alcance los 127,04 millones de dólares en 2027, con una tasa de crecimiento del 4,20%)[101].

El monopolímero de IA es muy transparente y se usa por ejemplo en aplicaciones para obtener gemas artificiales y lentes. En mezclas con otros elementos, aporta la capacidad de teñirse fácilmente y por eso se usa en compuestos con resinas para

---

[96] *Krull, S., et al., (2020). Ustilago Rabenhorstiana—An Alternative Natural Itaconic Acid Producer. Fermentation, 6(1), 4*

[97] *Asif Ali, M., et al., (2014) Syntheses of rigid-rod but degradable biopolyamides from itaconic acid with aromatic diamines. Polymer Degradation and Stability 109 367-372*

[98] *Magalhaes, A.I.; et al., (2017). Downstream process development in biotechnological itaconic acid manufacturing. Appl. Microbiol. Biotechnol., 101, 1–12.*

[99] *Robert, T.; et al., (2016). Itaconic acid—A versatile building block for renewable polyesters with enhanced functionality. Green Chem., 18, 2922–2934.*

[100] *Blazeck, J., et al., (2015). Metabolic engineeringof Yarrowialipolytica for itaconic acid production. Metabolic Engineering, 32, 66–73*

[101] *Global Itaconic Acid Market – Industry Trends and Forecast to 2027. https://www.databridgemarketresearch.com/reports/global-itaconic-acid-market*

pinturas así como en recubrimientos de fibras sintéticas (**impregna muy bien la coloración**). Asimismo aporta impermeabilidad y presenta capacidad anticorrosiva. Además, el ácido itacónico es un excelente agente excelente tanto para reticular como para funcionalizar biopolímeros y otros aditivos o refuerzos (e.g. agente liberador de fármacos[102], metales[103], nanopartículas…[104,105]).

[102] *Callesa, J.A., et al., (2013). Novel bioadhesive hyaluronan–itaconic acid crosslinked films forocular therapy. International Journal of Pharmaceutics 455, 48– 56*

[103] *Klement, T., et al., (2013). Review Itaconic acid – A biotechnological process in change. Bioresource Technology 135, 422–431*

[104] *Eyiler, E., et al., (2014). Magnetic iron oxide nanoparticles grafted with poly(itaconic acid)-block-poly(N-isopropylacrylamide). Colloids and Surfaces A: Physicochemical and Engineering Aspects, 444, 5, 321-325*

[105] *Pourjavadi, A., et al., (2016). Mesoporous silica nanoparticles with bilayer coating of poly(acrylic acid-co-itaconic acid) and human serum albumin (HSA): A pH-sensitive carrier for gemcitabine delivery. Materials Science and Engineering: C, 61, 1, 782-790*

APORTACIONES ORIGINALES / INNOVACIONES TÉCNICO-CIENTÍFICAS

Las aportaciones originales de los trabajos que conforman la tesis son:

- **Desarrollo de biocompuestos termoplásticos basados en bioPBS con aditivos cromóforos** (colorante) **y auxócromos** (auxiliares en fijación de color) mediante extrusión-compounding. Se ha demostrado que tanto los pigmentos como el uso de ácidos orgánicos reblandecen la matriz polimérica, asesorando en la cantidad aproximada de incorporación en la mezcla y que es necesario utilizar un tercer componente que refuerce las propiedades mecánicas y la dureza superficial, siendo el ZrO_2 un buen candidato para tal propósito (preferentemente a cargas bajas del 2wt%).
- **Desarrollo de biocompuestos termoplásticos mediante extrusión-compounding en base PHA con nanoarcillas** (sepiolitas y montmorillonitas) capaces de actuar con una **doble funcionalidad** como es la **captación de volátiles** mitigando olores desagradables así como actuando como **agente reforzante** en matriz. Se ha validado una correlación entre la tipológica de los volátiles encontrados, la causa de los mismos, así como la nanoarcilla más adecuada para su captura y se ha demostrado que la polaridad de la nanoarcilla afecta directamente a la afinidad por el polímero, su adecuada dispersión y la calidad de entrefase creada.
- Se ha desarrollado una **metodología para caracterizar en detalle biopolímeros comerciales** que parten de formulaciones complejas no detalladas en las hojas de características de los materiales y que resulta imprescindible conocer desde el punto de vista del desarrollador de granzas (punto de vista industrial) dado que pueden interferir en el propósito final.
- **Validar el efecto de distintas estrategias de compatibilización**: desde la **modificación del material** mediante la funcionalización superficial de los aditivos (nanoarcillas organomodificadas) **hasta la modificación de procesos industriales** como es la extrusión reactiva (REX) que genera injertos y entrecruzamiento entre polímeros originalmente inmiscibles. Por un lado, mediante la necesidad de mejorar la compatibilidad entre el ácido orgánico (itacónico en este caso) y el bioPBS.

- Se ha demostrado cómo es posible **adaptar una máquina de extrusión** con doble husillo convencional para producir mediante **REX** en aplicaciones con biopolímeros y que el proceso de **extrusión reactiva con los biopolímeros** utilizados afecta al color de la mezcla como resultado de la reacción en el husillo. Aunque es útil para mejorar otras propiedades ingenieriles como la estabilidad térmica y mejoras en propiedades mecánicas del material, **no resulta a priori el método más adecuado para propiedades enfocadas a la fijación o mejora de un color**.
- Se ha desarrollado y validado una **metodología útil para la identificación y cuantificación de volátiles** causantes del enranciamiento oxidativo en PHAs así como una propuesta para mitigar dicho efecto basada en los biocompuestos con nanoarcillas previamente mencionados.

BLOQUE 2

SOLUCIÓN: TECNOLOGÍAS DE PROCESADO DE MEZCLAS

CARACTERIZACIÓN DE LAS MUESTRAS

SOLUCIÓN: TECNOLOGÍAS DE PROCESADO DE MEZCLAS

El objetivo final del diseño y desarrollo de nuevos materiales es el de obtener o bien materiales sustitutos o bien mejorar las propiedades de los existentes para satisfacer los requisitos de aplicaciones específicas. Los procesos de *extrusión-compounding* y extrusión reactiva (REX) permiten realizar mezclas en masa para obtener compuestos poliméricos ad-hoc.

PROCESO DE EXTRUSIÓN - COMPOUNDING

Es un proceso termomecánico, de fusión y mezclado a alta temperatura. Se basa en la acción de uno o dos husillos que giran en una camisa cilíndrica hermética dotada de control de temperatura. La aplicación de una temperatura base (que garantice el fundido del polímero) acompañada de las fuerzas de cizalla generadas al hacer girar el plástico fundido entre el husillo y el cilindro, resulta en una temperatura y presión elevadas a lo largo del extrusor que mediante su giro mezcla y empuja al fundido. La longitud del husillo tiene tres zonas principales: zona de alimentación, zona de compresión o transición y zona de dosificación. La mezcla fundida es empujada por una boquilla con un orificio de salida de sección circular. Se forma entonces un hilo o filamento que acto seguido se sumerge en un baño de agua a temperatura ambiente para que la mezcla se solidifique y enfríe. A continuación, el filamento pasa por una estación de secado y corte o granceado que lo trocea formando la granza o “pellets”.

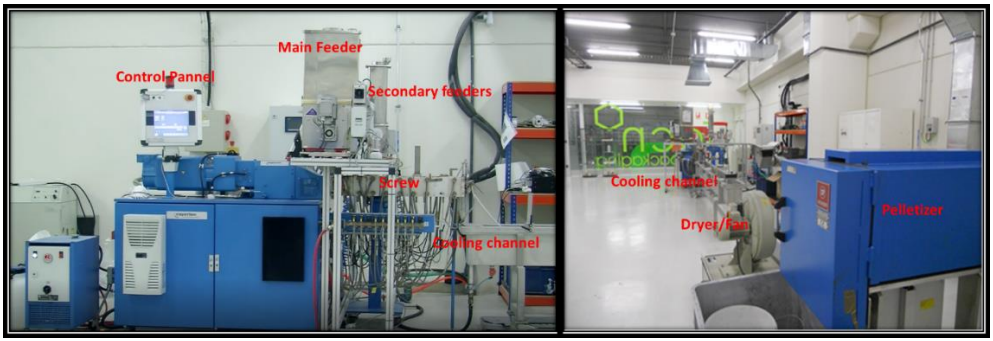

Figura 23: *Extrusora Coperion ZSK 26*

Para el desarrollo de las granzas en la presente tesis se utilizó una extrusora Coperion ZSK 26 de doble husillo con dos tolvas gravimétricas de alimentación. Mediante la regulación del flujo de entrada de cada material al husillo se controla la proporción de la mezcla. El polímero matriz se incorpora por la tolva de alimentación principal y éste es fundido en el husillo donde se mezcla con el aditivo que normalmente se introduce en forma de polvo por la tolva secundaria. El doble husillo está formado por dos tornillos que giran en el mismo sentidos de manera co-rotante para garantizar que la mezcla sea lo más homogénea posible.

El perfil del husillo es modular, y está compuesto por secciones más cortas que permiten adaptar dicho perfil de extrusión a las características del polímero con el que se va a trabajar. De esta manera se puede controlar la cizalla y el volumen libre generados, logrando una mezcla óptima y evitando cualquier degradación indeseada en el material. Esto se consigue modificando el paso de la rosca del husillo así como la forma o dibujo de la misma.

Figura 24: Ejemplos de módulos de husillo

Para el desarrollo de las formulaciones diseñadas en la presente tesis, se realizaron mezclas en masa para obtener granzas mediante este proceso (ver ARTICULOS 1[45],2[55] y 3[86]).

En la línea de fijación del color, tras cuatro semanas de haber desarrollado los materiales y obtenido las probetas para su caracterización, se observaron ciertos problemas de migración del IA. Ante la necesidad de mejorar la integración del mismo en las mezclas se modificó el proceso convencional de extrusión-*compounding* para abordar el problema de compatibilidad mediante un proceso de extrusión reactiva (REX).

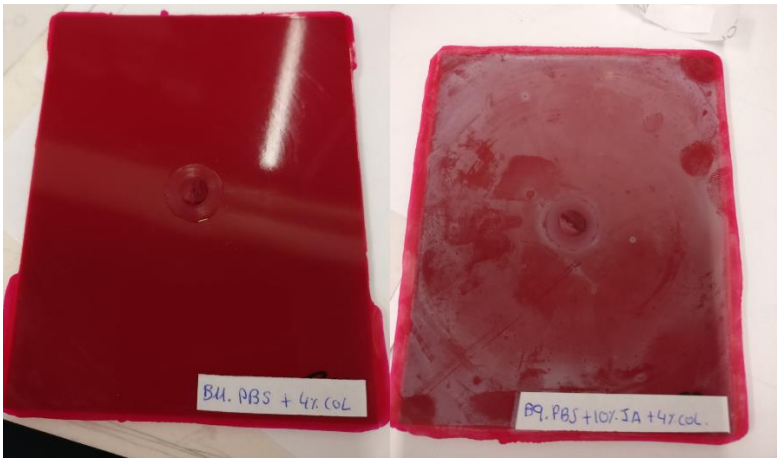

Figura 25: Ejemplo de envejecimiento de muestras de bioPBS con colorante y con y sin IA a las cuatro semanas.

PROCESO DE EXTRUSIÓN REACTIVA

En la extrusión reactiva (REX) se producen reacciones químicas en el husillo de la extrusora y por tanto se consiguen materiales con aditivos mejor integrados. Uno de los objetivos más comunes de la REX es la compatibilización de materiales poliméricos heterogéneos. El proceso implica la formación in situ de enlaces covalente de las distintas fases en estado fundido. Los métodos de compatibilización reactiva normalmente se llevan a cabo mediante oxidación, esterificación o eterificación. Dependiendo de la estructura química de los reactivos y los productos resultantes se pueden diferenciar las reacciones de copolimerización por injerto (*grafting*), de acoplamiento (*coupling*) y de reticulación (*crosslinking*). El aspecto común de estos métodos es la formación in situ de un copolímero en bloque o de injerto, cuyos bloques respectivos son miscibles[4].

Esta técnica se ha utilizado para validar la integración del ácido itacónico (IA) en la matriz de bioPBS con colorante. Para ello, es necesario realizar una serie de modificaciones en la máquina de extrusión-*compounding* convirtiéndola en un reactor dinámico. Las extrusoras de doble husillo son adecuadas para llevar a cabo

un proceso de REX debido a su excelente control de la mezcla y un mayor control del tiempo de residencia del material en el husillo.

Para ello, se procedió a modificar la extrusora adecuando los elementos que conforman el perfil del husillo para obtener un paso más corto con una baja cizalla, permitiendo un alto tiempo de remanencia y algo más de volumen libre para permitir la reacción. También se incorporó una bomba de vacío para desgasificar los gases que se generan por la reacción en el husillo. Además, sobre la formulación original fue necesario incorporar un peróxido (peróxido de dicumilo) que actuase como iniciador de la reacción.

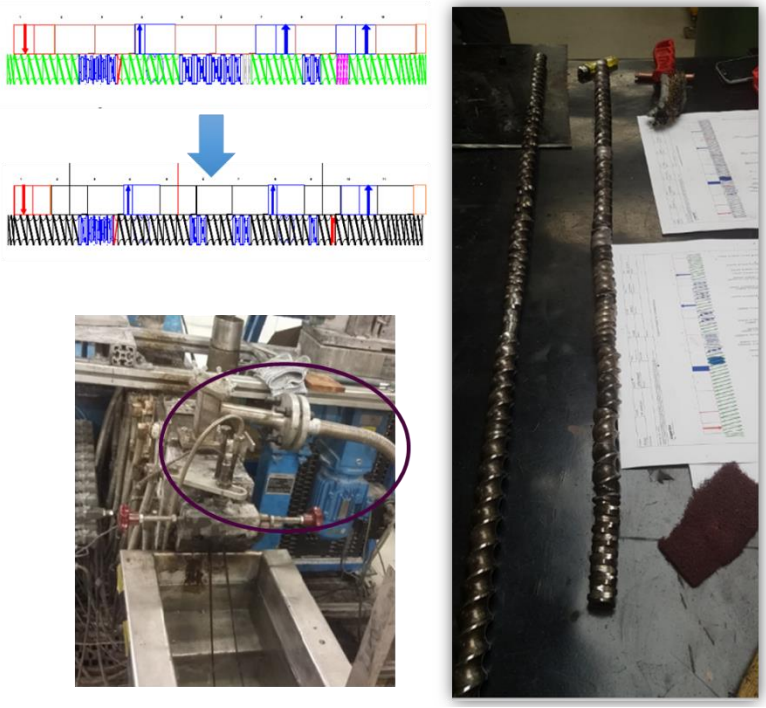

Figura 26: Cambio en el perfil del husillo para y acople de bomba de vacío para proceso REX

Como resultado de la reacción exotérmica producida se obtuvo un material que químicamente sí había mejorado la integración del ácido en la matriz pero que dio

como resultado un material con un color marrón oscuro (posiblemente debido a cierta degradación del material por un exceso de temperatura). Estos resultados relacionados con la extrusión reactiva, en principio no se han contemplado para publicación de artículo científico.

CARACTERIZACIÓN DE LAS MUESTRAS

PREPARACIÓN DE LAS MUESTRAS

Para la mayoría de las técnicas de caracterización basta con unos pocos gramos en formato “pellet” del material desarrollado: TGA, DSC, NMR, HS-SPME…

Figura 27: Ejemplo de granzas desarrolladas en la tesis (mezclas de PHAs con distintos porcentajes de T1)

Para el caso particular de los ensayos mecánicos, su posterior análisis estructural mediante SEM, así como XRD, dureza, ángulo de contacto y medición del color por espectrofotometría; fue necesario obtener probetas con la superficie adecuada para cada caso. Las probetas se obtuvieron mediante moldeo por inyección con las máquinas y parámetros que se describen en los ARTÍCULOS 1, 2 y 3 (JSW 85 EL II semi-industrial & Xplore microinyectora de laboratorio).

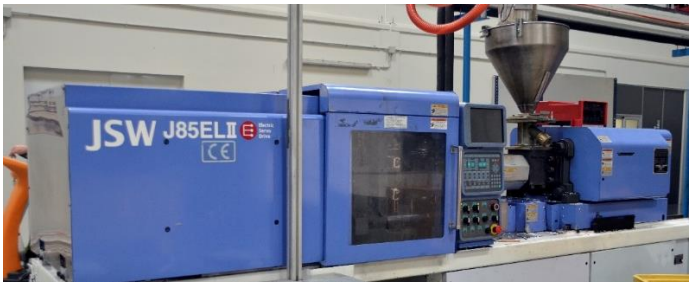

Figura 28: Ejemplo de Máquina Inyectora

En el proceso de inyección los pellets o la granza de material se introducen en la tolva de alimentación. Los pellets van cayendo hacia el interior de la cavidad del husillo. Dicha cavidad está rodeada de calentadores que proporcionan la temperatura idónea para cada sección de la unidad de inyección, fundiendo el material y permitiendo que el husillo empuje el material hacia la boquilla de inyección. Se utiliza además una presión de compactación para asegurar el llenado total de la cavidad del molde y evitar rechupes en las piezas. Los principales parámetros de proceso a controlar son: Temperatura del husillo, de la boquilla de expulsión y del molde (en caso de que necesite un enfriamiento controlado), velocidad de rotación del husillo, tiempo de llenado del molde, de enfriado y total del ciclo, presión de llenado y dosis o cantidad de polímero fundido inyectado.

A partir de la granza se inyectaron diferentes tipos de probetas:

- Probetas para ensayos mecánicos y XRD: tipo hueso de perro (para tracción) y rectangulares (para flexión y dureza superficial), siguiendo las dimensiones que se especifican en las normas ISO 178 and ISO 527 respectivamente.
- Probetas para ángulo de contacto, dureza y medición de color: discos circulares de 50 mm de diámetro y 2 mm de espesor.
- *Probetas rectangulares (80 mm x 100 mm x 2 mm). Se inyectaron inicialmente para testeo de color y dureza. También para usarlas como sustrato en un periodo inicial de la tesis para pruebas con recubrimientos (disolución de PBS y colorante) que se descartaron poco después para focalizar avances experimentales en la línea de PHA-olor. Sobre dichas probetas se observó el envejecimiento producido por la migración del IA. En relación a tests realizados sobre estas probetas no se han llegado a publicar resultados en papers, sí se han usado para un poster divulgativo en el congreso BIOPOL de 2019. (Ver Figura 24)*

INTRODUCCIÓN A LAS TÉCNICAS DE CARACTERIZACIÓN USADAS

Ensayos mecánicos: ensayo uniaxial de tracción y flexión por tres puntos:

Se utilizó una máquina de ensayos mecánicos universal: Zwick Roell Z 2.5 (Zwick, Germany). De las curvas tensión-deformación ensayadas se puede obtener información del módulo elástico, tensión de fluencia, tensión máxima, deformación y tenacidad o trabajo hasta fractura…

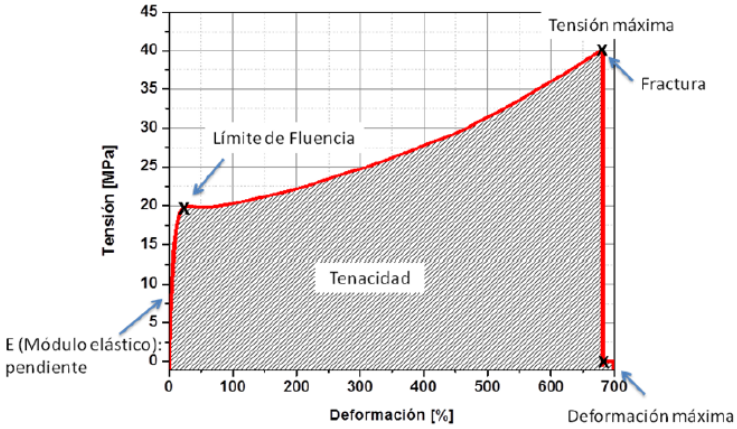

Figura 29: Curva estándar de un ensayo mecánico (ejemplo de curva con ensayo uniaxial de tracción)[106]

El módulo de Young o módulo de elasticidad longitudinal es una constante que caracteriza el comportamiento de un material elástico relacionando la tensión y la deformación según la tangente a la curva tensión-deformación en cada punto. La ley de Hooke gobierna el comportamiento elástico lineal del material durante la primera parte de la curva donde que los enlaces covalentes de los átomos de

[106] *García-Quiles L. (2013). Caracterización del ácido poliláctico (PLA) procesado por inyección y extrusión-compounding. estudio de la influencia de aditivos: espumante y nanoarcillas (Proyecto Fin de Carrera, Ingeniería Industrial, Mención en Materiales)*

carbono de la cadena principal del polímero sufren deformación elástica produciendo el alargamiento de los mismos y cuando la tensión se elimina la distorsión de la cadena desaparece. El esfuerzo es proporcional a la deformación unitaria y representa el grado de rigidez del material.

El límite de fluencia indica la tensión que soporta una probeta durante el ensayo de tracción en el momento de producirse el fenómeno de la fluencia, que consiste en una deformación brusca de la probeta sin incremento de la carga aplicada. Hasta el punto de fluencia el material se comporta elásticamente, siguiendo la ley de Hooke, y por tanto se puede definir el módulo de Young, previamente comentado. Este fenómeno tiene lugar por tanto en la zona de transición entre las deformaciones elástica y plástica. Superado este límite, si se retira la carga, el material sólo recupera la parte correspondiente a la deformación elástica permaneciendo la deformación plástica o permanente. La deformación plástica es consecuencia del deslizamiento de unas cadenas del polímero sobre otras rompiendo los enlaces débiles de Van der Waals. Al retirar el esfuerzo las cadenas permanecen en sus nuevas posiciones y de este modo el material se deforma de manera permanente.

La tensión a fractura es la máxima tensión que un material puede soportar previo a su rotura. Es una propiedad intensiva; por lo tanto, su valor no depende del tamaño de la probeta de ensayo. Sin embargo, depende de otros factores, tales como la preparación de la probeta, la presencia o no de defectos superficiales, y la temperatura del ambiente y del material al realizar el ensayo.

La elongación total es la deformación que sufre el material ante la tracción producida hasta la rotura de la probeta. Este incremento de longitud se expresa en porcentaje con respecto a la longitud inicial de la probeta.

La tenacidad o resistencia a tracción se define como la energía total absorbida que se corresponde con el área comprendida bajo la curva tensión-deformación hasta la rotura. Es por tanto el máximo esfuerzo que un material puede resistir antes de su rotura por estiramiento desde ambos extremos con temperatura y velocidad especificadas.

La elongación total y la tenacidad, se modifican cuando se introducen refuerzos en el material. Cualquier segregación de fases entre polímeros (e.g. PBS y el IA) o aglomerados de las nanoarcillas utilizadas (e.g. T1, T2, T3 y los PHAs, o ZrO_2 y PBS)

generan defectos en la muestra por los que falla el material durante el ensayo. Ambos comportamientos pueden verse en los artículos presentados.

Dureza (Metaltest – Rockwell)

El ensayo de dureza Rockwell mide la dureza del material ensayado mediante una medición de profundidad diferencial. El ensayo se realizó con un durómetro que determina la dureza del material comparando la profundidad de la identación creada por una precarga y una carga. Primero, se presiona el indentador sobre la superficie del material con una precarga y se mide la profundidad de la hendidura. A continuación, se baja el identador con una fuerza determinada durante un tiempo de permanencia específico y se suelta. La profundidad de la nueva hendidura se mide y se compara con la hendidura previa.

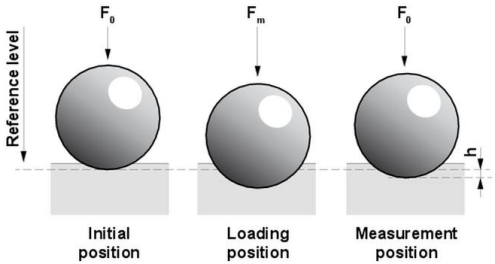

Figura 30: Ensayo de dureza Rockwell

Propiedades Estructurales: SEM Hitachi S3400N

La morfología del material estudiado fue examinada mediante microscopía por barrido electrónico (SEM). En el SEM, se barre la superficie de la muestra con un haz de electrones acelerados que viajan a través del cañón situado en la columna del microscopio. Un detector formado por lentes basadas en electroimanes mide la cantidad e intensidad de electrones que devuelve la muestra (principalmente electrones secundarios y retrodispersados), ofreciendo una imagen del barrido de la superficie de la misma.

El área examinada de cada probeta fue la superficie de rotura generada en los ensayos mecánicos. Al no ser el polímero un material conductor, fue necesario recubrir la zona de estudio con una capa de oro mediante la técnica de "sputtering".

Las muestras fueron observadas perpendicularmente a esta superficie, permitiendo estudiar la dispersión de los aditivos utilizados (nanoarcillas, ZrO_2,

colorante), así como variaciones en el comportamiento frágil-dúctil del material (en el que afectan tanto las cargas, carencia en la compatibilidad entre polímeros y fases, o incluso se pueden observar indirectamente modificaciones inducidas por parámetros de proceso como la temperatura). En relación a los aditivos, además de la dispersión, se puede observar su morfología, ver la formación de agregados o apilamiento y su tamaño, e incluso defectos en la entrefase entre la carga y el polímero.

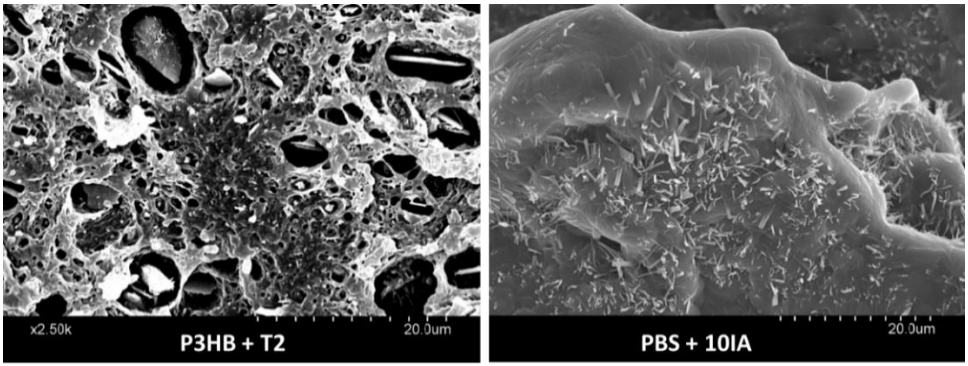

Figura 31: Ejemplo de micrografía obtenida por SEM. A la izquierda muestra de PHA con Sepiolita y a la derecha de PBS con cristales de IA.

Análisis termogravimétrico (TGA - Mettler-Toledo TGA/SDTA 851e)

El análisis termogravimétrico (TGA) es una técnica que se utiliza para caracterizar térmicamente al material. Se coloca un fragmento de la muestra de unos pocos gramos en una termobalanza y éste se monitoriza en función del tiempo y/o la temperatura en una atmósfera controlada. Es un método dinámico en el que se determina la variación de masa. El registro de estos cambios nos dará información sobre si la muestra se descompone (pérdida de masa) o reacciona con otros componentes (ganancia de masa).

Las curvas TGA primarias muestran la variación de masa (pérdida de masa) relacionada con la descomposición del polímero; por lo que permite predecir su estabilidad térmica a temperaturas muy altas. En general, las causas del cambio de

masa son debidas a: reacciones de descomposición, reacciones de oxidación, vaporización, sublimación y desorción.

En nuestro caso, podemos conocer la humedad o agua libre, el agua ligada o coordinada (estructural) y los elementos volátiles contenidos en la muestra (e.g. solventes) y descomposición multietapa de otros monómeros (como es el caso del PBA en la muestra de P3HB); así como los restos no orgánicos existentes.

Además, mediante su derivada con respecto al tiempo, se puede conocer la cinética de descomposición del material. Es lo que se conoce como curva secundaria o DTG.

La discusión en detalle de las curvas TGA tanto de los polímeros como de las nanoarcillas se puede encontrar en el ARTICULO 2[55].

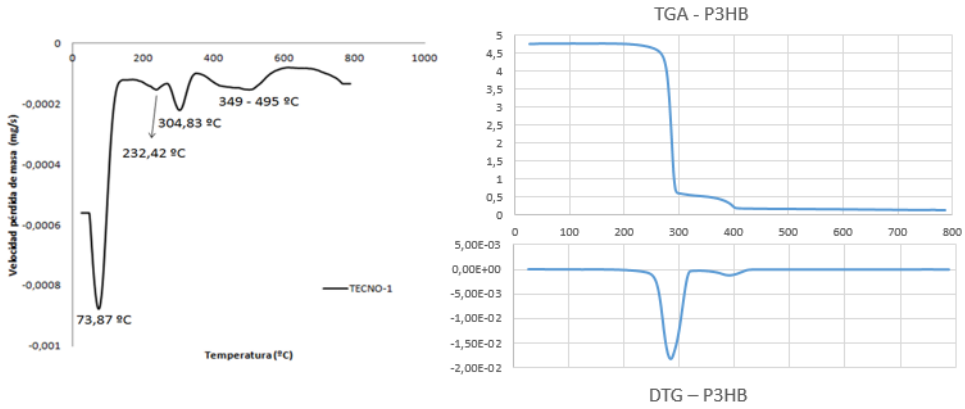

Figura 32: Ejemplos de DTG - T1 (Sepiolita modificada con organosilanos, se aprecia la desorción del disolvente y otros compuestos orgánicos) y TGA & DTG – P3HB donde se aprecia la degradación multietapa del P3HB y el PBA.

Calorimetría Diferencial de Barrido (DSC – Mettler Toledo 223E)

El DSC es una técnica cuantitativa, de alta sensibilidad, para detectar transiciones débiles y fenómenos térmicos que permite obtener información de la temperatura a la cual tiene lugar el cambio energético en estudio y del calor involucrado en el proceso: C_p, ΔH_m, ΔH_c (transiciones de primer y segundo orden). Se mide la

variación en el flujo de calor entre la muestra (unos pocos mg) y una referencia cuando dicha muestra se somete a un programa de temperatura en una atmósfera controlada.

Las señales de interés en las curvas DSC son aquellas que se desvían de la línea base, y ésta no siempre está bien establecida. Para definir y cuantificar un pico sobre una curva DSC, se ha de hacer respecto a una línea base calibrada.

Las muestras se calientan por encima del punto de fusión y se enfrían una primera vez para eliminar la historia térmica del material. Así, se restablecen las muestras bajo las mismas condiciones iniciales térmicas. El segundo calentamiento es el consideramos válido o fiable para la lectura de datos (desde un punto de vista industrial es más realista con las etapas y procesos realizados). Todas las curvas DSC comparadas en el ARTICULO 1[45] se corresponden con el segundo calentamiento.

Aplicado sobre polímeros y en particular sobre biopolímeros termoplásticos como los que se estudian en la presente tesis, permite conocer información térmica de interés como es la T_g (temperatura de transición vítrea), T_m (temperatura a la que funde el material – rango de fusión) y conocer información sobre la cristalización del material (X_c% en un polímero semicristalino y cualitativamente poder comparar entre muestras similares variaciones en el tamaño de los cristales).

- La temperatura de transición vítrea (T_g) es aquella para la cual un polímero amorfo vitrificado se vuelve en un estado gomoso, más flexible. Es esta transición no hay absorción o desprendimiento de calor, por lo que no da lugar a ningún cambio en la entalpía. Es lo que se conoce como transición de segundo orden. Sin embargo, sí que se produce un cambio en el calor específico del material C_p, consecuencia de cambios en los grados de libertad locales de las cadenas, provocándose un descenso de la línea base.

- Al aumentar la temperatura de un sólido amorfo por encima de su T_g, las cadenas moleculares se mueven hacia una nueva configuración estructural provocando un reagrupamiento que origina zonas cristalinas. Esta cristalización que tiene lugar desde el estado amorfo es la llamada cristalización fría (pico exotérmico en la curva DSC). El material no puede alcanzar un estado plenamente cristalino pues existe una importante

fracción de volumen entre las lamelas ocupada por segmentos amorfos. El área bajo este pico representa la ΔH_c entalpía de cristalización fría.

- El pico de la temperatura de fusión (T_m), endotérmico, corresponde a una fusión completa en materiales orgánicos y da información sobre el tamaño de los cristales formados. Si el material tiene una mayor temperatura de fusión indica que el tamaño o grosor de sus cristales es también mayor. A la energía que se requiere para producir la transición de fusión se le conoce como entalpía de fusión (ΔH_m) y da información sobre la cantidad de cristales que se forman, por lo tanto un aumento en la entalpía de fusión indicaría un mayor número de cristales formados. El grado de cristalinidad (X_c) se calcula comparando ΔH_m respecto de la variación de entalpía que corresponde con la fusión de un cristal puro (100% cristalino) del polímero estudiado (ΔH^o_m). Para el caso del PHB se ha tomado de la literatura ΔH^o_m = 146 J/g[107].

[107] *Kumar, S.; et al., (2010). Practical Guide to Microbial Polyhydroxyalkanoates. Chapter 6: Crystalline and Solid-State Structures of Polyhydroxyalkanoates (PHA); Smithers Rapra: Shrewsbury, UK; pp. 1–160. ISBN 1847351174*

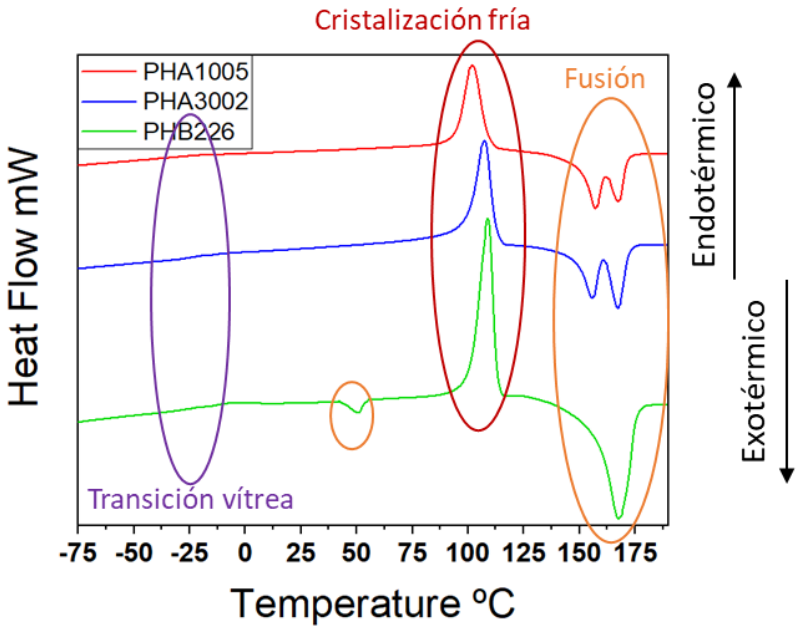

Figura 33: Ejemplo de curvas DSC (2º calentamiento) para las tres matrices de PHA utilizadas en la tesis. Se observan claramente los picos de cristalización fría así como los picos de fusión. La transición de T_g queda algo más difusa. Ver la discusión en detalle en ARTICULO 1[45].

Microextracción en fase sólida del espacio cabeza combinada con cromatografía de gases con trampa de iones y espectrometría de masas: HS-SPME – GC-IT/MS (Agilent 7890A acoplado a detector Agilent 5975 C)

La microextracción en fase sólida (HS-SPME) es un método rápido y sencillo para poder **extraer** compuestos químicos volátiles de una muestra, combinada además con el cromatógrafo de gases permite **identificar y cuantificar** un gran número de compuestos volátiles.

Las variables a ajustar son la cantidad de muestra, tiempo y temperatura de extracción. La fibra seleccionada para la sorción (captura de los volátiles y semivolátiles y posterior desorción en el puerto del cromatógrafo) fue DVB/CAR/PDMS. De este modo la fibra captura los volátiles en el espacio cabeza (cámara donde está situada la muestra) y los libera en el cromatógrafo, el cual los cuantifica y permite identificarlos mediante su comparación con librerías y patrones (para asegurar la fiabilidad y reproducibilidad del método).

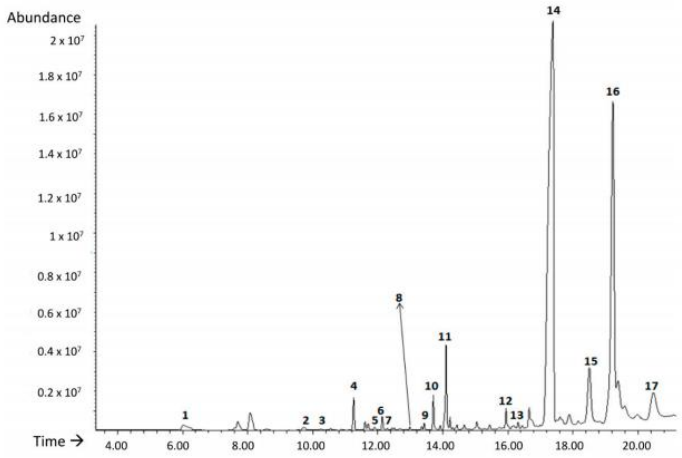

Figura 34: Ejemplo de cromatograma obtenido para PHB226 - (P3HB). Volátiles identificados: ***1**, 1-butanol; **2**, p-xylan; **3**, heptanal; **4**,α-methylstyrene; **5**, benzaldehyde; **6**, octanal; **7**, limonene; **8**, 1-hexanol; **9**, undecane; **10**, 1-octanol; **11**, nonanal; **12**, decanal; **13**, 1-chloro-decane; **14**, 1-decanol; **15**, tetradecane; **16**, biphenyl; **17**, 2,6-bis (1-methylethyl)-benzeneamide.*

Éstos pueden utilizarse como marcadores para determinar el grado de oxidación de los lípidos (técnica que se utiliza en la alimentación), puntualmente se ha utilizado para evaluar la degradación de polímeros convencionales y en la tesis se ha aplicado el método para tratar de identificar aquellos volátiles que son causantes del olor a rancio del PHA. La principal fuente de olores desagradables provocados por la oxidación de los lípidos son los hidroperóxidos, que son inestables y se descomponen fácilmente para formar aldehídos alifáticos, cetonas y alcoholes.

Del cromatograma se puede obtener el valor del área bajo la curva de los principales picos obtenidos (correspondientes a esos aldehídos, cetonas y alcoholes). Comparando la variación entre las áreas de las muestras con y sin nanoarcillas podemos cuantificar (% comparativo) la capacidad secuestrante de las nanoarcillas o el efecto que producen como atenuantes de dicho olor: si el pico obtenido en el cromatograma por una muestra con nanoarcilla para un determinado volátil es menor que para la muestra sin nanoarcilla bajo las mismas condiciones de ensayo, podemos deducir que los volátiles han sido capturados por la arcilla evitando su liberación al ambiente. El método, así como la discusión de resultados se puede encontrar detallado en el ARTICULO 2[55] aunque merece la pena destacar que los volátiles encontrados en mayor proporción son aquellos volátiles tipo alcohol con mayor peso molecular o con estructuras más complejas que contienen grupos aromáticos. Éstos, son más difíciles de extraer del PHA y de limpiar durante las etapas de purificación (menos accesibles a disolventes), y es por ello que podemos observarlos en cantidades mayores.

Difracción de Rayos X (WAX - XRD)

Esta técnica se basa en la difracción de las ondas. Es el resultado de la interacción de una radiación de rayos X con los átomos ordenados de los cristales. Cuando un haz de rayos X encuentra un obstáculo comparable con su longitud de onda (λ), se produce la difracción del haz. Se utilizan rayos X con una longitud de onda en torno a 1Å ya que es el orden de magnitud de las distancias interatómicas en los cristales, lo que posibilita la aparición de fenómenos de interferencia y de direcciones de difracción.

$$Ley\ de\ Bragg \rightarrow n\lambda = 2dsen\theta$$

Si la orientación de la radiación incidente y la distancia interplanar satisfacen la ley de Bragg el haz difracta y se obtiene una respuesta en el equipo que se traduce en un espectro con una serie de picos de intensidad apreciable cuando la interferencia entre los haces reflejados por un conjunto de planos separados una cierta distancia (d), es constructiva.

Esta técnica se utiliza para analizar estructuras de polímeros semicristalinos. Cada compuesto cristalino posee su propia distancia interplanar que origina una serie propia de ángulos de difracción de rayos X (θ) que permite su identificación de forma directa. El uso de rayos X permite identificar cambios en la estructura cristalina de las mezclas del material. Los patrones grabados con y sin aditivos muestran el carácter cristalino (pico estrecho y bien definido) u amorfo (pico ancho a modo de campana) del material, y si ha habido buena interacción entre el refuerzo y la matriz.

En la tesis esta tecnología se ha utilizado para ver los patrones cristalinos de los distintos PHAs, para los que se observaron dos polimorfismos (α y β) y preferencias en la ordenación de los cristales para los dos copolímeros (P3HB-co-P4HB) diferentes del P3HB. Además, se buscan desplazamientos de los picos a otros planos de difracción, que indican cambios en el empaquetamiento de las cadenas de los cristales poliméricos inducidos por la adición de refuerzos. También se pueden valorar cualitativamente diferencias en la interacción entre las nanoarcillas y el polímero matriz, observando si se mantienen los picos propios de las arcillas o se atenúan (indicando por ejemplo exfoliación en el caso de la Montmorillonita o desagregación de la Sepiolita).

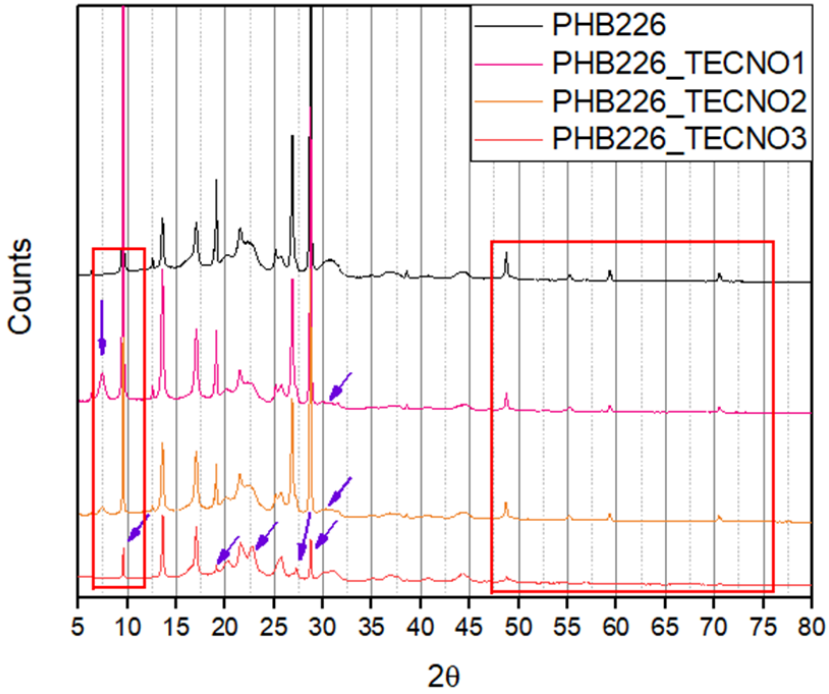

Figura 35: Ejemplo de difractograma para P3HB virgen y reforzado. Se marcan variaciones observadas en los patrones. Los resultados se discuten en el ARTICULO 1[45].

Resonancia Magnética Nuclear (1H - RMN) (Bruker Instrument)

La caracterización de polímeros por espectroscopia de resonancia magnética nuclear (RMN) proporciona información molecular detallada. Cualquier átomo con Número atómico o Masa atómica impar tiene spin nuclear y se puede analizar mediante un equipo de resonancia. Se pueden analizar diferentes núcleos, aunque los más utilizados en química orgánica son el (^{1}H) y el ^{13}C, principales componentes de las moléculas orgánicas. Permite estudiar propiedades físicas y químicas de muestras en estado cristalino o amorfo. La RMN permite determinar cómo y entre que átomos se realizan las interacciones, estudiando los desplazamientos que

sufren las señales de unos espectros con respecto a otros. Además, se puede determinar la estequiometria.

Una señal en RMN se caracteriza básicamente por tres propiedades:

1. Posición (desplazamiento químico, δ, ppm). Indica la cantidad de los diferentes tipos de protones presentes en la molécula.
2. Intensidad (integrales). Área bajo el pico es proporcional al número de átomos de hidrógeno que contribuyen a la señal.
3. Multiplicidad (patrón de desdoblamiento)-acoplamientos: podemos obtener información sobre los protones del entorno.

Las principales interacciones responsables del ensanchamiento de las señales son la anisotropía del desplazamiento químico, los acoplamientos dipolares (homo y heteronucleares) y el acoplamiento cuadrupolar.

Table 14.1 Approximate Values of Chemical Shifts for ^{1}H NMR[a]

Type of proton	Approximate chemical shift (ppm)	Type of proton	Approximate chemical shift (ppm)
$(CH_3)_4Si$	0		6.5–8
$-CH_3$	0.9		
$-CH_2-$	1.3		9.0–10
	1.4		2.5–4
	1.7		
			2.5–4
	2.1		
			3–4
	2.3		
			4–4.5
$-C\equiv C-H$	2.4		
$R-O-CH_3$	3.3	RNH_2	Variable, 1.5–4
	4.7	ROH	Variable, 2–5
		ArOH	Variable, 4–7
	5.3		Variable, 10–12
			Variable, 5–8

[a]The values are approximate because they are affected by neighboring substituents.

Table 14.2 Multiplicity of the Signal and Relative Intensities of the Peaks in the Signal

Number of equivalent protons causing splitting	Multiplicity of the signal	Relative peak intensities
0	singlet	1
1	doublet	1:1
2	triplet	1:2:1
3	quartet	1:3:3:1
4	quintet	1:4:6:4:1
5	sextet	1:5:10:10:5:1
6	septet	1:6:15:20:15:6:1

Figura 36: tablas para interpretar picos respecto del desplazamiento y acoplamientos[108]

[108] *https://www.ehu.eus/documents/1468013/5943652/RMN*

Se utilizaron pellets disueltos en cloroformo deuterado (cuya señal en ^{1}H es 7,26 ppm) y se filtraron las muestras para eliminar cualquier precipitado (como por ejemplo el talco). De este modo se evitan las señales de los protones del disolvente en los espectros de protón a estudiar (unas 10.000 veces intensas que las del producto). Disponer de la señal de deuterio permite corregir la inestabilidad del campo magnético y optimizar la homogeneidad.

En nuestro caso ha permitido por un lado cuantificar la estructura co-polimérica de los P3HB-co-P4HB (conociendo así el porcentaje de P4HB mediante la integración de las áreas bajo los picos propios) y también identificar aditivos orgánicos que llevan en nuestro caso las matrices comerciales de PHA y de las que desconocemos su formulación original como es el uso de pequeños porcentajes de otros biopoliésteres a modo de plastificantes (se identifica PBA).

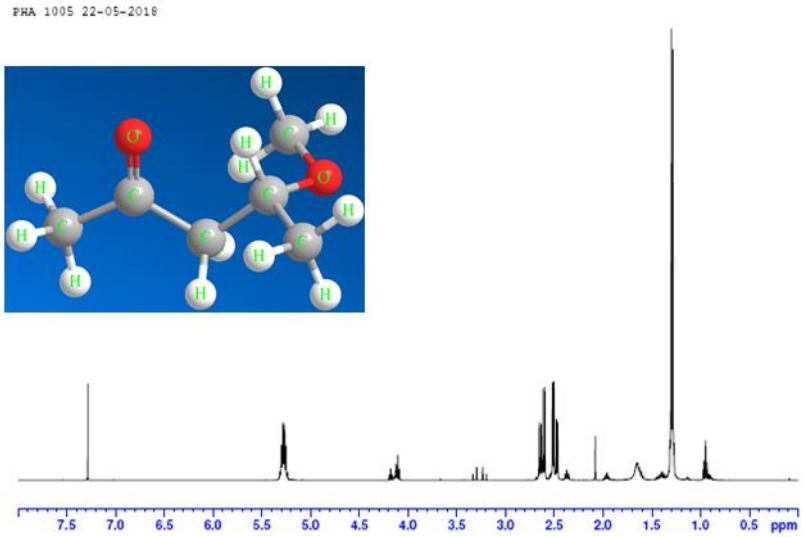

Figura 37: Ejemplo "en crudo" de espectro del PHA 1005 (P3HB-co-P4HB). Interpretación y resultados en ARTICULO 1[45].

Espectofotometría (CM-2300d Konica Minolta)

El espectrofotómetro es un instrumento que tiene la capacidad de proyectar un haz de luz monocromática a través de una muestra y medir la cantidad de luz que **es absorbida** por dicha muestra. El equipo utilizado en particular es adecuado para medir el color en muestras planas y mostrar un valor en una escala de color. El haz de luz se midió sobre las muestras inyectadas (opacas). El equipo permite ser usado como colorímetro y como brillómetro y muestra por tanto el porcentaje de luz que **se refleja** en una muestra coloreada.

Normalmente se recurre a la diferencia de color total (ΔE*) para la representación de los cambios de color, que es una distancia euclidiana. Es la longitud de la línea recta que une los dos puntos en un espacio tridimensional. Fue definido en 1976 por Hermann von Helmholtz y Ewald Hering y se conoce como el espacio de color CIELAB[109], también denominado L*a*b*, definido por la Comisión Internacional de Iluminación: $\Delta E^* = \sqrt{(\Delta L^*)^2 + (\Delta a^*)^2 + (\Delta b^*)^2}$

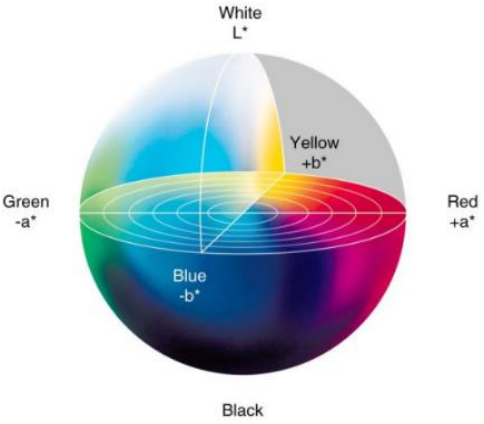

*Figura 38: El espacio de color CIE L*A*B*

Donde "*L*" mide la variación de negro a blanco, "*a*" de verde a rojo y "*b*" de azul a amarillo. Un objeto negro no refleja ninguna luz a través de todo el espectro (0% de reflexión), mientras que una superficie blanca ideal refleja casi toda la luz (100% de reflexión). Todos los demás colores reflejan la luz solamente en ciertas partes del espectro definiendo su propia curva espectral (dentro del espectro de luz visible

[109] *Backhaus, W., et al., (1999). Color Vision: Perspectives from Different Disciplines, Ethology, 105(2), 184–185*

UV-VIS). Además, en las muestras desarrolladas en el ARTICULO 3[86] se midió la variación en el brillo (G). El color se mide independientemente del brillo (G) y cambios en el brillo no implican variaciones en el tono del color. Lo que sí afecta al brillo de una muestra es la textura superficial que va a modificar la forma de reflejar la luz (más brillante cuanto más pulido y homogéneo o más mate al introducir imperfecciones y rugosidad). La discusión detallada de los resultados puede consultarse en el ARTICULO 3[86] de esta memoria.

Mojabilidad (propiedades superficiales) mediante ángulo de contacto

Se define el ángulo de contacto como el ángulo que forma la superficie de un líquido al entrar en contacto con la superficie de un sólido. La mojabilidad es la capacidad de un cuerpo sólido para formar una interfase con un líquido y viene determinada por el ángulo de contacto. El perfil que adopta la gota es el resultado del balance entre las fuerzas de la superficie y de la interfase, que tienden a minimizar la energía superficial libre del sistema. Según la afinidad del sistema el ángulo de contacto determinará si una superficie es hidrófila o hidrófoba (cuando se realicen las mediciones con agua como medio líquido, como es el caso de las mediciones realizadas en esta tesis, y siendo la superficie sólida muestras de los materiales desarrollados en base bioPBS). Si la superficie es hidrófila la gota se extiende sobre el mismo formando un ángulo entre 0 ^{o} y 30^{o}. Si la superficie del sólido es hidrófoba el ángulo de contacto será mayor que 90^{o}. En superficies muy hidrófobas el ángulo puede ser mayor a 150^{o} e incluso cercano a 180^{o}.

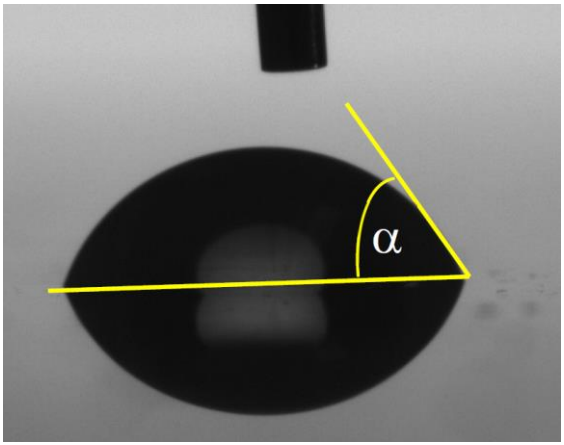

Figura 39: Ejemplo de medición del ángulo de contacto, gota de agua sobre muestra bioPBS.

BLOQUE 3

METODOLOGÍA

METODOLOGÍA

Con el objetivo de mejorar las propiedades estéticas de los biopolímeros para poder incrementar su uso en un mayor número de aplicaciones, se planteó la siguiente metodología adaptada a las matrices biopoliméricas de estudio. Primero fue necesario valorar la problemática en cuestión y separar las líneas en dos para poder abordarlas con mayor detalle. Por ello se decidió por un lado buscar una solución para mitigar el olor en PHAs y limitar las estrategias de fijación de color al bioPBS. Para la consecución del objetivo general, esta tesis aborda cuatro fases principales que son comunes para ambas líneas: 1) conceptualización y diseño de los materiales, 2) desarrollo físico de las formulaciones, 3) caracterización e interpretación de resultados y 4) discusión y comparación de los mismos con respecto a otros trabajos científico-técnicos respecto del estado del arte.

A su vez, dentro de cada línea, se pueden detallar en los siguientes pasos:

LÍNEA DE MITIGACIÓN DEL OLOR EN PHAs:

1. Evaluar el potencial del PHA como material alternativo a poliolefinas convencionales como el PP. Estudiar las propiedades del PHA. En particular de las matrices seleccionadas para desarrollar y validar las formulaciones a desarrollar (P3HB y P3HB-co-P4HB).
2. Revisar el estado del arte y estudiar las propiedades de las nanoarcillas (como agentes adsorbentes de volátiles) así como distintas funcionalizaciones que permitan modificar superficialmente su afinidad por los polímeros matriz.
3. Diseñar las formulaciones objetivo a estudiar: componentes finales de la mezcla y porcentaje en masa.
4. Optimizar el proceso de mezclado para introducir los aditivos seleccionados en las matrices objetivo mediante el proceso de extrusión-compounding: ventana de proceso, particularidades de cada aditivo y pre-tratamientos como secado o molienda, selección de tolva de entrada según características del aditivo y necesidades de mezclado (a inicio de husillo o a mitad de husillo), orden en el mezclado en función del nº de extrusiones etc.

5. Desarrollar formulaciones de matriz + aditivo utilizando distintas concentraciones para evaluar saturación y buscar una síntesis o formulación óptima.
6. Obtener probetas por moldeo por inyección para completar los sustratos necesarios junto con la granza para su posterior caracterización.
7. Caracterización de las formulaciones desarrolladas del material con una particular evaluación de propiedades estéticas.
8. Lectura e interpretación de resultados.
9. Explorar la utilidad de las formulaciones desarrolladas en mercados dominados por el PP según los resultados obtenidos. Comparativa con estado del arte, selección del mejor candidato y/o propuestas de mejora (tanto en la formulación como en el proceso).

LÍNEA DE FIJACIÓN DEL COLOR EN bioPBS:

1. Evaluar el potencial del bioPBS como material alternativo a poliolefinas convencionales como el PP. Estudiar las propiedades del bioPBS.
2. Revisar el estado del arte en cuanto a ácidos orgánicos y sus usos en biopolímeros. Seleccionar y estudiar las propiedades del ácido itacónico como agente para mejorar propiedades estéticas en la fijación de color.
3. Estudiar aditivos complementarios que puedan balancear la merma de propiedades producida por los ácidos orgánicos.
4. Diseñar las formulaciones objetivo a estudiar: componentes finales de la mezcla y porcentaje en masa.
5. Optimizar el proceso de mezclado para introducir los aditivos seleccionados en las matrices objetivo mediante el proceso de extrusión-compounding: ventana de proceso, particularidades de cada aditivo y pre-tratamientos como secado o molienda, selección de tolva de entrada según características del aditivo y necesidades de mezclado (a inicio de husillo o a mitad de husillo), orden en el mezclado en función del nº de extrusiones etc.
6. Desarrollar formulaciones de matriz + aditivo utilizando distintas concentraciones para evaluar saturación y buscar una síntesis o formulación óptima.
7. Obtener probetas por moldeo por inyección para completar los sustratos necesarios junto con la granza para su posterior caracterización.

8. Caracterización de las formulaciones desarrolladas del material con una particular evaluación de propiedades estéticas.
9. Lectura e interpretación de resultados.
10. Revisar el estado del arte en cuanto a la funcionalización y estrategias para mejorar la miscibilidad y afinidad entre los componentes (en cuanto al envejecimiento producido por la segregación de fases, para mejorar la compatibilidad entre aditivos).
11. Aplicación de acciones correctoras en REX (extrusión reactiva) para validar aspectos básicos de las propiedades estéticas objetivo (mejora en fijación del color).
12. Explorar la utilidad de las formulaciones desarrolladas en mercados dominados por el PP según los resultados obtenidos. Comparativa con estado del arte, selección del mejor candidato y/o propuestas de mejora (tanto en la formulación como en el proceso).

BLOQUE 4

JUSTIFICACIÓN DE LA UNIDAD TEMÁTICA & PRESENTACIÓN DE LOS TRABAJOS

OTROS TRABAJOS DE INTERÉS

JUSTIFICACIÓN DE LA UNIDAD TEMÁTICA & PRESENTACIÓN DE LOS TRABAJOS

HILO CONDUCTOR DE LA INVESTIGACIÓN

En la presente tesis se proponen alternativas a las poliolefinas convencionales como el polipropileno (PP). Por ello se parte de dos biopolímeros que se consideran hasta la fecha sus principales sustitutos potenciales: los polihidroxialkanoatos (PHAs) y el polibutileno succinato (PBS). Dentro de la línea de mejoras de propiedades estéticas de dichos materiales se identifican dos con mayor relevancia: 1) la fijación del color y 2) mitigar el marcado olor desagradable que desprenden (desodorizar). Por esta razón los cuatro artículos publicados se dividen a razón de dos para tratar de mejorar cada una de las líneas.

Por un lado, aunque ambos polímeros biobasados proceden de fermentación bacteriana (PHA) y de levaduras (los elementos precursores del PBS), es en el PHA donde destaca la necesidad de rebajar el olor que emana del material para intentar conseguir una mayor aceptación y ampliar el horizonte de aplicaciones del mismo. Para ello, dentro del *Artículo 1*[45]*: Polymers 2019, 11, 696 - "Sustainable Materials with Enhanced Mechanical Properties Based on Industrial Polyhydroxyalkanoates Reinforced with Organomodified Sepiolite and Montmorillonite*", se realizó una selección de tres matrices las cuales se caracterizaron en detalle para poder entender la estructura del material y proponer así agentes secuestrantes de olor. Estos agentes secuestratantes se basaron en nanaoarcillas de distinta naturaleza tanto morfológica como química y se evaluó la afinidad de cada una por las matrices seleccionadas. Además, se estudió el impacto sobre las propiedades térmicas y mecánicas fundamentales para asegurar la funcionalidad de materiales en aplicaciones industriales. En el *Artículo 2*[55]*: Polymers 2019, 11, 945 - "Reducing off-Flavour in Commercially Available Polyhydroxyalkanoate Materials by Autooxidation through Compounding with Organoclays"*, se describe y aplica una metodología propia sobre las formulaciones de PHA con los agentes secuestrantes, que es capaz de identificar y medir los principales compuestos volátiles causantes del desagradable olor producido por la oxidación lipídica del material (particular de estos polímeros debido a su origen bacteriano y a los procesos de purificación) y evaluar la capacidad secuestrante de las nanoarcillas introducidas.

Por otro lado, los avances en la línea de fijación del color se centran en la matriz del bioPBS, la cual tiene una base más blanquecina sobre la que poder evaluar las estrategias de fijación. En el *Artículo 3*[86]*: Polymers 2021, 13, 79 - "Color Fixation Strategies on Sustainable Poly-Butylene Succinate Using Biobased Itaconic Acid"*, se realizaron mezclas en masa de bioPBS con un colorante rojo, al que se le añadió un fijador de color (ácido itacónico) propiamente utilizado en el sector de las resinas termoestables y pinturas con dicho fin. Durante el desarrollo de la investigación se observó una marcada tendencia del material a migrar hacia la superficie produciendo un efecto de envejecimiento acelerado que repercutía negativamente en las propiedades del material (tanto pérdida de color como de propiedades mecánicas y dureza). Por ello, se realizó una búsqueda y un análisis de estrategias para anclar químicamente el fijador de color, las cuales se publican en el marco del *Artículo 4*[4]*: Carbohydrate Polymers 2019, 209, 20-37 - "Reactive Compatibilization of Plant Polysaccharides and Biobased Polymers: Review on Current Strategies, Expectations and Reality",* realizando especial hincapié en la extrusión reactiva (REX), dado que es un proceso industrializable por empresas de transformación de plástico como es el caso de Tecnopackaging. Además, se adjuntan algunos resultados de las pruebas realizadas en la planta piloto tras la modificación del proceso, que no han sido publicados.

ARTICULO 1

Sustainable Materials with Enhanced Mechanical Properties Based on Industrial Polyhydroxyalkanoates Reinforced with Organomodified Sepiolite and Montmorillonite

García-Quiles L.G, Fernández A., & Castell P. (2019).
Polymers, 11(4), 696
Impact Factor: 3.426 (2019); 5-Year Impact Factor: 3.636 (2019) – Q1

Este artículo tiene como **objetivo** principal el desarrollo de materiales compuestos biobasados y biodegradables basados en PHA comercial y mejorados con nanoarcillas con el fin de introducir agentes captadores de volátiles (o secuestrantes) que no produzcan mermas o incluso mejoren las propiedades termomecánicas de este biopolímero, abordando así dos desventajas clave de los PHA. El artículo muestra una caracterización completa de las formulaciones desarrolladas a nivel estructural, térmico y mecánico. Se estudian los mecanismos de compatibilidad que tienen lugar entre la matriz y el refuerzo con el fin de ser capaces de sugerir las combinaciones más adecuadas para aplicaciones industriales como por ejemplo el envasado y el sector de la automoción.

En el presente trabajo se estudiaron doce formulaciones diferentes teniendo en cuenta las tres matrices de control más el desarrollo de nueve materiales nanobiocompuestos con una carga de nanoarcilla del 3% en masa, basados en:

- Tres tipos de Matrices PHA: un poli (3-hidroxibutirato) lineal (P3HB) y dos copolímeros a base de poli (3- hidroxibutirato) -co-poli (4-hidroxibutirato) (P3HB-co-P4HB); y,
- Tres nanoarcillas (T1, T2 y T3) con diferente carácter polar (con y sin modificaciones superficiales). Las arcillas T1 (polar) y T2 (neutral) son sepiolitas y T3 (apolar) montmorillonita. Entre ellas difieren en geometrías, siendo las sepiolitas agujas y la montmorillonita fibras conformadas por láminas.

El grado de mejora en las propiedades de los PHA resulta de una combinación entre la morfología de las arcillas, su dispersión en la matriz del polímero y las interacciones entre el polímero y la superficie de la arcilla. Cabe destacar la dispersión lograda para ser un proceso industrial, la cual es muy relevante en comparación con los resultados encontrados en la literatura, así como las propiedades mecánicas mejoradas en particular para la matriz P3HB reforzada con T1 (sepiolita modificada superficialmente con aminosilanos), resultado de la excelente afinidad entre el poliéster y la nanoarcilla. Por ello, se puede **concluir** que el comportamiento polar/funcional resulta predominante sobre la dispersión de la nanoarcilla en el polímero cuando se trata de lograr buenas propiedades termomecánicas en sistemas poliméricos complejos como los seleccionados aunque una buena dispersión sea fundamental para maximizarlo.

Aportes técnico-científicos:

- La optimización de los parámetros del proceso de extrusión-compounding en el desarrollo de nanobiocompuestos: siendo crítico: obtener el perfil de temperatura más bajo posible, usar una velocidad de husillo media-alta y un perfil de husillo de baja cizalla. (Obtener un buen mezclado sin degradar el polímero).
- El método de caracterización detallado basado en técnicas complementarias (H-NMR, DSC y WAX) para entender la estructura química y las interacciones generadas entre el refuerzo y la matriz, y cómo se ven reflejadas en las propiedades mecánicas, que son las que principalmente se realizan a nivel industrial (por rapidez y coste) para validar la calidad del material en aplicaciones determinadas.

polymers

MDPI

Article

Sustainable Materials with Enhanced Mechanical Properties Based on Industrial Polyhydroxyalkanoates Reinforced with Organomodified Sepiolite and Montmorillonite

Lidia García-Quiles [1,*], Ángel Fernández Cuello [2] and Pere Castell [3,*]

[1] Tecnopackaging, Polígono Industrial Empresarium C/Romero N° 12 50720 Zaragoza, Spain
[2] University of Zaragoza, Escuela de Ingeniería y Arquitectura, Av. Maria de Luna, 3, 50018 Zaragoza, Spain; afernan@unizar.es
[3] Fundación Aitiip, Polígono Industrial Empresarium C/Romero N° 12 50720 Zaragoza, Spain
* Correspondence: lgarcia@tecnopackaging.com (L.G.-Q.); pere.castell@aitiip.com (P.C.); Tel.: +34 607 01 88 03 (L.G.-Q.); +34 976 46 45 44 (P.C.)

Received: 21 March 2019; Accepted: 15 April 2019; Published: 16 April 2019

Abstract: Microplastics have become one of the greatest environmental challenges worldwide. To turn this dramatic damage around, EU regulators now want to ensure that plastic itself is fully recyclable or biodegradable. The aim of the present work is to develop a biobased and biodegradable biocomposite based on commercial polyhydroxyalkanoates (PHAs) and nanoclays, with the objective of achieving a reduction of rancid odour while avoiding any loss in thermomechanical properties, thus tackling two key disadvantages of PHAs. This research aims at completely characterising the structural, thermal and mechanical behaviour of the formulations developed, understanding the compatibility mechanisms in order to be able to assess the best commercial combinations for industrial applications in the packaging and automotive sectors. We report the development of nine nanobiocomposite materials based on three types of commercial PHA matrices: a linear poly(3-hydroxybutyrate) (P3HB); two copolymers based on poly(3-hydroxybutyrate)-*co*-poly(4-hydroxybutyrate) (P3HB-*co*-P4HB); and nanoclays, which represent a different polar behaviour. Dispersion achieved is highly relevant compared with literature results. Our findings show impressive mechanical enhancements, in particular for P3HB reinforced with sepiolite modified via aminosilanes.

Keywords: biopolymers; nanoclays; nanobiocomposites; extrusion-compounding; polyhydroxyalkanoates; thermal properties; mechanical properties; differential scanning calorimetry; nuclear magnetic resonance; X-ray diffraction

1. Introduction

At least 8 million tonnes of plastics leak into the ocean each year, which is equivalent to dumping the contents of one bin truck into the ocean per minute. In 2016, 27.1 million tonnes of plastic waste were collected through official schemes in Europe, from which 31.1% of plastic post-consumer waste was recycled, 41.6% was dedicated to energy recovery and 27.3% was landfilled [1]. Moreover, landfill rates are very uneven across Europe. In countries where landfill bans are in effect (Belgium, Luxembourg, Netherlands, Germany, Denmark, Switzerland, Austria, Norway and Sweden), less than 10% of plastic waste is landfilled. In other countries, such as Spain and Greece, a staggering amount of over 50% of all plastic waste still finds its way to landfill [2]. Furthermore, the option of exporting plastic waste to EU or non-EU counties has been foreseen and allowed by the existing EU

legislation given that there is evidence that recovery of materials is taking place under conditions that are equivalent to the EU legislation [3]. This situation is starting to change. For decades, China was the world's largest importer of waste, but this has been changing after Beijing banned 24 types of scraps from entering its borders starting January 2018. This decision has forced other countries, such as Europe, USA and Japan, to improve management of their own waste [4]. The problem is even accentuated when talking about microplastics. It is estimated that between 75,000 and 300,000 tonnes of microplastics are released into the environment each year in the EU [5]. These are reasons why EU regulators now want to ensure that the plastic itself is fully recyclable or biodegradable.

In December 2015, the European Commission adopted an EU Action Plan for a circular economy, and in January 2018, the European Commission published its Communication 'A European Strategy for Plastics in a Circular Economy' as an ambitious step towards making the European plastics system more resource-efficient and to drive the change from a linear to a circular system [5]. A circular economy aims to keep products, components and materials at their highest utility and value at all times, emphasising the benefits of recycling residual waste materials [6]. The New Plastics Economy has three main ambitions:

1. Create an effective after-use plastics economy by improving the economics and uptake of recycling, reuse and controlled biodegradation for targeted applications;
2. Drastically reduce leakage of plastics into natural systems (in particular, the ocean);
3. Decouple plastics from fossil feedstocks by exploring and adopting renewably sourced feedstocks.

Therefore, a new sustainable solution for the plastic sector needs to tackle three pillars: eco-design, functionality and end-of-life. In this sense, various investigations are aimed at decreasing the amounts of plastic waste and manufacturing products with less environmental impact via recycling strategies or via the use of biodegradable materials. Aware of the environmental impacts of the production of synthetic polymers from nonrenewable resources, a promising solution could be the usage of mixtures of biopolymers that gradually replace those synthetic polymers. It is relevant to recall that biopolymers, also referred to in some cases as bioplastics, can be classified into two main groups. When referring to their origin, they can be biobased or fossil-based, and when alluding to end-of-life, they can be biodegradable or nonbiodegradable. Different families and combinations can be found. For example, polylactic acid (PLA) as well as polyhydroxyalkanoates (PHAs) are renewable resource-based biopolyesters, in contrast to polycaprolactone (PCL), polybutylene succinate (PBS) and aliphatic–aromatic polyesters, which are petroleum-based biodegradable polyesters [7–9].

Nowadays, bioplastics represent about one percent of the approximately 320 million tonnes of plastic produced annually [10]. By 2020, biodegradable plastics are expected to represent 18% of bioplastics production and biobased, nonbiodegradable plastics will rise to 82% [11].

The development of new biopolymer materials will require availability of the raw material (second- and third-generation feedstocks), surpassing of market barriers facing economic disadvantages, and additional technological improvements dealing, for example, with higher heat resistance, UV stabilization, controlled barrier properties to water vapour and gases, and better mechanical properties. Blending is a useful strategy to modify material properties for specific applications. In addition to incorporation of fibres or nanoclays, the mentioned technical properties of biopolymers may be improved by chemical and physical crosslinking, or even with the use of surface treatments, such as grafting and coating. The economical barrier is expected to be compensated once disposal costs are taken into consideration and/or production volumes have increased further [12].

Polyhydroxyalkanoates (PHAs) are gaining attention in the biopolymers market due to their high biodegradation rates as well as processing versatility, thus representing a potential sustainable replacement for fossil oil-based commodities. PHAs are most relevant when referring to new biopolymer applications [13]. Polyhydroxyalkanoates (PHA) are polyesters which are intracellularly deposited by bacteria for energy storage. When carbon sources are alternated over time during the bacterial fermentation process, microorganisms synthesize PHA block copolymers. PHA biopolymers are formed mainly from saturated and unsaturated hydroxyalkanoic acids. Each

monomer unit harbours a side-chain R group, which is usually a saturated alkyl group. These features give rise to diverse PHA combinations [14]. PHA biopolyesters include isotactic poly(3-hydroxybutyrate) P3HB, with a high melting point, being very crystalline and brittle; and the poly(3-hydroxybutyrate-*co*-valerate) PHBV copolymer, with a lower crystallinity and lower melting point. More recently, new customised copolymers have been developed by randomly incorporating controlled amounts of flexible linear aliphatic spacers along the main chain; for example, 3-hydroxypropionate (3HP) or 4-hydroxybutyrate (4HB) [15]. The results are semicrystalline copolymer structures designed to have a tailored melting point between 80 °C and 150 °C and that are less susceptible to thermal degradation during processing. Their properties range from brittle thermoplastics to gummy elastomers and can be controlled by the choice of substrate, bacteria and fermentation conditions. These biopolymers have attracted much interest for many new products in the medical and pharmaceutical sectors due to their natural ability to control drug release [16,17] and intrinsic biocompatibility properties [18]. More recently, the material has found new niches in the replacement of conventional oil-based plastic products. Good examples can be found in the food and cosmetic packaging sectors [19], mulch films for agricultural purposes [20], as bio-fuels [21] and even as interior automobile parts. However, PHA biopolymers face a technical barrier which is unique and intrinsic to this biopolyester family and the way it is produced: rancid odour [22]. Lipid residues and endotoxins often remain attached to the biopolymer after extraction. These lipids are oxidised to odourless and flavourless intermediates that could break into molecules giving off-flavours. These conditions are associated with the production of free radicals by autoxidation, which has been recognized as a potential shortcoming of PHA for many applications [23,24]. Different solutions can be approached in order to avoid polymer autoxidation. Most of them deal with the extraction and purification stages of the polymer, but these stages are the most expensive ones, especially if high purity is required. However, the current situation is that nowadays, plastic product converters purchase commercial-grade PHA with unsatisfactory smell, which is a handicap for many potential applications. Our proposed solution approaches the compounding stage of customised blends for industrial applications. It tackles the use of nanoclays with high adsorbance properties which are able to capture volatile compounds responsible for the displeasing fragrance.

Commercial PHAs purchased for plastic parts production are usually blended with other copolyesters and contain small amounts of plasticisers and metal elements, such as Na^{+}, Ca^{2+} and Mg^{2+}. These additives have an effect on the crystallisation, thermal stability [25], mechanical properties [26] and biodegradability of the commercial materials. However, this behaviour is not always functional enough for many industrial applications, and the use of other additives or fillers such as fibres [27–29] or nanoparticles [30,31] is needed. Their use gives rise to thermoplastic nanobiocomposite structures. To enhance the compatibility between the nanoparticle and the polymer is key to better fit the requirements of a certain application, although improving the compatibility of a heterogeneous system is often accompanied by the deterioration of other properties [32,33]. Sepiolite nanoclay fibres form ribbons with inner channels called zeolitic tunnels, offering interesting characteristics such as microporosity and large specific surface area. Due to its natural morphology, sepiolite is considered a good reinforcing agent as well as presenting an outstanding sorption capacity [34]. Moreover, there is much literature demonstrating that its surface functionalisation also helps to improve the transference of properties to the polymeric matrix [35]. In this work, natural sepiolite and sepiolite functionalised via aminosilanes are compared, and with montmorillonite as well. Montmorillonite falls into the smectite group and is largely used for its swelling and adsorption properties [36].

The objective of this research is to develop biobased and biodegradable biocomposites based on commercial PHA and nanoclays, enhancing their thermomechanical properties. This research aims at completely characterising the structural, thermal and mechanical behaviour of the formulations developed and tackles the understanding of the compatibility mechanisms that take place in order to be able to assess the best commercial combinations for industrial applications in the packaging and automotive sectors.

In the present work, three grades of PHAs were reinforced with modified and unmodified sepiolite and montmorillonite kindly provided by TOLSA (Spain). The clays differ in geometries, with sepiolites being T1 and T2 needles and montmorillonite being T3 fibres formed by sheets. The degree of improvement in the PHAs' properties is a combination of the morphology of the clays, their dispersion in the polymer matrix and their interfacial polymer–clay interactions. The three candidates selected present different behaviours, from polar (T1) and neutral (T2) to nonpolar (T3) features, which directly affect the affinity for the PHA polyesters and therefore affects the matrix's final properties in a different manner.

2. Materials and Methods

2.1. Materials

Three grades of PHAs were used as polymer matrixes: Mirel PHA1005, Mirel PHA3002 (both food contact-grade P3HB-*co*-P4HB grades, purchased from Metabolix USA) and Biomer PHB P226 (isotactic and linear short chain length scl-PHA homopolymer P3HB grade purchased from Biomer, Germany).

Three different modified and unmodified organoclays were kindly provided by TOLSA (hereby referred to as T1, T2 and T3, which have been previously characterised by other studies [34,37–39]), being:

- T1: Modified sepiolite: organically modified through aminosilane groups on the surface;
- T2: Natural sepiolite without modifications on its surface (naturally containing silanol groups, commercially marketed as Pangel 9);
- T3: Natural sodium montmorillonite (Na-MMT) modified with a quaternary ammonium salt; it is an anionic organoclay (highly compatible with nonpolar polymers).

2.2. Nanobiocomposite Preparation

PHA/clay formulations were prepared by extrusion-compounding with a 26-mm twin-screw Coperion ZSK 26 compounder machine (Germany). Twelve different formulations were studied in total, accounting for the three control matrixes plus nine developed materials prepared on the compounder machine by loading them with the three nanoclays at 3 wt. % in all cases (see description in Table 1). The melted polymers and nanoclay powder were mixed at a screw speed of 125 rpm; temperature was increased from 150 °C in the feeding zone up to 165 °C at the nozzle for PHA1005 and PHA3002 (P3HB-*co*-P4HB formulations) and slightly decreased from 140 °C in the feeding zone up to 160 °C at the nozzle when blending PHB226 (P3HB). The compounding was extruded through a 2-mm diameter die for a constant output of 10 kg/h. The extrudate was quenched in a water bath at room temperature, dried and cut into pellets.

Specimens for mechanical and tensile testing were obtained by injection moulding with a JSW 85 EL II electric injection machine (JSW, Tokyo, Japan) following ISO 178 and ISO 527 standards. Temperature profile was increased from 160 °C at the hopper up to 200 °C at the nozzle. Dosage and filling pressure were varied for each formulation injected. A packing pressure of 25% was applied.

Table 1. Summary of material formulations based on poly(3-hydroxybutyrate) (P3HB); poly(3-hydroxybutyrate)-co-poly(4-hydroxybutyrate) (P3HB-co-P4HB) and nanoclays

Material formulation	Commercial matrix used	Nature of the PHA	Type of reinforcement (3 wt. %)
PHA1005	PHA1005	P3HB-*co*-P4HB	17% P4HB/P3HB and talc
PHA1005_T1	PHA1005	P3HB-*co*-P4HB	T1: Aminosilane sepiolite
PHA1005_T2	PHA1005	P3HB-*co*-P4HB	T2: Natural sepiolite
PHA1005_T3	PHA1005	P3HB-*co*-P4HB	T3: Sodium montmorillonite: quaternary ammonium salt
PHA3002	PHA3002	P3HB-*co*-P4HB	23.5% P4HB/P3HB and talc
PHA3002_T1	PHA3002	P3HB-*co*-P4HB	T1: Aminosilane sepiolite
PHA3002_T2	PHA3002	P3HB-*co*-P4HB	T2: Natural sepiolite

PHA3002_T3	PHA3002	P3HB-*co*-P4HB	T3: Sodium montmorillonite: quaternary ammonium salt
PHB226	PHB226	P3HB	Traces of PBA (polybutyladipate), plasticiser, and talc found
PHB226_T1	PHB226	P3HB	T1: Aminosilane sepiolite
PHB226_T2	PHB226	P3HB	T2: Natural sepiolite
PHB226_T3	PHB226	P3HB	T3: Sodium montmorillonite: quaternary ammonium salt

2.3. General Characterisation Methods

Mechanical tests were conducted under ambient conditions using a Zwick Roell Z 2.5 (Zwick, Germany). At least five specimens per material were tested, according to ISO 178 and ISO 527 methodology.

Nuclear magnetic resonance (NMR) spectra were measured on a Bruker instrument at 25 °C using 400 MHz for the three neat biopolymers (PHB226, PHA1005 and PHA3002) (Bruker, Karlsruhe, Germany). Samples were dissolved in $CDCl_3$ and washed to clean them up from mineral fillers. ^1H NMR spectra were obtained.

Thermal characterisation was carried out by differential scanning calorimetry (DSC) using a Mettler Toledo 223E (Mettler, Columbus, OH, USA). Dynamic heating was performed from room temperature to 220 °C at a rate of 10 °C/min for 8 mg samples placed into standard 40 μL aluminium crucibles, under a 100 mL/min flow of nitrogen. DSC tests were duplicated to ensure the reproducibility of results.

Energy-dispersive X-ray spectroscopy (EDX) was also used for samples' chemical characterization in a Hitachi S3400N (Hitachi, Tokyo, Japan). The diffraction pattern was determined using a Bruker D8 X-ray diffraction (XRD) equipment using Cu Kα irradiation at 44 kV (Bruker, Karlsruhe, Germany). The diffractogram was carried out between 5° and 80° at a step of 0.5°/min. XRD was used to identify changes in PHA/clay blends' crystalline structure. XRD tests were duplicated to ensure the reproducibility of results.

3. Results and Discussion

3.1. Mechanical Results (Flexural and Tensile)

The mechanical properties of composite materials are always a compromise between stiffness and toughness. These properties are generally mutually exclusive. The elastic modulus (E), tensile strength (σ_M) and elongation at break (ε_B) are useful parameters which describe the mechanical behaviour of the developed materials and are closely related to the internal microstructure. Toughness (U_T) was calculated by integrating the stress–strain curves and obtaining the area under the curves. The mechanical properties determined from uniaxial tensile and flexural tests are summarized in Table 2.

Table 2. Mechanical properties under tensile and flexural forces: modulus (E), flexural strength (σ_M), elongation at break (ε_B) and toughness (U) for all characterised materials.

Material	E (MPa)	σ_M (MPa)	ε_B (%)	U_T (MPa)	E_f (MPa)	σ_{fM} (MPa)	ε_{fB} (%)	U_{fT} (MPa)
PHB 226	2028 ± 68	21.8 ± 0.5	3.1 ± 0.3	53.9	1316 ± 28	30.2 ± 0.4	4.4 ± 0.2	98.8
PHB 226_T1	2004 ± 66	23.7 ± 0.6	4.6 ± 0.7	83.9	1306 ± 17	30.1 ± 1.0	4.8 ± 0.3	115.8
PHB 226_T2	2435 ± 88	22.1 ± 1.1	1.9 ± 0.3	33.6	1318 ± 68	34.1 ± 0.9	4.7 ± 0.4	111.5
PHB 226_T3	2006 ± 65	22.5 ± 0.3	4.2 ± 0.3	69.9	1871 ± 9	42.3 ± 0.3	3.6 ± 0.1	99.3
PHA 1005	2770 ± 99	22.4 ± 0.7	2.0 ± 0.1	32	1801 ± 39	31.5 ± 0.4	3.9 ± 0.1	92.8
PHA 1005_T1	3411 ± 98	25.2 ± 0.5	1.8 ± 0.1	33.9	2066 ± 71	32.2 ± 0.8	3.2 ± 0.1	71.9
PHA 1005_T2	3420 ± 218	25.9 ± 0.6	1.9 ± 0.2	38.2	2240 ± 88	33.9 ± 1.7	2.7 ± 0.1	60.3
PHA 1005_T3	3755 ± 41	23.8 ± 0.6	1.4 ± 0.1	24.9	2980 ± 90	47.6 ± 2.3	2.6 ± 0.2	81.6
PHA 3002	2263 ± 37	24.7 ± 0.5	2.8 ± 0.1	50	1342 ± 71	33.9 ± 1.5	5.0 ± 0.2	121.9
PHA 3002_T1	1997 ± 48	26.2 ± 0.3	4.1 ± 0.2	84.6	1485 ± 35	34.3 ± 1.1	4.2 ± 0.1	97.6

PHA 3002_T2	2961 ± 87	28.7 ± 0.3	2.9 ± 0.2	65.7	1807 ± 85	43.1 ± 1.1	4.4 ± 0.8	128.9
PHA 3002_T3	2463 ± 115	27.4 ± 0.2	3.3 ± 0.3	68.9	2358 ± 7	57.0 ± 0.7	4.3 ± 0.3	134.1

It is well-documented that P3HB seems to be more crystalline, mechanically stiffer, stronger and less ductile than its copolymers [40]. According to Koller et al., pure P3HB presents a tensile strength of 40 MPa and 6% elongation at break, while pure P4HB presents 104 MPa and 1000%, respectively [41]. Cong et al. demonstrated that the addition of a 4HB copolymer at up to 30 wt. % into P3HB causes reductions in the storage modulus, stress at yield and stress at break, while the elongation at yield and at break increases [42]; however, our results show a different situation. It has to be taken into account that even our commercial-grade P3HB (PHB226) may contain small percentages of talc, plasticiser and other polyesters. The presence of these and other additives will be explored and discussed by DSC and NMR analysis. Therefore, the general statements and results obtained by other authors in similar research works where the polymers were synthetised and blended in a laboratory with nanoparticles might not always correspond to others' findings. In addition, NMR results established the molar ratio of the P3HB-*co*-P4HB blends, with PHA3002 being the one containing the highest percentage of P4HB. The amounts of talc that each blend contains highly affects the elongation at break and toughness of the blends, and it is not possible to find a correlation due to its random behaviour.

Our results show that PHA1005 is the stiffest matrix with the highest elastic modulus under tensile and flexural stress, followed by PHA 3002 and finally by PHB226. However, PHB226 presents a high elongation at break, probably due to the PBA, and in consequence, it presents the highest toughness under tensile efforts. PHA3002 maintains an intermediate behaviour under tensile and flexural stresses.

A common behaviour found in many nanobiocomposites when nanoparticles are introduced is an increase in the elastic modulus, a preservation or even a slight increase in the tensile stress and a decrease in elongation at break [43]. Botana et al. demonstrated that the incorporation of small quantities of montmorillonite (2–10% in mass) with a certain degree of exfoliated structure have a great influence on the properties of the final material, such as mechanical strength, stiffness, thermal stability, conductivity and gas barrier properties [44]. Our samples comply partially with this generally observed behaviour, depending on the nanoclay reinforcing the matrix.

In the PHA1005 blends, the three nanoclays generally improved the stiffness of the material (both under flexural and tensile forces), with T3 (montmorillonite) being the one introducing the greatest enhancement. PHA1005_T3 shows a 35% higher Young's modulus and 65% higher flexural modulus than neat PHA1005, although toughness was clearly compromised. Only for PHA1005_T2 was toughness enhanced under tensile forces, by 19%.

PHA3002 T1 (sepiolite modified via aminosilanes) greatly improves elongation at break, by 46%, and the increase in toughness by 69% compared to neat PHA3002 is therefore noticeable (although the elastic modulus is slightly compromised, falling by 13%). The modified surface of T1 may have acted as plasticiser with this matrix, favouring the interphase affinity. When testing the same material, PHA3002_T1, under flexural forces, an opposite behaviour was found, with the flexural modulus being increased and the elongation at break and toughness reduced. The authors consider that the alignment or orientation of the sepiolite ribbons with the flow when extruding the material may have also an important effect on the final strain and toughness. For PHA3002_T2, there was an increase of 31% in the Young's modulus, while the elongation at break was maintained, as for PHA3002, and hence the tenacity was improved. The same tendency of behaviour was found for this material under flexural stress. Finally, a significant improvement was found when adding T3. The exfoliation of the layers (see XRD results) induced mechanical improvements for all parameters under tensile forces and was even more significant under flexural ones. PHA3002_T3 had its flexural modulus increased by 75%. The elongation at break was slightly reduced, but the improvement in stiffness was so high that final toughness was also increased by 10% compares to neat PHA3002.

For PHB226, the greatest improvement in mechanical properties is observed for T1, as it maintains the elastic modulus while substantially improving the elongation at break and therefore

toughness. PHB226_T1 is the only material developed for which all the mechanical properties were maintained or increased. Under tensile stress, strain is increased by 48% and toughness by 55%, while under flexural stress, strain is increased by 9% and toughness by 17%. Probably the combination of a good dispersion in the blend, the large surface area of sepiolite and the organic modification of T1 produces a better interaction and affinity due to the aminosilane modification, which may present a better compatibility with the P3HB matrix.

This behaviour disappears for T2 (sepiolite without the functional modification). Despite the large amount of silanol groups, T2 acts as a filler, enhancing the stiffness of the material by 20% for tensile stress, but reducing elongation at break and toughness considerably. The material has similar mechanical properties to neat PHB226 under flexural stresses. Finally, when T3 is added, the overall stiffness of the material is improved, in particular increasing by 42% under flexural forces, but strain and toughness are compromised. The exfoliation of montmorillonite probably leads to the enhancement in toughness under tensile forces, but this is not as significant as the one produced by T1.

As a global pattern in all nanobiocomposites developed, T1 (modified sepiolite) probably has a better interphase, as elongation at break enhances while flexural modulus is maintained, whereas T2 formulations show higher rigidity and poorer toughness. T3 produces significant overall mechanical improvements, which may be induced due to exfoliation of clay layers leading to an increase of the effective aspect ratio, but probably the nonpolar behaviour of montmorillonite hinders a better polymer–matrix interaction.

Mechanical analysis demonstrates that PHA1005 is the matrix with the least overall improvement in mechanical properties when reinforcing the matrix with organoclays, while PHB226_T1 shows the greatest enhancement (modified sepiolite). However, it has to be taken into account that for all reinforced nanocomposites, there is an optimum load of filler, over which the matrix appears to be oversaturated. The combination of talc plus nanoclay may lead to this point being reached, which produces a loss of mechanical properties, especially regarding elongation at break and toughness. The results obtained for PHA1005 suggest that the material may contain larger amounts of talc than PHA3002.

Czerniecka-Kubicka et al. developed Biomer P3HB samples loaded with modified montmorillonite (cloisite 30B: natural montmorillonite modified with methylbis(2-hydroxyethyl)tallowalkylammonium cations) at 1 wt. %, 2 wt. % and 3 wt. % and evaluated the mechanical properties under flexural stress. The flexural modulus values found for nanocomposite containing 1 wt. % nanoclay increased by approximately 20% in relation to the nonmodified sample. Further increase of nanofiller content caused a decrease in flexural modulus values, but they were still higher than that of neat P3HB [45]. Our findings have shown an increase of 42% in flexural modulus when adding 3 wt. % of montmorillonite to Biomer P3HB (PHB226). The increase in the flexural modulus with PHA1005 and PHA3002 is even higher (65% and 75%, respectively). Therefore, we can confirm that either the dispersion or the surface modification has an extremely important effect on the composite. Dispersion is directly related to the extrusion-compounding process, where the temperature and shear force induced are key parameters in obtaining a homogenous blend without degrading the biopolymer. Compared to Czerniecka-Kubicka et al., our samples were mixed at lower temperatures, but at much higher rotation speeds (inducing higher shear and therefore favouring dispersion and delamination of montmorillonite in this case).

3.2. NMR

The ^{1}H NMR spectra of P3HB (PHB226) and P(3HB-*co*-4HB) (PHA1005 and PHA3002) polymers is shown in Figure 1, with the various peaks labelled for the different protons in the 3HB and 4HB units, as well as for additional polyesters identified (PBA, plasticiser).

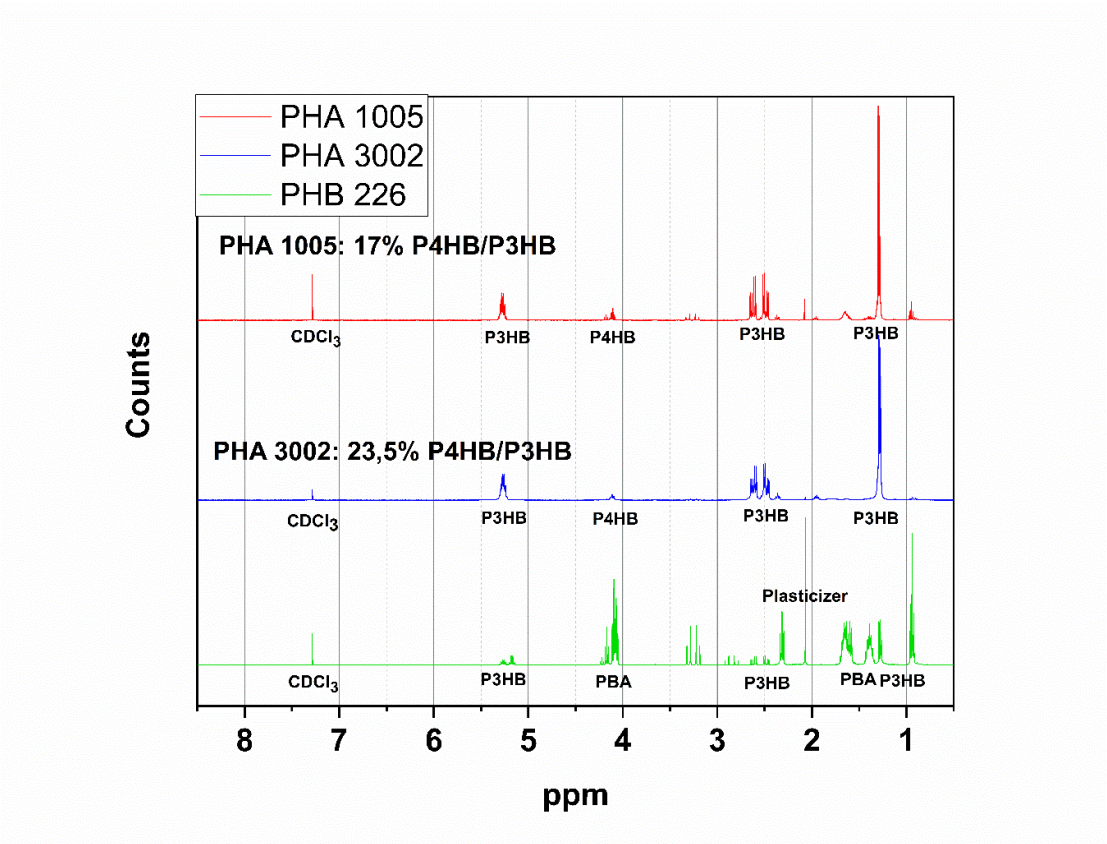

Figure 1. The ^{1}H-NMR spectra of PHB226, PHA1005 and PHA3002.

Very few articles have been dedicated to understanding the commercial grades of PHAs, which are the real ones that industry is incorporating in our daily products. Some characterisations have been done by Corre et al. [46] for commercial P3HB (PHB226), P3HB-*co*-P4HB (1006, 3002) and P3HB-*co*-3HV (Y1000P), but without explaining their composition in detail or giving further assessment on how to improve their weak properties.

Modification of PHA with plasticisers and other copolymers is a conventional technique for the improvement of the processability and brittleness of PHA. Nuclear magnetic resonance (NMR) is a useful analytical method to obtain information about the organic chemical structure of our blends.

The ^{1}H NMR spectra of PHB226, PHA1005 and PHA 3002 were obtained. Results revealed the domain structure of P3HB in all samples. Specific peaks associated to P3HB and P4HB [47,48] protons were identified and the molar relation between PH3B and PH4B in PHA1005 and PHA3002 samples was obtained by integrating the peaks. The content found for P4HB corresponds to 23.5 mol % in PHA3002 and 17 mol % in PHA1005.

The presence of peaks different from P3HB were found in PHB226 samples (according to the product datasheet, it is 89.8% biobased P3HB). These are probably related to the addition of another biopolyester used as a plasticiser. Those peaks did not appear for PHA1005 or PHA 3002 polymers. Taking into account the nature of PHB, two candidates have been found to be potential copolymers in the blend: polybutylene adipate (PBA) components and triacetin (or citrate ester) [49,50]. Specific peaks that may be associated to PBA appeared between 1.3 and 1.7 ppm [48]. The presence of PBA is corroborated in DSC results, with the melting peak found at 50°C, which is characteristic of this polyester [51]. Initially, the addition of Polybutyrene adipate terephtalate (PBAT) was considered as it is a frequent additive used in many biopolymer formulations. However, the lack of a single peak at 8 ppm [43] confirms that no terephthalate had been added into any of the formulations. Often, these polyesters are added on purpose as plasticisers, and other times, they may be considered to be impurities from the purification stage of the PHA. It has to be taken into consideration that different

batches of these materials may show slight differences due to additive traces used during polymer growth as carbon sources for the strain of microbe. For example, acetic acid, adipic acid, propionic acid or dodecanioic acid are used as precursors in the production of P3HB-*co*-P4HB or PHBHV4HB polymers [52]. The ^{1}H-NMR spectrum of PHB226, PHA1005 and PHA3002 can be found in Figure 1.

3.3. DSC—Differential Scanning Calorimetry

DSC measurements were performed in order to observe the melting behaviour of the crystals and to determine the changes induced in the highly ordered structure. The DSC analysis of the samples was carried out over three cycles, involving a first heating cycle followed by a second cooling cycle and finally a third heating. This method ensures the removal of residual thermal behaviour in the polymers.

According to the literature data, the T_g of PHA biopolymers may vary between −1 and −48 °C, depending on the type and molar fraction of the second monomer (4HB, 3HV, 3HO, 3HHx) [53,54]. The T_g of P3HB has been reported to vary between −3 and 5 °C, and the T_g of P4HB at −46 °C [55]. Our thermograms for the neat matrixes are aligned to those of other neat PHAs reported by Corre et al. [46].

Comparing the T_g of our three raw matrixes, we can observe that the T_g of PHA1005 and the T_g of PHA3002 have almost no deviations around −24°C, which is about 10 °C lower than the T_g of PHB226. This behaviour is expected as the P4HB side groups in PHA1005 and PHA3002 increase the free volume in the molecule, resulting in a decrease of T_g.

The increase in the T_g transition appreciated in the DSC diagram for PHA3002_3T1 should be highlighted, which might be induced by an increase of the amorphous phase in the interphase between the matrix and the nanoclay. For the case of PHA1005 bionanocomposite formulations, it can be observed that the three nanoclays (T1, T2 and T3) induce a decrease of T_g, being especially remarkable in the case of T3. In addition, the transition becomes almost indiscernible, which suggests that nanoclays induce a plasticiser effect in the three cases. Moreover, T_g lowering could result from some interfacial interactions between the clay and the matrix producing disorganized molecular arrangements within the interphase, probably due to an agglomeration of filler, which might become a predominant factor for T_g decrease [56,57]. This tendency in behaviour can be observed for PHB226 too. T1 and T2 produce a clear decrease of T_g. PHB226 is the polymer with the highest crystallinity in comparison with PHA1005 and PHA 3002. Thus, T_g results are difficult to be obtained as the transition is not clear in the DSC diagram due to the very low amorphous range. In the case of T3, it is not possible to find an approximate value. This is an indication about the good dispersion achieved with this nanoclay and is in coherence with the results obtained in XRD.

In Figure 2, we can observe that all diagrams show a clear crystallization peak, which indicates that our compounds undergo some small amount of crystallization while heating. Comparing the three matrixes, it can be corroborated that PHB226 is the one with highest crystallinity, followed by PHA3002 and finally PHA1005. This result is in contradiction to the findings of Bayari et al., who confirmed the fact that the degree of crystallinity of P(3HB-*co*-4HB) copolymers decreased with an increase in the amount of the 4HB content [58]. However, these are based on lab-produced PHA materials, not commercial blends, in which the use of additives tailors the crystallisation rates. Our results agree with the findings shown by Corre et al. [46], in which similar Mirel matrixes (P3HB-*co*-P4HB) under polarized optical microscopy (POM) featured larger spherulites with lower nucleation density than PHB226 (P3HB). The introduction of inorganic nanoparticles to increase the nucleation density and decrease the spherulite size is a common practice in commercial PHAs. Examples of these inorganic particles include tungsten disulphide inorganic nanotubes (INT-WS2), boron nitride (BN), talc ($Mg_3Si_4O_{10}(OH)_2$), hydroxyapatite (HA) and zinc stearate (ZnSt) [59], used as nucleation agents to modify the properties of P3HB-*co*-4HB. Wang et al. [59] suggested that the addition of talc increased the crystallisation degree of P3HB-*co*-4HB, but had little effect on the crystallisation rate. This cheap material is used at the industrial level by commercial material producers and it can be found in our neat PHB226, PHA1005 and PHA3002 matrices (according to EDX results carried out by the authors, in which Mg^{2+} cations and silicon are clearly identified).

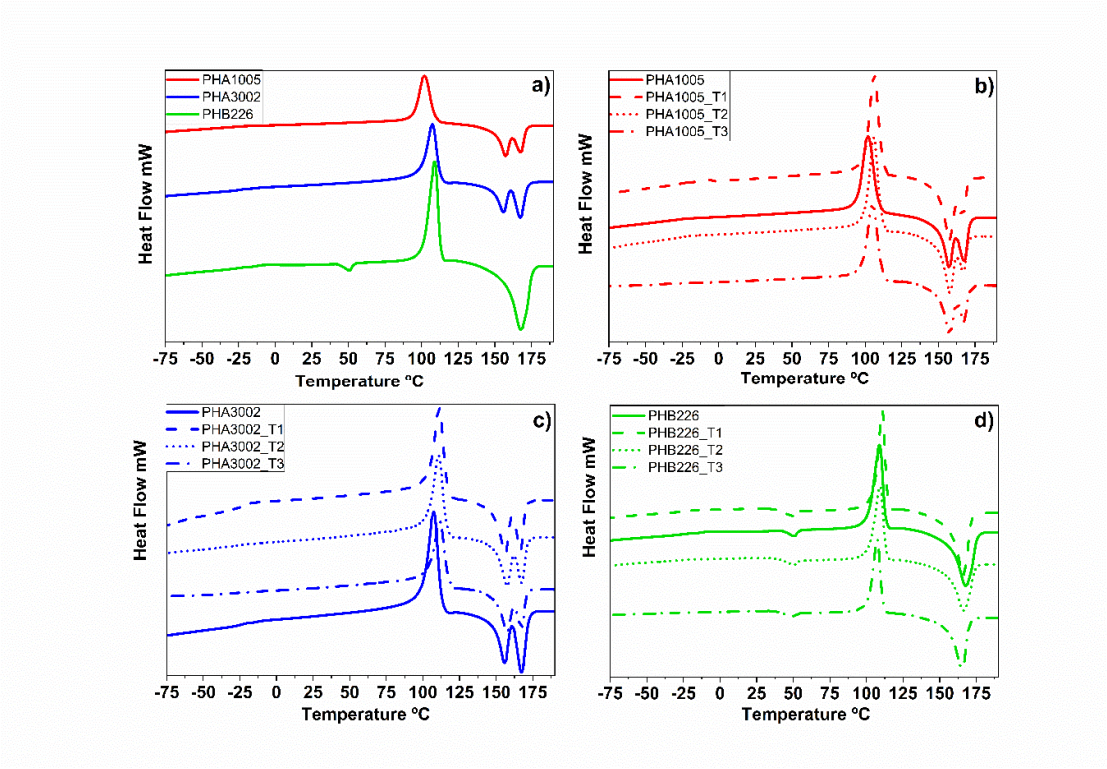

Figure 2. Differential scanning calorimetry (DSC) thermograms. (**a**) Raw matrices: PHA1005, PHA3002 and PHB226; (**b**) PHA 1005 loaded with 3 wt. % T1, T2 and T3; (**c**) PHA 3002 loaded with 3 wt. % T1, T2 and T3; (**d**) PHB 226 loaded with 3 wt. % T1, T2 and T3.

The PHA1005 DSC diagram is accompanied by a rise in the cold crystallisation temperature and crystallisation enthalpy, with T1 being the nanoclay that induces the highest augmentation. Crystallization temperature (T_c) increases by almost the same ratio in all cases (3–4%) for PHA3002 formulations when adding any of the three nanoclays with respect to the neat matrix. A similar tendency is obtained for PHB226 compounds, except for the case of PHB226_T3, which suffers a slight decrease with respect to neat PHB226. High Tc implies that the polymer crystallisation ability of the material is better [29].

The crystallinity of the samples was calculated for the second heating from the general equation: X_c (%) = ($\Delta H_m/\Delta H°_m$*(1-w_t))*100, where w_t is the clay fraction and $AH°_m$ is the theoretical melting enthalpy of 100% crystalline PHB polymer, taken as 146 J/g [60].

P3HB chains typically form spherulites that are crystallised from the melt polymer. The nucleation density for P3HB is known to be excessively low, leading to the development of extremely large spherulites which grow radially within P3HB materials. The size varies from several micrometres to a few millimetres, depending on the crystallisation temperature and molecular weight [61]. Lamellar thicknesses in spherulites range from 5 nm to 10 nm, depending on the crystallisation temperature. It is well known that P3HB exhibits two crystal polymorphs: α and β crystals. It is assumed that the β-crystals appear from amorphous chains present between the lamellar crystals of the α-crystal (tie-chain). The β-form is introduced by the orientation of free chains in the amorphous regions between α-form lamellar crystals. The authors understand that these crystals form part of the so-called rigid amorphous phase (RAF) for this particular case of PHA structure. Di Lorenzo et al. assigned a peak around 45 °C to the RAF structure [62]. The presence or absence of this peak depends on the thermal history of the material. Our DSC results corresponds to the second heating, and therefore the thermal history of our matrixes has already been removed and the peak does not appear. However, our XRD results show the presence of β-crystals. The rigid amorphous structure growths during the first stage of cold crystallisation and slows down crystallisation before

completion, creating an immobilised amorphous layer that surrounds the crystals. The physical state of the rigid amorphous fraction affects the crystallisation kinetics of P3HB. The crystal dimensions of P3HB and P4HB have been deeply characterised in the literature.

Our DSC results show the two peaks related to the two distinct populations of crystals (P3HB and P4HB) for all composite formulations. To understand the effects induced on crystallinity, it is important to take into account the differences in the kinetics and crystal formation in the copolymers between P3HB and P4HB, as well as the particular modifications that the nature of each nanoclay (with different polar affinity and structure) is introducing into the system. When adding the nanoclays, different behaviours can be observed according to the interphase created, which is directly related to the dispersion grade and interaction of the nanoclays with each polymer.

According to the literature [63], crystals related to P3HB exhibit a higher T_m than those corresponding to PH4B. Different authors report the Tm for pure 3HB to be 171–175 °C [58], while the Tm for pure 4HB appears at 56–58 °C [38]. The Tm for P3HB reported in the literature ranges between 162 °C and 197 °C [64]. The differences in Tm indicate that the size or thickness of P3HB crystals is greater than those for P4HB. Volova et al. compile quite a lot of information related to thermal behaviour and the structure of the different monomers and polymers that form PHAs, in particular for P3HB, P4HB, PHV and PHH [65].

In this research, PHA1005 and PHA3002 samples showed two endothermic peaks which correspond to the two crystalline phases: the 3HB-rich crystalline microregion at 167 °C and the 4HB-rich crystalline microregion around 157 °C. According to the literature [47], P(3HB-*co*-4HB) crystallises like P(3HB), with the 4HB units acting as defects in the crystal lattice when the 4HB content is less than 30 mol % (which has been confirmed in this study with the NMR results). Thus, the multiple melting behaviour of P(3HB-*co*-4HB) samples corresponding to PHA1005 and PHA3002 originates from microphase separation [66]. Kabe et al. studied the transition of spherulite morphology and measured the radial growth rate of spherulites in the blend of polyesters composed of P(3HB-*co*-3HH) and neat PHB with polarisation optical microscopy. They concluded that the radial growth rate of spherulites of neat P3HB was 0.25 mm/min, and complete crystallisation took about 5 min, while for the copolymer, they were 0.0008 mm/min and 9 h, respectively [67]. Therefore, it might be deduced that P3HB crystals appear to present the fastest radial growth rate.

In addition, PHB226 shows a melting peak at 50 °C, indicating the presence of another polymer or plasticiser, as suspected from the NMR results. Mohanty et al. described the presence of citrate plasticiser in this Biomer grade without providing further information [49]. Other authors consider that the material may contain small amounts of other copolymers, such as PBAT or PLA [55,68,69]. Our characterisation results (NMR and DSC) confirm that the formulation contains small amounts of PBA (with a Tm reported between 50 °C and 60 °C) [70], but not PBAT, as there is no trace of terephthalate. Anyhow, comparing the three neat matrixes, it can be observed that PHB226 presents the highest crystallinity of 79.5%, followed by PHA3002 with 44.2% and PHA1005 with 41.2%. Knowing that PHA3002 contains the highest P4HB/P3HB ratio, the crystallinity of PHA3002 should have been lower than that for PHA1005. However, both materials present high loads of mineral fillers (talc, according to EDX results) that most probably influence the crystallisation of the samples, varying the nucleation points and kinetics. The system becomes even more complex when the nanoclays are introduced. There is a decrease in the melting temperature (Tm) of the nanocomposites compared with pure matrixes, as the presence of the nanoclay seemed to induce crystal defects. This observation suggests the formation of smaller crystals with larger imperfections, which melt at lower temperatures [37].

In the case of the PHA1005 copolyester, when incorporating T1 (sepiolite modified with aminosilanes), an increase in crystallinity is achieved, while when introducing T2 (natural sepiolite), it seems not to affect the crystallisation of the original matrix. On the contrary, the tendency of T3 (Na-montmorillonite) is to decrease crystallinity slightly. For the matrix PHA3002, the introduction of sepiolites (T1 and T2) decreases the crystallinity of the material in a similar rate. Furthermore, when T3 is incorporated, the effect is even more acute, which suggests a global tendency for the rigidisation of the side chains when the nanoclays are dispersed. It can be observed that nanoclays

particularly affect the peaks which correspond to a major concentration of P3HB crystals, so these are mostly hindering the rearrangement of short P3HB crystals. This result can be explained according to an induced modification in the crystallisation kinetics.

In PHB226, both Tm and ΔH_m decreases, and so does the global Xc. For both sepiolite nanoclays, a clear difference can be found. The superficial aminosilane groups of T1 seem not to be modified as much as natural sepiolite does, neither in the amount of crystals formed nor in their size. Therefore, the global crystallinity of the polymer is maintained. Some authors have demonstrated that nanoclay surfaces can be useful in providing nucleation points [38]. When PHB crystallises in the presence of the clay mineral particles, crystals could grow on the particle surfaces. In these cases, fillers (such as sepiolite, montmorillonite, cellulose nanowhiskers or fine lignin powder) reduce the energy barrier for polymer crystallisation and increase the nucleating density, originating smaller spherulites in higher number than in neat PHB [57]. We can find a slight decrease in Tm for all nanoclays, indicating a small reduction in size of the crystals formed. In addition, we can observe that T2 (natural sepiolite) may present a worse dispersion inside the blend, favouring the formation of agglomerates and therefore reducing the amount of crystals formed (as ΔH_m decreases with respect to neat PHB226 or PHB226_T1). The discontinuity of the silica sheets on the outer edges in sepiolite fibre leads to the presence of numerous silanol groups (Si–OH) at their external surface, which allows easy functionalisation based on their reaction with coupling agents such as organosilanes [39,71]. In T1 nanoclay, sepiolite has been grafted with aminosilane groups which are very stable, generating an organophilic clay that can be more easily dispersed in low-polarity polymers than unmodified clays [72]. Chemical covalent functionalisation is believed to counteract the stacking forces in the nanoparticles and to lead to debundling [73]. This effect may be caused by the intercalation of the attached moieties that finally results in a more effective dispersion within the polymeric matrix. Therefore, the affinity T1 inside the PHB226 may be scattered enough to keep a similar amount of nucleating points.

Anyhow, the most noticeable drop in T_m and ΔH_m is found for PHB226_T3. The exfoliation of montmorillonite may lead to a very high dispersion of the nanoclay. Exfoliation of T3 has been confirmed by XRD results. A good exfoliation should give rise into an increment in crystallinity, as it favours the creation of nucleation points. Nevertheless, the reaction can be so fast that crystals formed may be irregularly arranged, which increases the amorphous regions (RAF) between lamellae, and hence a decrease of the global crystallinity of the material [67], which means that it may hinder PHB226 chain movements by absorbing PHB226 segments on its surface [74]. Botana et al. studied the kinetics and dispersion of organically modified montmorillonites (among them, Na-montmorillonite) in PHB blends under polarised microscopy. The polarised optical micrographs indicated differences in the spherulite size [44]. In particular, Na-montmorillonite produced a large amount of spherulites, but being smaller in comparison to neat PHB. The appearance of disordered areas surrounding some spherulites corroborate that intercalated/exfoliated montmorillonite produces larger amorphous regions.

3.4. WAX—X-ray Diffraction

The XRD spectra of the samples revealed the crystallisation pattern of our PHA samples, which follows the trend of standard P3HB and P3HB-*co*-P4HB. P3HB exhibits two crystal polymorphs: α and β crystals. Diffraction patterns can be found in Figure 3.

The profile of PHB226 exhibits distinct diffraction peaks patterns of 2θ at 13.58, 17.03, 19.93, 21.5; 22.26, 25.69 and 30.69, corresponding to orthorhombic crystal planes (0,2,0), (1,1,0), (0,2,1), (1,0,1), (1,1,1), (1,2,1) and (0,1,2) [75], respectively. Sharp peaks at 2θ = 13.58 and 17.03 show typical α-crystals, while 2θ = 19.93 reveals that β-crystal structure also appears. This peak is also observed for PHA3002 with lesser intensity than PHB226, while for PHA1005, it disappears. This behaviour suggests that PHA3002 presents higher crystallinity than PHA1005, which is in coherence with the results obtained in DSC. For PHA1005 and PHA3002, a new peak not found for PHB226 is observed at 2θ = 27.13, which is attributed to the crystal plane (0,4,0) [76], indicating a preferential order of the copolymer blend P3HB-*co*-P4HB for this crystal structure.

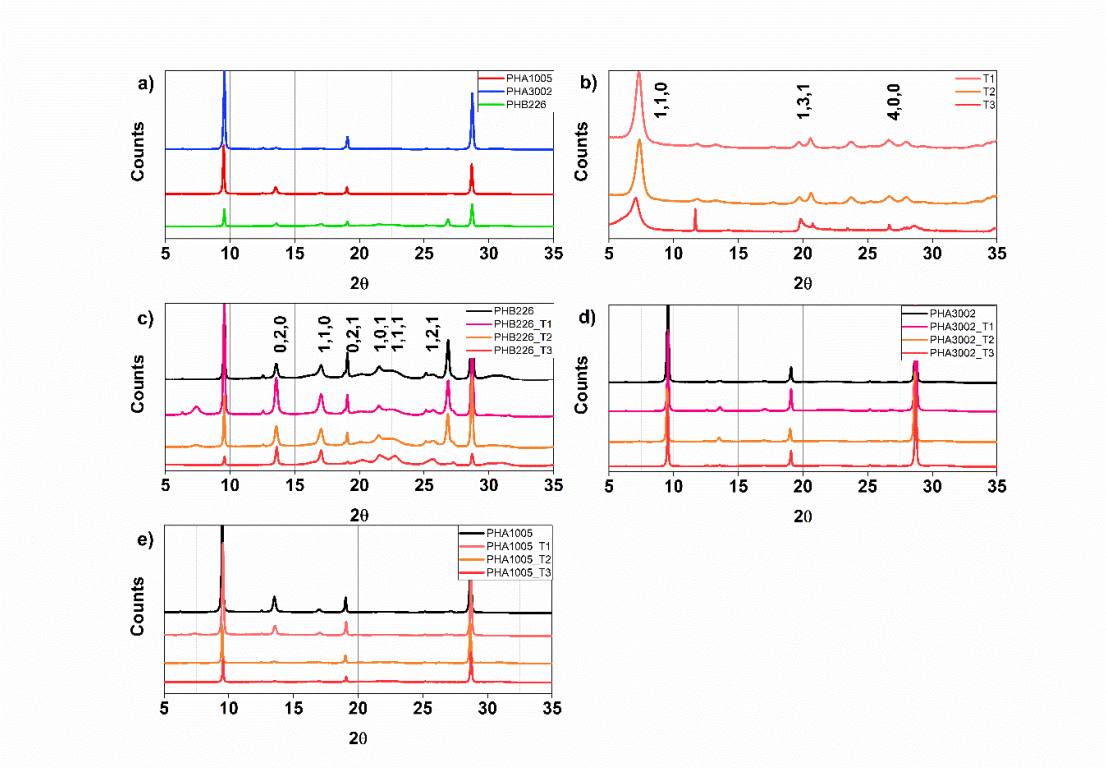

Figure 3. X-Ray diffraction patterns. (**a**) Raw matrixes: PHA1005, PHA3002 and PHB226; (**b**) Nanoclays: T1, T2 and T3; (**c**) Neat PHB226 and loaded with 3 wt. % T1, T2 and T3; (**d**) Neat PHA3002 and loaded with 3 wt. % T1, T2 and T3; (**e**) Neat PHA1005 and loaded with 3 wt. % T1, T2 and T3.

In the neat polymers (PHB226, PHA1005 and PHB3002), X-ray diffraction patterns show three peaks at 2θ = 9.55, 19.07 and 28.71 that correspond to the addition of talc (usually used by manufacturers to control the nucleation of the polymer). To corroborate the chemical structure of the original clay included in the neat polymers, EDX was carried out. The results confirmed the incorporation of talc.

The diffraction patterns of T1 and T2 shows the expected structure for sepiolite organoclays, with the principle peak being at 2θ = 7.29, showing highest intensity. Results agree with those of Penning et al. as the basal interlayer distance of pristine sepiolite seems not to be altered by the silanisation process [77], and as the authors had corroborating calculations for the basal distance for d(1,2,1) and d(1,2,0), respectively (see Table 3). In addition, T3 presents three well-differentiated peaks at 2θ = 14.03, 19.83 and 61.9, which are typical of montmorillonite organoclay. These outcomes agree well with results previously reported in the literature [78–82].

The effects of each nanoclay on PHB226 and therefore on P3HB are different for each case. The peak associated with 2θ = 7.29 suffers from variations when blending the polymers with the nanoclays. T1 presents higher intensity than T2, which indicates that T2 presents a more effective interaction with the polymer. This result may be contradictory to the findings of DSC. At times, the greater the amount of organic modifier in clays, the greater the impediment to debundle (T2) or exfoliate (T3), and this seems to be the behaviour observed between T1 (modified) and T2 (natural). Moreover, for T3, the peak has completely disappeared, which may indicate the complete intercalation or exfoliation of the clay sheets, which was expected due to the laminar structure of this nanoclay. PHB226_T1 presents sharper peaks for 2θ = 13.58 and 17.03 than for PHB226_T2 and PHB226_T3 or even the neat PHB226, suggesting a preferred α-crystal orientation for planes (0,2,0) and (1,1,0) and a more ordered structure, which is aligned to the increase in crystallinity observed in DSC results (raising X_c by 5%). Moreover, a well-defined peak can be observed for the blend PHB226_T3 at 2θ = 19.93, indicating that T3 favours the introduction of the β form, which

corroborates the creation of further amorphous regions due to the speeding up of crystallisation kinetics. In addition, the peaks corresponding to talc, 2θ = 19.07 and 28.71, had much lower intensity for PHB226T3, which suggests an intercalation with the talc of the PHB226 blend, producing a high dispersion of these mineral additives.

Table 3. Main crystallographic planes and d-spacing calculated from X-ray diffraction.

Material	D-spacing (Å)								
	(0,2,0)	**(1,1,0)**	**(0,2,1)**	**(1,0,1)**	**(1,1,1)**	**(1,2,1)**	**(1,3,1)**	**(1, 9, 1)**	**(4, 0, 0)**
PHB226	6.517	5.204	4.453	4.131	3.991	3.466	-	-	-
PHA1005	6.546	5.216	4.470*	-	3.995	3.468	-	-	-
PHA3002	6.536	5.204	4.424*	-	3.484	3.285	-	-	-
T1	-	12.120	-	-	-	-	4.311	2.565	3.344
T2	-	12.012	-	-	-	-	4.307	2.561	3.339
T3	-	12.444	-	-	-	-	4.282	2.565	3.342
PHB226_T1	6.514	5.203	4.439	4.060	3.953	3.463	-	-	3.317
PHB226_T2	6.524	5.203	4.389	4.137	3.976	3.465	-	-	3.320
PHB226_T3	6.505	5.197	4.368	4.118	3.912	3.470	-	-	3.268
PHA1005_T1	6.524	5.197	-	-	-	3.536	-	-	-
PHA1005_T2	6.542	5.227	-	4.118	3.929	3.545	-	-	-
PHA1005_T3	6.514	5.215	-	4.096	3.893	3.534	-	-	-
PHA3002_T1	6.514	5.197	-	-	-	3.534	-	-	3.322
PHA3002_T2	6.552	5.215	-	-	-	3.545	-	-	-
PHA3002_T3	6.524	*disappeared	-	4.104	-	3.534	-	-	-

* Almost not discernible/not found.

A global decrease of crystallisation for both P3HB-*co*-4HB blends (PHA1005 and PHA3002) can be observed, as not as many and such well-defined peaks can be found compared to PHB226 (higher-purity P3HB). Regarding PHA1005, 2θ = 13.58 and 17.03 are attenuated for PHA1005_T1 and are supressed for PHA1005_T2 and PHA1005_T3, indicating again the debundling and exfoliation of T2 and T3, respectively. For PHA3002, the addition of sepiolite T1 and T2 accentuates the α-form crystal formation, as again, the peaks at 2θ = 13.58 and 17.03 appear to sharpen compared to neat PHA3002 and PHA3002_T3. Often, if a peak is shifted to a lower angle or is reduced in intensity, it can be produced by the increase in the interplanar distance. It is usually an indication of good dispersion. The d-spacing calculated from the XRD figures for all samples is listed in Table 3. D-spacing for (P3HB-*co*-P4HB) apparently decreases when 4HB content is increased (PHA3002). These differences in basal distance can be appreciated in Table 3 for all diffracted angles and with particular attention at d(1,1,1) and d(1,2,1).

The basal distance has been increased for the main α-crystal planes in the case of T2 for PHB226 and PHA3002. Disappearance of the associated peak for PHA3002_T3 is also a relevant signal for a new order in the structure, probably induced due to exfoliation.

4. Conclusions

The present work demonstrates an industrial methodology to produce novel nanobiocomposite materials. Nine formulations were developed by adding 3 wt. % of sepiolite (T2), modified sepiolite via aminosilanes (T1) and montmorillonite (T3). Each nanoclay represents a different polar behaviour passing from one extreme to the other (polar, medium polarity and nonpolar). The different nanoclays were compounded into three types of commercial PHA matrixes: PHB226 (P3HB), PHA1005 and PHA3002 (P3HB-*co*-P4HB with different molar ratios of 4HB, being 17 % and 23.5 %, respectively). Results of NMR and EDX permitted us to better understand the composition of the

commercial blends, as these contain talc, plasticisers, and even other polyesters. Therefore, we are dealing with complex quaternary and quinary composites.

For PHA1005 and PHA3002, two characteristic melting zones rich in 4HB and 3HB crystals are found at around 157 °C and 167 °C, respectively. A higher degree of crystallinity is observed for PHA1005 than for PHA3002, which a priori may seem contradictory. However, the results show the importance of nucleation kinetics which greatly affects the crystallisation process, as well as the appearance of RAF zones. The addition of nanoclays decreases Tm, which indicates the formation of smaller crystals. As a general conclusion, although minor exceptions appear, it can be said that T1 increases the Xc of the matrixes, T2 does not seem to modify it and T3 tends to decrease the overall Xc.

From the XRD patterns, we notice the appearance of α and β crystals typical of P3HB, as well as natural peaks proper tosepiolite, talc and montmorillonite. The appearance of β crystals confirms the formation of RAF zones, particularly for PHA1005. In addition, XRD confirms the exfoliation of montmorillonite, as well as the lack of complete debundling of both sepiolites. The grafting of aminosilane groups on top of the sepiolite surface is intended to favour the affinity and compatibility of the clay for the polymer; however, in this case, it acts as an impediment for dispersion. A good interaction between the nanoclay and the polymer is confirmed when mechanical properties are evaluated. The greatest mechanical improvement in terms of higher stiffness and toughness under tensile and flexural forces can be found for PHB226_T1. T3 produces significant overall improvement of the matrixes, but not as much as T1 does, and hence the polar/functional behaviour may predominate over dispersion to achieve good thermomechanical properties in complex polymer systems such as the ones selected. Anyhow, dispersion achieved in T1, T2 and T3 is highly relevant compared with literature results.

Our findings show impressive mechanical enhancements. Therefore, we believe that optimisation of the production parameters of the blend during extrusion compounding is critical to maximise the potential of any nanoparticle in the production of nanobiocomposites (being the lowest temperature as possible, medium to high screw speed and an low shear screw profile).

Author Contributions: L.G.-Q. conceived the work, carried out the experimental work, contributed to the scientific discussion and wrote the manuscript.; A.F. contributed to scientific discussion and reviewed the manuscript; P.C. designed the methodology, contributed in the interpretation of results and scientific discussion, obtained funding and reviewed the manuscript.

Funding: The authors gratefully acknowledge the Government of Aragón (DGA) under the project T08_17R (I+AITIIP) for support in financial aid for this publication.

Acknowledgments: The authors acknowledge TOLSA for kindly providing the nanoclays used for this research.

Conflicts of Interest: The authors declare no conflict of interest.

References

1. Plastics Europe, Plastics—the Facts 2018. An analysis of European plastics production, demand and waste data. (https://www.plasticseurope.org/es/resources/publications/619-plastics-facts-2018) (accessed on 1 March 2019).
2. PlasticsEurope, Plastics—the Facts 2015. An analysis of European plastics production, demand and waste data. (https://www.plasticseurope.org/93-plastics-facts-2015) (accessed on 1 March 2019).
3. Available online: https://www.cnbc.com/2018/04/16/climate-change-china-bans-import-of-foreign-waste-to-stop-pollution.html (accessed on 1 March 2019).
4. Available online: https://www.reuters.com/article/us-eu-environment/eu-targets-recycling-as-china-bans-plastic-waste-imports-idUSKBN1F51SP (accessed on 1 March 2019).
5. European Commission. *Communication from the Commission to the European Parliament, the Council, the European Economic and Social Committee and the Committee of the Region*s; A European Strategy for Plastics in a Circular Economy; European Commission: Brussels, Belgium, 2018.

6. European Commision. A European Strategy for Plastics in a Circular Economy, 2015. Available online: http://ec.europa.eu/environment/circular-economy/pdf/plastics-strategy-brochure.pdf (accessed on 1 March 2019).
7. Kuang, T.; Ju, J.; Yang, Z.; Geng, L.; Peng, X. A facile approach towards fabrication of lightweight biodegradable poly(butylene succinate)/carbon fiber composite foams with high electrical conductivity and strength, *Compos. Sci. Technol.* **2018**, *159*, 171–179, doi:10.1016/j.compscitech.2018.02.021.
8. Gao, S.; Tang, G.; Hua, D.; Xiong, R.; Han, J.; Jiang, S.; Zhang, Q.; Huang, C. Stimuli-responsive bio-based polymeric systems and their applications. *J. Mater. Chem. B* **2019**, 1–21, doi:10.1039/c8tb02491j.
9. Kuang, T.; Chang, L.; Chen, F.; Sheng, Y.; Fu, D.; Peng, X. Facile preparation of lightweight high-strength biodegradable polymer/multi-walled carbon nanotubes nanocomposite foams for electromagnetic interference shielding. *Carbon* **2016**, *105*, 305–313, doi:10.1016/j.carbon.2016.04.052.
10. European Bioplastics. *Bioplastics Market Data Report*; 2016. (https://docs.european-bioplastics.org/publications/EUBP_Bioplastics_market_data_report_2016.pdf) (accessed on 1 March 2019).
11. Dreizen, C. *2020 Bioplastics Market Forecast*; Sustainable Packaging Coalition (GREENBLUE); 2017. https://sustainablepackaging.org/2020-bioplastics-market-forecast/ (accessed on 1 March 2019).
12. La Rosa, A.D. *Biopolymers and Biotech Admixtures for Eco-Efficient Construction Materials*, 1st ed.; Woodhead Publishing: Cambridge, UK, 2016; ISBN: 9780081002148.
13. Ipsita; R.; Visakh, P.M. Polyhydroxyalkanoate (PHA) Based Blends, Composites and Nanocomposites. *R. Soc. Chem.* **2015**, doi:10.1039/9781782622314-FP001.
14. Wang, S.; Chen, W.; Xiang, H.; Yang, J.; Zhou, Z.; Zhu, M. Modification and Potential Application of Short-Chain-Length Polyhydroxyalkanoate (SCL-PHA). *Polymers* **2016**, *8*, 273, doi:10.3390/polym8080273.
15. Sudesh, K.; Iwata, T. Sustainability of Biobased and Biodegradable Plastics. *Clean* **2008**, *36*, 433–442, doi:10.1002/clen.200700183.
16. Jirage, A.; Baravkar, V.; Kate, V.; Payghan, S.: Disouza, J. Poly-β-Hydroxybutyrate: Intriguing Biopolymer in Biomedical Applications and Pharma Formulation Trends. *Int. J. Pharm. Biol. Arch.* **2013**, *4*, 1107–1118.
17. Shrivastav, A.; Kim, H.Y.; Kim, Y.R. Advances in the Applications of Polyhydroxyalkanoate Nanoparticles for Novel Drug Delivery System. *Biomed Res. Int.* **2013**, 1–12, doi:10.1155/2013/581684.
18. Kok, F.; Hasirci, V. Chapter 15: Polyhydroxybutyrate and Its Copolymers: Applications in the Medical Field. In *Tissue Engineering and Novel Delivery Systems*; Marcel Dekker: New York, NY, USA, 2004.
19. Chaos, A.; Sangroniz, A.; Gonzalez, A.; Iriarte, V.; Sarasua, J.R.; del Río, J.; Etxeberria, A. Tributyl citrate as an effective plasticizer for biodegradable polymers: Effect of the plasticizer on the free volume, transport and mechanical properties. *Polym. Int.* **2018**, doi:10.1002/pi.5705.
20. Milani, P.; França, D.; Balieiro, A.G.; Faez, R. Polymers and its applications in agriculture. *Polímeros* **2017**, *27*, 256–266.
21. Mozejko-Ciesielska, J.; Kiewisz, R. Bacterial polyhydroxyalkanoates: Still fabulous? *Microbiol. Res.* **2016**, *192*, 271–282.
22. Choi, J.I.; Lee, S.Y. Efficient and economical recovery of poly(3-hydroxybutyrate) from recombinant Escherichia coli by simple digestion with chemicals. *Biotechnol. Bioeng.* **1999**, *62*, 546–553.
23. Koller, M.; Bona, R.; Chiellini, E.; Braunegg, G. Extraction of short-chain-length poly- [(R)-hydroxyalkanoates] (scl-PHA) by the antisolvent acetone under elevated temperature and pressure. *Biotechnol. Lett.* **2013**, *35*, 1023–1028, doi:10.1007/s10529-013-1185-7.
24. Khosravi-Darani, K.; Vasheghani-Farahani, E. Application of supercritical fluid extraction in biotechnology. *Crit. Rev. Biotechnol.* **2005**, *25*, 1–12, doi:10.1080/07388550500354841.
25. Peelman, N.; Ragaert, P.; Ragaert, K.; Erkoç, M.; Van Brempt, W.; Faelens, F.; Cardon, L. Heat resistance of biobased materials, evaluation and effect of processing techniques and additives. *Polym. Eng. Sci.* **2017**, *58*, 513–520.
26. Kai, D.; Chong, H.M.; Chow, L.P.; Jiang, L.; Lin, Q.; Zhang, K.; Loh, X.J. Strong and biocompatible lignin/poly(3-hydroxybutyrate) composite nanofibers. *Compos. Sci. Technol.* **2018**, *158*, 26–33.
27. Han, H.; Wang, X.; Wu, D. Isothermal Crystallization Kinetics, Morphology, and Mechanical Properties of Biocomposites Based on Poly(3-hydroxybutyrate-*co*-4-hydroxybutyrate) and Recycled Carbon Fiber. *Ind. Eng. Chem. Res.* **2012**, *51*, 14047−14060, doi:10.1021/ie3012352.
28. Zini, E.; Focarete, M.L.; Noda, I.; Scandola, M. Bio-composite of bacterial poly(3-hydroxybutyrate-*co*-3-hydroxyhexanoate) reinforced with vegetable fibers. *Compos. Sci. Technol.* **2007**, *67*, 2085–2094.

29. An, S.; Ma, X. Properties and structure of poly(3-hydroxybutyrate-*co*-4-hydroxybutyrate)/wood fiber biodegradable composites modified with maleic anhydride. *Ind. Crop. Prod.* **2017**, *109*, 882–888.
30. Al, G.; Aydemir, D.; Kaygin, B.; Ayrilmis, N.; Gunduz, G. Preparation and characterization of biopolymer nanocomposites from cellulose nanofibrils and nanoclays. *J. Compos. Mater.* **2017**, *52*, 689–700.
31. Larsson, M.; Hetherington, C.J.D.; Wallenberg, R.; Jannasch, P. Effect of hydrophobically modified graphene oxide on the properties of poly(3-hydroxybutyrate-*co*-4-hydroxybutyrate). *Polymer* **2017**, *108*, 66–77.
32. Bumbudsanpharoke, N.; Ko, S. Nanoclays in Food and Beverage Packaging—Review article. *J. Nanomater.* **2019**, 1–13, doi:10.1155/2019/8927167.
33. Ramos, Ó.L.; Pereira, R.N.; Cerqueira, M.A.; Martins, J.R.; Teixeira, J.A.; Malcata, F.X.; Vicente, A.A. Bio-Based Nanocomposites for Food Packaging and Their Effect in Food Quality and Safety. *Food Packag. Preserv.* **2018**, 271–306, doi:10.1016/b978-0-12-811516-9.00008-7.
34. Franchini, E. Structuration of Nano-Objects in Epoxy-Based Polymer Systems: Nanoparticles & Nanoclusters for Improved Fire Retardant Properties, Institut National des Sciences Appliquées de Lyon, Lyon. Ph.D. Thesis, INSA Lyon, Villeurbanne, France, 2008.
35. Falco, G.; Giulieri, F.; Volle, N.; Pagnotta, S.; Sbirrazzuoli, N.; Peuvrel Disdier, E.; Mija, A. Self-organization of sepiolite fibbers in a biobased thermoset. *Compos. Sci. Technol.* **2019**, *171*, 226–233.
36. Zheng, Y.; Zaoui, A. Mechanical behavior in hydrated Na-montmorillonite clay. *Phys. A* **2018**, *505*, 582–590.
37. Wang, S.; Song, C.; Chen, G.; Guo, T.; Liu, J.; Zhang, B.; Takeuchi, S. Characteristics and biodegradation properties of poly(3-hydroxybutyrate-*co*-3-hydroxyvalerate)/organophilic montmorillonite (PHBV/OMMT) nanocomposite. *Polym. Degrad. Stab.* **2005**, *87*, 69–76.
38. Peinado, V.; García, L.; Fernández, A.; Castell, P. Novel lightweight foamed poly(lactic acid) reinforced with different loadings of functionalised sepiolite. *Compos. Sci. Technol.* **2014**, *101*, 17–23, doi:10.1016/j.compscitech.2014.06.025.
39. Khandal, D.; Pollet, E.; Avérous, L. Elaboration and behavior of poly(3-hydroxybutyrate-*co*-4-hydroxybutyrate)- nano-biocomposites based on montmorillonite or sepiolite nanoclays. *Eur. Polym. J.* **2016**, *81*, 64–76, doi:10.1016/j.eurpolymj.2016.05.025.
40. Reinsch, V.; Kelley, S. Crystallization of poly(hydroxybutyrate-cohydroxyvalerate) in wood fiber-reinforced composite. *J. Appl. Sci.* **1997**, *64*, 1785–1796.
41. Koller, M. Poly(hydroxyalkanoates) for Food Packaging: Application and Attempts towards Implementation. *Appl. Food Biotechnol.* **2014**, *1*, 3–15.
42. Cong, C.; Zhang, S.; Xu, R.; Lu, W.; Yu, D. The Influence of 4HB Content on the Properties of Poly(3-hydroxylbutyrate-*co*-4-hydroxylbutyrate) based on Melt Molded Sheets. *J. Appl. Polym. Sci.* **2008**, *109*, 1962–1967.
43. Avérous, L. Nano- and Biocomposites. *Mater. Today* **2010**, *13*, 57, doi:10.1016/S1369-7021(10)70063-8.
44. Botana, A.; Mollo, M.; Eisenberg, P.; Torres Sanchez, R.M. Effect of modified montmorillonite on biodegradable PHB nanocomposites. *Appl. Clay Sci.* **2010**, *47*, 263–270, doi:10.1016/j.clay.2009.11.001.
45. Czerniecka-Kubicka, A.; Fracz, W.; Jasiorski, M.; Błazejewski, W.; Pilch-Pitera, B.; Pyda, M.; Zarzyka, I. Thermal properties of poly(3-hydroxybutyrate) modified by nanoclay. *J. Therm. Anal. Calorim.* **2017**, *128*, 1513–1526, doi:10.1007/s10973-016-6039-9.
46. Corre, Y.M.; Bruzaud, S.; Audic, J.L.; Grohens, Y. Morphology and functional properties of commercial polyhydroxyalkanoates: A comprehensive and comparative study. *Polym. Test.* **2012**, *31*, 226–235, doi:10.1016/j.polymertesting.2011.11.002.
47. Hu, D.; Chung, A.L.; Wu, L.P.; Zhang, X.; Wu, Q.; Chen, J.C.; Chen, G.Q. Biosynthesis and Characterization of Polyhydroxyalkanoate Block Copolymer P3HB-b-P4HB. *Biomacromolecules* **2011**, *12*, 3166–3173, doi:10.1021/bm200660k.
48. Wang, H.-H.; Zhou, X.-R.; Liu, Q.; Chen, G.Q. Biosynthesis of polyhydroxyalkanoate homopolymers by Pseudomonas putida. *Appl. Microbiol. Biotechnol.* **2010**, *89*, 1497–1507, doi:10.1007/s00253-010-2964-x.
49. Mohanty, A.K.; Parulekar, Y. Methods of Making Nanocomposites and Compositions of Rubber Toughened Polyhydroxyalkanoates. U.S. Patent US20070015858A1, 2005.
50. Xiao, N.; Chen, Y.; Shen, X.; Zhang, C.; Yano, S.; Gottschaldt, M.; Schubert, U.S.; Kakuchi, T.; Satoh, T. Synthesis of miktoarm star copolymer Ru(II) complexes by click-to-chelate approach. *Polym. J.* **2013**, *45*, 216–225, doi:10.1038/pj.2012.100.

51. Sun, X.; Liu, J.; Takahashi, I.; Yan, S. Melting and β to α transition behavior of β-PBA and the β-PBA/PVPh blend investigated by synchrotron SAXS and WAXD. *RSC Adv.* **2014**, *4*, 39101, doi:10.1039/c4ra04752d.
52. Koller, M.; Maršálek, L.; de Sousa Dias, M.M.; Braunegg, G. Producing microbial polyhydroxyalkanoate (PHA) biopolyesters in a sustainable manner. *New Biotechnol.* **2017**, *37*, 24–38, doi:10.1016/j.nbt.2016.05.001.
53. Madison, L.L.; Huismann, G.W. Metabolic engineering of poly(3- hydroxyalkanoates): From DNA to plastic. *Microbiol. Mol. Biol. Rev.* **1999**, *63*, 21–53.
54. Sudesh, K.; Abe, H.; Doi, Y. Synthesis, structure and properties of polyhydroxyalkanoates: Biological polyesters. *Prog. Polym. Sci.* **2000**, *25*, 1503–1555, doi:10.1016/S0079-6700(00)00035-6.
55. Wang, H.H.; Zhou, X.R.; Liu, Q.; Chen, G.Q. Biosynthesis of polyhydroxyalkanoates homopolymers by Pseudomonas putida. *Appl. Microbiol. Biotechnol.* **2011**, *89*, 1497–1507, doi:10.1007/s00253-010-2964-x.
56. Utracki, A.L.; Jamieson, A.M. *Polymer Physics: From Suspensions to Nanocomposites and Beyond*; Wiley: Hoboken, NJ, USA, 2010; ISBN 978-0-470-19342-6.
57. Thiré, R.M.; Arruda, L.C.; Barreto, L.S. Morphology and thermal properties of poly(3-hydroxybutyrate-*co*-3-hydroxyvalerate)/attapulgite nanocomposites. *Mater. Res.* **2011**, *14*, 340–344, doi:10.1590/S1516-14392011005000046.
58. Bayarı, S.; Severcan, F. FTIR study of biodegradable biopolymers: P(3HB), P(3HB-*co*-4HB) and P(3HB-*co*-3HV). *J. Mol. Struct.* **2005**, *744–747*, 529–534, doi:10.1016/j.molstruc.2004.12.029.
59. Wang, L.; Wang, X.J.; Zhu, W.F.; Chen, Z.F.; Pan, J.Y.; Xu, K.T. Effect of nucleation agents on the crystallization of poly(3-hydroxybutyrate-*co*-4-hydroxybutyrate) (P3HB4HB). *J. Appl. Polym. Sci.* **2009**, *2*, 1116–1123, doi:10.1002/app.31588.
60. Inoue, Y.; Yoshie, N. Structure and physical properties of bacterially synthesized polyesters. *Prog. Polymer. Sci.* **1992**, *17*, 571–610, doi:10.1016/0079-6700(92)90002-G.
61. Kumar, S.; Hideki, A. *Practical Guide to Microbial Polyhydroxyalkanoates. Chapter 6: Crystalline and Solid-State Structures of Polyhydroxyalkanoates (PHA)*; Smithers Rapra: Shrewsbury, UK, 2010; pp. 1–160, ISBN 1847351174.
62. Di Lorenzo, M.L.; Gazzano, M.; Righetti, M.C. The Role of the Rigid Amorphous Fraction on Cold Crystallization of Poly(3-hydroxybutyrate). *Macromolecules* **2012**, *45*, 5684–5691, doi:10.1021/ma3010907.
63. Zhang, J.; Chu, T.L. Property analysis of biodegradable material P(3HB-*co*-4HB). *Adv. Mater. Res.* **2012**, *380*, 168–172, doi:10.4028/www.scientific.net/AMR.380.168.
64. Akhtar, S.; Pouton, C.W.; Notarianni, L.J. Crystallization behaviour and drug release from bacterial polyhydroxyalkanoates. *Polymer* **1992**, *33*, 117–126, doi:10.1016/0032-3861(92)90570-M.
65. Volova, T.G.; Vinogradova, O.N.; Zhila, N.O.; Peterson, I.V.; Kiselev, E.G.; Vasiliev, A.D.; Sukovatiy, A.G.; Shishatskaya, E.I. Properties of a novel quaterpolymer P(3HB/4HB/3HV/3HHx). *Polymer* **2016**, *101*, 67–74, doi:10.1016/j.polymer.2016.08.048.
66. Kunioka, M.; Tamaki, A.; Doi, Y. Crystalline and Thermal Properties of Bacterial Copolyesters: Poly(3-hydroxybutyrate-*co*-3-hydroxyvalerate) and Poly(3- hydroxybutyrate-*co*-4-hydroxybutyrate). *Macromolecules* **1989**, *22*, 694–697, doi:10.1021/ma00192a031.
67. Kabe, T.; Sato, T.; Kasuya, K.; Hikima, T.; Takata, M.; Iwata, T. Transition of spherulite morphology in a crystalline/crystalline binary blend of biodegradable microbial polyesters. *Polymer* **2014**, *55*, 271–277, doi:10.1016/j.polymer.2013.11.038.
68. Alavi, S.; Thomas, S.; Sandeep, K.P.; Kalarikal, N.; Varghese, J.; Yaragalla, S. *Polymers for Packaging Applications*; Appe Academic Press, CRC Press: Boca Raton, FL, USA, 2014; ISBN 9781926895772.
69. Ray, D. *Biocomposites for High-Performance Applications, Current Barriers and Future Needs Towards Industrial Development*; Woodhead Publishing Series in Composites Science and Engineering: Elsevier, Cambridge, UK, 2017; pp. 1–336, ISBN 9780081007945.
70. Penning, J.P.; St John Manley, R. Miscible Blends of Two Crystalline Polymers. 1. Phase Behavior and Miscibility in Blends of Poly(vinylidene fluoride) and Poly(1,4-butylene adipate). *Macromolecules* **1996**, *29*, 77–83, doi:10.1021/ma950651t.
71. Ruiz-Hitzky, E.; Aranda, P.; Alvarez, A.; Santarén, J.; Esteban-Cubillo, A. *Developments in Palygorskite-Sepiolite Research. A New Outlook on These Nanomaterials*; Galán, E., Singer, A., Eds.; Elsevier, B.V.: Oxford, UK, 2011; pp. 393–452, ISBN 9780444536082.
72. Ruiz-Hitzky, E.; Van Meerbeek, A. *Handbook of Clay Science*, Development in Clay Science, ed.; Bergaya, F., Theng, B.K.G., Lagaly, G., Eds.; Elsevier: Amsterdam, The Netherlands, 2006; pp. 583–621, ISBN 9780080457635.

73. Lvov, Y.; Guo, B.; Fakhrullin, R.F. Functional Polymer Composites with Nanoclays. *REC Smart Mater.* **2016**, doi:10.1039/9781782626725.
74. Karami, S.; Ahmadi, Z.; Nazockdast, H.; Rabolt, J.F.; Noda, I.; Chase, B.D. The effect of well-dispersed nanoclay on isothermal and non-isothermal crystallization kinetics of PHB/LDPE blends. *Mater. Res. Express* **2018**, *5*, 015316, doi:10.1088/2053-1591/aaa747.
75. Bruckner, S.; Meille, S.V.; Malpezzi, L. The Structure of Poly(D-(-)-@-hydroxybutyrate). A Refinement Based on the Rietveld Method. *Macromolecules* **1988**, *21*, 967–972, doi:10.1021/ma00182a021.
76. Anbukarasu, P.; Sauvageau, D.; Elias, A. Tuning the properties of polyhydroxybutyrate films using acetic acid via solvent casting. *Sci. Rep.* **2015**, *5*, 17884; doi:10.1038/srep17884.
77. Jalali, A.M.; Taromi, F.A.; Atai, M.; Solhi, L. Effect of reaction conditions on silanisation of sepiolite nanoparticles. *J. Exp. Nanosci.* **2016**, *11*, 1171–1183, doi:10.1080/17458080.2016.1200147.
78. Patrício, A.C.L.; da Silva, M.M.; de Sousa, A.K.F.; Mota, M.F.; Freire Rodrigues, M.G. SEM, XRF, XRD, Nitrogen Adsorption, Fosters Swelling and Capacity Adsorption Characterization of Cloisite 30 B. *Mater. Sci. Forum* **2012**, *727–728*, 1591–1595, doi:10.4028/www.scientific.net/msf.727-728.1591.
79. Xue, M.-L.; Yu, Y.-L.; Li, P.; Preparation, Dispersion, and Crystallization of the Poly(trimethylene terephthalate)/Organically Modified montmorillonite (PTT/MMT) Nanocomposites. *J. Macromol. Sci. Part B* **2010**, *49*, 1105–1116, doi:10.1080/00222341003609385.
80. Sarier, N.; Onder, E.; Ersoy, S. The modification of Na-montmorillonite by salts of fatty acids: An easy intercalation process. *Colloids Surf. A Physicochem. Eng. Asp.* **2010**, *371*, 40–49, doi:10.1016/j.colsurfa.2010.08.061.
81. Høgsaa, B.; Fini, E.H.; Christiansen, J.D.; Hung, A.; Mousavi, M.; Jensen, E.A.; Pahlavan, F.; Pedersen, T.H.; Sanporean, C.G. A Novel Bioresidue to Compatibilize Sodium montmorillonite and Linear Low Density Polyethylene. *Ind. Eng. Chem. Res.* **2018**, *57*, 1213–1224, doi:10.1021/acs.iecr.7b04178.
82. Krupskaya, V.V.; Zakusin, S.V.; Tyupina, E.A.; Dorzhieva, O.V.; Zhukhlistov, A.P.; Belousov, P.E.; Timofeeva, M.N. Experimental Study of montmorillonite Structure and Transformation of Its Properties under Treatment with Inorganic Acid Solutions. *Minerals* **2017**, *7*, 49, doi:10.3390/min7040049.

ARTICULO 2

Reducing off-Flavour in Commercially Available Polyhydroxyalkanoate Materials by Autooxidation through Compounding with Organoclays

García-Quiles, L.; Valdés, A.; Cuello, Á.F.; Jiménez, A.; Garrigós, M.C.; Castell, P.
Polymers 2019, 11, 945.
Impact Factor: 3.426 (2019); 5-Year Impact Factor: 3.636 (2019) – Q1

Los polihidroxialcanoatos (PHA) comerciales emiten un olor desagradable que puede afectar negativamente a la calidad del producto plástico final. La causa de este olor a rancio se atribuye a la forma en la que es producido: primero mediante fermentación bacteriana (habitualmente gram-negativas), seguido de una etapa de extracción del polímero del interior de las bacterias y posteriormente purificado. Tas la etapa de extracción, los glicolípidos de la membrana celular se oxidan y frecuentemente quedan restos adheridos a los gránulos de PHA. Además, el uso de disolventes para poder extraer el PHA también puede afectar al olor final del material.

El **objetivo** de este artículo es el desarrollo de bionanocompuestos de PHA personalizados para aplicaciones industriales. Compuestos que contienen nanoarcillas organomodificadas con altas propiedades de adsorbancia capaces de capturar compuestos volátiles responsables del olor desagradable. Para ello, se ha definido una metodología ad-hoc para la detección e identificación de los volátiles más relevantes (aquellos a los que se les puede atribuir el olor a rancio) liberados debido a la degradación oxidativa del material. La metodología establecida utiliza la técnica de *microextracción en fase sólida de espacio de cabeza (HS-SPME)*, y se completa con una caracterización térmica (TGA) y estructural (SEM) de los bionanocompuestos estudiados. Dichas formulaciones son las desarrolladas y caracterizadas en el Artículo 1.

Como **conclusión** principal el estudio demuestra que el efecto secuestrante alcanzado depende tanto de la naturaleza del volátil (teniendo una gran dependencia con el peso molecular y su estructura – si es lineal o si contiene grupos

aromáticos) como de la afinidad de la nanoarcilla con cada matriz. La Figura 37 resume qué nanoarcilla funciona mejor con cada PHA para reducir la liberación de compuestos volátiles.

Volatile	PHA 1005	PHA 3002	PHB 226
1-Hexanol	T3	T1	T1
Heptanal	T2	T1	T1
Octanal	T3	T2	T1
Decanal	T2	T3	T2
α-Methylstyrene	T2	T3	T2
Benzaldehyde	T2	T2	T2

Figura 40: Resultados Artículo 2

No obstante, si un transformador de plástico no desease abordar un subgrupo particular de volátiles sino tratar de cubrir la mayor cantidad posible de ellos, T2 resultaría la candidata más versátil.

Aportes técnico-científicos:

- Desarrollo de una metodología basada en HS-SPME por primera vez aplicada, bajo el uso de patrones, en la identificación de volátiles en PHAs y que con el conjunto de tests de caracterización desarrollados por la doctoranda, aportan una visión clara del efecto que producen las nanoarcillas modificadas en la captación de compuestos volátiles producidos por la autooxidación del polímero. La técnica HS-SPME se utiliza en algunas aplicaciones del sector alimentación para evaluar por ejemplo los volátiles que conforman la fragancia en el vino, o en este caso particular, se replicó un protocolo originalmente ideado para detectar volátiles en alimentos grasos (frutos secos) por una tesina anterior de una doctoranda de la Universidad de Alicante.

polymers

MDPI

Article

Reducing off-Flavour in Commercially Available Polyhydroxyalkanoate Materials by Autooxidation through Compounding with Organoclays

Lidia García-Quiles [1,*], Arantzazu Valdés [2], Ángel Fernández Cuello [3], Alfonso Jiménez [4], María del Carmen Garrigós [4] and Pere Castell [5,*]

1 Tecnopackaging, Polígono Industrial Empresarium C/Romero N° 12, 50720 Zaragoza, Spain
2 Analytical Chemistry, Nutrition & Food Sciences Department, University of Alicante, P.O. Box 99, 03080 Alicante, Spain; arancha.valdes@ua.es
3 Escuela de Ingeniería y Arquitectura, University of Zaragoza, Av. María de Luna, 3, 50018 Zaragoza, Spain; afernan@unizar.es
4 NANOBIOPOL Research Group, University of Alicante, San Vicente del Raspeig, 03690 Alicante, Spain; alfjimenez@ua.es (A.J.); mc.garrigos@ua.es (M.d.C.G.)
5 Fundación Aitiip, Polígono Industrial Empresarium C/Romero N° 12, 50720 Zaragoza, Spain
* Correspondence: lgarcia@tecnopackaging.com (L.G.-Q.); pere.castell@aitiip.com (P.C.); Tel.: +34-607-018-803 (L.G.-Q.); +34-976-46-45-44 (P.C.)

Received: 30 April 2019; Accepted: 29 May 2019; Published: 31 May 2019

Abstract: Polyhydroxyalkanoates (PHAs) are nowadays considered competent candidates to replace traditional plastics in several market sectors. However, commercial PHA materials exhibit unsatisfactory smells that can negatively affect the quality of the final product. The cause of this typical rancid odour is attributed to oxidized cell membrane glycolipids, coming from Gram-negative production strains, which remain frequently attached to PHAs granules after the extraction stage. The aim of this research is the development of customised PHA bio-nano-composites for industrial applications containing organomodified nanoclays with high adsorbance properties able to capture volatile compounds responsible for the displeasing fragrance. To this end, a methodology for the detection and identification of the key volatiles released due to oxidative degradation of PHAs has been established using a headspace solid-phase microextraction technique. We report the development of nine bio-nano-composite materials based on three types of commercial PHA matrices loaded with three species of nanoclays which represent a different polar behaviour. It has been demonstrated that although the reached outcoming effect depends on the volatile nature, natural sepiolite might result in the most versatile candidate for any the PHA matrices selected.

Keywords: biopolymers; nanoclays; bio-nanocomposites; extrusion-compounding; polyhydroxyalkanoates; thermal properties; microstructure; volatiles; autoxidation; thermal gravimetric analysis; scanning electron microscope; headspace solid phase microextraction

1. Introduction

The poly(hydroxyalkanoates) (PHAs) market is poised to grow during the next decade at a compounded annual growth rate of 6.3% gaining more and more attention in the biopolymers market [1]. PHA biopolyesters are increasingly used owing to its biodegradable nature and processing versatility representing a potential sustainable replacement for fossil oil-based commodities [2]. PHA biopolymers are formed mainly from saturated and unsaturated hydroxyalkanoic acids in which the monomer unit harbours a side chain R group which is usually a saturated alkyl group. These polymers are generally classified in two categories depending on the number of carbon atoms in their monomer

units: small chain length (*scl*)-PHA when the monomer units contain from three to five carbon atoms and medium chain length (mcl)-PHA with monomer units possessing from six to 14 carbon atoms [3,4]. These features give rise to diverse PHA monomers and polymers with tailored molecular weights and melting points providing broad properties, such as isotactic poly(3-hydroxybutyrate) P3HB; poly(3-hydroxybutyrate-*co*-hydroxyvalerate) PHBV copolymer; 3-hydroxypropionate (3HP); 3-hydroxyoctanoate (3HO); or 4-hydroxybutyrate (4HB) among others [2,5].

Accumulation of PHA seems to be a common metabolic strategy adopted by many bacteria to cope with a series of various stress factors in the environment [6]. PHA biopolyesters are used as carbon and energy storage and are accumulated by various prokaryotes as intracellular "carbonosomes" [7] in the form of granules of 0.2–0.5 microns inside these bacterial cells in an amorphous state (chain disordered) are covered by an outer monolayer of phospholipids and proteins [8]. To recover the PHA granules is necessary to break bacterial cells, remove the monolayer and isolate the PHA with high molecular chains (unbroken chains). To this end, a combination of solvents is used, usually based in organic solvents and/or chlorinated. These solvents modify the cell membrane permeability and dissolve the PHA, which is able to escape through the monolayer and cell wall [9,10]. Recent works have studied the effect that carbon sources may have on the final odours released by PHA monomers [11].

The proposal of efficient methods to purify microbial PHAs to meet the legislative requirements in the pharmaceutical, medical or food sectors has been investigated [12,13]. Simple chemical methods, such as combinations of organic PHA solvents and anti-solvent or high-pressure extraction, can be applied to remove the remaining lipids and endotoxins that are frequently attached to PHAs from Gram-negative production strains [14]. In the case of PHAs, lipid residues often remain attached to the biopolymer after extraction, causing a typical rancid odour and smell that can negatively affect the quality of the final product. The flavour threshold of a particular chemical can vary greatly and is defined as the minimum quantity of a substance, which can be detected by 50% of the taste panel [15]. Regardless of the oxidation mechanism, it is recognised that lipids are oxidised to odourless and flavourless intermediates that could break into molecules giving off-flavours. These conditions are associated with the production of free radicals by autoxidation which have been recognized as a potential source of food quality shortcomings of PHA for many applications such as packaging [16,17]. Nowadays, plastic product converters purchase commercial PHA materials with unsatisfactory smelling because current PHA production methods are not solving this particular disadvantage. Our proposed solution approaches the compounding stage of customised blends for industrial applications by using nanoclays with high adsorbance properties able to capture volatile compounds responsible for the displeasing fragrance.

Up to now, microextraction methods have been used for the separation of specific analytes from complex matrices with high reproducibility, selectivity and sensitivity [18]. This is a very important process commonly used in the food sector in order to analyse the aroma properties. Among several extraction methods widely used for the extraction and determination of flavour compounds, the most frequently applied are those based on headspace (HS) analysis. Solid phase microextraction (SPME) is a sample preparation technique based on sorption that constitutes a reliable tool for the analysis of organic volatile and semi-volatile compounds [19]. In the plastic sector, the analysis of volatile organic compounds emissions from plastic and rubber materials through HS-SPME and other techniques such as (MAE)-GC-MS, (SPM)-GC-MS, (TGA)-GC-MS etc have been performed as a useful method for understanding polymer degradation and object damage made of conventional oil-based polymers such as high-density polyethylene (HDPE), low density polyethylene (LDPE), polyacrylonitrile (PAN), polyvinyl chloride (PVC), polypropylene (PP), polystyrene (PS), polymethyl methacrylate (PMMA), polyurethane (PU), and nylon 6,6 (PA) [20–22] Specific volatile emissions can be related to deterioration, including loss of additives and polymer degradation [23].

However, headspace solid-phase microextraction (HS-SPME) has not been used for the analysis of those volatile compounds released from PHAs. This technique used by the authors is combined with gas chromatography ion-trap/mass spectrometry (GC-IT/MS) in order to quantify a large number of

volatile compounds in PHA samples. To the best of our knowledge, this is the first time that a method for analysis of volatiles is used in PHA final/commercial materials for such purpose.

In the present work, three PHA materials were reinforced with organically modified and unmodified Sepiolite and Montmorillonite as described in the materials section. Clays and zeolite exchanged with various cationic surfactants have been shown to be effective adsorbents for a variety of organic compounds [24]. Sepiolite has outstanding sorption capacity and may adsorb a large variety of molecules as vapours as well as liquids due to its natural structure that forms inner zeolitic channels that provides a high microporosity and large specific surface area [25]. Sepiolite fibre leads to the presence of numerous silanol groups (Si–OH) all along the edges of the fibre [26] which are useful as fillers providing reinforcing characteristics with polar polymers [27]. Sodium montmorillonite (Na-MMT) is a smectite nanoclay that has two tetrahedral sheets of silica sandwiching a central octahedral sheet of alumina and largely used in industry too due to its swelling and adsorption properties [28,29].

The aim of this research was the development and characterization of novel composite materials based on different PHA matrices to diminish the release of undesirable oxidised lipid molecules through the introduction of organoclays. The objective is to establish a methodology for the identification of the key volatiles released by commercial PHAs which are responsible for unpleasant odours, and demonstrate that the introduction of commercial organoclays can be an efficient approach to capture those volatiles and reduce the displeasing aroma. The studied techniques used in this paper can be useful for processors in order to monitor the oxidative degradation of PHAs with storage time and to evaluate their acceptance on the market.

2. Materials and Methods

2.1. Materials

Three commercial PHA materials were used as a matrix. These were Mirel PHA1005 and Mirel PHA3002 (food contact P3HB-*co*-P4HB, purchased from Metabolix, Cambridge, MA, USA), and Biomer PHB P226 (homopolymer P3HB grade purchased from Biomer, Krailling, Germany).

Three different modified and unmodified organoclays were kindly provided by TOLSA (Madrid, Spain). A natural sepiolite (T2), a modified Sepiolite with aminosilane groups on its surface (T1) and a sodium montmorillonite modified with a quaternary ammonium salt (T3). The three candidates selected present different behaviours from polar (T1) and neutral (T2) to non-polar (T3) feature which directly affects their affinity for the PHAs polyesters (Table 1).

Table 1. Summary of material formulations. Table reproduced with permission of García-Quiles et al. [30].

Material Formulation	Commercial Matrix Used	Nature of the PHA	Type of Reinforcement (3 wt %)
PHA1005	PHA1005 (Metabolix)	P3HB-*co*-P4HB	(3HB-*co*-17 mol % 4HB) & Talc
PHA1005_T1	PHA1005 (Metabolix)	P3HB-*co*-P4HB	T1: Aminosilane Sepiolite
PHA1005_T2	PHA1005 (Metabolix)	P3HB-*co*-P4HB	T2: Natural Sepiolite
PHA1005_T3	PHA1005 (Metabolix)	P3HB-*co*-P4HB	T3: Sodium Montmorillonite-quaternary ammonium salt
PHA3002	PHA3002 (Metabolix)	P3HB-*co*-P4HB	(3HB-*co*-23.5 mol % 4HB) & Talc
PHA3002_T1	PHA3002 (Metabolix)	P3HB-*co*-P4HB	T1: Aminosilane Sepiolite
PHA3002_T2	PHA3002 (Metabolix)	P3HB-*co*-P4HB	T2: Natural Sepiolite
PHA3002_T3	PHA3002 (Metabolix)	P3HB-*co*-P4HB	T3: Sodium Montmorillonite-quaternary ammonium salt
PHB226	PHB226 (Biomer)	P3HB	Traces of PBA and plasticizer found, & Talc
PHB226_T1	PHB226 (Biomer)	P3HB	T1: Aminosilane Sepiolite
PHB226_T2	PHB226 (Biomer)	P3HB	T2: Natural Sepiolite
PHB226_T3	PHB226 (Biomer)	P3HB	T3: Sodium Montmorillonite-quaternary ammonium salt

Chemical patterns for volatile quantification (considered as main responsible for the odour), were purchased from Sigma-Aldrich. These are 1-hexanol, heptanal, octanal, decanal, α-Methylstyrene, 4-methylstyrene and Benzaldehyde.

2.2. Nano-Bio-Composites Preparation

A 26-mm twin-screw Coperion ZSK 26 compounder machine (Stuttgart, Germany) was used to prepare PHA/nanoclay formulations by extrusion-compounding. Twelve different formulations were studied in total accounting for the three control matrixes plus nine composite materials loading them with the three nanoclays at 3 wt % in all cases. The melted polymers and nanoclay powder were mixed at a screw speed of 125 rpm; temperature was increased from 150 °C in the feeding zone up to 165 °C at the nozzle for PHA1005 and PHA3002 (P3HB-*co*-P4HB formulations) and slightly decreased from 140 °C in the feeding zone up to 160 °C at the nozzle when blending PHB226 (P3HB). The compound was extruded through a 2 mm diameter die for a constant output of 10 kg/h. The extrudate was quenched in a water bath at room temperature, dried and cut into pellets. A total amount of 3 to 5 kg per material was produced.

Specimens for mechanical testing were obtained by injection moulding with a JSW 85 EL II electric injection machine (Tokyo, Japan) by following ISO 178 and ISO 527 standards. These were tested and broken samples were used to study the structural properties (results on mechanical properties are out of the scope of this paper). A complete characterization covering the structural, thermal and mechanical behaviour of the formulations developed, understanding the compatibility mechanisms between the different organoclays and the matrices can be found in a previous work carried out by the authors and published at García-Quiles et al.) [30].

2.3. General Characterisation Methods

2.3.1. Scanning Electron Microscopy

Structural properties were evaluated by scanning electron microscopy (SEM) with Hitachi S3400N equipment (Tokyo, Japan) in order to determine the morphology and dispersion of the nanoclay through the biopolymer-based materials. Samples for SEM observation were obtained from fractured mechanical specimens.

Energy-dispersive X-ray spectroscopy (EDX) was also used for samples for chemical characterization.

2.3.2. Thermogravimetric Analysis

Thermal characterisation was carried out by using thermogravimetric analysis (Mettler-Toledo TGA/SDTA 851e, Greifensee, Switzerland). Samples (5.0 ± 0.1 mg) were heated from 25 to 800 °C at 5 °C/min under N_2 atmosphere (50 mL/min).

2.3.3. Analysis of Volatile Compounds by HS-SPME-GC-MS

HS-SPME Extraction Procedure

The sample (1.00 ± 0.01 g) was mixed with 1 mL of distilled water and 2 µL of internal standard 4-methylstyrene (8 mg/kg, Sigma-Aldrich Inc., St. Louis, MO) and a small magnetic stirrer were placed in a 20 mL amber vial sealed with an aluminium pressure cap provided with a pierceable silicone septum. The extraction was carried out using the SPME fibre made of divinylbenzene/carboxen/polydimethylsiloxane (DVB/CAR/PDMS) 50/30 mm, StableFlex, 1 cm long, mounted on a manual support set SPME (Supelco, Bellefonte, PA, USA) [31,32]. The vial with the sample was placed in a water bath under a specific temperature. After 10 min of equilibrium of the sample, the SPME needle was inserted into the vial and exposed to the headspace of the vial for a specific time. After extraction, the fibre desorption was performed in the GC-MS injection port at

250 °C for 12 min (splitless mode). Blank tests were performed prior to the analysis of the samples to ensure that there was no contamination that could cause memory effects.

GC-MS Parameters

The analysis of the volatiles was carried out using an Agilent 6890N GC model gas chromatograph coupled to an Agilent 5973N MS mass spectrometer (Agilent Technologies, Palo Alto, CA, USA) with impact ionization source of electrons (EI 70 eV) and quadrupole analyzer. The temperatures of the transfer line "ion source" and GC-MS were 230 and 250 °C, respectively. A TRB-624 column (30 m × 0.25 mm × 1.4 µm) of Teknokroma was used, which was programmed from 50 °C (maintaining 2 min) to 250 °C (isotherm for 7 min) at 10 °C/min. Helium was used as the carrier gas (1.5 mL/min). The volatile compounds were identified in "scan" mode (m/z 30–550) by comparing their mass spectra with those of the standard compounds and the Wiley compound library. When standards were not available, volatile compounds having ≥80% similarity with Wiley library were tentatively identified using GC-MS spectra only. All patterns obtained from the commercial house Sigma-Aldrich, St. Louis, were quantified by HS-SPME-GC-MS using standard calibration curves. For this, mother solution (5 mg/kg) and working solutions were prepared using distilled water as a solvent. The HS-SPME and GC-MS sampling procedures were carried out as described for the samples. The analytical method used for the quantification was validated in terms of linearity, repeatability and limits of detection (LOD) and quantification (LOQ). The calibration curves were performed at five concentration levels, in triplicate, using adequately diluted standards and adjusted by linear regression.

Optimization of HS-SPME Extraction Parameters Box-Benhken Experimental Design (BBD)

The extraction of volatile compounds from PHAs was performed under different extraction conditions according to the experimental design shown in Table 2. The parameters considered during HS-SPME optimization were extraction temperature (50, 70 and 90 °C), and extraction time (15, 37.5 and 60 min) and sodium chloride addition (0, 0.5 and 1 M) in a final vial volume of 1 mL. The P3HB sample was selected for the optimization of HS-SPME conditions. The range of studied variables was selected on the basis of results obtained in previous studies reported in the literature [31–33]. A Box–Behnken design (BBD), comprising 12 experimental runs and four central points, was used, and experiments were carried out in randomized order from the experimental design were evaluated in terms of the sum of the peak areas of volatile compounds identified with a library similarity higher than 80%

Table 2. Box-Benkhen experimental design proposed for the headspace solid-phase microextraction (HS-SPME) optimization procedure.

Run	Temperature (°C)	Time (min)	NaCl (1 M)
1	70	37.5	0.5
2	50	60	0.5
3	90	60	0.5
4	70	60	0
5	90	15	0.5
6	70	15	1
7	70	37.5	0.5
8	90	37.5	0
9	90	37.5	1
10	70	15	0
11	50	37.5	1
12	70	37.5	0.5
13	50	37.5	0
14	70	60	1
15	50	15	0.5
16	70	37.5	0.5

2.3.4. Statistical Analysis

Statgraphics-Plus software 5.1 (Statistical Graphics, Rockville, MD, USA) was employed to generate and analyse the results of the BBD. Statistical significance of model parameters was determined at the 5% probability level ($\alpha = 0.05$).

All analytical tests were performed in triplicate. ANalysis Of VAriance (ANOVA) was applied to the results by using SPSS software (Version 15.0, Chicago, IL, USA). Tukey's test was used to assess differences between means and the significance of differences was considered at the level of $p < 0.05$.

3. Results & Discussion

3.1. SEM—Scanning Electron Microscopy

SEM micrographs (Figure 1) showed the dispersion and affinity between the nanoclays and each of the biopolymer matrices used. The good dispersion, debundling (T1 and T2) and exfoliation (T3) of the nanoclays may highly increase the capture of volatiles. The natural chemical behaviour (higher or lower polarity) of each organoclay surface show a clear effect in the interaction mode with each biopolymer matrix. The organophilic clays are not compatible with hydrophobic organic matrices as the spacing between the nanoclay sheets (T3) and inner channels (T1 and T2) is extremely narrow, and hence diffusion of polymer chains in the nanoclay galleries is not possible. This often leads to aggregation of clay particles, acting as stress-concentration sites in the polymer matrix [34]. The organic modification aims at broadening these channels and helps the polymer to penetrate and get fixed onto the surfaces.

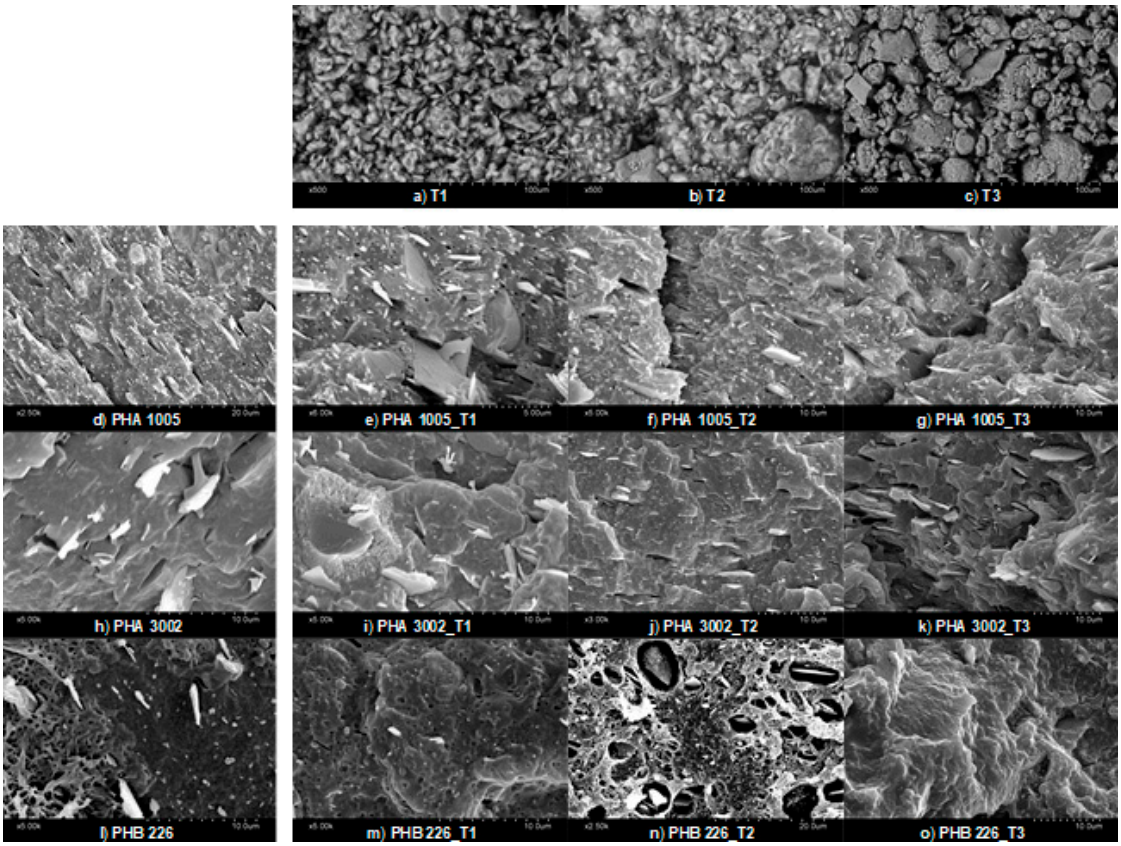

Figure 1. SEM micrographs of nanoclays (**a**–**c**); neat matrices (**d**,**k**,**l**) and composites: PHA1005 composites (**e**–**g**), PHA3002 composites (**i**–**k**); PHB226 composites (**m**–**o**).

On the one hand, analysing PHA3002 micrographs, T2 seems to appear better dispersed than T1 or at least better oriented in one direction. In addition, sepiolites (T1 and T2) appear to show a better

affinity with this P3HB-co-P4HB matrix as T3 micrographs show a lack of wetting contact layer or interphase between the nanoclay and the polymer. On the other hand, for PHA1005 matrix, T1 presents some agglomerates, which in principle should be avoided due to the aminosilane modification. At times, the greater the amount of organic modifier in nanoclays, the greater the impediment to debundle [35] and this might be the behaviour observed between T1 (modified) and T2 (natural) for this matrix.

Finally, when analysing PHB226 compounds, a clear lack of affinity for T2 PHB226 was observed. Similar behaviour was found for T1 in which a similar bubble-like reaction during the blend compounding might have started. However, the polar affinity between T1 and PHB226 probably cuts the kinetics of the reaction while for T2 (non-modified) the process is more pronounced. Therefore, a better interphase interaction between T1 and PHB226 can be observed when comparing to T2. This enhanced interaction was sought with the organoclay modification. However, a completely different affinity behaviour can be found for T3 and PHB226, for which the surface structure complies with a more ductile fracture. Montmorillonite layers are found well integrated and interphases are not discernible as in the other two cases. These results are in agreement with Mechanical and XRD results already published by authors, in which Montmorillonite seemed to be highly intercalated and even exfoliated, while sepiolite debundling was not so effective [30]. This favourable interaction between T3 and PHB226 may be attributed to the lack of P4HB and the appearance of PBA, which modifies the polar behaviour or the matrix, and indirectly affects the overall viscosity of the molten polymer when the blend is developed favouring or hindering miscibility [36].

Finally, for neat matrices, the difference in the amount of talc used by the manufacturer for PHA1005 and PHA3002 formulations respect to PHB226 can be observed, which seems in coherence with TGA findings.

3.2. TGA—Thermogravimetric Analysis

The thermal stability of the nanocomposite materials was evaluated through TGA. The temperature corresponding to the onset of decomposition (T onset) for the samples studied is essential for evaluating their thermal stability and is shown in Table 3.

Table 3. Thermal results obtained by TGA. T_{onset} %, T_{max} %, and T_{50} % represent the temperature of the initial degradation, the maximum degradation rate of decomposition, and 50 wt % loss of the samples, respectively. FR represents the final residue and DTG first derivative.

Materials	T_{onset} [°C]		T_{max} [°C]		T_{50} wt % [°C]	FR [%]
PHA1005	268.13		278.33		279.62	9.45
PHA1005_T1	267.94		275.51		278.89	12.93
PHA1005_T2	265.75		278.33		278.52	13.56
PHA1005_T3	263.20		278.33		277.25	13.27
PHA3002	290.01		307.67		305.34	8.39
PHA3002_T1	287.46		307.67		305.61	11.71
PHA3002_T2	283.63		302.33		300.23	10.93
PHA3002_T3	284.73		299.67		298.95	11.26
PHB226	275.97	386.87	297.00	403.70	293.84	2.73
PHB226_T1	283.63	384.31	299.82	411.67	301.50	5.61
PHB226_T2	278.52	383.03	297.00	407.30	296.40	5.83
PHB226_T3	272.14	347.29	291.49	382.86	287.46	6.37

In addition, the appearance of volatile traces in the first section of the DTG was evaluated. Theoretically, high amounts of some identified volatiles that might be found in the neat matrices, may have been released during the extrusion-compounding of the bio-nanocomposites due to the temperature profile reached during the material development (over 150 °C) [21,32]. However, the release rate is unknown and there is not a clear perception of volatile release. Nevertheless, the DTG range

between 100 and 220 °C was studied trying to observe substantial peaks. The signal noise of the apparatus seems too high compared to the amount of volatiles released in order to be able to obtain reliable results. Therefore the correct volatile analysis is left for the accurate technique HS-SPME and authors will focus the TGA results to study the thermal stability and the non-organic residue.

The degradation of PHA 3002 occurred in one step while PHA 1005F shows a smooth second step at higher temperatures which may correspond to a greater amount of inorganic fillers. Several steps occurred for the PHB226 sample too, distinctly exhibiting two decomposition platforms. This behaviour has been previously reported in the literature for some pure P3HB polymers and for different P3HB-*co*-P4HB co-blends. According to literature, pure P3HB thermally decomposes at around 270 °C, above its melting point (around 180 °C). However, a short exposure of PHB to temperatures near its melting point induce a severe degradation producing degraded products such as olefinic and carboxylic acid compounds due to the random chain scission reaction that takes place [37]. Wang et al. studied the thermal degradation of P3HB-*co*-P4HB composites [38]. The results showed that thermal degradation of P3HB occurs almost exclusively by random chain-scission involving a six-member ring formation while P4HB decomposes through intermolecular ester exchange reaction and generates a decomposition product ɣ-butyrolactone. Therefore, P4HB crystals are thermally more stable than P3HB. In addition, in a previous analysis carried out by the authors for these composites, the presence of PBA was corroborated in the NMR and DSC analyses for PHB226 [30]. Maximum degradation temperature of PBA is defined at T_{dmax} = 385.1 °C [39] which is aligned with the TGA results shown in Table 3. The presence of multi-component nature for PHB226 commercial formulation containing organic additives and polyesters has been also corroborated by further authors such as Y.M. Corre et al. [40].

Different residual weights remaining at 800 °C can be found for the three matrices being higher for P3HB-co-P4HB blends than for P3HB. Usually, two inorganic fillers are commonly used in polymers as nucleating agents to reduce crystallization rates: $Mg_3Si_4O_{10}(OH)_2$ and $CaCO_3$ [41,42]. Complementary EDS was used for the elemental analysis of the final residues revealing their correspondence to talc. In addition, the final amount of inorganic residue found for the bio-nano-composites developed, reveals an effective dosage of the nanoclays load introduced.

The thermal degradation of Sepiolite and montmorillonite nanoclay additives was characterised in order to better understand the effect these have over the final bio-nano-composites.

The T2 thermograph (Figure 2a) shows a typical curve for non-modified sepiolite. T1 thermograph shows a few deviations from respect to T2 due to the modification through organosilanes containing amine groups [25,27]. Our TGA results are in concordance with the aminosilane grafted Sepiolite (T1) characterisation made by G. Tartaglione et al., in previous publication [43]. In particular, four degradation steps are appreciated for T1. The clay presents degradations around 74, 232 and 305 °C. In addition, a less defined degradation phase is observed at 349–495 °C. To try to better define this area and separate the overlap of peaks, the heating rate was lowered from 10 to 5 °C/min. The first loss corresponds to mainly methanol, probably used as a solvent for the modification of the clay, followed by dehydration of water: moisture and zeolitic water (below 180 °C).

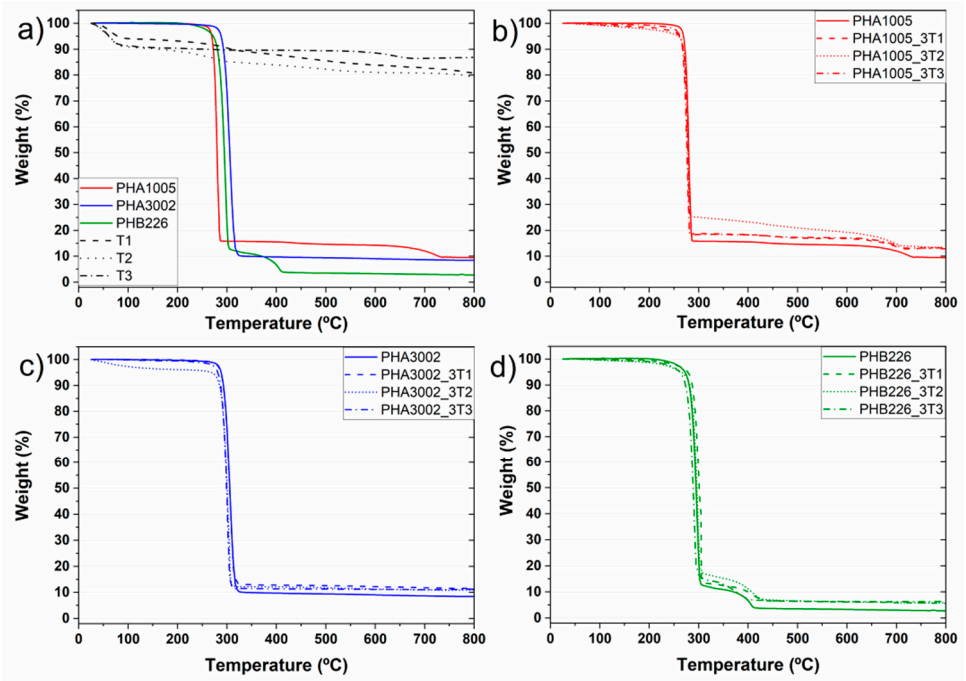

Figure 2. TGA curves: (**a**) neat matrices and nanoclays; (**b**) PHA1005 composites; (**c**) PHA3002 composites; (**d**) PHB226 composites.

The volatilization of the modifier takes place in two steps, the first one related to adsorbed molecules (non-grafted) at 215–250 °C. The grafted modifier is likely to volatilize over 400 °C. The grafted groups are very stable, being eliminated by heating at temperatures above 400 °C. In this way, the characteristic hydrophilic surface of Sepiolite becomes organophilic and the fibrous clays can then be easily dispersed in low-polar polymers [44]. The last loss observed approximately at 750 °C has been described in the literature to be related to a complete oxidation of the carbonaceous residue formed during previous thermal oxidation of the grafted molecules [45].

T3 (Na-MMT) presents a chemical structure modified with a quaternary alkyl ammonium surfactant which has a noticeable effect on the thermal stability of the organoclay itself. Analysing its thermal degradation behaviour, it can be observed that T3 DTG shows a water/solvent release at 68 °C and at 116 °C. In addition, two small mass loss peaks are found for 295 °C and for 526 °C, and finally an accentuated peak corresponding to 674 °C. According to the literature (Botana et al. [46] and Cervantes et al. [47]) free water loss in MMT nanoclays containing hydroxyl groups in the alkylammonium anion, shows free water loss at around 80 °C. Peaks in at 200–600 °C are attributed not only to structural water but also to the decomposition of the alkylammonium ions. In particular, peaks found at 297 and 528 °C are associated to the following chemical species for this organoclay sample: H_2O, CO_2, alkanes, alkenes, CHO's, COOH's, amines [47]. Finally, peaks attributed between 610 and 674 °C are attributed to some further structural water release.

In all the developed bio-nano-composites a decrease in T_{onset} and T_{max} can be appreciated except for PHB226-T1. Han et al. reported that P3HB-*co*-P4HB samples containing a 10 wt % silica presented a higher T_{onset} and T_{max} than that of pure P3HB-*co*-P4HB, in particular being 2.08 and 6.28 °C higher, respectively [48]. Our samples containing a 3 wt % of nanoclay content seems not to induce a high thermal stability increase. Nevertheless, results show that sepiolites (T1 and T2) seem more suitable for these polyhydroxyalkanoates materials than montmorillonite for thermal stability purposes, as sepiolites maintain the thermal stability of the original matrix. For P3HB-*co*-P4HB composites, it can be observed that T1 presents the same T_{onset}, T_{max} and T_{50} while a slight decrease is found for T2. For T3, the overall decrease for T_{onset}, T_{max} and T_{50} is noticeable. A similar tendency is found for P3HB composites. T1 is the nanoclay inducing a higher thermal stability for both degradation

steps (including PBA), while T2 tends to maintain the original matrix behaviour and T3 induces a remarkable decrease. Results are detailed in Table 3.

3.3. HS-SPME-GC-MS—Headspace Solid-Phase Microextraction Coupled to Gas Chromatography-Mass Spectrometry

3.3.1. Optimization of the HS-SPME Extraction Process

Seventeen different volatile compounds were identified with a library similarity higher than 80% in all runs of the BBD carried out in this study (Figure 3): 1, 1-butanol; 2, p-xylan; 3, heptanal; 4, α-methylstyrene; 5, benzaldehyde; 6, octanal; 7, limonene; 8, 1-hexanol; 9, undecane; 10, 1-octanol; 11, nonanal; 12, decanal; 13, 1-chloro-decane; 14, 1-decanol; 15, tetradecane; 16, biphenyl; 17, 2,6-bis (1-methylethyl)-benzeneamide.

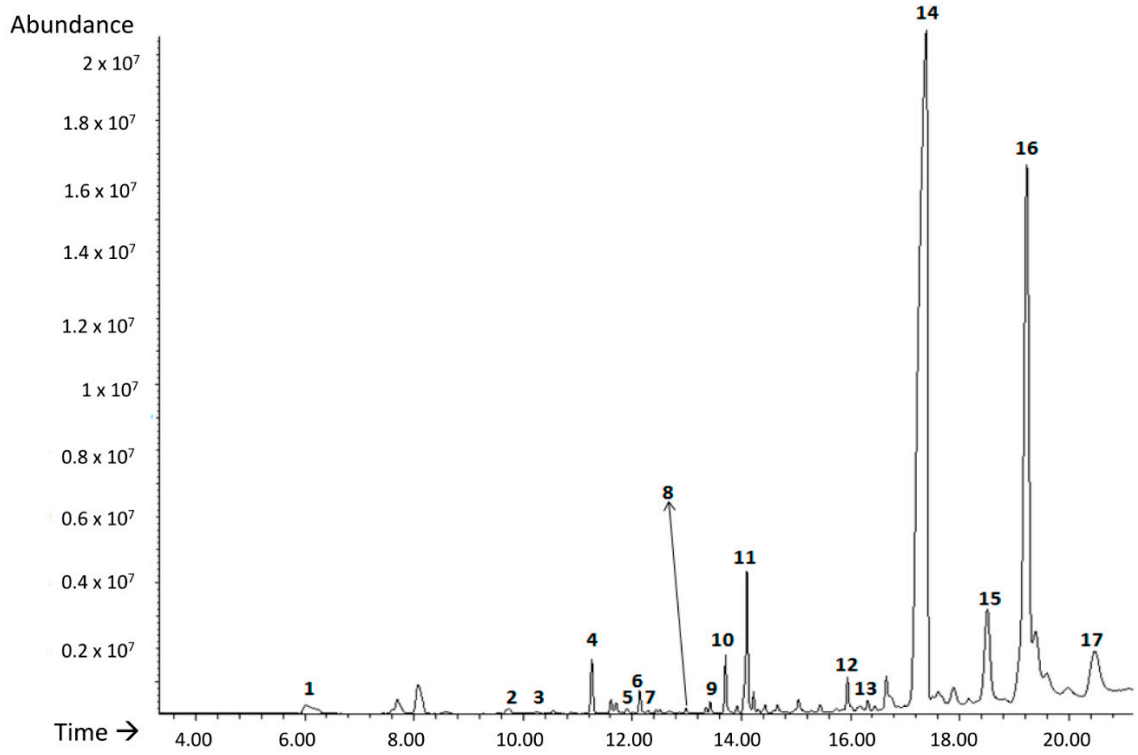

Figure 3. TIC chromatogram obtained for PHB 226 sample under run 3 of the BBD. * *Time refers to s.*

Benzaldehyde, heptanal, octanal, nonanal and decanal belong to the family of aldehydes. The presence of benzaldehyde in other matrices such as polystyrene has been related to oxidation processes together with p-xylan and α-methylstyrene [21]. Furthermore, heptanal, octanal, nonanal, decanal, are secondary oxidation compounds, which are characterized by strong and unpleasant odours characteristic of lipid degradation [49]. In addition, four alcohols were identified (butanol, 1-hexanol, octanol and decanol). In particular, 1-hexanol is one of the most important alcohols used for several processes of synthesis and degradation product of one of the most used plasticizers since 1950, the phthalate DEHP [50]. This compound has been detected in emissions of different plastics with undesirable odour [51]. As expected, some organic volatile compounds identified are linear or branched chain alkanes such as undecane and tetradecane due to the high affinity for SPME fibre coating [32]. Regarding limonene, it is a terpene which has acquired great importance in recent years due to its demand as a biodegradable solvent. Apart from industrial solvent it also has applications as an aromatic component and is widely used to synthesize new compounds [52].

The influence of extraction temperature (A), extraction time (B) and NaCl addition (C) in the sum of the peak areas of these seventeen compounds was evaluated by using standardized Pareto diagrams

(Figure 4). This kind of diagram allows for the determination of the magnitude and the importance of each independent variable or factors in a response. Figure 4 shows that only the extraction time was significant and it has a positive effect. That means that extraction by HS-SPME improves when the time increases from 15 min to 60 min. Nonetheless, the extraction temperature and the addition of NaCl and all possible interactions (AB, AC, BC, AA, BB, CC) do not have a significant effect with a confidence level of 95% ($\alpha = 0.05$). Based on the obtained results, the optimum HS-SPME extraction conditions were 60 min at 90 °C without the addition of NaCl.

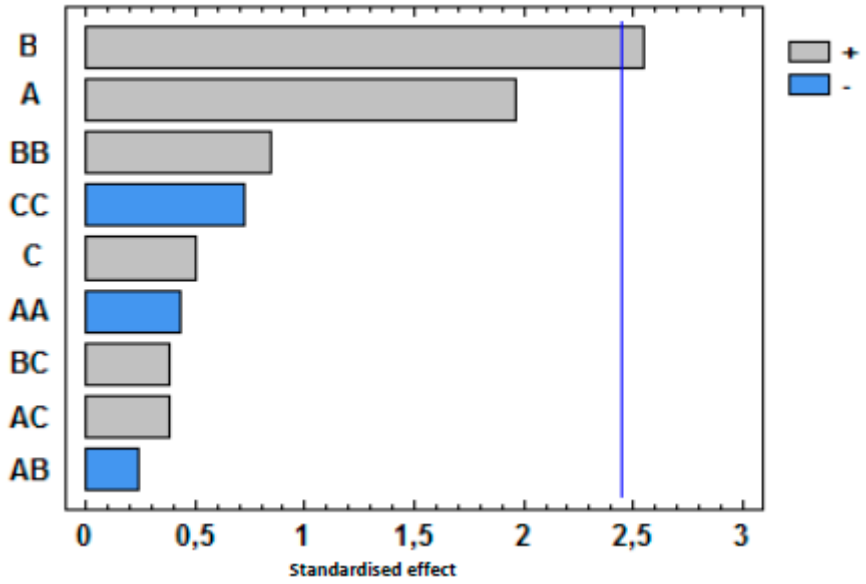

Figure 4. Pareto charts of factors and interactions obtained from the BBD for the sum of the volatile compounds. The vertical line indicates the statistical significance at 5% of the effects.

Finally, it was decided to quantified six main volatile compounds in the present work as a result of this negative effect on the final odour of samples: heptanal, α-methylstyrene, benzaldehyde, octanal, 1-hexanol and decanal. The adequacy of the fitted models was determined by evaluating the lack of fit, the coefficient of determination (R^2) and F test obtained from the analysis of variance (ANOVA). The computing program showed that the fitted models were considered satisfactory as the lack of fit was not significant with values of 0.852 for heptanal, 0.659 for α-methylstyrene, 0.457 for benzaldehyde, 0.940 for octanal, 0.816 for 1-hexanol and 0.983 for decanal. ($p > 0.05$). On the other hand, R^2 is defined as the ratio of the explained variation to the total variation and is a measurement of the degree of fitness. The model can fit well with the actual data when R^2 approaches unity with values of 0.733 for heptanal, 0.767 for α-methylstyrene, 0.775 for benzaldehyde, 0.861 for octanal, 0.853 for 1-hexanol and 0.681 for decanal. These values indicated a relatively high degree of correlation between the actual data and predicted values, indicating that models could be used to predict the studied responses.

3.3.2. Validation method

The analytical method used for the quantification of volatile compounds by HS-SPME-GC-MS was validated in terms of linearity, repeatability and detection (LOD) and quantitation (LOQ) limits. An acceptable level of linearity was obtained for all analytes (R^2 between 0.9076 and 0.9929), showing relative standard deviation (RSD) values lower than 5%. LOD and LOQ values were determined using the regression parameters of the calibration curves (3 Sy/x/a and 10 Sy/x/a, respectively, where Sy/x is the standard deviation of the residues and "a" is the curve slope). LOD and LOQ values obtained for heptanal ranged between 0.001 and 0.004 µg/kg, α-methylstyrene ranged between 2.76 and 9.19 µg/kg, benzaldehyde ranged between 0.003 and 0.011 µg/kg, octanal ranged between 0.071 and 0.236 µg/kg, 1-hexanol and decanal ranged between 0.001 and 0.002 µg/kg.

Volatile Compounds Quantification

Lipid oxidation is a complex process where unsaturated fatty acids react with molecular oxygen via a free radical mechanism or in a photosensitised oxidation process. The principal source of off-flavours developed by lipid oxidation is hydroperoxides, which are unstable and readily decompose to form aliphatic aldehydes, ketones and alcohols. Many of these secondary oxidation products have undesirable odours with particularly low odour thresholds [53,54]. As it is shown in Tables 3 and 4, the effect of studied nanoclays (T1, T2 and T3) were different depending on the polymer matrix (PHB226, PHA1005 or PHA3002).

In general, the volatile compound quantified in greater quantity for all the samples has been the decanal as it is the volatile with the highest M_w. Table 4 results suggest that there is a clear tendency which indicates that the content of the volatiles is related to the molecular weight, as the higher the M_w is, the more difficult the volatiles are to extract from the polymer and to clean during purification stages. Therefore, we can observe them in higher amounts. For the case of α-methylstyrene and benzaldehyde, these are more complex volatiles containing aromatic groups which may be also less accessible to solvents to be extracted and cleaned. Hence, they can be found also in higher quantities than simpler alcohols.

According to García-Quiles et al. [30], the addition of nanoclays may modify the structure of the polymers studied affecting the release of the studied undesirable volatile compounds. Regarding the control matrix polymers, PHB 226 initially shows lower contents of heptanal, α-methylstyrene, octanal and 1-hexanol while its content in decanal was the highest respect to the other two PHA matrices. However, benzaldehyde was initially quantified in similar amounts in all control matrices.

Concerning the effect of the addition of T1, T2 and T3, each studied volatile showed a different behaviour depending on the matrix and organoclay used (Figure 5 and Table 5).

Regarding 1-hexanol, PHB 3002 showed the lowest content in contrast to PHA1005 and PHB226. In this sample, no significant enhancement was found between the three nanoclays, although T1 at least maintained the level of release, while T3 and T2 showed non-desirable and remarkable increasing peaks of 200% and 515% respectively. For PHA 1005 all the nanoclays reduced the release of this compound, but it seems that T3 clay was much more effective reducing it in a 72%.

Heptanal, together with Decanal, seemed to be the most difficult volatile to be adsorbed by any of the organoclays. In this sense, T1 seemed to be more efficient maintaining heptanal release for PHA1005 and PHA3002 and reducing a 20% the release PHB226. In contrast, it seems that the addition of T3 could modify the structure of PHA1005 and PHA3002 polymers increasing the heptanal release in more than 400% while reducing 13% for PHB226.

Concerning octanal behaviour, the initial concentration was lower in PHB 226 but for this matrix, it seems that all organoclays provoke increases in the release of this volatile instead of retaining them. On the contrary, T3 prevents the release of octanal in PHA 1005 decreasing its release in a remarkable 92%. However, for PHA 3002, it seems that T2 suits better as it hinders the release of this volatile compound more efficiently than T3, 66%.

PHB 226 showed the highest decanal initial content. T2 was the most effective clay reducing the release of this compound in a 43%. T2 nanoclay was also the most efficient for the PHA 1005 matrix although there was no decrease for any of the three organoclays. The same tendency was found for PHA 3002, being in this case T3 the nanoclay increasing the release to a lesser extent.

Regarding α-methylstyrene, the lowest content was determined in PHB 226 and PHA1005 at equal rates by decreasing its release in 75%. For this compound and in particular for PHA 3002_T3 the developed formulation seems to be especially effective since it was not possible to detect the presence of this volatile compound therein.

Finally, Benzaldehyde was initially present in a similar quantity in all formulations. In this case, T2 could be more effective in PHB 226 and PHA 1005 matrices whereas for PHA 3002 no significant effect was observed.

Table 4. Volatile compounds content for the PHB 226 PHA 1005 and PHA 3002 controls and the T1, T2 and T3 formulations, expressed as the mean ± SD (n = 3).

Sample Material	Volatile Compound											
	1-Hexanol		Heptanal		Octanal		Decanal		α-Methylstyrene		Benzaldehyde	
	Average (μg/g sample)	SD	Average (μg/g sample)	SD	Average (μg/g sample)	SD	Average (μg/g sample)	SD	Average (μg/g sample)	SD	Average (μg/g sample)	SD
PHA 1005	18.8	3.8	14.8	6.8	68.6	14.9	900	500	102.8	35.4	6.4	0.3
PHA 1005_T1	13.2	1.1	15.8	1.5	68.1	7.1	2100	500	283.6	12.2	5.7	1.2
PHA 1005_T2	8.2	1.3	15.3	3.2	78.1	13.9	1300	200	25.7	10.0	4.3	0.3
PHA 1005_T3	5.3	0.7	81.2	29.3	5.3	0.7	5300	700	89.6	33.5	5.3	0.7
PHA 3002	2.7	1.0	18.8	10.0	75.4	18.8	1000	300	135.4	28.4	4.5	1.5
PHA 3002_T1	2.8	1.0	27.9	1.7	41.2	6.5	3300	500	279.5	17.6	7.1	0.3
PHA 3002_T2	16.6	2.9	41.4	16.3	25.3	7.4	2400	400	59.3	11.6	4.6	0.7
PHA 3002_T3	8.1	2.7	98.8	11.1	53.6	16.8	1800	400	nd	nd	6.7	1.1
PHB 226	3.7	0.9	4.0	0.6	26.7	0.5	2300	100	40.4	4.6	7.7	0.7
PHB 226_T1	1.2	0.9	3.2	1.1	32.6	6.0	1900	200	43.4	7.1	7.2	2.6
PHB 226_T2	2.3	0.6	10.3	0.9	39.3	7.7	1300	300	10.3	2.3	4.9	0.5
PHB 226_T3	1.6	0.6	3.5	7.6	71.3	17.9	2800	700	39.6	17.3	6.5	2.7

nd = no data.

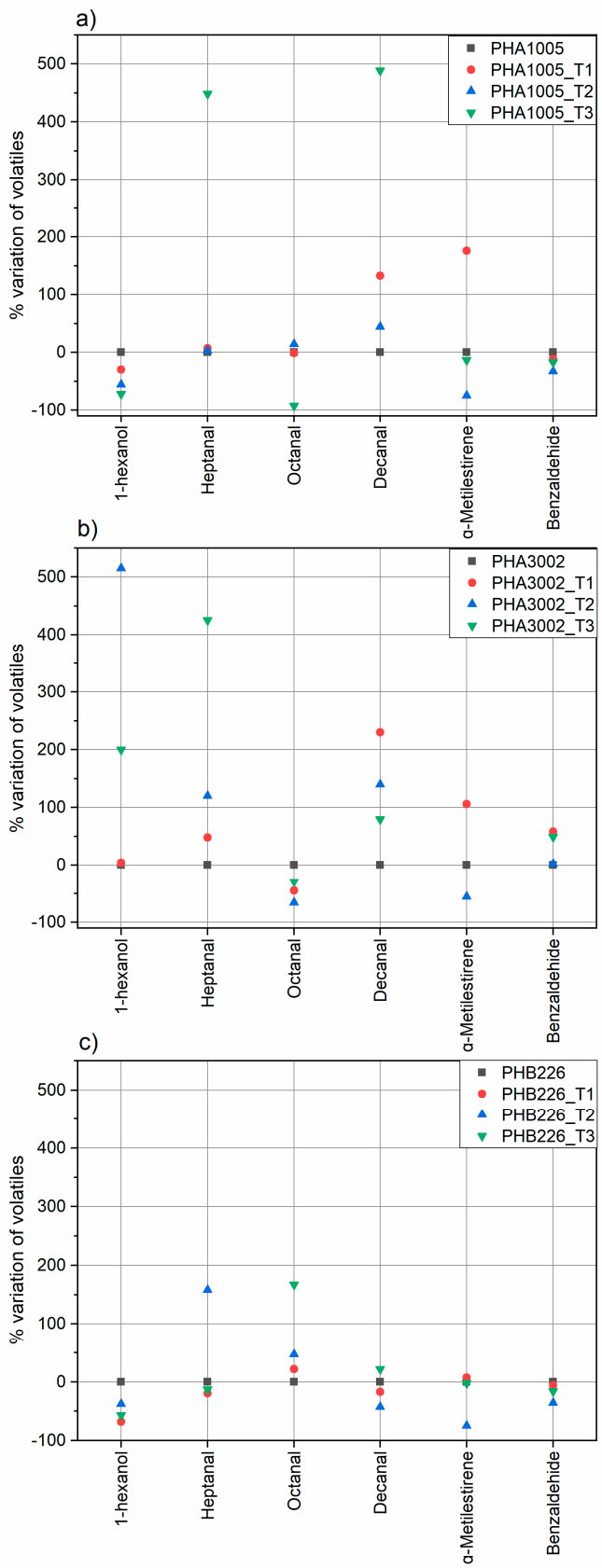

Figure 5. Percentage variation of volatile substances in the samples of study: (**a**) PHA1005, (**b**) PHA3002, (**c**) PHB226.

Table 5. Summary of the organoclay that works best to reduce the release of the volatile compounds studied for each polymer matrix.

Volatile	PHA 1005	PHA 3002	PHB 226
1-Hexanol	T3	T1	T1
Heptanal	T2	T1	T1
Octanal	T3	T2	T1
Decanal	T2	T3	T2
α-Methylstyrene	T2	T3	T2
Benzaldehyde	T2	T2	T2

4. Conclusions

The incorporation of organoclays to PHAs greatly affects the dispersion and integration of the nanoclay in the polymer matrix due to surface modification. SEM micrographs confirm how important is adequate the surface polarity of nanoclays for a particular matrix, having found largest differences between T2 which showed a lack of surface adhesion and voids formation and T3 apparently exhibiting better surface interaction and delamination. There is also a clear difference between micrographs containing T1 and T2, especially for PHB226, where the aminosilane modification clearly accentuates affinity for the PHAs matrices. Moreover, T1 has been demonstrated to be the unique nanoclay really enhancing the thermal stability of the composites developed according to TGA results while T2 maintains the original behaviour and T3 induces a remarkable decrease on T_{onset} and T_{max}.

In addition, TGA analysis has allowed us to identify thermal decomposition peaks for our composites and understand the degradation phases of matrices and the decomposition and volatilization of the organic modifiers employed onto nanoclays. However, the release of volatile compounds coming from matrix aldehydes and ketones at thermal rates between 100 and 220 °C cannot be identified with this technique and therefore the determination of this off-flavour compounds has been optimised by applying headspace analysis. The obtained results from the experimental design demonstrate the suitability of the HS-SPME technique followed by GC-MS to be used in biopolymer analysis to identify and monitor the release of volatile compounds in PHAs matrices.

It has been demonstrated that the reached effect depends on the volatile nature and the affinity of the organoclay with each matrix. On the one hand, for PHB226, T1 seems more suitable for low M_w volatiles whileT2 could be more effective to reduce the released volatiles with higher M_w, which indeed are present in a major proportion. On the other hand, for PHA 1005 compounds, T2 seems to be the most effective to reduce heptanal and decanal and also α-Methylstyrene and benzaldehyde. However, T3 was of great relevance in the reduction of the octanal and 1-hexanol compounds. Finally, for PHA 3002 formulations T1 seems the most effective to reduce 1-hexanol and heptanal (lowest M_w), while T2 would tackle best octanal and benzaldehyde (medium M_w) and T3 would be the most effective for decanal and α-Methylstyrene (highest M_w).

As a general outcome from this commercial PHA off-flavour analysis, if a plastic converter would not desire to tackle a particular subgroup of volatiles, but try to comprise as much of them as possible, T2 might result in the most versatile candidate. However, the compromise with other properties such as mechanical or barrier properties for example for food or cosmetics packaging should also be taken under consideration.

Author Contributions: L.G.-Q. Conceived the work, carried out the experimental work related to materials development, contributed to the scientific discussion and wrote the major part of the manuscript.; A.V. conceived the volatile designed of experiments and carried out the analysis, contributed to the scientific discussion and wrote part of the manuscript; Á.F.C. contributed to scientific discussion and reviewed the manuscript; A.J. contributed to scientific discussion and reviewed the manuscript; M.d.C.G. contributed to scientific discussion and reviewed the manuscript; P.C. designed the methodology, contributed to the interpretation of results and scientific discussion, got funding and reviewed the manuscript.

Funding: The authors gratefully acknowledge the Government of Aragón (DGA) under the project T08_17R (I+AITIIP) for support and financial aid for this publication.

Acknowledgments: The authors acknowledge TOLSA for kindly provide the nanoclays used for this research.

Conflicts of Interest: The authors declare no conflict of interest.

References

1. Research and Markets. Global Polyhydroxyalkanoate (PHA) Market Analysis & Trends—Industry Forecast to 2025. Available online: https://www.researchandmarkets.com/reports/4375504/global-polyhydroxyalkanoate-pha-market-analysis (accessed on 1 August 2017).
2. Wang, S.; Chen, W.; Xiang, H.; Yang, J.; Zhou, Z.; Zhu, M. Modification and Potential Application of Short-Chain-Length Polyhydroxyalkanoate (SCL-PHA). *Polymers* **2016**, *8*, 273. [CrossRef] [PubMed]
3. Pramanik, K.; Patra, J.K. Polyhydroxyalkanoates: Biodegradable Plastics for Environmental Conservation. In *Industrial & Environmental Biotechnology*; Studium Press: New Delhi, India, 2014; Chapter 1.
4. Rehm, B.H.A. Polyester synthases: Natural catalysts for plastics. *Biochem. J.* **2003**, *376*, 15–33. [CrossRef] [PubMed]
5. Sudesh, K.; Iwata, T. Sustainability of Biobased and Biodegradable Plastics. *Clean* **2008**, *36*, 433–442. [CrossRef]
6. Obruca, S.; Sedlacek, P.; Krzyzanek, V.; Mravec, F.; Hrubanova, K.; Samek, O.; Kucera, D.; Benesova, P.; Marova, I. Accumulation of Poly(3-hydroxybutyrate) Helps Bacterial Cells to Survive Freezing. *PLoS ONE* **2016**, *11*, e0157778. [CrossRef] [PubMed]
7. Koller, M.; Braunegg, G. Advanced approaches to produce polyhydroxyalkanoate (PHA) biopolyesters in a sustainable and economic fashion. *EuroBiotech J.* **2018**, *2*, 89–103. [CrossRef]
8. Kabasci, S. *Bio-Based Plastics: Materials and Applications*; John Wiley & Sons Ltd.: Hoboken, NJ, USA, 2014; Chapter 7.3.2, ISBN 9781119994008.
9. Koller, M.; Maršálek, L.; de Sousa Dias, M.M.; Braunegg, G. Producing microbial polyhydroxyalkanoate (PHA) biopolyesters in a sustainable manner. *New Biotechnol.* **2017**, *37*, 24–38. [CrossRef] [PubMed]
10. Ong, S.Y.; Kho, H.-P.; Riedel, S.L.; Kim, S.-W.; Gan, C.-Y.; Taylor, T.D.; Sudesh, K. An integrative study on biologically recovered polyhydroxyalkanoates (PHAs) and simultaneous assessment of gut microbiome in yellow mealworm. *J. Biotechnol.* **2018**, *265*, 31–39. [CrossRef]
11. Brigham, C.J.; Riedel, S.L. The Potential of Polyhydroxyalkanoate Production from Food Wastes. *Appl. Food Biotechnol.* **2018**, *6*, 7–18. [CrossRef]
12. Kunasundari, B.; Sudesh, K. Isolation and recovery of microbial polyhydroxyalkanoates. *Express Polym. Lett.* **2011**, *5*, 620–634. [CrossRef]
13. Jacquel, N.; Lo, C.-W.; Wei, Y.-H.; Wu, H.-S.; Wang, S.S. Isolation and purification of bacterial poly(3-hydroxyalkanoates). *Biochem. Eng. J.* **2008**, *39*, 15–27. [CrossRef]
14. Fung, F.M.; Su, M.; Feng, H.; Li, S.F.Y. Extraction, separation and characterization of endotoxins in water samples using solid phase extraction and capillary electrophoresis-laser induced fluorescence. *Sci. Rep.* **2017**, *7*, 10774. [CrossRef] [PubMed]
15. Hamilton, R.J. Oxidative rancidity as a source of off-flavours. In *Taints and Off-Flavours in Food*; Woodhead Publishing Limited: Cambridge, UK, 2003; pp. 140–158.
16. Koller, M.; Bona, R.; Chiellini, E.; Braunegg, G. Extraction of short-chain-length poly-[(R)-hydroxyalkanoates] (scl-PHA) by the antisolvent acetone under elevated temperature and pressure. *Biotechnol. Lett.* **2013**, *35*, 1023–1028. [CrossRef] [PubMed]
17. Khosravi-Darani, K.; Vasheghani-Farahani, E. Application of supercritical fluid extraction in biotechnology. *Crit. Rev. Biotechnol.* **2005**, *25*, 231–242. [CrossRef] [PubMed]
18. Kokosa, J.M. Recent Trends in Using Single-Drop Microextraction and Related Techniques in Green Analytical Methods. *Trends Anal. Chem.* **2015**, *71*, 194–204. [CrossRef]
19. Barros, P.; Moreira, E.; Elias Pereira, N.; Leite, G.; Moraes Rezende SG, F.; Guedes de Pinho, P. Development and validation of automatic HS-SPME with a gas chromatography-ion trap/mass spectrometry method for analysis of volatiles in wines. *Talanta* **2012**, *101*, 177–186. [CrossRef] [PubMed]
20. Curran, K.; Strlič, M. Polymers and volatiles: Using VOC analysis for the conservation of plastic and rubber objects. *Stud. Conserv.* **2014**, *60*, 1–14. [CrossRef]

21. Vilaplana, F.; Martínez-Sanz, M.; Ribes-Greus, A.; Karlsson, S. Emission pattern of semi-volatile organic compounds from recycled styrenic polymers using headspace solid-phase microextraction gas chromatography–mass spectrometry. *J. Chromatogr. A* **2010**, *1217*, 359–367. [CrossRef]
22. Kaykhaii, M.; Linford, M.R. Application of Microextraction Techniques Including SPME and MESI to the Thermal Degradation of Polymers: A Review. *Crit. Rev. Anal. Chem.* **2016**, *47*, 172–186. [CrossRef]
23. Hashemi, S.H.; Kaykhaii, M.; Khajeh, M. Molecularly Imprinted Polymers for Stir Bar Sorptive Extraction: Synthesis, Characterization, and Application. *Anal. Lett.* **2015**, *48*, 1815–1829. [CrossRef]
24. Wang, S.; Peng, Y. Natural zeolites as effective adsorbents in water and wastewater treatment. *Chem. Eng. J.* **2010**, *156*, 11–24. [CrossRef]
25. Franchini, E. Structuration of Nano-Objects in Epoxy-based Polymer Systems: Nanoparticles & Nanoclusters for Improved Fire Retardant Properties. Ph.D. Thesis, Institut National des Sciences Appliquées de Lyon, Lyon, France, 2008.
26. Volle, N.; Giulieri, F.; Burr, A.; Pagnotta, S.; Chaze, A.M. Controlled interactions between silanol groups at the surface of sepiolite and an acrylate matrix: Consequences on the thermal and mechanical properties. *Mater. Chem. Phys.* **2012**, *134*, 417–424. [CrossRef]
27. Peinado, V.; García, L.; Fernández, A.; Castell, P. Novel lightweight foamed poly(lactic acid) reinforced with different loadings of functionalised Sepiolite. *Compos. Sci. Technol.* **2014**, *101*, 17–23. [CrossRef]
28. Zheng, Y.; Zaoui, A. Mechanical behavior in hydrated Na-montmorillonite clay. *Physica A* **2018**, *505*, 582–590. [CrossRef]
29. Wang, S.; Song, C.; Chen, G.; Guo, T.; Liu, J.; Zhang, B.; Takeuchi, S. Characteristics and biodegradation properties of poly(3-hydroxybutyrate-co-3-hydroxyvalerate)/organophilic montmorillonite (PHBV/OMMT) nanocomposite. *Polym. Degrad. Stab.* **2005**, *87*, 69–76. [CrossRef]
30. García-Quiles, L.; Fernández, A.; Castell, P. Sustainable Materials with Enhanced Mechanical Properties Based on Industrial Polyhydroxyalkanoates Reinforced with Organomodified Sepiolite and Montmorillonite. *Polymers* **2019**, *11*, 696. [CrossRef] [PubMed]
31. Félix, J.S.; Domeño, C.; Nerín, C. Characterization of wood plastic composites made from landfill-derived plastic and sawdust: Volatile compounds and olfactometric analysis. *Waste Manag.* **2013**, *33*, 645–655. [CrossRef]
32. Lattuati-Derieux, A.; Egasse, C.; Thao-Heu, S.; Balcar, N.; Barabant, G.; Lavédrine, B. What do plastics emit? HS-SPME-GC/MS analyses of new standard plastics and plastic objects in museum collections. *J. Cult. Herit.* **2013**, *14*, 238–247. [CrossRef]
33. Espert, A.; de las Heras, L.A.; Karlsson, S. Emission of possible odourous low molecular weight compounds in recycled biofibre/polypropylene composites monitored by head-space SPME-GC–MS. *Polym. Degrad. Stab.* **2005**, *90*, 555–562. [CrossRef]
34. Mahesh, K.R.V.; Murthy, H.N.N.; Kumaraswamy, B.E.; Raghavendra, N.; Sridhar, R.; Krishna, M.; Pattar, N.; Pal, R.; Sherigara, B.S. Synthesis and characterization of organomodified Na-MMT using cation and anion surfactants. *Front. Chem. China* **2011**, *6*, 153–158. [CrossRef]
35. Jalali, A.M.; Taromi, F.A.; Atai, M.; Solhi, L. Effect of reaction conditions on silanisation of sepiolite nanoparticles. *J. Exp. Nanosci.* **2016**, *11*, 1171–1183. [CrossRef]
36. González-Ausejo, J.; Gámez-Pérez, J.; Balart, R.; Lagarón, J.M.; Cabedo, L. Effect of the addition of sepiolite on the morphology and properties of melt compounded PHBV/PLA blends. *Polym. Compos.* 2017. [CrossRef]
37. Wang, H.H.; Zhou, X.R.; Liu, Q.; Chen, G.Q. Biosynthesis of polyhydroxyalkanoates homopolymers by Pseudomonas putida. *Appl. Microbiol. Biotechnol.* **2011**, *89*, 1497–1507. [CrossRef] [PubMed]
38. Wang, X.; Zhang, H.; Liu, M.; Jia, D. Thermal stability of poly(3-hydroxybutyrate-co-4-hydroxybutyrate)/modified montmorillonite bio-nanocomposites. *Polym. Compos.* **2015**, *38*, 673–681. [CrossRef]
39. Tang, D.; Noordover BA, J.; Sablong, R.J.; Koning, C.E. Metal-free synthesis of novel biobased dihydroxyl-terminated aliphatic polyesters as building blocks for thermoplastic polyurethanes. *J. Polym. Sci. A Polym. Chem.* **2011**, *49*, 2959–2968. [CrossRef]
40. Corre, Y.M.; Bruzaud, S.; Audic, J.L.; Grohens, Y. Morphology and functional properties of commercial Polyhydroxyalkanoates: A comprehensive and comparative study. *Polym. Test.* **2012**, *31*, 226–235. [CrossRef]
41. Ipsita, R.; Visakh, P.M. *Polyhydroxyalkanoate (PHA) Based Blends, Composites and Nanocomposites*; Royal Society of Chemistry: Cambridge, UK, 2015.

42. Wypych, G. *Handbook of Nucleating Agents*; Chemtech Publishing: Toronto, ON, Canada, 2016; ISBN 978-1-895198-93-5.
43. Tartaglione, G.; Tabuani, D.; Camino, G. Thermal and morphological characterisation of organically modified sepiolite. *Microporous Mesoporous Mater.* **2008**, *107*, 161–168. [CrossRef]
44. Lvov, Y.; Guo, B.; Fakhrullin, R.F. *Functional Polymer Composites with Nanoclays*; RSC Smart Materials: Cambridge, UK, 2016; ISBN 1782624228.
45. Lemić, J.; Tomašević-Čanović, M.; Djuričić, M.; Stanić, T. Surface modification of sepiolite with quaternary amines. *J. Colloid Interface Sci.* **2005**, *292*, 11–19. [CrossRef]
46. Botana, A.; Mollo, M.; Eisenberg, P.; Torres Sanchez, R.M. Effect of modified montmorillonite on biodegradable PHB nanocomposites. *Appl. Clay Sci.* **2010**, *47*, 263–270. [CrossRef]
47. Cervantes-Uc, J.M.; Cauich-Rodríguez, J.V.; Vázquez-Torres, H.; Garfias-Mesías, L.F.; Paul, D.R. Thermal degradation of commercially available organoclays studied by TGA–FTIR. *Thermochim. Acta* **2007**, *457*, 92–102. [CrossRef]
48. Han, L.; Han, C.; Cao, W.; Wang, X.; Bian, J.; Dong, L. Preparation and characterization of biodegradable poly(3-hydroxybutyrate-co-4-hydroxybutyrate)/silica nanocomposites. *Polym. Eng. Sci.* **2011**, *52*, 250–258. [CrossRef]
49. Hongchao, Z.; Kanishka, B.; Pengqun, K.; Juming, T.; Barbara, R.; Scott, M.; Shyam, S. Effects of Oxygen and Water Vapor Transmission Rates of Polymeric Pouches on Oxidative Changes of Microwave-Sterilized Mashed Potato. *Food Bioprocess Technol.* **2016**, *9*, 341–351. [CrossRef]
50. Wilson, A.S. *Plasticisers: Principles and Practice*; The Institute of Materials: London, UK, 1995.
51. Järnström, H.; Saarela, K.; Kalliokoski PPasanen, A.-L. Comparison of VOC and ammonia emissions from individual PVC materials, adhesives and from complete structures. *Environ. Int.* **2008**, *34*, 420–427. [CrossRef] [PubMed]
52. Ohkado, Y.; Kawamura, Y.; Mutsuga, M.; Tamura, H.-O.; Tanamoto, K. Analysis of residual volatiles in recycled polyethylene terephthalate. *J. Food Hyg. Soc. Jpn.* **2005**, *46*, 13–20. [CrossRef]
53. Hu, M.; Jacobsen, C. *Oxidative Stability and Shelf Life of Foods Containing Oils and Fats*; Subchapter 13.5.5 Aldehyde Scavenging Packaging; Elsevier: Amsterdam, The Netherlands, 2016; ISBN 978-1-63067-056-6.
54. Azarbad, M.H.; Jeleń, H. Determination of Hexanal—An Indicator of Lipid Oxidation by Static Headspace Gas Chromatography (SHS-GC) in Fat-Rich Food Matrices. *Food Anal. Methods* **2014**, *8*, 1727–1733. [CrossRef]

ARTICULO 3

Color Fixation Strategies on Sustainable Poly-Butylene Succinate Using Biobased Itaconic Acid

G. Quiles, L.; Vidal, J.; Luzi, F.; Dominici, F.; Fernández Cuello, Á.; Castell, P.
Polymers 2021, 13, 79.
Impact Factor: 3.426 (2019); 5-Year Impact Factor: 3.636 (2019) – Q1

El presente artículo versa sobre la necesidad de mejorar las propiedades estéticas y mecánicas del succinato de biopolibutileno (bioPBS). El **objetivo** es mejorar la fijación del colorante en la matriz sin disminuir sus propiedades mecánicas para lograr que el bioPBS pueda ser comparable con sus homólogos actuales como el polipropileno (PP) en aplicaciones industriales como por ejemplo salpicaderos y puertas en automoción o paneles de operación y frontales en electrodomésticos.

En el artículo se desarrollan, caracterizan y comparan un total de trece materiales, siendo doce biocompuestos que contienen combinaciones de tres aditivos diferentes: un colorante comercial rojo (4wt%), ácido itacónico (IA - al 4wt% y 10wt%) para mejorar la fijación del color y nanopartículas de zirconia (ZrO_2 – al 2wt% y 4wt%) que fue necesario incorporar para mantener al menos las propiedades mecánicas del PBS natural. La naturaleza del pigmento rojo utilizado muestra un comportamiento blando, el cual al ser utilizado en conjugación con el IA que en la industria química se utiliza para la formulación de elastómeros, podía acentuar un excesivo ablandamiento superficial del material. Por ello, se incluye en la investigación la adición de Zirconia, una cerámica muy dura utilizada habitualmente como agente endurecedor en recubrimientos.

Los ensayos de caracterizaron realizados fueron: mecánicos (universales de tracción y flexión), dureza (Rockwell), mojabilidad (ángulo de contacto), estructura macromolecular (SEM) y cambios en color y brillo (espectrofotometría).

Los resultados muestran que la combinación de IA y el colorante tiende a amarillear ligeramente la mezcla debido a los espectros de absorbancia de IA y también a modificar el brillo debido a la formación de nanocristales que afectan a la dispersión

de la luz mostrando acabados superficiales en mate. Además, para cantidades bajas de IA las propiedades mecánicas del material mejoran, manteniendo la rigidez y aumentando la tenacidad respecto del bioPBS virgen. Inesperadamente, tras cuatro semanas de inyectar las probetas que se usaron para los ensayos de caracterización, se observó un fuerte efecto de envejecimiento apareciendo una fragilidad extrema, ablandamiento del material así como una película blanquecina en la superficie. Los resultados revelan que el IA aumenta el comportamiento hidrófilo de las muestras y por tanto parece acelerar la hidrolización de la matriz (degradación), que viene acompañada de una acusada desagregación de fases entre el IA y el PBS, causantes de la merma en las propiedades mecánicas. Además, la adición de bajas cantidades de ZrO_2 parece proporcionar el efecto deseado para endurecer la superficie sin afectar casi a las otras propiedades; sin embargo, cantidades más altas tienden a formar agregados que saturan los compuestos.

Como **conclusión**, el uso de IA podría ser un buen candidato para usarse como agente de fijación del color en polímeros biobasados, sin embargo, es necesario mejorar la fijación o acople del IA en la matriz para favorecer la compatibilidad y miscibilidad entre ambos, evitando así la separación de fases. Además, debido a los rangos de absorbancia natural de IA, se recomienda su uso preferentemente pigmentos amarillos o azules.

Aportes técnico-científicos:

- Desarrollo de nuevos materiales compuestos biobasados usando agentes cromóforos (pigmentos que imparten color) y auxocromos (agentes que intensifican el color y mejoran la afinidad). Se migra el concepto de usar IA como auxocromo en otras aplicaciones como desarrollo de pinturas en el que la resina matriz es un sustrato totalmente diferente al termoplástico; o el de su uso como precursor en la producción de polímeros elastómeros (*building-block*), para investigar un nuevo uso como fijador de color en mezclas en masa para bio-poliésters.
- El método de caracterización en su conjunto para poder evaluar y comparar el efecto de envejecimiento producido por el IA, tanto sobre las propiedades estéticas como sobre las mecánicas, para lo que es fundamental una lectura comparativa teniendo en cuenta también los resultados del SEM, los cambios en su energía superficial y por tanto mojabilidad, o la dureza.

polymers

MDPI

Article

Color Fixation Strategies on Sustainable Poly-Butylene Succinate Using Biobased Itaconic Acid

Lidia G. Quiles [1,*], Julio Vidal [2], Francesca Luzi [3], Franco Dominici [3], Ángel Fernández Cuello [4] and Pere Castell [2,*]

1 Tecnopackaging, Polígono Industrial Empresarium C/Romero Nº, 12, 50720 Zaragoza, Spain
2 Fundación Aitiip, Polígono Industrial Empresarium C/Romero Nº, 12, 50720 Zaragoza, Spain; julio.vidal@aitiip.com
3 Department of Civil and Environmental Engineering, University of Perugia, 05100 Terni, Italy; francesca.luzi@unipg.it (F.L.); franco.dominici@unipg.it (F.D.)
4 Escuela de Ingeniería y Arquitectura, University of Zaragoza, Av. María de Luna, 3, 50018 Zaragoza, Spain; afernan@unizar.es
* Correspondence: lgarcia@tecnopackaging.com (L.G.Q.); pere.castell@aitiip.com (P.C.); Tel.: +34-976-46-45-44 (P.C.)

Abstract: Biopo-lybutylene succinate (bioPBS) is gaining attention in the biodegradable polymer market due to its promising properties, such as high biodegradability and processing versatility, representing a potential sustainable replacement for fossil-based commodities. However, there is still a need to enhance its properties for certain applications, with aesthetical and mechanical properties being a challenge. The aim of the present work is to improve these properties by adding selected additives that will confer bioPBS with comparable properties to that of current counterparts such as polypropylene (PP) for specific applications in the automotive and household appliances sectors. A total of thirteen materials have been studied and compared, being twelve biocomposites containing combinations of three different additives: a commercial red colorant, itaconic acid (IA) to enhance color fixation and zirconia (ZrO_2) nanoparticles to maintain at least native PBS mechanical properties. The results show that the combination of IA and the coloring agent tends to slightly yellowish the blend due to the absorbance spectra of IA and also to modify the gloss due to the formation of IA nanocrystals that affects light scattering. In addition, for low amounts of IA (4 wt %), Young's Modulus seems to be kept while elongation at break is even raised. Unexpectedly, a strong aging affect was found after four weeks. IA increases the hydrophilic behavior of the samples and thus seems to accelerate the hydrolization of the matrix, which is accompanied by an accused disaggregation of phases and an overall softening and rigidization effect. The addition of low amounts of ZrO_2 (2 wt %) seems to provide the desired effect for hardening the surface while almost not affecting the other properties; however, higher amounts tends to form aggregates saturating the compounds. As a conclusion, IA might be a good candidate for color fixing in biobased polymers.

Keywords: biopolymers; biocomposites; polybutylene succinate; itaconic acid; zirconium oxide; colorant; hardness; color fixing; gloss; aging effect

Citation: G. Quiles, L.; Vidal, J.; Luzi, F.; Dominici, F.; Fernández Cuello, Á.; Castell, P. Color Fixation Strategies on Sustainable Poly-Butylene Succinate Using Biobased Itaconic Acid. *Polymers* **2021**, *13*, 79. https://doi.org/10.3390/polym13010079

Received: 26 November 2020
Accepted: 23 December 2020
Published: 28 December 2020

1. Introduction

Technical biopolymers are becoming increasingly attractive as sustainable and good-performing polymeric materials [1]. One of the most promising biopolymers is biopolybutylene succinate (bioPBS). BioPBS is an aliphatic polyester synthesized from the polymerization of two biobased building blocks: succinic acid (or dimethyl succinate) and 1,4-butanediol [2,3], all coming from renewable sources. The materials and products derived from bioPBS are soft, flexible and have become a promising replacement for commodities [4] such as polyethylene terephthalate (PET), polypropylene (PP) and polyethylene (PE) as they exhibit nearly comparable mechanical properties [5] to these synthetic plastics for

several applications such as packaging, construction applications, houseware, furniture or agriculture [6]. In addition, bioPBS undergoes biodegradation during disposal in compost, moist soil, fresh water and seawater [7], which reduces its potential environmental impact and makes it a promising candidate to enhance the sustainability of plastic products—as currently demanded by the markets and consumers.

However, a general drawback of biopolymers, among them bioPBS, is that they present poor aesthetic appearance compared to oil-based counterparts. Every thermoplastic material has its own innate color. A thermoplastic material in its innate color state is referred to as natural. The natural color of biopolymers usually vary from yellowish, brownish to crude whitish, that many times is not the preference of the consumer. Thus, the use of pigments or additives to tailor the appearance of biopolymers is required. In terms of color, bioPBS has a whitish bright matrix. The need to introduce these materials in the market requires the improvement of such properties, allowing customization of the final color.

The term "colorant or coloring agent" denotes a series of colored substances that affect a material's appearance. Therefore, the introduction of a coloring agent would increase the attractiveness of the bioplastic and the potential acceptance of the material in more applications. Nevertheless, how the material responds to the colorant is a critical aspect of the overall appearance that also involves gloss and texture. Gloss is used to describe the manner in which a surface reflects light: specular reflection (shiny), diffuse reflection or it can absorb the light (dull). Regarding texture, smooth surfaces reflect light in the specular direction, whereas diffuse reflection dominates in the case of rough surfaces.

Two kinds of coloring agents are usually used to color plastics: pigments and dyes. Pigments may be either organic or inorganic in structure and are insoluble both during processing of the plastics and in the end product [8,9]. Dyes, on the other hand, are organic molecules that dissolve into the substrate to which they are applied. Azo colorants are the most important class of synthetic dyes and pigments, representing 60–80% of all organic colorants [10]. These colorants contain one or more nitrogen–nitrogen double bonds (–N = N–) in their chemical structure and may possess other functional groups [11]. They have excellent coloring properties, mainly in the yellow to red range, as well as good lightfastness. Azo colorants are used widely in substrates such as textile fibers, leather, plastics, papers, hair, mineral oils, waxes, foodstuffs, rubbers and paints.

The colorant not only needs to match the desired color but it should also satisfy other constraints such as to be chemically compatible with the base polymer matrix and to be chemically stable. In order to be able to provide a wide palette of colors, it is important to reach a good color fixation and gloss, making it long-lasting (durable), and that it also does not affect other functional key properties such as hardness or mechanical performance. Other factors influencing color strength are particle size and dispersion in the plastic matrix.

Ideally, when a biobased material is conceived, the colorants and additives used in the formulation should come from a bio-based origin [12,13]. Natural pigments and dyes present poor color fastness and yield compared to synthetic ones [14]. For this reason, it is necessary to introduce a linking agent that enhances compatibility with the polymeric matrix. Most of the natural dyes present hydroxylic groups (–OH) in their structure and for example can be esterified with polycarboxylic acids such as citric acid or itaconic acid (IA) [15]. These, and others such as amino groups, are considered color helpers. They are known as auxochromes [16], which are able to alter both the intensity and the wavelength of absorbed light influencing the physical-chemical properties of the material while they do not produce color by themselves. These are often used as color fixation chemicals enhancing the overall stability of the colored part.

Among the different linking agents used in polymer science, IA has demonstrated good performance in oil-based polymers [17]. Today, IA is exclusively produced by fermentation with carbohydrates by filamentous fungi, mainly *Aspergillus terreus* [18]. Thus, it has the potential to be produced exclusively from biomass. IA is a fully sustainable industrial building block, an ionic hydrophilic co-monomer, with a myriad of chemical applications due to its structural similarity to acrylic and methacrylic acids [17]. In fact, it presents a

viable solution to replace acrylic acid in biodegradable polymers. For example, it is used in the production of lubricants, active agents, dyes, plastics, chemical fibers, etc. [19]. Other promising uses are unsaturated polyester resins, phosphate-free detergents, and in the food industry [20]. It is stable at acidic, neutral and middle basic conditions at moderate temperatures, so it was considered a good candidate for the extrusion-compounding process in which high temperatures and shear forces are achieved.

However, as it is a component usually used in the formulation of gums/elastomers and latex, one of the drawbacks of using IA in different thermoplastics is the softening effect, which might be accentuated by the organic nature of the diazo pigment. The use of inorganic fillers has been demonstrated to be a good strategy in composites for enhancing mechanical properties [21–25]. Among these fillers, nanoparticles such as ZrO_2 have been used in several applications [26,27]. Its natural whitish color, and its excellent dimensional stability, mechanical and chemical properties, has made zirconia a highly attractive ceramic material in medical applications such as hip head replacement instead of titanium or alumina prostheses and in particular for prosthodontics [28,29]. Zirconia has also been used to produce hard coatings for plastic surfaces with antifogging, anti-wetting and antistatic properties [30]. Due to this reason, it was decided to add zirconium dioxide to harden bioPBS surface as well as prevent it from losing mechanical properties.

The objective of this study is to develop an enhanced biobased material showing good aesthetical properties in terms of color fixing while keeping at least the mechanical properties of the original matrix polymer (bioPBS) in order to make it attractive for a plethora of applications in the market such as automotive, householding or furniture. In this research, IA has been selected as functional color helper to better fix and increase the lightfastness of an organic red diazo pigments in bioPBS matrix. To enhance the resulting material mechanical properties ZrO_2 was as a reinforcing agent. A complete and detailed characterization has been conducted using micro and macroscopical techniques such as SEM, wettability, color change, hardness, and mechanical analysis. Additionally, an aging effect was evaluated during the realization of the experimental work and their effects were characterized and compared.

2. Materials and Methods

2.1. Materials

The polymer matrix used was a biobased polybutylene succinate BioPBS FZ71 PD which was purchased from Japan Pulp and Paper GmbH (Düsseldorf, Germany).

The IA 99% pure, was purchased from Sigma Aldrich (Darmstadt, Germany). It is a white crystalline powder, unsaturated dicarboxylic acid ($C_5H_6O_4$), in which one carboxyl group is conjugated to the methylene group [31]. It presents a hygroscopic property, and it is odor-free [32,33]. Its melting point is 167–168 °C and the boiling point is 268 °C [34].

The coloring agent was purchased from UNNOX GROUPS (Esquiroz, Spain) which is an organic red diazo pigment with the commercial code: PR57:1, MDN-1153.

Finally, the Zirconia nanoparticles were kindly provided by the TORRECID group (L'Alcora, Spain). Zirconia is a crystalline dioxide of zirconium. Its mechanical properties are very similar to those of metals (it has been called 'ceramic steel' [35]). Zirconia crystals can be organized in three different patterns: monoclinic (found at room temperature, under ambient pressure and upon heating up to 1170 °C), tetragonal (between 1170 and 2370 °C), and cubic (above 2370 °C and up to the melting point) [36].

2.2. Nano-Bio-Composites Preparation

Twelve different formulations were prepared by extrusion-compounding with a 26-mm twin-screw Coperion ZSK 26 compounder machine (Stutgart, Germany). Firstly, binary blends were extruded: F2 and F3; F4 and F5 and F6. The three additives were introduced in a powder format from a secondary feeder different from the bioPBS main hopper. IA was introduced at the beginning of the barrel while the ZrO_2 and the coloring agent at the middle of the barrel. The melted polymer and powders were mixed at a screw speed of

200 rpm; temperature was in-creased from 160 °C in the feeding zone up to 180 °C at the nozzle. The compounding was extruded through a 2 mm diameter die for a constant output of 15 kg/h. The extrudate was quenched in a water bath at room temperature, dried and cut into pellets. A total of 3 kg of per blend were produced. Ternary and quaternary formulations were produced by re-extruding in a second step using the conditions above. To this end, the colorant and the zirconia were added into bioPBS/IA extruded matrices, by introducing them at the middle of the barrel as for the first extrusion-compounding step. No modifications were required regarding the parameters and conditions of the extrusion process. Table 1 summarizes the composition of all references.

Table 1. Summary of material formulations based on bioPBS FZ71PD matrix.

Reference	bioPBS Matrix	IA	Colorant	ZrO_2
F1	100%	-	-	-
F2	96%	4%	-	-
F3	90%	10%	-	-
F4	96%	-	4%	-
F5	98%	-	-	2%
F6	96%	-	-	4%
F7	94%	-	4%	2%
F8	92%	4%	4%	-
F9	86%	10%	4%	-
F10	94%	4%	-	2%
F11	88%	10%	-	2%
F12	90%	4%	4%	2%
F13	84%	10%	4%	2%

Samples were analyzed at week 0 (W0), just after their preparation and after aging in ambient conditions at week 4 (W4).

2.3. General Characterisation Methods

2.3.1. Two Types of Specimens Were Developed for Material Characterization

- Injected specimens for mechanical (tensile or dog-bone following ISO 178 standard) and hardness (parallelepiped specimens of 80 × 100 × 4 mm) testing were obtained by injection molding with a JSW 85 EL II electric injection machine.

The temperature profile was increased from 150 °C at the hopper up to 180 °C at the nozzle with 40 rpm. The dosage and filling pressure were varied for each formulation injected. A packing pressure of 35% (55 bar during 20 s) was applied. When injecting samples containing IA, temperatures were decreased from 140 °C at the hopper up to 160 °C at the nozzle and cooling time increased by 10 s so that it was cooled enough to be expelled from the mold.

- Circular specimens of 50 mm diameter and 2 mm thick from all the formulations were produced for measuring wettability and color change. The same processing parameters were considered. The materials were mixed for 120 s at 90 rpm in a co-rotating twin-screw extruder Microcompounder at 5 and 15 cc, DSM (Sittard, The Netherlands), using a temperature profile of 120–125–130 °C. Due to the low viscosity of the formulations containing IA, a pressure-time injection molding profile of 1.0–5; 1.1–15; 1.1–15 in bar-seconds was used. The mold and injection temperatures were set at 30 and 150 °C, respectively.

2.3.2. Measurements

Mechanical tests were conducted under ambient conditions using a Zwick Roell Z 2.5 (Ulm, Germany). At least five specimens per material were tested, according to ISO 178 and ISO 527 Methodology

Structural properties were evaluated by scanning electron microscopy (SEM) with a Hi-tachi S3400N (Tokyo, Japan) equipment in order to determine the morphology and dispersion. Broken samples coming from the mechanical tests were used.

Hardness was measured using a portable hardness tester, the METALTEST tester model T500 (Barcelona, Spain), to verify material hardness with load-cell technology for Vickers, Brinell and Rockwell testing. The Rockwell B scale was used for this study.

The surface properties of produced materials were evaluated by static contact angle measurements (FTA1000 Analyzer (Newark, NJ, USA)). The wettability of the surfaces was studied by using the sessile drop method, in air, in contact with HPLC grade water. When a surface is hydrophilic, the drop extends over the material at an angle between 0° and 30°. If the surface of the solid is hydrophobic, the contact angle will be greater than 90°. On surfaces that are very hydrophobic, the angle can be greater than 150° and even close to 180°.

Color change and gloss of samples was investigated by means of a spectrophotometer (CM-2300d Konica Minolta, Japan). Data were acquired by using the SCI 10/D65 method, CIELAB color variables, as defined by the Commission Internationale de 1′Éclairage (CIE 1995), were used.

Samples were placed on a white standard plate and L^*, a^*, and b^* parameters were de-termined. L^* value ranges from 0 (black) to 100 (white); a^* value ranges from −80 (green) to 100 (red); and b^* value ranges from −80 (blue) to 70 (yellow). For each sample, 3 measurements were taken at random location. The total color difference or distance between colors (Euclidean distance) ΔE^* between white and the samples was calculated as indicated in Equation (1) [37]: color-difference formula:

$$\Delta E* = \sqrt{(\Delta L*)^2 + (\Delta a*)^2 + (\Delta b*)^2} \quad (1)$$

3. Results and Discussion

3.1. Mechanical Tests

The mechanical properties of biocomposite materials are always a compromise between stiffness and toughness which are generally mutually exclusive. The elastic modulus (E) and elongation at break (ε_B) are useful parameters to describe the mechanical behavior of the developed materials and are closely related to the internal microstructure. The mechanical properties determined from uniaxial tensile tests are summarized in Table 2 and their com-parison among the different formulations and aged samples are shown in Figure 1.

Table 2. Mechanical properties under tensile force: Young's modulus and elongation at break for all characterized materials; surface hardness and contact angles measurement (wettability). Measurements done at week 0 (W0) and after 4 weeks aging (W4).

Material	Young's Modulus (MPa) W0	Young's Modulus (MPa) W4	Elongation at Break (%) W0	Elongation at Break (%) W4	Hardness (HRB) W0	Hardness (HRB) W4	WCA (°) W0	WCA (°) W4
F1	590 ± 30	685 ± 20	268 ± 27	262 ± 9	6.2 ± 1.3	5.1 ± 0.9	76 ± 1	69 ± 3
F2	473 ± 37	866 ± 33	289 ± 119	1.5 ± 0.8	20.6 ± 2.6	Break	54 ± 3	54 ± 0
F3	528 ± 49	953 ± 63	317 ± 75	0.67 ± 0.05	5.1 ± 0.4	Break	66 ± 3	47 ± 3
F4	645 ± 24	740 ± 14	258 ± 16	60 ± 4	2.6 ± 1.4	2 ± 1.3	68 ± 3	70 ± 3
F5	625 ± 13	740 ± 60	258 ± 7	173 ± 18	6.6 ± 1.1	1.6 ± 0.5	75 ± 3	66 ± 1
F6	726 ± 31	960 ± 351	205 ± 68	192 ± 18	4.3 ± 1.3	1.1 ± 0.6	76 ± 3	71 ± 2
F7	631 ± 31	739 ± 23	249 ± 16	225 ± 32	1.1 ± 0.8	1.1 ± 0.8	70 ± 3	66 ± 3
F8	634 ± 59	966 ± 32	75 ± 65	0.88 ± 0.2	10.4 ± 1.5	Break	63 ± 4	56 ± 3
F9	626 ± 52	946 ± 39	259 ± 133	0.27 ± 0.01	6.4 ± 0.7	Break	65 ± 3	58 ± 4
F10	659 ± 52	1052 ± 67	247 ± 42	0.97 ± 0,4	17.4 ± 0.3	Break	59 ± 2	44 ± 3
F11	587 ± 34	937 ± 24	279 ± 45	0.56 ± 0.28	5.0 ± 1.2	Break	67 ± 2	61 ± 3
F12	610 ± 52	1027 ± 66	57 ± 7	0.88 ± 0.2	10.2 ± 1.6	Break	60 ± 3	61 ± 3
F13	585 ± 103	979 ± 53	145 ± 108	0.3 ± 0.05	5.6 ± 0.6	Break	60 ± 4	59 ± 3

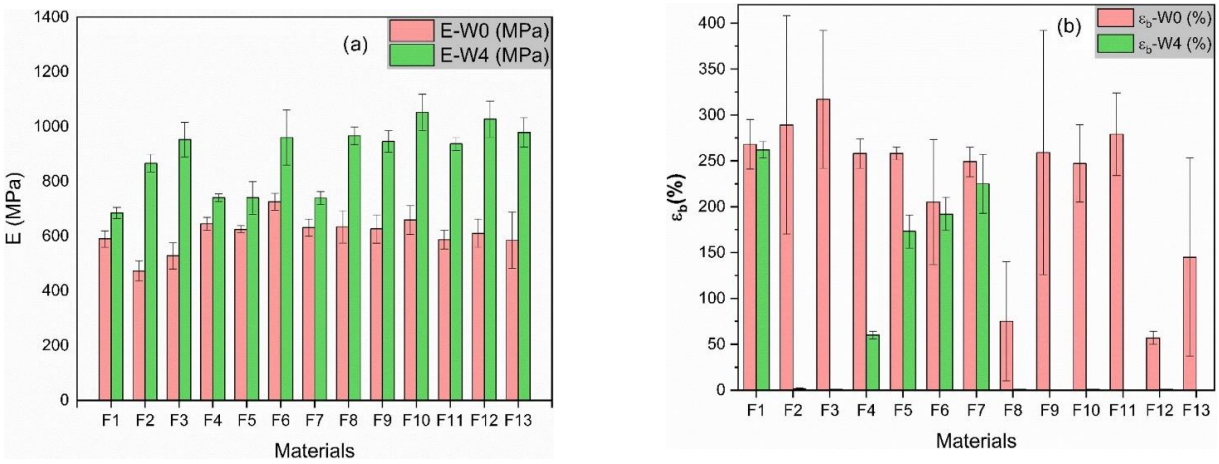

Figure 1. Young's moduli (**a**) and elongation at break values (**b**) for all specimens evaluated at W0 and W4.

3.1.1. Comparative Results among Formulations at W0 (Comparisons among Pink Columns—Young's Modulus; and among Green Columns—Elongation at Break)

When IA is added to neat PBS a reduction in the Young's modulus by 11% for F2 and by 26% for F3 is observed, while an increase in the elongation at break by 8% for F2 and by 18% for F3 is found. Thus, IA seems to induce a plasticizing effect, which is in coherence with Kirimura et al. [34] who explained the use of this component in rubber-like polymers due to its excellent strength and flexibility, making the PBS tougher. This result is also aligned with Krishnan et al. [38], who used IA to design an aliphatic copolyester elastomer that was used as PLA toughener.

The addition of the colorant (F4) as well as low amounts of ZrO_2 (F5) slightly increases the Young's modulus, while the material stiffness is considerable raised by 23% when a 4 wt % of ZrO_2 is incorporated (F6). On the one hand, Zirconia affects in the elongation at break and an overall fall can be observed (F6 decreases a 24%). Nevertheless, the data dispersion is broad, that indicates the appearance of agglomerates producing a stress concentrating effect favoring a premature rupture [39]. All in all, this decrease is noticeably found for 4 wt % of ZrO_2, which is a quite positive result for such a high content of zirconium if compared with other similar studies using it as reinforcement agent in polymers. For example, Mishra T.K. et al. [40] found the same decrease in the elongation at break for PEEK/ZrO2 compounds with just a 1 wt %. On the other hand, when the colorant is incorporated to PBS (F4) elongation at break values remain almost unchanged. Consequently, the colorant appears to be better dispersed and integrated than the ZrO_2 probably due to its organic nature which is more compatible with the blend.

Ternary formulations (F5, F6, F8, F9, F10, F11) and quaternary blends (F12, F14), lead to a complex mechanical behavior in which the rigidity of the materials is kept or even scarcely in-creased when compared to neat PBS. The combination of these additives induce a remarkable fall in the elongation at break respect to neat PBS. The most prominent decrease is found for F8 by 72% and F12 by 79%, closely followed by F13. Both formulations are complex blends combining a 4% wt % of IA and colorant. The high scattering of the data confirms a lack of integration between the IA, the matrix and the additives, probably forming regions of high and low IA concentration peaks; and the formation of zirconia and colorant aggregates with insufficient dispersion (a result that has been corroborated with SEM micrographs).

3.1.2. Comparative Results of Same Formulations between W0 and W4 (Aging Effect)

All plastic materials suffer from aging with time. They tend to recrystallize as the polymer chains end their ordering. The plastic gets stiffer and in a long-term becomes brittle. Kimble et al. [41], studied aging in PLLA/PBS blends including annealing and

creep studies. As conclusion, blends with high content of PBS tend to decrease its Mw with time produced by degradation and showing and embrittlement of samples. Thus, their results also highlighted the importance of appropriate storage conditions for ductility retention. In this study, the Young's modulus of neat PBS increased by 16% (F1) after 4 weeks. The elongation at break was maintained, that indicated the good integrity of the material and, apparently, an absence of degradation.

The effect of the IA was remarkable. In F2 and F3 samples, the Young's modulus raised by 80%, which clearly indicated the rigidization effect. The blends lost their toughness and became very brittle. A drop in the elongation at break by more than 98% was observed in all the formulations containing IA.

When adding the colorant (F4) and a 2 wt % of ZrO_2 (F5), the material became a 15% stiffer in both cases, while when increasing the addition of ZrO_2 by 4 wt % (F6) the Young's modulus doubled by reaching a 32% higher value. Stiffness and toughness are usually compromised properties, and we can find a reduction in elongation at break by 6% for F6 and by 33% for F5. These results draw a better dispersion of ZrO_2 for F6 rather than F5. The colorant also seems to highly affect this property, falling by 77% (F4), that may indicate a disaggregation of the organic phases with time that weakens the interphase between the colorant and the additive.

When ternary and quaternary blends are studied (F8–F13), we can observe a rise in the Young's modulus between 60% and 70%, as expected, and practically an absence of elongation at break effect induced by the IA.

3.2. Hardness

3.2.1. Hardness Results at W0

The highest value on hardness is found for F2 (4 wt % IA), which multiplies almost by four the hardness value for neat PBS, while for F3 (10 wt %) it decreases a 18% down neat PBS value. It is likely that a 10 wt % IA has saturated the blend, showing a lack of miscibility among the two phases (polybutylene succinate (PBS) and IA). The shear forces or thermodynamics produced during the compounding process might not have been enough to disperse and homogenize the components, which seem not to be compatible and which tend to form separated phases inside the blend. Moreover, as these phases are distinct, the IA apparently seems to crystallize into the surface of the injected specimen. Using the SEM micrographs we can observe the IA crystals, and when the indenter finds a high concentration of IA in the surface it also finds a fragile and brittle point.

When observing F4, the PBS phase mainly contains the colorant, which is a soft pigment, and the overall hardness of the blend decreases by 58%. On the other hand. when characterizing F5 and F6, we can find a hardening effect by 6% for the 2 wt % of zirconia. However, when adding a 4 wt % of zirconia, hardness decreases by 31%, probably due to a saturation of the blend accompanied by the apparition of agglomerates. The high surface energy of nanoparticles is prone to induce the formation of nanoparticles aggregation [42]. Thus, phase separation often takes place owing to the great differences in the properties of polymer and inorganic materials.

When combining the colorant and the ZrO_2 (F7), there is a negative synergistic effect, decreasing the hardness value by 82%, while the combination of any of them with the 4 wt % IA induces a positive synergy in which the IA dominates the behavior of the complex blends (F8 by 68%, F10 by 181% and F12 by 65%). However, with a 10 wt % IA added instead, it still dominates the blend keeping similar values to those found for F3.

3.2.2. Hardness Results at W4

When hardness was measured at W4, the authors found a clear embrittlement of the samples. Especially in those containing IA (F2, F3 and F8–F13), to which it was not possible to repeat the characterization test. The specimens broke when the indenter penetrated the sample, and some of the experiment samples even had a ductile fracture just from being manipulated.

3.3. Structural Properties (SEM)

The surface morphology of the developed formulations was studied by using scanning electron microscope (SEM). Micrographs of representative specimens are shown in Figure 2.

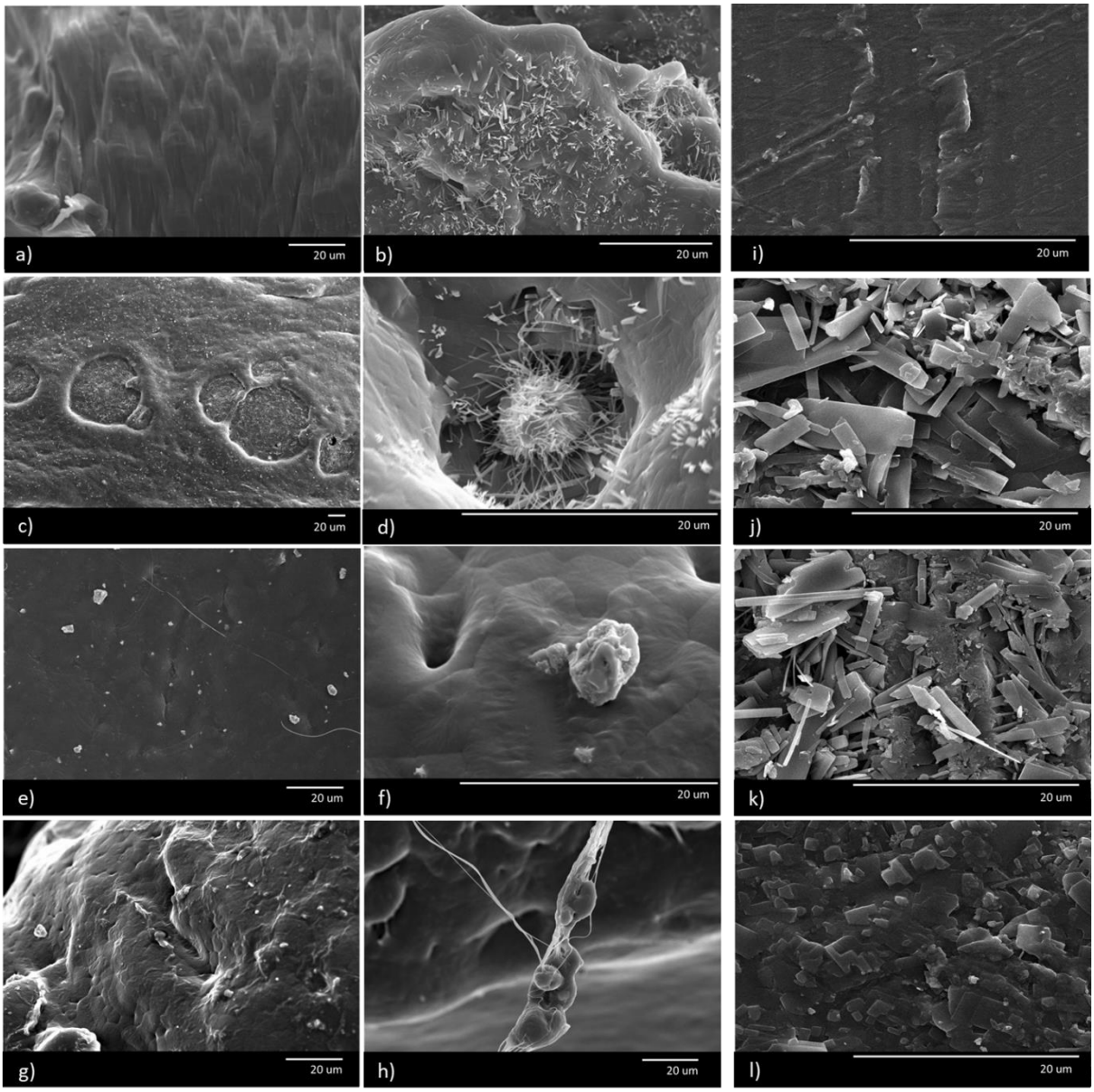

Figure 2. SEM—W0 (left—(**a**,**c**,**e**,**g**)—and central—(**b**,**d**,**f**,**h**)—columns) and W4 (right column—**i**,**j**,**k**,**l**). (**a**): F1; (**b**): F3; (**c**): F9; (**d**): F13; (**e**,**f**): F5; (**g**,**h**): F4; (**i**):F1; (**j**): F3; (**k**): F9; (**l**) F10.

3.3.1. Structural Results at W0

The micrographs confirm the tendencies observed in the mechanical and hardness results. IA crystallizes in the form of rectangular nanocrystals. It clearly manifests a special phase morphology constituted by the disperse phase of IA. These nanocrystals are found to group themselves in a heterogeneous way showing a lack of compatibility between the IA and the PBS (b,c). The IA nanocrystals are found to migrate to the surface of the part. The authors observed this phenomena: either over time outside to the external surface (Figure 2j,k are taken from the border perimeter), or within internal created surfaces such as for example in bubbles or defects generated during the injection process of the specimen

(Figure 2d). Therefore, we find a highly reinforced material at the surface level, but as it is not miscible, it is not well integrated, and a segregation of the phases is observed.

Apparently, as the pigment is highly organic, it displays a good interfacial bonding with the polymer (Figure 2g,h). The ZrO_2 seems to be well dispersed, although a few aggregates can be found (Figure 2e,f). When ternary and quaternary blends are studied, those containing IA nanocrystals tend to surround the colorant aggregates. This effect can be explained as probably being due to the combination of the polar–apolar performance of both materials, that generates a complex interface inducing a low adherence with the polymeric matrix, PBS. The IA is an acid, that means that the hydrogen on the OH group can easily be removed, leaving an anion. Both the colorant pigment as well as ZrO_2, may act as a salt to the IA, favoring the attraction between them (Figure 2d). These aggregates have a stress concentrating effect which reduces the toughness of the material, favoring a premature breaking, that explains the mechanical behavior found.

3.3.2. Structural Results at W4

Finally, a change in the type of fracture can be observed between W0 and W4. At W0 the fracture surface evidenced a ductile behavior (Figure 2a), while at W4 a more fragile surface is found showing a flat fracture surface of the polymer accompanied by some striations (Figure 2i), in which polymeric chains have had the time to rearrange. So does the IA, which is unstable in the blend and migrates to the surface of the specimen, seeking the state of minimum energy (Figure 2j,k,l). Thus, it can be confirmed that the materials suffer from aging that induces a rigidization mechanism and that it is clearly intensified with the addition of IA.

3.4. Hydrophobicity/Wettability

Wettability results are included in Table 2. The range WCA values for our bioPBS systems vary between 44° and 76°.

3.4.1. Structural Results at W0

The presence of IA in binary systems reduces WCA when compared with neat PBS (F1), this phenomenon is more pronounced in F2 than in F3 making the material more hydrophilic. It is also found a slight reduction in the WCA when colorant is added (F4) while the presence of ZrO_2 does not change the WCA value of reference PBS matrix (F5, F6). Mizuno et al. [5], showed the same tendency as with IA when introduced grafted Acrylic Acid into PBS to study and control the biodegradability of this aliphatic polyester. Their study demonstrated that a more hydrophilic surface had a considerable impact in the biodegradation of the PBS and thus it negatively affects the mechanical and structural properties.

In the samples where IA was combined with ZrO_2 (F10, F11 systems), the WCA seems to be influenced only by the presence of IA and the contact angle values are similar to the values recorded for PBS/IA binary systems.

The addition of ZrO_2 (F7) does not change the values of F4, influenced by the colorant pigment, as already noted in the case of ternary systems. The presence of IA reduces the values of F4, so the decrease in wettability in the presence of IA is confirmed even in colored samples (F8, F9). Moreover, as explained, the colored samples suffer from cleavage of the labile groups of the red pigment, thus accelerating even more this degradation process that is also translated in a more hydrophilic surface.

Including the ZrO_2 in the F12 and F13 systems only slightly changes the WCA values, when compared to ternary systems having IA but without ZrO_2 (F8, F9).

3.4.2. Structural Results at W4

An overall decrease on WCA was observed comparing the values obtained for PBS samples at W0 and at W4, making the matrix material more hydrophilic with time as a result of material degradation. According to Mizuno et al., wettability together with the

stereochemistry, the flexibility of molecular chains and the crystallinity, have been found to be decisive factors in the biodegradability of PBS [42]. Our results show the natural effect of conjugating the natural biodegradation process of PBS synergistically speed up by the acid transfer of IA to the PBS matrix.

3.5. Color Properties

Color properties of all formulations are presented in Table 3.

Table 3. Color coordinates and gloss of polybutylene succinate (PBS) based systems at W0 and W4.

Material Formulations	*L**	*a**	*b**	Δ*E**	Gloss (°)
White Control	99.47 ± 0.00	−0.08 ± 0.01	−0.08 ± 0.01	-	121 ± 0
F1–W0	85.80 ± 0.26	−1.22 ± 0.03	−1.04 ± 0.08	13.75 ± 0.26	78 ± 4
F1–W4	86.05 ± 0.43	−1.05 ± 0.03	−1.60 ± 0.08	13.54 ± 0.43	72 ± 1
F2–W0	86.84 ± 0.13	−1.34 ± 0.04	3.53 ± 0.08	13.20 ± 0.13	72 ± 2
F2–W4	87.34 ± 0.23	−1.07 ± 0.02	3.02 ± 0.19	12.56 ± 0.25	53 ± 3
F3–W0	84.01 ± 0.06	−2.27 ± 0.02	9.92 ± 0.10	18.54 ± 0.06	63 ± 2
F3–W4	84.37 ± 0.21	−1.68 ± 0.14	8.08 ± 0.06	17.23 ± 0.23	17 ± 2
F4–W0	35.09 ± 0.09	36.71 ± 0.26	16.06 ± 0.12	75.89 ± 0.08	77 ± 3
F4–W4	34.84 ± 0.12	35.72 ± 0.17	15.39 ± 0.15	75.49 ± 0.18	77 ± 4
F5–W0	86.43 ± 0.07	−0.41 ± 0.03	8.97 ± 0.05	15.87 ± 0.04	70 ± 2
F5–W4	86.50 ± 0.15	−0.46 ± 0.01	8.41 ± 0.13	15.51 ± 0.06	71 ± 4
F6–W0	88.34 ± 0.06	0.77 ± 0.03	13.29 ± 0.12	17.42 ± 0.09	68 ± 3
F6–W4	88.41 ± 0.10	0.73 ± 0.05	13.07 ± 0.10	17.20 ± 0.11	75 ± 2
F7–W0	39.30 ± 0.39	44.58 ± 0.12	12.51 ± 0.20	75.99 ± 0.30	66 ± 3
F7–W4	39.01 ± 0.23	43.73 ± 0.17	11.60 ± 0.27	75.57 ± 0.32	60 ± 3
F8–W0	36.18 ± 0.09	40.28 ± 0.65	15.7 ± 0.24	76.72 ± 0.38	66 ± 3
F8–W4	36.04 ± 0.36	40.81 ± 0.99	15.43 ± 0.22	77.05 ± 0.40	8 ± 2
F9–W0	34.88 ± 0.14	38.34 ± 0.38	15.39 ± 0.33	76.73 ± 0.20	66 ± 3
F9–W4	34.78 ± 0.51	39.33 ± 1.03	15.38 ± 0.41	77.32 ± 1.03	11 ± 2
F10–W0	87.62 ± 0.34	−0.56 ± 0.04	11.55 ± 0.20	16.62 ± 0.25	71 ± 3
F10–W4	88.05 ± 0.13	−0.78 ± 0.04	10.83 ± 0.40	15.81 ± 0.33	26 ± 1
F11–W0	85.44 ± 0.26	−0.46 ± 0.02	11.38 ± 0.07	18.12 ± 0.19	61 ± 3
F11–W4	85.82 ± 0.10	−0.44 ± 0.05	10.56 ± 0.10	17.31 ± 0.13	29 ± 3
F12–W0	38.25 ± 0.60	40.30 ± 0.13	12.70 ± 0.28	74.44 ± 0.52	63 ± 3
F12–W4	37.84 ± 0.52	42.11 ± 0.46	12.83 ± 0.13	75.79 ± 0.42	5 ± 1
F13–W0	38.88 ± 0.11	42.90 ± 0.11	12.98 ± 0.11	75.42 ± 0.11	67 ± 2
F13–W4	38.89 ± 0.29	44.20 ± 0.21	13.03 ± 0.20	76.17 ± 0.34	8 ± 1

3.5.1. Color Results at W0

On the one hand, IA (F2, F3), reduces the parameter *a* (a bit greener) and it also induces an increase in parameter *b* (more yellow), so the samples tend to have yellowish coloration (shift to warm tones). The absorbance range for red color in the UV-VIS spectra is about the 600 to 700 nm [43], while the natural absorbance peak for IA locates at 200–205 nm [44]. Therefore, the combination tends to move the overall material spectra to the lower wavelength absorbance spectra, moving down first to yellowish and then to greenish values. The gloss of the PBS–IA binary systems decreases as the IA concentration increases—probably due to the formation of nanocrystals which scatter the light in a number of different directions than the original matrix.

On the other hand, the presence of ZrO_2 in PBS (F5, F6) causes an increase in *L**, *a** and *b** parameters, due to its opaque white color. It can be observed that ZrO_2 whitens the specimens and decreases also the gloss of the material. This drop in gloss values may be produced by the roughening effect induced in the matrix structure by the ZrO_2 agglomerates.

For the ternary systems F10 and F11, that combine IA and ZrO_2, the *L* parameter increases when compared to F2 and F3 (IA based). Again, this effect may be produced because of the presence of ZrO_2. The gloss of F10 and F11 systems does not change if

compared to binary F5 and F6 (ZrO_2 binary systems) and F2 and F3 formulations. Thus, we can confirm that there is no sum of the effects of fillers in terms of gloss.

The presence of the 4 wt % colorant determines a considerable variation of the color parameters induced by the red color of the pigment. The combined species formed in the samples absorbs and attenuates the light [45]. The *L* parameter decreases when compared to the value recorded for PBS (that makes darker the material), *a** and *b** increases as expected following the red color scale. The addition of this red pigment does not change the values of the gloss (F4). The presence of ZrO_2 in F7, F8 and F12 samples causes *L* and a parameters to increase while *b* to decrease (bluish) respect to F4, which we consider now as the sample of control. The presence of IA and ZrO_2 in the F12 and F13 system reduces gloss, and no combined effect of the two fillers is revealed.

3.5.2. Color Results at W4

After 4 weeks a considerable reduction of gloss parameter was recorded in all PBS based samples containing IA. The same behavior was also found when colorant was added. Moreover, a synergistic effect appeared when both additives are combined. The azo bond, which is known to be the most labile portion of an azo colorant, can readily undergo cleavage photochemical degradation [46]. Both, the effect of the cleavage in the polymer structure and the formation and re-grouping of IA nanocrystals vary the manner in which the surface reflects light. The internal structure of the material becomes rougher and gloss is dominated by a diffuse reflection.

For PBS samples with ZrO_2 (F5 and F6), the gloss tends to increase with time. However, any combination of ZrO_2 either with IA or colorant or both, is dominated by the other two, obtaining fully dull gloss samples.

4. Conclusions

The present work demonstrates an industrial technology to produce biobased composites with enhanced coloring properties through extrusion-compounding of complex blends. A methodology was proposed to design a biobased material with enhanced and ad hoc aesthetical properties while maintaining the natural polymer performance. To this end, a diazo red colorant has been added to a bioPBS matrix. In order to increase the color fixing, IA has been used with the aim of acting as compatibility agent between the matrix and the pigment, as its structure is quite similar to acrylic acid (we were looking for a behavior similar to paint formulations). Lastly, as IA was also modifying other fundamental properties of bioPBS, ZrO_2 nanoparticles which have a similar natural color as the bioPBS matrix, were incorporated to avoid decreasing stiffness and hardness. An aging effect was observed during the realization of the experimental work and their effects were characterized and compared (week 0 and week 4).

Regarding the mechanical properties, at W0 the addition of the colorant and low amounts of ZrO_2 makes the material stiffer, while it almost does not affect the elongation at break, making the material tough and ductile. The addition of IA provokes the desired effect as it maintains or even increases the Young's modulus (26% for 10 wt % IA) while increasing the elongation at break (18% for 10 wt % IA). Concerning hardness, it is reduced by the addition of the diazo pigment, as expected, while it is augmented by the zirconia at low loads. Combinations of colorant and ZrO_2 are found to produce a negative synergistic effect, decreasing by 82% the hardness value. In contrast, for low amounts of IA, the hardness value is multiplied almost by four times, while higher amounts tend to soft the blend. Complex blends combining the colorant, ZrO_2 and IA shows a dominant behavior induced by IA.

At W4, a prominent embrittlement is found due to an aging effect. A drop in the elongation at break by more than 98% can be observed in all the formulations containing IA, while the Young's modulus rises by 60% to 70% showing a rigidization effect. This behavior is accompanied by a softening of all samples being outstanding for those blends containing IA, losing their plastic deformation capacity. The loss in mechanical and hardness

properties was corroborated by SEM and wettability results. When SEM micrographs were studied, IA nanocrystals were found to group themselves in a heterogeneous way showing a lack of compatibility between the IA and the matrix and a clear separation of the phases. In addition, the WCA results showed a tendency for the material to become more hydrophilic when IA was incorporated, inducing biodegradability (hydrolyzing effect with the water of the environment) and thus accelerating the degradation of the material.

Our findings on color fixing show that, on the one hand, IA has an absorbance range somewhat lower than the red spectrum, so the material tends to slightly yellow the matrix; and, on the other hand, the high formation of IA nanocrystals shown by SEM micrographs produces such a variation in the structure of the material that it modifies the way of scattering and absorbing light and decreases the gloss of the blend which is translated into a more matte finish. This effect is accentuated with time. ZrO_2 by itself increments the gloss of the material with time, but in ternary systems IA governs the overall behavior.

To sum up, the use of IA might be a good candidate to be used as a color fixation agent. However, coupling techniques such as the use of reactive polymers (grafting to with, i.e., peroxide initiators) or the use of compatibilizers (grafting from with, i.e., amphiphilic structures) of IA with the PBS matrix should be further explored as these could favor the compatibility of the materials, therefore increasing their miscibility and avoiding the quick undesirable aging effect found on the materials (and avoiding the separation of phases and accelerated biodegradation), which would also affect the color fastening and keep the gloss. These coupling techniques may be industrialized through adapted extrusion-compounding processes, e.g., reactive extrusion (REX). Moreover, due to the natural absorbance ranges of IA, a recommended strategy is for it to be used for yellow to blue colorant pigments.

Author Contributions: L.G.Q. conceived the work, carried out the preparation of the materials and the mechanical experimental work, contributed to the scientific discussion and wrote the manuscript.; J.V. collaborated in the hardness measurements; F.D. carried out the WCA measurements; F.L. performed the color measurements and collaborated in the description of color results; Á.F.C. contributed to scientific discussion and reviewed the manuscript; P.C. designed the methodology, contributed to the interpretation of results and scientific discussion, got funding and reviewed the manuscript. All authors have read and agreed to the published version of the manuscript.

Funding: This research was funded by the Government of Aragón (DGA) under the project T08_17R 614 (I+AITIIP).

Acknowledgments: The authors acknowledge TORRECID for kindly provide the zirconia used for this research.

Conflicts of Interest: The authors declare no conflict of interest.

References

1. Resch-Fauster, K.; Klein, A.; Blees, E.; Feuchter, M. Mechanical recyclability of technical biopolymers: Potential and limits. *Polym. Test.* **2017**, *64*, 287–295. [CrossRef]
2. Ma, P. Tailoring the Properties of Bio-Based and Biocompostable Polymer Blend. Ph.D. Thesis, Technische Universiteit Eindhoven, Eindhoven, The Netherlands, 2011.
3. Totaro, G.; Sisti, L.; Celli, A.; Askanian, H.; Hennous, M.; Verney, V.; Leroux, F. Chain extender effect of 3-(4-hydroxyphenyl) propionic acid/layered double hydroxide in PBS bionanocomposites. *Eur. Polym. J.* **2017**, *94*, 20–32. [CrossRef]
4. Rudnik, E. Properties and applications. *Compost. Polym. Mater.* **2019**, 49–98. [CrossRef]
5. Mizuno, S.; Maeda, T.; Kanemura, C.; Hotta, A. Biodegradability, reprocessability, and mechanical properties of polybutylene succinate (PBS) photografted by hydrophilic or hydrophobic membranes. *Polym. Degrad. Stab.* **2015**, *117*, 58–65. [CrossRef]
6. Joy, J.; Jose, C.; Varanasi, S.B.; Thomas, S.; Pilla, S. Preparation and Characterization of Poly(butylene succinate) Bionanocomposites Reinforced with Cellulose Nanofiber Extracted from Helicteres isora Plant. *J. Renew. Mater.* **2016**, *4*, 351–364. [CrossRef]
7. Śmigiel-Gac, N.; Pamuła, E.; Krok-Borkowicz, M.; Smola-Dmochowska, A.; Dobrzyński, P. Synthesis and Properties of Bioresorbable Block Copolymers of l-Lactide, Glycolide, Butyl Succinate and Butyl Citrate. *Polymers* **2020**, *12*, 214. [CrossRef]
8. Marzec, A. The Effect of Dyes, Pigments and Ionic Liquids on the Properties of Elastomer Composites. Polymers. Ph.D. Thesis, Université Claude Bernard-Lyon I, Villeurbanne, France, Uniwersytet lódzki Lodz, Łódźc, Poland, 2014.
9. Tolinski, M. Colorants. *Addit. Polyolefins* **2009**, 137–156. [CrossRef]
10. Püntener, A.; Page, C. *European Ban on Certain Azo Dyes, Quality and Environment*; TFL: Jalandhar, India, 2012.

11. Lassen, P. Description of development of an analytical method for measurement of PAA in tattoo ink and PMU. In *The Danish Environmental Protection Agency*; Aarhus University: Aarhus, Denmark, 2017; ISBN 978-87-93614-03-1.
12. Delgado-Vargas, F.; Jiménez, A.R.; Paredes-López, O. Natural Pigments: Carotenoids, Anthocyanins, and Betalains—Characteristics, Biosynthesis, Processing, and Stability. *Crit. Rev. Food Sci. Nutr.* **2000**, *40*, 173–289. [CrossRef]
13. Heer, K.; Sharma, S. Microbial pigments as a natural color: A review. *Int. J. Pharm. Sci. Res.* **2017**, *8*, 1913–1922. [CrossRef]
14. Fernández-López, J.; Fernández-Lledó, V.; Angosto, J.M. New insights into red plant pigments: More than just natural colorants. *RSC Adv.* **2020**, *10*, 24669–24682. [CrossRef]
15. Das, D.; Datta, D.B.; Bhattacharya, P. Simultaneous Dyeing and Finishing of Silk Fabric with Natural Color and Itaconic Acid. *Cloth. Text. Res. J.* **2014**, *32*, 93–106. [CrossRef]
16. Aromatic Azo- and Benzidine-Based Substances. Draft Technical Background Document. The Chemicals Management Plan Substance Groupings Initiative. Environment Canada. Health Canada, July 2012. Available online: https://www.canada.ca/en/health-canada/services/chemical-substances/substance-groupings-initiative/aromatic-azo-benzidine-based.html (accessed on 24 November 2020).
17. Robert, T.; Friebel, S. Itaconic acid—A versatile building block for renewable polyesters with enhanced functionality. *Green Chem.* **2016**, *18*, 2922–2934. [CrossRef]
18. Praveen Kumar, R.; Gnansounou, E.; Kenthorai Raman, J.; Baskar, G. Refining Biomass Residues for Sustainable Energy and Bioproducts. *Technol. Adv. Life Cycle Assess. Econ.* **2019**. [CrossRef]
19. Carvalho, J.C.; Magalhaes, A.; Soccol, C. Biobased itaconic acid market and research trends - is it really a promising chemical? *Chim. Oggi Chem. Today* **2018**, *36*, 56.
20. Teleky, B.-E.; Vodnar, D. Biomass-Derived Production of Itaconic Acid as a Building Block in Specialty Polymers. *Polymers* **2019**, *11*, 1035. [CrossRef]
21. Peinado, V.; García, L.; Fernández, Á.; Castell, P. Novel lightweight foamed poly(lactic acid) reinforced with different loadings of functionalised Sepiolite. *Compos. Sci. Technol.* **2014**, *101*, 17–23. [CrossRef]
22. García, L.; Fernández, Á; Castell, P.; García-Quiles, L. Sustainable Materials with Enhanced Mechanical Properties Based on Industrial Polyhydroxyalkanoates Reinforced with Organomodified Sepiolite and Montmorillonite. *Polymers* **2019**, *11*, 696. [CrossRef]
23. Szeluga, U.; Kumanek, B.; Trzebicka, B. Synergy in hybrid polymer/nanocarbon composites. A review. *Compos. Part A Appl. Sci. Manuf.* **2015**, *73*, 204–231. [CrossRef]
24. Mirica, I.C.; Furtos, G.; Bâldea, B.; Lucaciu, O.P.; Ilea, A.; Moldovan, M.; Campian, R.S. Influence of Filler Loading on the Mechanical Properties of Flowable Resin Composites. *Materials* **2020**, *13*, 1477. [CrossRef]
25. Liu, X.; Wang, T.; Chow, L.C.; Yang, M.; Mitchell, J.W. Effects of Inorganic Fillers on the Thermal and Mechanical Properties of Poly(lactic acid). *Int. J. Polym. Sci.* **2014**, *2014*, 827028. [CrossRef]
26. Daou, E.E. The Zirconia Ceramic: Strengths and Weaknesses. *Open Dent. J.* **2014**, *8*, 33–42. [CrossRef] [PubMed]
27. Özkurt-Kayahan, Z. Monolithic zirconia: A review of the literatura. *Biomed. Res.* **2016**, *27*, 4.
28. Rahaman, M.N.; Li, Y.; Bal, B.S.; Huang, W. Functionally graded bioactive glass coating on magnesia partially stabilized zirconia (Mg-PSZ) for enhanced biocompatibility. *J. Mater. Sci. Mater. Med.* **2008**, *19*, 2325–2333. [CrossRef] [PubMed]
29. Kim, D.J.; Myung-Hyun, L.; Lee, D.Y.; Han, J.S. Mechanical properties, phase stability, and biocompatibility of (Y, Nb)-TZP/Al(2)O(3) composite abutments for dental implant. *J. Biomed. Mater. Res.* **2000**, *53*, 438–443. [CrossRef]
30. Chang, C.-C.; Hsieh, C.-Y.; Huang, F.-H.; Cheng, L.-P. Preparation of zirconia loaded poly(acrylate) antistatic hard coatings on PMMA substrates. *J. Appl. Polym. Sci.* **2015**, *132*, 42411. [CrossRef]
31. Sakthivel, M.; Franklin, D.; Guhanathan, S. pH-sensitive Itaconic acid based polymeric hydrogels for dye removal applications. *Ecotoxicol. Environ. Saf.* **2016**, *134*, 427–432. [CrossRef]
32. Raghu, C.; Raghuveer, P. Itaconic acid Production—A short review. *Int. J. Adv. Eng. Technol. Manag. Appl. Sci.* **2017**, *4*, 8–15.
33. Willke, T.; Vorlop, K.D. Biotechnological production of itaconic acid. *Appl. Microbiol. Biotechnol.* **2001**, *56*, 289–295. [CrossRef]
34. Kirimura, K.; Honda, Y.; Hattori, T. Gluconic and Itaconic Acids. *Compr. Biotechnol.* **2011**, 143–147. [CrossRef]
35. Garvie, R.C.; Hannink, R.H.; Pascoe, R.T. Ceramic steel? *Nature* **1975**, *258*, 703. [CrossRef]
36. Manicone, P.F.; Iommetti, P.R.; Raffaelli, L. An overview of zirconia ceramics: Basic properties and clinical applications. *J. Dent.* **2007**, *35*, 819–826. [CrossRef] [PubMed]
37. Color Vision. Perspectives from Different Disciplines. *Ethology* **1999**, *105*, 184–185. [CrossRef]
38. Krishnan, S.; Mohanty, S.; Nayak, S.K. An eco-friendly approach for toughening of polylactic acid from itaconic acid based elastomer. *J. Polym. Res.* **2017**, 25. [CrossRef]
39. Takahashi, M.; Osawa, S.; Jinnai, H.; Yamane, H.; Shiomi, H. Dispersion State of Zirconium Oxide Particles in Polymer Blends and Viscoelastic Behavior of the Composites. *Nihon Reoroji Gakkaishi* **2007**, *35*, 1–9. [CrossRef]
40. Mishra, T.; Kumar, A.; Verma, V.; Pandey, K.; Kumar, V. PEEK composites reinforced with zirconia nanofiller. *Compos. Sci. Technol.* **2012**, *72*, 1627–1631. [CrossRef]
41. Kimble, L.D.; Bhattacharyya, D. In Vitro Degradation Effects on Strength, Stiffness, and Creep of PLLA/PBS: A Potential Stent Material. *Int. J. Polym. Mater.* **2014**, *64*, 299–310. [CrossRef]
42. Fan, F.; Xia, Z.; Li, Q.; Li, Z.; Chen, H. ZrO2/PMMA Nanocomposites: Preparation and Its Dispersion in Polymer Matrix. *Chin. J. Chem. Eng.* **2013**, *21*, 113–120. [CrossRef]

43. Gentili, P.L. The Fuzziness of the Molecular World and Its Perspectives. *Molcules* **2018**, *23*, 2074. [CrossRef]
44. Available online: https://pubchem.ncbi.nlm.nih.gov/compound/Itaconic-acid#section=UV-Spectra (accessed on 24 November 2020).
45. Zagórski, Z.P. Diffuse reflection spectrophotometry (DRS) for recognition of products of radiolysis in polymers. *Int. J. Polym. Mater.* **2003**, *52*, 323–333. [CrossRef]
46. Ciccòla, A.; Guiso, M.; Domenici, F.; Sciubba, F.; Bianco, A. Azo-pigments effect on UV degradation of contemporary art pictorial film: A FTIR-NMR combination study. *Polym. Degrad. Stab.* **2017**, *140*, 74–83. [CrossRef]

ARTICULO 4

Reactive Compatibilization of Plant Polysaccharides and Biobased Polymers: Review on Current Strategies, Expectations and Reality

Imre, B., García, L., Puglia, D., & Vilaplana, F. (2018).
Carbohydrate Polymers 209 (2019) 20–37
Impact Factor: 7.182 (2019), 5-Year Impact Factor: 6.890 – Q1

En general, los biopolímeros presentan varias desventajas en cuanto a propiedades se refiere respecto de los polímeros "commodities" derivados del petróleo, como son: la estabilidad térmica, la absorción de humedad y ciertas limitaciones en el rendimiento mecánico; que dificultan su aplicación directa en ciertas aplicaciones, máxime cuando hablamos de sistemas de materiales avanzados o materiales para aplicaciones técnicas o ingenieriles. Es por ello que la combinación con otros biopolímeros en forma de "blendas" y el uso de refuerzos se convierte en una estrategia necesaria para superar dichas barreras en propiedades del material; y que tales mezclas requieren de la compatibilización de los compuestos para que sean efectivas.

El cuarto artículo surge como una necesidad para encontrar estrategias que permitan resolver el problema de miscibilidad y compatibilidad resultante del artículo 3 entre el bioPBS y el IA. Por ello, se decide realizar una búsqueda exhaustiva en colaboración con expertos en química de biopolímeros, para tratar de encontrar aquella que mejor se pudiera ajustar a las necesidades tanto del material como del proceso, teniendo siempre en cuenta la potencial industrialización del mismo. En el artículo se aborda la compatibilización reactiva como la estrategia más adecuada para lograr este propósito, poniendo un especial énfasis en el proceso de extrusión reactiva (REX) que es la forma de pasar al ámbito industrial dicha estrategia de compatibilización de mezclas.
Aunque el artículo es en su formato un *Review*, la doctoranda ha llevado a la práctica el proceso de REX, modificando la extrusora de doble husillo convencional para convertirla en un reactor dinámico que sea capaz de que genere enlaces covalentes entre los componentes.

Carbohydrate Polymers 209 (2019) 20–37

Contents lists available at ScienceDirect

Carbohydrate Polymers

journal homepage: www.elsevier.com/locate/carbpol

Reactive compatibilization of plant polysaccharides and biobased polymers: Review on current strategies, expectations and reality

Balázs Imre[a], Lidia García[b,c], Debora Puglia[d], Francisco Vilaplana[a,*]

[a] Division of Glycoscience, Department of Chemistry, School of Engineering Sciences in Chemistry, Biotechnology and Health, KTH Royal Institute of Technology, Stockholm, Sweden
[b] Fundación Aitiip, Polígono Industrial Empresarium, C/Romero Nº 12, Zaragoza 50720, Spain
[c] Tecnopackaging S.L., Polígono Industrial Empresarium, C/Romero Nº 12, Zaragoza 50720, Spain
[d] Department of Civil and Environmental Engineering, University of Perugia, Terni, Italy

ARTICLE INFO

Keywords:
Plant polysaccharides
Bioplastics
Compatibilization
Reactive extrusion
Starch

ABSTRACT

Our society is amidst a technological revolution towards a sustainable economy, focused on the development of biobased products in virtually all sectors. In this context, plant polysaccharides, as the most abundant macromolecules present in biomass represent a fundamental renewable resource for the replacement of fossil-based polymeric materials in commodity and engineering applications. However, native polysaccharides have several disadvantages compared to their synthetic counterparts, including reduced thermal stability, moisture absorption and limited mechanical performance, which hinder their direct application in native form in advanced material systems. Thus, polysaccharides are generally used in a derivatized form and/or in combination with other biobased polymers, requiring the compatibilization of such blends and composites. In this review we critically explore the current status and the future outlook of reactive compatibilization strategies of the most common plant polysaccharides in blends with biobased polymers. The chemical processes for the modification and compatibilization of starch and lignocellulosic based materials are discussed, together with the practical implementation of these reactive compatibilization strategies with special emphasis on reactive extrusion. The efficiency of these strategies is critically discussed in the context on the definition of blending and compatibilization from a polymer physics standpoint; this relies on the detailed evaluation of the chemical structure of the constituent plant polysaccharides and biobased polymers, the morphology of the heterogeneous polymeric blends, and their macroscopic behavior, in terms of rheological and mechanical properties.

1. Introduction

Bioplastics have been in the focus of academic and industrial research and development efforts for more than two decades now. Their global production reached 4 million metric tons in 2015 and keeps sharply increasing. The robust growth of this emerging field of industry is driven by multiple factors including environmental awareness and changing consumer preferences, new policies and legislation as well as product development. Nevertheless, the estimated market share of bioplastics still has not exceeded 1% of the global plastics production (European Bioplastics ö nova-Institute, 2017). Increasing the market share of bioplastics plays a crucial role in reducing the dependence on fossil-based resources towards the transition to a bio-based society, lessening the environmental impact of polymeric materials and achieving a circular economy. This, however, requires the overall improvement and careful tailoring of the performance of existing materials as well as the development of novel biopolymer grades.

Physical blending, i.e. the simple mixing of thermoplastics in the melt state, is a convenient and cost-efficient route to create new polymeric materials with the desired set of properties. The compatibility of most polymer pairs, however, is not sufficient to ensure the satisfactory performance of their blends – biopolymers are no exception. In our present publication, we review the techniques developed in order to improve compatibility in biopolymer blends by reactive methods. In a recent paper (Imre ö Pukánszky, 2013), we already emphasized the importance of the proper, and preferentially quantitative analysis of miscibility-structure-properties correlations. Following the same approach, here we also aim to explore the chemistry of the process in more detail. We also limit our study to the blends of plant polysaccharides with other biopolymers, for several reasons. Polysaccharides such as starch and cellulose represent the most abundant natural polymers in the biosphere, and therefore have a considerable

* Corresponding author.
E-mail address: franvila@kth.se (F. Vilaplana).

https://doi.org/10.1016/j.carbpol.2018.12.082
Received 19 September 2018; Received in revised form 27 November 2018; Accepted 24 December 2018
Available online 29 December 2018

market share. However, due to their inherently less favorable characteristics, such as high hydrophilicity and lack of thermoplasticity, they are in most cases applied in combination with other polymeric materials. The unique chemical structure of polysaccharides, and the abundance hydroxyl moieties in particular, also enables a wide range of reactive compatibilization techniques.

In the following sections, we discuss some commonly used – and often misused – definitions of the field, such as those of natural, biobased and biopolymers as well as miscibility and compatibility. This is followed by the review of compatibilization strategies in polysaccharide blends, both from a chemical perspective and according to more pragmatic considerations regarding the implementation of such strategies. Finally, we aim to provide a practical guide for the compatibilization of heterogeneous polymeric materials based on plant polysaccharides and biobased polymers.

2. Biopolymers, natural and synthetic biobased polymers

What exactly do we mean when we talk about bioplastics and biopolymers? At present, these terms are applied to describe several different classes of materials, depending on the background and field of expertise of the user. Common usage covers natural, bio-based and biodegradable macromolecules as well as biocompatible polymers for biomedical applications. From an environmental point of view, the origin of raw materials and degradability are the most critical factors. Based on these, polymers fall into four overlapping categories, as illustrated by Fig. 1a that also lists the most significant examples in each category.

The European standard CEN/TR 15932:2010 (Plastics - Recommendation for terminology ö characterisation of biopolymers ö bioplastics, 2010) aims to address the ambiguity regarding the definitions in this field, while taking into consideration both public perception and the current use of biopolymer-related terms. According to the standard, the polymeric materials generally labelled as biopolymers (or bioplastics) fulfill the criteria of one or more of the below categories.

- Biobased polymers: Polymers with constitutional units that are totally or in part from biomass origin. Natural (synthesized by living organisms) and synthetic biobased polymers (whose monomers derive from renewable resources) both belong to this category.
- Biodegradable polymers: A polymeric item that can be biodegraded (according to the relevant standards, e.g. EN 13432 Packaging - Requirements for packaging recoverable through composting and biodegradation - Test scheme and evaluation criteria for the final acceptance of packaging (2000)) and EN 14995 (Plastics - Evaluation of compostability - Test scheme ö specifications, 2006). Biodegradability is linked to the structure of the polymer chain; it does not depend on the origin of the raw materials.
- Biocompatible polymers: Polymers that are compatible with human or animal tissues and suitable for medical therapy. The polymer does not harm the body or its metabolism in any way while fulfilling the expected function.

As the above classification reflects, the standard essentially affirms the current practice by acknowledging 'biopolymer' as an umbrella term for a rather wide range of polymeric materials. The guide also emphasizes the need to use specific terms whenever possible. Naturally, listing the complete terminology exceeds the scope of this review. Instead, we turn our attention to two specific groups of biopolymers, i.e. synthetic biobased polymers and plant polysaccharides. The latter group belongs to the family of natural polymers and accounts for the largest fraction of all biomass, therefore representing the main renewable resource for biofuel and materials production (Field, Behrenfeld, Randerson, ö Falkowski, 1998; Martínez-Abad, Ruthes, ö Vilaplana, 2016). Here, we focus our attention to the most significant representatives of plant polysaccharides, namely cellulose, hemicelluloses

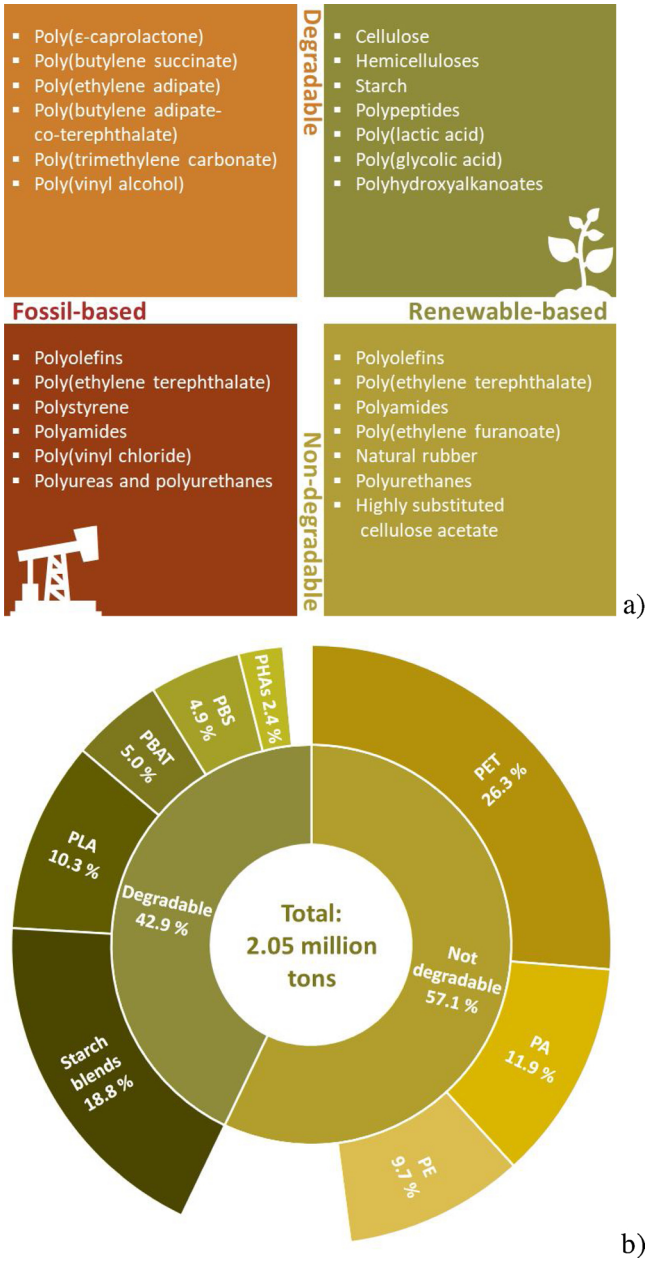

Fig. 1. Biobased and degradable polymers; **a)** the classification of biopolymers; **b)** global production capacities of bioplastics in 2017 according to European Bioplastics (European Bioplastics & nova-Institute, 2017); degradable grades (fossil- or biobased): PLA – poly(lactic acid), PBAT – poly(butylene adipate-co-terephthalate, PBS – poly(butylene succinate), PHAs – polyhydroxyalkanoates; biobased, non-degradable grades: PE – polyethylene, PA – polyamide, PET – poly(ethylene terephthalate).

and starch. The industrial application of starch and lignocellulosic biomasses is growing rapidly due to the abundance, low cost and renewable nature of these feedstocks. Nevertheless, few studies have been published on the global availability of biomass resources and most of these focuses on fuel and electricity production without considering other applications. Some recent publications aim to fill this gap, providing a detailed analysis of starch (Marques, Moreno, Ballesteros, ö Gírio, 2018) and lignocellulosic materials (Alzagameem, El Khaldi-Hansen, Kamm, ö Schulze, 2018; Tye, Lee, Wan Abdullah, ö Leh, 2016), respectively.

In lignocellulosic biomass, cellulose microfibrils are the main structural component, embedded within a matrix of hemicelluloses,

pectins, and polyphenolic lignins (Burgert ö Keplinger, 2013; Cosgrove ö Jarvis, 2012). The cellulose macromolecule itself consists of (1→4)-linked β-D-glucopyranosyl units that form long, linear polymeric chains, which aggregate in partially crystalline microfibrils of few nanometers in diameter. The term hemicellulose comprises several different classes of plant polysaccharides that vary substantially in composition and primary molecular structure not only between plant species but also between tissues and developmental stages within the same species. Hemicelluloses are structurally-complex glycan copolymers (xylans, mannans, xyloglucans, and mixed-linkage β-glucans), sharing with cellulose a similar backbone of β-(1→4)-linked monosaccharides (mainly glucose, mannose or xylose), decorated with a wide pattern of neutral sugar and uronic acid substitutions. Starch consists of two types of polysaccharides based on α-D-glucose monomers (Chen et al., 2015). Amylose is typically the minor component; it is a linear polymer with a molar mass in the range of 10^5-10^6 g/mol. Amylopectin, on the other hand, has a hyperbranched structure with a molar mass of ca. 10^8 g/mol. The starch industry is currently growing, and about 180 million tons of starch and starch derivatives are expected to be produced worldwide by 2022 (Marques et al., 2018).

A common feature of plant polysaccharides is their rather recalcitrant structure due to strong intra- and intermolecular interactions, and in some cases a high degree of crystallinity. The large number of highly polar hydroxyl groups present in these natural polymers plays a crucial role in both these characteristics, by enabling the formation of H-bonds. Therefore, plant polysaccharides are not intrinsically thermoplastic, i.e. they cannot be processed in the melt state without chemical modification and/or plasticization. Plasticizers, however, have a tendency of migrating to the surface, resulting in unstable mechanical characteristics over time, and various other issues during application. Thermoplastic starch is also prone to slow recrystallisation after processing, which leads to the embrittlement of the material (Huneault ö Li, 2007). Another consequence of their rather polar, hydrophilic nature is the moisture sensitivity of plant polysaccharides. Therefore, they generally contain a considerable amount of water, depending on environmental conditions such as temperature and humidity. This, in turn can lead to considerable hydrolysis and molar mass decrease during processing and to unstable properties during application.

The above issues can and often are addressed by blending the polysaccharides with more hydrophobic matrices. Due to environmental concerns and practical considerations, these latter commonly belong to the family of biobased or biodegradable polymers, resulting in fully biobased and/or degradable compositions. According to data collected by European Bioplastics (European Bioplastics ö nova-Institute, 2017), the market share of degradable starch-based blends alone added up to almost a fifth of the global production of biobased and degradable polymers (Fig. 1b). Moreover, this figure does not contain non-degradable grades and a range of other polysaccharide-based materials such as wood plastic composites. The development of such blends and composites with satisfactory performance profiles – according to the desired application – depends on the control of structure and interfacial adhesion in order to facilitate stress transfer between the respective phases. This, however, is seldom achievable without the implementation of a range of physical or chemical modification techniques commonly referred to as compatibilization.

3. Compatibilization of heterogeneous polymeric compounds

Although several papers discuss the distinction between miscibility and compatibility (Imre ö Pukánszky, 2013; Koning, Van Duin, Pagnoulle, ö Jerome, 1998; Zeng, Li, ö Du, 2015), these two terms are still often confused. Miscibility (Koning et al., 1998; Olabisi, Robeson, ö Shaw, 1979) describes the number of phases as well as the composition thereof upon blending two polymers. It is determined by thermodynamic factors, namely the free enthalpy of mixing:

$$\Delta G_{mix} = \Delta H_{mix} - T\,\Delta S_{mix} \quad (1)$$

The resulting blend is homogeneous (i.e. the respective polymers do not form separate phases) only in case the free enthalpy of mixing (ΔG_{mix}) is negative. Since the entropy contribution (ΔS_{mix}) is largely negligible when blending high molar mass polymers, the resulting morphology is in a great part determined by the change of enthalpy (ΔH_{mix}). The extent of the latter, on the other hand, depends on the intra- and intermolecular interactions between the blend components. Due to the lack of specific interactions, complete miscibility rarely occurs in practice (Koning et al., 1998). The great majority of polymer pairs are partially miscible at most, i.e. their blends consist of two distinct phases, both being rich in one polymer, while containing a fraction of the other blend component. The extent of mixing on a molecular level is, however, negligible in most cases, thus it does not affect properties to a significant degree.

Compatibility is essentially a technical term that concerns the property profile of a blend in connection with a certain application. Although mechanical characteristics are generally in the focus of attention when assessing compatibility in a multi-component polymeric material, a multitude of other properties such as processability, transparency, permeability, surface quality or degradability might also be taken into consideration. Improving the compatibility of its components alters the property profile of a heterogeneous system in order to better fit the requirements of a certain application. One should keep in mind, though, that the enhancement of some characteristics is often accompanied by the deterioration of others.

The rule of mixtures estimates the properties, e.g. the tensile strength of polymer blends (σ_b) as the linear combination of the respective properties of the components (σ_1 and σ_1) multiplied by their volumetric fraction (f) in the blend:

$$\sigma_b = f\sigma_1 + (1 - f)\sigma_2 \quad (2)$$

The properties of homogeneous blends tend to follow this hypothetical correlation relatively well. The mechanical behavior of materials based on immiscible polymeric components, on the other hand, generally deviate from the rule of mixtures, due to their more complex morphology and the resulting micromechanical deformation processes. In Fig. 2, we compare two typical examples. PLA and thermoplastic starch (TPS) are largely incompatible, thus the relative tensile strength of their blends (○) is well below the 100% value suggested by the rule of mixtures across the whole composition range. PLA and poly(methyl methacrylate) (PMMA) (◇), on the other hand, form strong interactions, and are in fact partially miscible. This is also reflected by the SEM micrographs that reveal well-dispersed, submicron sized PMMA particles in the PLA/PMMA blend, while the large starch particles are easy to observe in PLA/TPS even at 10× lower magnification. Thus, the relative tensile strength of the PMMA-based material even exceeds 100%. Therefore, it is considered a blend of compatible polymers. The successful compatibilization of a blend or composite of incompatible components is sometimes attributed to reaching or exceeding the values predicted by the rule of mixing for a certain characteristic. Although the correlation indeed serves as a convenient threshold, in practice the requirements of the application determine the success or failure of any compatibilization effort.

Miscibility and compatibility are of course not fully independent terms. As mentioned above, most polymer pairs are immiscible, their blends having a heterogeneous morphology. In general, compatibility in such polymeric systems can be considered a function of structure and interfacial adhesion. Interfacial adhesion is governed by the strength and number of interfacial interactions; the chemical structure of the respective polymer chains plays a crucial role in determining both. Some polymeric materials, e.g. polyolefins, are only capable of weak Van der Waals-type secondary interactions. The presence or absence of functional groups capable of specific interactions (induced dipole, dipole-dipole interactions and hydrogen bonding) as well as the nature

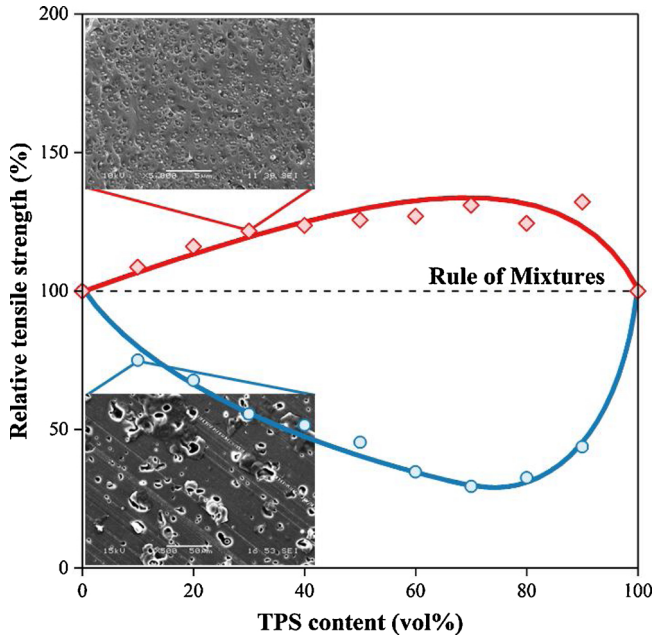

Fig. 2. The relative strength of two PLA blends, (◯) PLA/TPS and (◇) PLA/PMMA; SEM micrographs: PLA/TPS – 10 vol% TPS, 500× magnification; PLA/PMMA – 30 vol% PMMA, 5000× magnification (Imre, Renner, & Pukanszky, 2014; Müller et al., 2016).

and arrangement of such functional groups are decisive in terms of not only miscibility but also compatibility of immiscible polymer pairs. Naturally, the number of interfacial interactions correlates with the number of the functional groups at the interface connecting the phases, but also with the specific surface area of said interface. In short, good compatibility requires the formation of a large number of strong interactions across an extensive interface.

Aside from a few exceptions, such as reactor blends, most polymer blends are prepared by melt mixing. While the composition of the phases can be estimated solely based on miscibility, blend morphology shows a great degree of variety and complexity as a function of polymer characteristics and processing conditions. Besides blend composition and interactions, temperature, shear rate as well as the viscosity and elasticity of the phases also must be considered. During the melt mixing of two immiscible polymers, shear forces tend to break up larger drops of one phase that in turn becomes dispersed in the other phase, i.e. the matrix. This process continues until an equilibrium particle size is reached. The equilibrium particle size may vary to a large extent, from tens of nanometers to several micrometers, depending on a number of factors. Higher shear rates and stronger interfacial interactions, for instance, facilitate finer phase dispersion. The effect of the viscosity ratio of the two polymers is more diverse, depending on the mechanism of drop formation and coalescence during processing (Janssen ö Meijer, 1993; Koning et al., 1998; Wu, 1987).

A finely dispersed morphology has several advantages in terms of optical properties and permeability, among other characteristics. More importantly, it results in an increased specific surface area of the dispersed phase, thus in a more effective interfacial adhesion, and improved mechanical properties (consider the morphology and relative strength of PLA/PMMA blends in Fig. 2. Consequently, compatibility can be improved up to a certain point simply by optimizing processing conditions. The improvement achievable with this approach is, however, rather limited. In order to considerably enhance the performance of a polymer blend, a wide range of modification strategies is available that are commonly referred to as compatibilization.

Most compatibilization techniques involve the introduction of an additive – i.e. compatibilizer – that exerts its activity at the blend interface in order to facilitate interfacial adhesion. In the case of non-reactive compatibilization, pre-made amphiphilic compounds are used. Such molecules are able to interact with the respective polymers in both phases. The most common representatives of non-reactive compatibilizers are block-copolymers (Cai, Wan, Bei, ö Wang, 2003; Duquesne, Rutot, Degee, ö Dubois, 2001; Na et al., 2002; Vilay, Mariatti, Ahmad, Pasomsouk, ö Todo, 2010), one constitutive end or block of which is miscible with one blend phase (**Phase A**), while the other with the second phase (**Phase B**). Macromolecules with various structures can be used for this purpose, e.g. diblock, triblock or graft copolymers, as illustrated in Fig. 3. The compatibilization effect is most commonly associated with the formation of an interphase facilitating interfacial adhesion as well as a finer morphology with reduced average diameter of the dispersed particles (Koning et al., 1998). Amphiphilic low-molar mass compounds (Yokesahachart ö Yoksan, 2011), ionomers (Landreau, Tighzert, Bliard, Berzin, ö Lacoste, 2009) or third polymers – at least partially – miscible with both components (Parulekar ö Mohanty, 2007) work in a similar manner.

In the case of reactive methods, amphiphilic structures form in situ during blending. This can be achieved through the addition of low molar mass (Jang, Shin, Lee, ö Narayan, 2007; Jun, 2000; Ma et al., 2014; Piming Ma, Hristova-Bogaerds, Schmit, Goossens, ö Lemstra, 2012; Wang, Yu, ö Ma, 2007; Zhang ö Sun, 2004), oligomeric (Al-Itry, Lamnawar, ö Maazouz, 2012; Quiles-Carrillo, Montanes, Sammon, Balart, ö Torres-Giner, 2018) or polymeric (Shi et al., 2011, Avella et al., 2000; Detyothin, Selke, Narayan, Rubino, ö Auras, 2015;

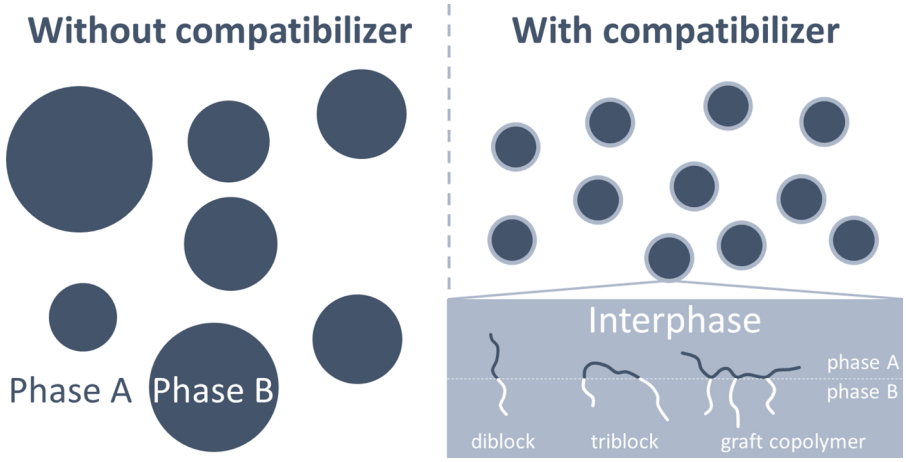

Fig. 3. The effect of compatibilization on the morphology of polymer blends due to the activity of amphiphilic polymer structures at the interface. Image drawn using inspiration from (Koning et al., 1998).

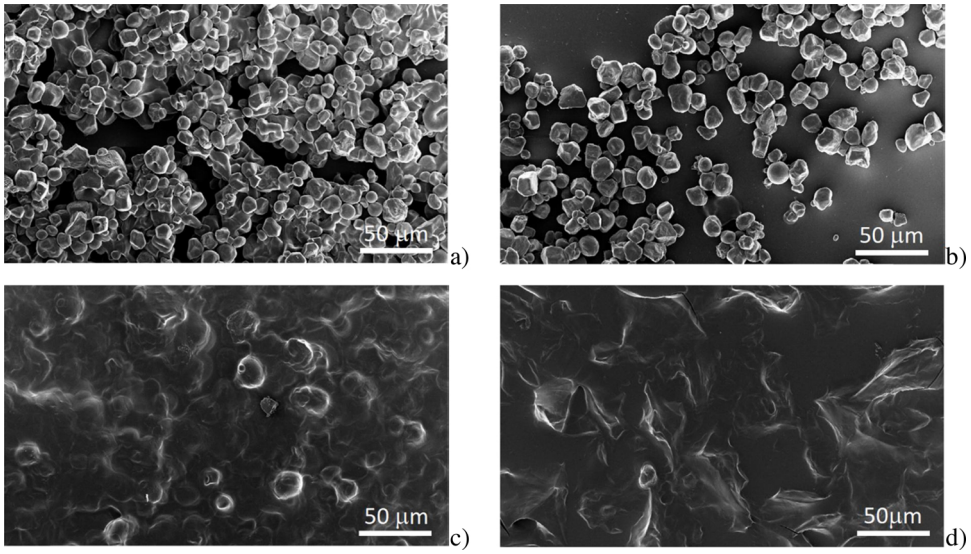

Fig. 4. The morphology of **a)** native corn starch compared with its propionylated counterparts having a DS of **b)** 0.05; **c)** 0.13; and **d)** 1.59, respectively. SEM images, 1000× resolution (Di Filippo et al., 2016).

Huneault ö Li, 2007; Jang et al., 2007; Kumar, Mohanty, Nayak, ö Rahail Parvaiz, 2010; Li ö Huneault, 2011; Ren, Fu, Ren, ö Yuan, 2009; Wu, 2003; Zeng, Jiao et al., 2011; Zeng, Wang, Xiao, Han, ö Meng, 2011) reactive compounds that act as coupling agents, forming covalent bonds between the phases. Another type of reactive compatibilization involves the formation of graft or block copolymers from their monomers (Don, Chung, Lai, ö Chiu, 2010; Dubois ö Narayan, 2003; Lai, Sun, ö Don, 2015; Lönnberg, Larsson, Lindström, Hult, ö Malmström, 2011), the respective chain sections of which are miscible with different phases of the blend. Throughout this review we focus our attention to such reactive techniques, for several reasons. First of all, although physical compatibilization strategies are also commonly applied, reactive methods prove to be more efficient in general (Imre ö Pukánszky, 2013; Koning et al., 1998). Furthermore, the large number of available hydroxyl moieties on polysaccharide chains offers a convenient site for reactive modification.

4. Reactive compatibilization strategies in polysaccharide-based compositions

The rich palette of carbohydrate chemistry offers almost unlimited possibilities for the modification and substitution of hydroxyl groups in polysaccharides (Chen et al., 2015; Heinze ö Liebert, 2001; Klemm, Philipp, Heinze, Heinze, ö Wagenknecht, 1998; Söderqvist Lindblad ö Albertsson, 2004; Vilaplana, Zou, ö Gilbert, 2018). Therefore, in the following sections we focus our attention to reactive compatibilization methods. Typically, this can be implemented through oxidation, esterification or etherification. Depending on the chemical structure of the reagents and the resulting products one can differentiate graft copolymerization, coupling and crosslinking reactions, as discussed in more detail below. The common aspect of these methods is the *in-situ* formation of a block or graft copolymer, the respective blocks of which are miscible with different blend phases.

4.1. Substitution with monofunctional reagents

The substitution of hydroxyl groups of plant polysaccharides has a long history. Cellulose acetate (CA), for instance was first described by Schutzenberger (Schützenberger, 1865) as early as 1865, while studies on the chemical modification of starch have been performed in the early 1940s (Chen et al., 2015). In the case of cellulose acetate, the main purpose of this modification is the thermoplasticization of cellulose. The substitution of starch −OH groups with more hydrophobic moieties, however, often aims to decrease the moisture absorption of this natural-based material, thus the properties of starch become more stable. Nevertheless, the chemical modification also affects the structure and morphology of the native polysaccharides, as well as their mechanical characteristics, transition temperatures and thermal stability. The origin of the polysaccharide substrate, methods, conditions and types of reagents all have a significant effect on the outcome of the modification. The products are often characterized by their degree of substitution (DS). In the case of starch and cellulose, for instance, this value ranges from 0 to 3, a DS of 3 meaning that on average all three hydroxyl groups of the anhydroglucose repeating units have been substituted.

One of the most commonly applied chemical modifications of polysaccharides is the substitution of their hydroxyl groups by esterification. The reaction can be performed using acids, acid chlorides (Aburto et al., 1999; Fang, Fowler, Sayers, ö Williams, 2004) or anhydrides (Chi et al., 2008; Lopez-Rubio, Clarke, Scherer, Topping, ö Gilbert, 2009; Shogren, 1996, 2003; Xu, Miladinov, ö Hanna, 2004). With the increasing proportion of acetyl moieties (Jiang, Qiao, ö Sun, 2006; Tupa, Maldonado, Vázquez, ö Foresti, 2013; Tupa, Ávila Ramírez, Vázquez, ö Foresti, 2015; Xu et al., 2004; Liming Zhang, Xie, Zhao, Liu, ö Gao, 2009) or longer nonpolar side-groups (Di Filippo et al., 2016; Miladinov ö Hanna, 2000; Namazi, Fathi, ö Dadkhah, 2011; Tupa et al., 2013), besides itself becoming more hydrophobic, starch also loses its original, highly crystalline granular structure (Fig. 4a). Due to the disruption of inter- and intra-molecular hydrogen bonds induced by the progressive replacement of −OH groups, the surface of the particles first starts to show increased roughness (Fig. 4b). Finally, the complete disruption of the granular structure and the fusion of the particles might also occur (Fig. 4c and d).

In terms of compatibilization of heterogeneous polymeric materials, the effect of substituting the hydroxyl groups of polysaccharides with rather hydrophobic, monofunctional reagents is not easy to interpret. While this type of modification decreases inter- and intramolecular interactions within the polysaccharide phase, it also leads to less interaction between the blend or composite components, i.e. less adhesion at the interface. Thus, it is not surprising that in many cases such modification was found to result in a strongly phase separated morphology with no specific interactions between blend components, nor any improvement in mechanical properties compared with unmodified starch (Jiang et al., 2006; Koenig ö Huang, 1995; Zhang, Deng, Zhao, ö

Huang, 1997), or even a deterioration thereof (Koenig ö Huang, 1995).

There are studies, however, that claim to have achieved improved compatibility in starch-based blends by this method (Wokadala, Emmambux, ö Ray, 2014; Zeng, Jiao et al., 2011; Zeng, Wang et al., 2011), as in their view, the hydrophilic nature of thermoplastic starch hinders compatibility with more hydrophobic polymers (Wokadala et al., 2014). There is some truth to that claim, although the complete picture is a little more complex than that. As discussed above, esterification and etherification generally hinder interfacial interactions, which is undesirable from a compatibilization point of view. By decreasing intra- and intermolecular interactions within the polysaccharide phase, however, such modifications can drastically alter blend or composite morphology, leading to decreased particle size and a more homogeneous dispersion of the dispersed phase. This, in turn equals increased interfacial area and the development of a more homogeneous stress-field under deformation, thus potentially leading to higher tensile strength. Therefore, it is well understandable that such behavior was mostly observed in heterogeneous materials based on non-plasticized starch (Wokadala et al., 2014; Zeng, Jiao et al., 2011; Zeng, Wang et al., 2011), in which the polysaccharide essentially acts as a filler. As Fig. 4 also suggests, the properties (e.g. thermoplasticity) and especially the morphology of native starch changes drastically as an effect of substitution, resulting in the improved composite morphology and mechanical characteristics described earlier. In the case of thermoplastic starch, the change in blend morphology due to such modifications is much subtler and is to a great extent governed by other factors, e.g. plasticizer content, therefore real compatibilization due to substitution with monofunctional reagents is rarely observed in such materials.

4.2. Coupling

4.2.1. Coupling with small molecules

By the term coupling we mean the establishment of chemical bonds between the respective phases of a heterogeneous polymeric material. It is a rather common and conventional form of reactive compatibilization, as it involves the in-situ formation of amphiphilic compounds, in this case typically block and graft copolymers, in order to facilitate interfacial adhesion. As Fig. 5a illustrates, one way to achieve this is the introduction of small molecules with at least one functional group being able to react with one phase, and another being able to react with the other phase. Naturally, these two moieties can be identical, and they very often are. The application of such compounds can also lead to crosslinking in one or both polymer phases, in case both functional groups react with one polymeric component. Excessive crosslinking, on the other hand, might lead to the formation of a polymer network, and thus thermoset behavior, i.e. the material can no longer be brought into the melt state. Thus, in order to preserve the thermoplastic nature of the blend or composite, coupling agents are applied in limited concentrations.

Due to their numerous hydroxyl groups, numerous bifunctional compounds can form covalent bonds with polysaccharides. These include organic bi- and trifunctional acids (Olivato, Grossmann, Bilck, ö Yamashita, 2012), maleic (Raquez, Nabar, Narayan, ö Dubois, 2008; Raquez, Narayan, ö Dubois, 2008; Raquez, Nabar, Srinivasan et al., 2008; Stagner, Dias Alves, Narayan, ö Beleia, 2011; Tomasik, Wang, ö Jane, 1995) and succinic anhydride (Bao, Xing, Phillips, ö Corke, 2003; Bhosale ö Singhal, 2006; Hui, Qi-he, Ming-liang, Qiong, ö Guo-qing, 2009; Shih ö Daigle, 2003; Shogren, 2003; Tomasik et al., 1995) as well as silane compounds (Jariyasakoolroj ö Chirachanchai, 2014) and diisocyanates (Karagoz ö Ozkoc, 2013; Schwach, Six, ö Avérous, 2008). Finding appropriate reagents that are able to react with the other, typically more hydrophobic polymer tends to be more challenging, and the low number – or complete lack of – available functional groups limits the effectiveness of this type of modification.

In the cases where the coupling reaction between the two phases could be confirmed, significant improvement in the mechanical properties was observed (Jariyasakoolroj ö Chirachanchai, 2014; Quiles-Carrillo et al., 2018). Still, mechanical performance is often limited by the inherent properties – e.g. low tensile strength – of the dispersed polysaccharide phase (Karagoz ö Ozkoc, 2013), among other things as discussed in Section 6.3. Potential side-reactions represent another challenge; we have already mentioned possible cross-linking in the polysaccharide phase. In a rather elaborate paper, Schwach et al. (Schwach et al., 2008) compare different methods for the compatibilization of PLA/TPS blends. One technique discussed by the authors involves the use of a bifunctional reagent, 4,4′-methylenebis(phenyl isocyanate) (MDI). As the authors also note, the limited success of compatibilization might well be explained by the numerous side reactions diisocyanates can participate in plasticized starch blends. Besides

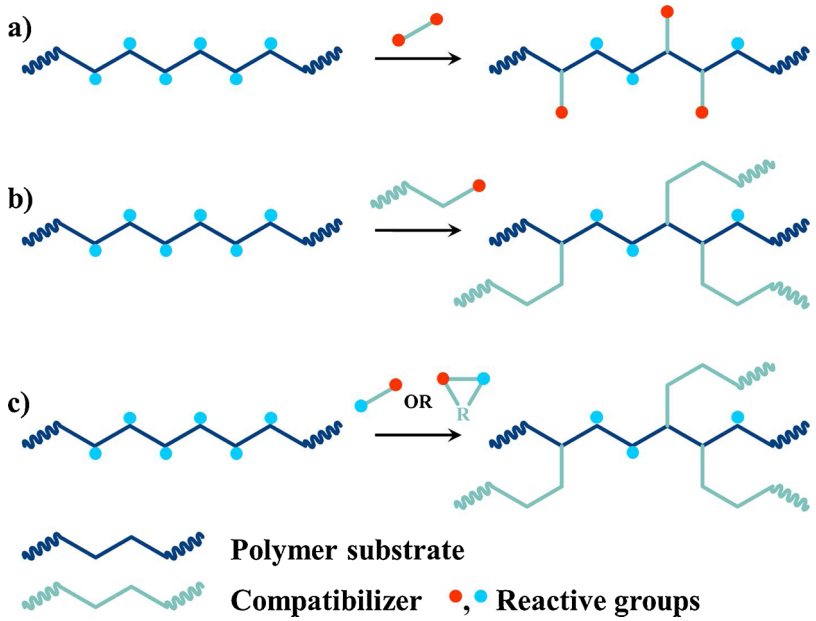

Fig. 5. Compatibilization strategies: **a)** coupling with bifunctional reagents; **b)** coupling with reactive polymers; **c)** graft copolymerization with bifunctional or cyclic monomers.

the hydroxyl groups of PLA and starch, such compounds can react with any traces of moisture as well as the hydroxyl-rich plasticizer forming low molar mass ureas and urethanes.

Due to the availability, low price, high reactivity and relatively benign nature of this unsaturated acid derivative, maleic anhydride (MA) has also been considered for the compatibilization of polysaccharide-based blends (Jang et al., 2007; Zhang ö Sun, 2004), with moderate success. The anhydride moiety can form covalent bonds with the available hydroxyl groups in the reaction mixture. Due to its double bond, MA can also radically react with the aliphatic chain of matrix polymers such as PLA in the presence of a peroxide initiator (Zhang ö Sun, 2004).

Several studies have also shown promising results regarding the use of poly(carboxylic acid)s – e.g. citric, malic and tartaric acids – as environmentally benign, non-toxic and non-volatile alternatives to MA. Moreover, these organic acids are inexpensive due to their abundance, since they can either be extracted from fruits and vegetables, or can be synthesized by microorganisms (Sailaja ö Seetharamu, 2008). Similarly to anhydrides, poly(carboxylic acid)s participate in esterification and transesterification reactions, resulting in the formation of reactive side-groups and cross-links between the polysaccharide chains and other polymers with appropriate reactive groups, e.g. the hydroxyl or amine end-groups of polyesters and polyamides, respectively. The effect of these agents on the properties of polymer blends is rather complex. Besides their compatibilization effect, and thus improved tensile strength, they can also exert a plasticizing effect and facilitate the acid hydrolysis of polysaccharide chains (Martins ö Santana, 2016; Olivato, Müller, Carvalho, Yamashita, ö Grossmann, 2014; Reddy ö Yang, 2010). Nevertheless, the consequent disruption of the granular structure of starch results in reduced viscosity, improving processing characteristics and the homogeneity of the material.

4.2.2. Reactive polymers

One way to overcome the challenge represented by the lack of available functional groups in most hydrophobic matrix polymers is the introduction of such reactive moieties to the macromolecule by using peroxide initiators. MA-grafted polymers have been used for decades for the compatibilization of polyolefin blends and composites that contain hydrophilic compounds such as lignocellulosic fibers (Danyadi et al., 2007; Klason, Kubat, ö Gatenholm, 1992; Renner, Móczó, ö Pukánszky, 2009) or starch (Wang, Yu, ö Yu, 2006; Bikiaris ö Panayiotou, 1998; Bikiaris et al., 1998; Senna, Hossam, ö El-Naggar, 2008; Shujun, Jiugao, ö Jinglin, 2005; Wang, Yu, ö Yu, 2005). The same concept has since been applied with success to polyesters (Arbelaiz, Fernández, Valea, ö Mondragon, 2006; Hwang et al., 2013; Muthuraj, Misra, ö Mohanty, 2017; Nabar, Raquez, Dubois, ö Narayan, 2005), and among them biobased and biodegradable polymers such as poly(lactic acid) (Detyothin et al., 2015; Hwang et al., 2013; Raghu, Kale, Raj, Aggarwal, ö Chauhan, 2018).

In contrast to using a combination of a peroxide and the anhydride for the in situ coupling of a polysaccharide with the matrix polymer (Zhang ö Sun, 2004), the reactive polymers introduced in this section are synthesized in a separate process step, similar to the one described in detail by Detyothin et al. (Detyothin, Selke, Narayan, Rubino, ö Auras, 2013) for the preparation of MA-grafted PLA by reactive extrusion. In a second step, this reactive compatibilizer is mixed with the other blend components during melt processing, forming graft copolymers by mainly reacting with polysaccharide hydroxyls through its anhydride moieties, according to Fig. 5b. Other moieties such as acrylic acid, oxazoline, and glycidyl methacrylate can also be grafted to confer reactivity to otherwise non-reactive polymers; however, MA grafting is generally preferred due to MA's easier handling, low toxicity and because it does not tend to homopolymerize during conventional free-radical melt-grafting conditions (Huneault ö Li, 2007).

The polymer backbone of the reactive compatibilizer is typically identical with that of the matrix (Dubois ö Narayan, 2003; Huneault ö Li, 2007), but this is not necessarily the case. Nevertheless, it is of critical importance that the long chains of the reactive polymer should be miscible with the matrix. The entanglements thus formed ensure the effective stress transfer during deformation between the covalently bonded matrix and dispersed phase. There are more complex approaches as well, such as the one described by Akrami et al. (Akrami, Ghasemi, Azizi, Karrabi, ö Seyedabadi, 2016). In this study, a reactive compatibilizer is prepared by first reacting MA with poly(ethylene glycol) (PEG) in solution, followed by the addition of starch, thus forming PEG-starch copolymers with free carboxylic groups. Once mixed with a blend of PLA and TPS, the carboxyls are anticipated to react with the hydroxyl moieties present in both blend components. Unfortunately, the reactions taking place during compatibilization were not analyzed in detail, which is a common deficiency of many studies in this field.

This approach (Akrami et al., 2016) resulted in a slight increase in tensile strength. This latter characteristic is a convenient and common measure of the success of compatibilization, as discussed in more detail in Section 6.3. Changes in blend or composite structure can also provide information on the effectiveness of a certain modification technique. Decreased particle size and a more homogeneous dispersion of the dispersed phase as a result of compatibilization are often reported. Improvements in mechanical performance, on the other hand, tend to be more moderate (Huneault ö Li, 2007).

Here, we must once more draw attention to the limiting effect of the inherently low strength of many plant polysaccharide materials on the mechanical performance of the blend or composite as a whole. Reactive polymers were successfully implemented for the compatibilization of lignocellulosic fillers with various polymer matrices (Plackett, 2004), resulting in significantly improved tensile properties. Nevertheless, in the case of strong interfacial adhesion between the phases, the dominating micromechanical deformation process was found to be the fraction of the fibers, limiting the ultimate strength of such composites (Faludi et al., 2014). Consequently, beyond ensuring strong interfacial adhesion, and effective stress transfer between the phases by compatibilization, one should also aim to modify the inherent properties of plant polysaccharide-rich materials, such as starch, hemicelluloses, cellulose or lignocellulosic fillers, in order to create biobased structural materials with a competitive set of properties.

4.3. Graft copolymerization

The amphiphilic copolymer structures acting as compatibilizer can also be synthesized via the graft copolymerization of various bifunctional and cyclic monomers initiated by the hydroxyl groups of plant polysaccharides, according to Fig. 5c. Such modifications are often referred to as "grafting from" as opposed to the "grafting to" approach discussed in Section 4.2. The advantage of this technique is that amphiphilic copolymer structures can be achieved in one step, often via reactive processing, while the easily accessible end-groups of the side-chains formed by graft copolymerization enable further reactive modification steps, if necessary.

4.3.1. Bifunctional monomers

Numerous studies have been published on the grafting of bifunctional monomers onto plant polysaccharides. Acrylate monomers (Hebeish, ElRafie, Higazy, ö Ramadan, 1996; Higazy, Bayazeed, ö Hebeish, 1987; Jyothi, Sajeev, ö Moorthy, 2010; Zou et al., 2012) have been the focus of research for many decades, aiming the synthesis of copolymer structures for various applications. Lately, biobased and/or degradable side-chains gained considerable importance, and thus novel monomers appeared, such as lactic acid (Ambrosio-Martín, Fabra, Lopez-Rubio, ö Lagaron, 2015; Hafren ö Cordova, 2007). In spite of a few exceptions (Ambrosio-Martín et al., 2015; Lai et al., 2015), bifunctional monomers never gained significant practical importance in the compatibilization of heterogeneous polymer systems, mostly due to

the convenience of ring-opening polymerization (ROP) techniques using cyclic monomers, as presented in Section 4.3.2. Therefore, we refrain from discussing them in much detail. The main drawback of many bifunctional monomers is the formation of low molar mass side-products (typically water) during their polymerization. These latter need to be constantly removed from the reaction mixture by vacuum or other means in order to shift the equilibrium towards the formation of the polymer. Nevertheless, achieving high molar masses still tends to be a challenge.

4.3.2. Ring-opening polymerization

Unlike the polycondensation of bifunctional compounds (e.g. hydroxy acids), the ring-opening polymerization of cyclic monomers proceeds without the accumulation of side-products, thus promoting the formation of high molar mass polymers and enabling the modification of polysaccharides via reactive processing. Nevertheless, proper drying protocols of the raw materials need to be set up to minimize moisture content that might lead to the hydrolysis of the growing side-chains. Another – generally undesirable – side reaction is the homopolymerization of the cyclic monomers initiated by water or other proton donors, such as hydroxyl-containing plasticizers, being present in the reaction mixture.

There are numerous cyclic organic compounds that can be used as monomers in ROP; the majority of them – at least those that have significant practical importance – belong to the family of cyclic esters, i.e. lactones. Fig. 6 shows the schematic representation of the ring-opening polymerization of a cyclic ester. The most commonly applied monomers for compatibilization purposes in polysaccharide blends and composites are ε-caprolactone (CL) and lactide (LA). The grafting of these compounds onto starch is typically carried out under anhydrous conditions either in bulk (Dubois, Krishnan, ö Narayan, 1999; Rutot-Houze et al., 2004; Yu et al., 2008), in organic solvents (Chen et al., 2005; Rutot-Houze et al., 2004; Sugih, Picchioni, Janssen, ö Heeres, 2009) or in ionic liquids (Xu, Kennedy, ö Liu, 2008). Although similar reactions have been reported also in aqueous media (Choi, Kim, ö Park, 1999; Gong, Wang, ö Tu, 2006), these techniques never gained much significance. The ROP reactions discussed above are almost without exception (Kim ö White, 2005) catalyzed by Lewis-acids, among which tin (II) 2-ethylhexanoate (Chen et al., 2005; Dubois et al., 1999; Dubois ö Narayan, 2003; Lönnberg et al., 2011; Yu et al., 2008) and various aluminum alkoxides (Dubois et al., 1999; Dubois ö Narayan, 2003; Sugih et al., 2009) are most commonly applied.

In two similar studies, Schwach et al. (Schwach et al., 2008) and Dubois et al. (Dubois ö Narayan, 2003) both compare different compatibilization strategies in polyester/starch blends. One such strategy in each case is the ex-situ synthesis of polyester-graft polysaccharides, PLA-graft amylose and PCL-graft dextran, respectively, followed by the incorporation of these copolymers into starch blends in the melt state. Strictly speaking, these modifications should be classified as physical compatibilization, of course. Nevertheless, we discuss them here, as in both cases the synthesis of the compatibilizer is in focus, and from a chemical point of view it is very similar to reactive compatibilization techniques based on graft copolymerization. In both cases, only moderate improvement could be achieved due to the addition of the compatibilizer. As Dubois et al. (Dubois ö Narayan, 2003) note, in addition to the time-consuming synthesis of the graft-copolymer, improved mechanical performance was obtained only when the compatibilizer was first precipitated onto the surface of starch granules in order to ensure they are localized at the interface. The in-situ graft-copolymerization of CL onto starch proved to be a much more favorable process that lead to considerably improved mechanical characteristics, highlighting the efficiency of reactive modification techniques.

As we discuss in more detail in Section 5.2, reactive processing – and reactive extrusion (REX) in particular – is a highly convenient technique for the ROP-synthesis of polyesters, both poly(ε-caprolactone) (PCL) (Balakrishnan, Krishnan, Narayan, ö Dubois, 2006; Kim ö White, 2003; Machado et al., 2008) and poly(lactic acid) (PLA) (Jacobsen, Fritz, Degee, Dubois, ö Jerome, 2000; Jacobsen, Fritz, Degée, Dubois, ö Jérôme, 2000). This method can also be applied for the in-situ formation of polyester-graft polysaccharides (Számel, Domján, Klébert, ö Pukánszky, 2008; Vidéki, Klébert, ö Pukánszky, 2005; Warth, Mülhaupt, ö Schätzle, 1997).

The use of silylated substrates, as reported in several studies (Dubois ö Narayan, 2003; Sugih et al., 2009), also deserves mentioning. Such modifications involve a pre-treatment step, in which some of the polysaccharide hydroxyls are substituted with silicon reagents, resulting in their respective silyl ethers. Besides enhancing the hydrophobicity and thermal stability of the polysaccharide, silylation has the additional benefit of "protecting" some of the −OH groups, thereby reducing the number of proton donors acting as initiators during the ROP of cyclic monomers. As a result, fewer but longer polyester side-chains form on the remaining free polysaccharide hydroxyls, potentially leading to more efficient compatibilization due to entanglement with the matrix polymer.

5. Implementation of compatibilization strategies

5.1. Bulk and solvent-based methods

Compatibilization by substitution and graft copolymerization reactions is commonly performed in bulk or in solution, especially at the laboratory scale. However, in case there are multiple polymeric components present in the reaction mixture, e.g. the coupling of two polymers with small molecules or reactive polymers, such techniques prove less convenient and melt processing techniques are favored even at smaller scales. A major challenge for synthesis in bulk is to maintain effective mixing and dissipate the excess heat arising due to the increasing molar mass, and thus increasing viscosity of the products.

Performing the reaction in a solvent, such as organic solvents (Chen et al., 2005; Rutot-Houze et al., 2004; Sugih et al., 2009), ionic liquids (Xu et al., 2008) or water (Choi et al., 1999; Gong et al., 2006), to some extent helps dealing with these problems, while also presenting new challenges. On the one hand, solution-based techniques make viscosity- and temperature-control more easily manageable, while they also

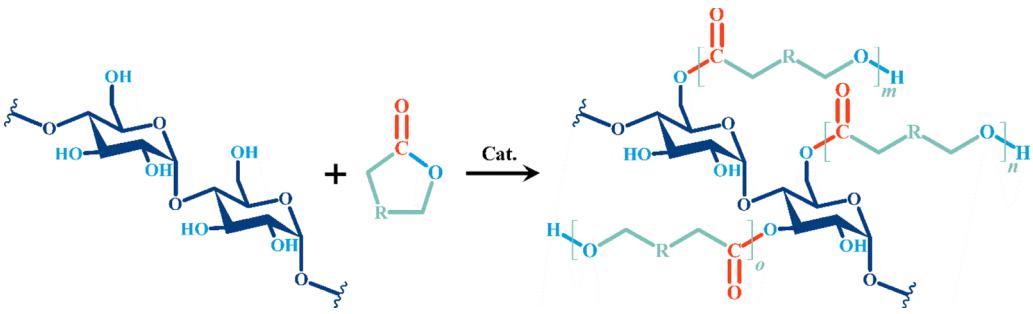

Fig. 6. Schematic representation of the ring-opening polymerization of a cyclic ester.

enable the purification of the product. However, the removal – and eventual recycling – of the solvent requires the introduction of additional process steps making such techniques costly and time-consuming compared to the melt processing methods discussed in the following section. Consequently, such methods are often difficult to scale up for industrial production (Raquez, Nabar, Narayan et al., 2008; Raquez, Narayan et al., 2008; Raquez, Nabar, Srinivasan et al., 2008).

5.2. Reactive processing

Extrusion is a thermo-mechanical process that is based on the action of one or two screws spinning in a tight barrel equipped with temperature control. The resulting high shearing forces between the plastic melt, the screw and the barrel lead to elevated temperature and pressure along the extruder. Two main categories of extrusion devices can be distinguished: single-screw and twin-screw extruders. The screw of single-screw extruders tends to be composed of one single piece, while twin-screw type devices often comprise shorter sections, i.e. screw elements that are selected and assembled according to the processed material and requirements regarding the product. These latter are referred to as modular extruders. There are three main types of screw elements that can be used: conveying screws, kneading blocks and reverse screws. Due to their different shape they affect the viscoelastic melt differently, facilitating material transport, mixing or shearing. The overall screw profile is one of the most crucial factors in extrusion processing. Additionally, twin-screw extruders can be classified as counter-rotating or co-rotating (Duque, Manzanares, ö Ballesteros, 2017; Erdmenger, 1957; Kohlgrüber ö Bierdel, 2008). In co-rotating devices, the shearing and plasticizing effect is axial (the maximum velocity being achieved at the intermeshing zone), while in counter-rotating twin-screw extruders, the effect is radial (highest velocity being achieved at the screw tips).

The ultimate goal of materials design and development is to obtain new materials or to enhance the properties of existing ones to meet the requirements of specific applications. By means of extrusion-compounding and reactive extrusion, a wide range of tailor-made polymer blends and composites can be produced. Due to their excellent mixing characteristics, intermeshing and co-rotating twin screw extruders are particularly suitable for this purpose. As opposed to single-screw extrusion, which produces mainly a distributive mixing and where the process throughput is dependent on the screw speed and the pressure profile, twin screw extrusion allows the adjustment of several independent process variables, including feed flow rate, screw rotation speed and temperature profile along the screw axis. This leads to a high process flexibility and optimization potential (Uitterhaegen ö Evon, 2017).

Reactive extrusion (REX) describes a special process in extrusion technology in which individual components are chemically modified during melt processing. Twin-screw extruders are typically used for REX purposes, due to their excellent control of mixing and residence time distribution (Raquez, Narayan et al., 2008). The stoichiometric ratio of the components needs to be ensured by using highly accurate feeders, while surplus reaction heat is dissipated through the barrel wall. One of the most common goals of REX is the compatibilization of heterogeneous polymeric materials, and polysaccharide-based ones among them. As illustrated by Fig. 7, the process involves the in-situ formation of amphiphilic structures, and thus covalently bonding the phases in the melt state, according to one of the chemical routes discussed in Section 4.

REX is a convenient and cost-effective technique for the esterification of polysaccharides using anhydride reagents (Hanna ö Fang, 2002; Miladinov ö Hanna, 2000; Raquez, Nabar, Narayan et al., 2008; Raquez, Narayan et al., 2008; Raquez, Nabar, Srinivasan et al., 2008; Rudnik, Matuschek, Milanov, ö Kettrup, 2005; Rudnik ö Zukowska, 2004; Tomasik et al., 1995; Wang, Shogren, ö Willett, 1997), the coupling of blend components using bifunctional reagents (Schwach et al., 2008) or reactive polymers (Dubois ö Narayan, 2003; Raquez, Nabar, Narayan et al., 2008; Raquez, Nabar, Srinivasan et al., 2008) as well as for the in-situ formation of graft-copolymers by ROP (Számel et al., 2008; Vidéki et al., 2005; Warth et al., 1997). Reactions that would otherwise require heavy equipment, such as batch reactors, can be performed more efficiently in a continuous manner by REX. Moreover, extruders are far more capable of dealing with the dramatic change of viscosity due to the increasing molar mass of one or more components of the reaction mixture during polymerization (Brown ö Orlando, 1998; Raquez, Narayan et al., 2008; Tzoganakis, 1989). One should keep in mind that unlike in the case of solvent-based methods, there is no practical solution for the purification of materials produced by reactive extrusion. Thus, catalysts, unreacted monomers and other reagents as well as side-products formed during the process cannot be removed from the finished product. Depending on their concentration, such chemical species might affect the characteristics of the material, and even prohibit its use in certain areas, e.g. food and medical applications.

The rheological behavior of polysaccharide-based blends is strongly affected by the blend composition, the properties of the components (viscosity ratio and elasticity ratio), the volume fractions, as well as by the morphology and interactions between phases (Biresaw ö Carriere, 2001). It should also be noted that rheological characteristics play a significant role during reactive processing in the melt state, regardless the reactivity of the components. Through melt viscosity and relative viscosity of the components, rheological properties affect residence time distribution (RTD) inside the extruder, shear viscosity in the screw channels and die as well as the dynamics of post-extrusion phenomena, e.g. die-swell. In polymerization processes carried out by reactive extrusion, the percentage monomer conversion has been found to be proportional to mean residence time and thus on RTD (De Graaf ö Janssen, 2000; Poulesquen, Vergnes, Cassagnau, Gimenez, ö Michel, 2001).

In general, the processing properties of polysaccharides and synthetic biobased polymers differ considerably. The viscosity of polysaccharides is much higher than that of conventional polymers, while the majority of biobased polymers, and aliphatic polyesters in particular, tend to form relatively low viscosity melts, often leading to difficulties with processing such blends. The complexity of the rheological behavior of thermoplastic starches and other polysaccharides further complicates melt processing: rheological properties depend on the botanical origins of the natural polymers (molar mass, and amylose/amylopectin ratio in the case of starch). The effect of chemical modifications such as esterification as well as the amount and type of plasticizers needs to be considered. Thermoplastic starch, for instance, was reported to behave similarly to a high molecular weight viscoelastic polymer at high amylopectin contents, while lower amylopectin/amylose ratios result in gel-like behavior. In both cases, plasticizer content only affected the viscosity of the polymer melt, but not its inherent rheological behavior (Della Valle, Buleon, Carreau, Lavoie, ö Vergnes, 1998).

It is well known that the precise control of such processes is rather challenging, due to the non-Newtonian behavior and high viscosity of polymer melts, the consequent high shear stresses occurring during extrusion, and the complex reactions taking place between the blend components during reactive extrusion. All these parameters affect the structure of the compatibilized blend to a high degree, therefore also influencing its macroscopic properties. Therefore, the study of rheological behavior during REX process, i.e. rheokinetics, is essential in modeling and optimizing processing conditions (Bao et al., 2018).

In any case, despite reactive extrusion certainly being an important way to modify and develop novel polymeric systems, it is a rather complex process that involves many interacting variables. Reactions in the melt state are governed by local flow conditions (residence time, temperature, mixing), while also affecting flow conditions through changes in molar mass, viscosity as well as temperature due to reaction

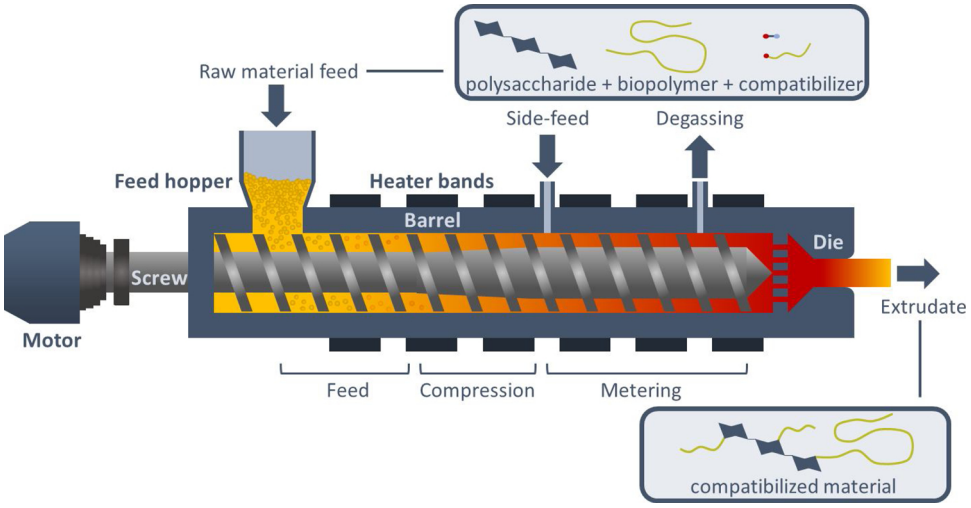

Fig. 7. The compatibilization of polysaccharide-based polymer blends and composites in the melt state by reactive extrusion.

heat. Moreover, the geometry and the kinematics of a twin-screw extruder are often rather complex, compared to a batch reactor. Therefore, the optimization of such processes is a highly challenging task (Jongbloed, Kiewiet, Van Dijk, ö Janssen, 1995). Consequently, studies generally focus either on the determination of general, theoretical correlations, or providing practical tools for the optimization and control of specific reactive extrusion processes (Janssen, 2004; Vergnes ö Berzin, 2006).

5.3. Catalysts

The substitution of the hydroxyl groups of plant polysaccharides with more hydrophobic moieties through esterification is a well-described in the literature (Simon, Müller, Koch, ö Müller, 1998; Whistler, 1945). The acylation reaction can be catalyzed by a wide range of organic and inorganic compounds including acids (Cheng, Dowd, Selling, ö Biswas, 2010), bases (Whistler, 1945), halogens (Biswas et al., 2008) or even enzymes (Alissandratos ö Halling, 2012). The formation of polyester chains through ROP is most commonly catalyzed by one family of metal-organic compounds, namely metal alkoxides ranging from aluminum (Dubois et al., 1999; Dubois ö Narayan, 2003) to lanthanide alkoxides. The efficiency of these Lewis-acid type catalysts is based on the in-situ formation of alkoxides with an alcohol or other protic impurities present in the reaction medium (Kowalski, Duda, ö Penczek, 1998). Accordingly, polysaccharides containing free hydroxyl groups such as starch (Dubois et al., 1999), dextran (Dubois ö Narayan, 2003) or cellulose and its derivatives (Hatakeyama, Yoshida, ö Hatakeyama, 2000; Számel et al., 2008; Vidéki et al., 2005; Warth et al., 1997) can be grafted with cyclic esters by this method conveniently. Among the metal alkoxides discussed above, tin(II) bis(2-ethylhexanoate), or stannous octoate [$Sn(Oct)_2$], is by far the most commonly applied. Its extensive use is mainly due to the fact that it is accepted by the American Food and Drug Administration (FDA) for polymer coating formulations in contact with food. Moreover, $Sn(Oct)_2$ is less sensitive towards water and other protic impurities than aluminum alkoxides, which facilitates its use in the laboratory and in industry as well (Lecomte ö Jérôme, 2011). Despite the FDA approval, the health and environmental effects of tin catalysts are rather ambiguous, as Hege et al. (Hege ö Schiller, 2014) discuss in some detail. Therefore, numerous other metal-organic compounds such as Li, Mg, Ca, Zn, Fe and Zr alkoxides have been considered as more environmentally benign catalyst in ROP syntheses (Kundys, Plichta, Florjańczyk, Frydrych, ö Żurawski, 2015). Due to their very low toxicity, iron compounds are often used as alternatives for the catalysis of ring-opening polymerization (Dobrzynski, Kasperczyk, Janeczek, ö Bero, 2002; Kundys et al., 2015; O'Keefe, Breyfogle, Hillmyer, ö Tolman, 2002; Stolt et al., 2005), with varying degrees of success. Among them, iron(III) acetylacetonate [$Fe(AcAc)_3$] (Dobrzynski et al., 2002; Kundys et al., 2015) has shown much promise, resulting in polymers with molar masses similar to those prepared with $Sn(Oct)_2$.

Organocatalysis is another concept that aims to reduce the environmental effect of catalysts (Domínguez de María, 2010) used for the esterification of polysaccharides (M. Tupa et al., 2013) or the ROP of lactones (Casas, Persson, Iversen, ö Córdova, 2004; Hafrén ö Córdova, 2005; Persson, Schröder, Wickholm, Hedenström, ö Iversen, 2004). Although the term originally comprises all reactions catalyzed by metal-free organic compounds, it is often applied to nontoxic, small organic molecules such as hydroxy (lactic, tartaric) and amino (proline, alanine) acids. These latter have been claimed to act as 'minimal hydrolyses' catalyzing reactions in a biomimetic fashion, thus being highly selective (Persson et al., 2004) and active under relatively mild conditions (Domínguez de María, 2010). Nevertheless, as chemical catalysts, they are able to withstand high temperatures and remain active under strongly basic or acidic conditions as well. Some of these claims, however, might be somewhat too optimistic. As studies show, in many cases high catalyst concentrations and elevated temperature are necessary for such catalysts to be efficient (M. V. Tupa et al., 2015). Another considerable drawback of such compounds is that their application for reactive processing purposes is questionable. Due to their acidic nature, besides catalyzing esterification and polymerization reactions, they might also facilitate the hydrolysis of certain polymeric components, in particular polyesters and polyamides.

6. Evaluation of the efficiency of compatibilization

6.1. Rheology

The viscoelastic behavior of polymer blends or composites plays a crucial role in the optimization of processing conditions as well as the development of phase morphology and macroscopic properties. Depending on the processing and/or testing conditions, the viscosity of heterogeneous polymeric materials in the melt state can deviate either in a negative or positive direction from the additive rule, this is, the logarithmic combination of the viscosities of its respective components. In general, a negative deviation indicates weak interfacial interactions, while the opposite behavior can be observed in the case of strong interactions. Thus, an increase in viscosity due to the addition of a compatibilizer suggests that the additive exerts interfacial activity, a pre-requisite for successful compatibilization. Although discussing the complex relation between compatibilization and rheological behavior

exceeds the scope of this paper, this topic is examined in detail in the excellent review of Koning et al. (Koning et al., 1998).

Plant polysaccharides and most synthetic biopolymers are thermodynamically dissimilar in nature, and hence are incompatible unless a compatibilizer is used (Maliger, McGlashan, Halley, ö Matthew, 2006). This latter is often added in the melt state, considerably affecting the rheological properties of the blend. Although many studies report the effect of compatibilizers on blend morphology and mechanical properties, much less attention has been paid to their effect on rheological properties (Démé, Peuvrel-Disdier, ö Vergnes, 2014).

As Van Puyvelde et al. (Van Hemelrijck, Van Puyvelde, ö Moldenaers, 2006; Van Puyvelde, Velankar, ö Moldenaers, 2001) point out, the presence of surface-active copolymers as compatibilizers significantly affect the rheological characteristics of blends. Nevertheless, rheological characterization is seldom considered for the determination of compatibilization efficiency. This is largely due to the complex nature of rheological processes that make the prediction of macroscopic properties challenging. Nevertheless, improved compatibility has been reported for modified polysaccharide blends based on the increased complex viscosities of the blends (Xie, Yu, Liu, ö Dean, 2006, 2007; Xu ö Finkenstadt, 2013). One should consider such claims with caution, since the viscosity and rheological behavior of polysaccharide blends depend on numerous factors besides compatibilization, including plasticizer content, changes in molar mass due to polymerization or degradation caused by the compatibilizer (Li ö Huneault, 2011) or residual humidity (Mittal, Akhtar, ö Matsko, 2015), and even the order of mixing the components (Ali Nezamzadeh, Ahmadi, ö Afshari Taromi, 2017).

6.2. Morphology

The mixing of miscible polymers results in a homogeneous, single-phase system, the properties of which largely depend on those of the components and the volumetric ratio thereof. In immiscible blends, on the other hand, it is commonly accepted and experimentally confirmed that the size and distribution of the dispersed particles are the result of a competitive process between breakup and coalescence phenomena. Interfacial interactions, the shear rate of mixing, as well as the viscosity ratio of the blend components are all key parameters determining the degree of dispersion (Van Hemelrijck et al., 2006; Van Puyvelde et al., 2001). Heterogeneous blends are labeled as compatible in case their property profile fits the requirement of a certain application; in general, strong adhesion between the respective phases at the interface is necessary to achieve this. As discussed earlier, interfacial interactions can be improved by the addition or in-situ formation of compatibilizers that also substantially affect the morphology of the blends, resulting in reduced average particle size of the dispersed phase (see Fig. 8a and b) as well as improved mechanical properties (Huneault ö Li, 2007; Imre ö Pukánszky, 2013; Martins ö Santana, 2016). This latter can be a consequence of both/either stronger interfacial interactions and/or the increased surface area of the interface due to morphological changes. One should keep in mind, however, that the purpose of compatibilization is never the conversion of immiscible blends into fully miscible ones, but the proper control of blend morphology and the enhancement of interfacial adhesion in order to tailor mechanical properties.

In most cases, the major component of the blend forms the continuous phase, whereas the minor component is the dispersed phase (Shujun et al., 2005). Depending on the volume fraction of the blend components, phase inversion takes at a certain composition at which the two phases switch their functions (Steinmann, Gronski, ö Friedrich, 2001). This occurs when both polymers are present in approximately equal amounts or at high concentrations of the minor phase (Schwach ö Avérous, 2004). A wide range of different morphologies can be obtained by melt mixing, such as spherical, lamellar, fibrillar, and even co-continuous (Rodriguez-Gonzalez, Ramsay, ö Favis, 2003; Steinmann et al., 2001). Co-continuous microstructures are distinguished by the mutual interpenetration of the phases (Galloway ö Macosko, 2004). This morphology is particularly interesting because both components can contribute fully to the properties of the blend, resulting in a synergistic improvement of the final properties.

The mechanical properties of heterogeneous polymeric materials are strongly related to their morphology. Consequently, the structure of polysaccharide blends should be closely monitored in order to determine the effect of compatibilization and tailor mechanical performance. Zhang and Sun (J.-F. Zhang ö Sun, 2004) and Jang et al. (Jang et al., 2007) both studied the morphology and mechanical performance of PLA/non-plasticized starch composites in the presence or absence of MA-based reactive compatibilizers, namely MA (Jang et al., 2007; Zhang ö Sun, 2004), MA-g-TPS (Jang et al., 2007) and MA-g-PLA (Zhang ö Sun, 2004). Since the polysaccharide component is not thermoplastic, it acts as a filler in the heterogeneous compositions, thus its average particle size does not change noticeably during processing. Nevertheless, one can still observe the effect of compatibilization based on the morphology of the materials.

These studies suggest that MA is an efficient compatibilizer both applied as an in-situ reactive agent (Jang et al., 2007; Zhang ö Sun, 2004), and grafted onto a PLA chain (Zhang ö Sun, 2004). MA-g-TPS, on the other hand is not as effective for PLA/starch blend systems (Jang et al., 2007). While sharp edges and large cavities can be observed around the starch granules in the unmodified composites (Fig. 8c), the SEM micrograph taken on the fracture surface of MA-compatibilized indicate stronger interfacial adhesion (Fig. 8d). The morphology of the samples prepared with MA-g-TPS strongly depend on the compatibilizer content: the interface between starch and the biopolymer matrix still has some cavities at rather low MA-g-TPS concentrations, while increasing copolymer contents (15 parts per hundred rubber (phr), Fig. 8e) result in a morphology similar to that of MA-compatibilized blends. The efficiency of MA as a compatibilizer might be in part explained by its plasticizing effect: as discussed by Wang et al. (H. Wang, Sun, ö Seib, 2002), good wetting at interface is needed to achieve strong adhesion. Thus, reducing the surface tension of starch due to the absorption of MA, and the lower viscosity of the PLA phase due to its plasticizing effect might be beneficial.

6.3. Mechanical properties

The effect of compatibilization is often reported based on morphological analysis (Dubois ö Narayan, 2003; Jang et al., 2007) without discussing mechanical properties. This is from our standpoint insufficient, since the improvement of the mechanical properties is often the most common goal of such modification techniques. Another common claim is to report improved compatibility based on increased Young's modulus (Hwang et al., 2013). Compatibilization most commonly aims to improve interfacial adhesion between the respective components. However, modulus, or stiffness, is determined at very low deformations, under which conditions the phases do not separate at the interface. Accordingly, this characteristic does not provide sufficient information on the strength of interfacial adhesion. The parameters that determine the stiffness of a heterogeneous polymeric material are the properties and volumetric ratio of its constituents, and the structure and morphology of the blend. Since compatibilization changes the composition of the material and often results in structural changes (e.g. reduced particle size of the dispersed phase), it can affect stiffness as well. This correlation, though, is hardly direct, and at the same time it is rather complex. Side-reactions, plasticization or crystallization due to the addition of a compatibilizer also have a similar effect. Consequently, the Young's modulus of a polymer blend or composite is not a proper indicator of compatibility.

A direct consequence of successful compatibilization is the enhanced tensile strength of the blend or composite in question. Consequently, numerous studies (Arbelaiz et al., 2006; Avella et al., 2000; Detyothin et al., 2015; Dubois ö Narayan, 2003; Gregorova,

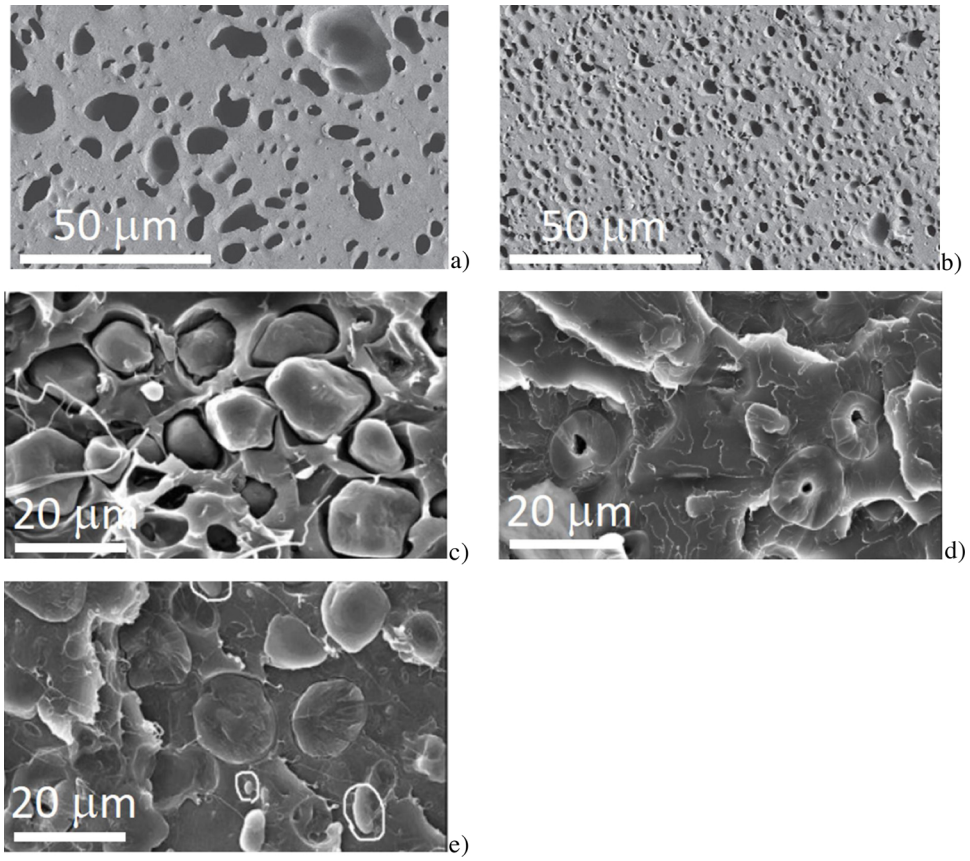

Fig. 8. The effect of reactive compatibilization on the morphology of thermoplastic and granular starch-based materials; PLA/TPS blends (43 wt% starch): **a)** no compatibilization; **b)** coupling the phases with MA-grafted PLA (Huneault & Li, 2007); PLA/starch composites (30 wt% starch): **c)** without compatibilizer, **d)** in presence of 3 phr of MA and **e)** 15phr of MA-grafted TPS (Jang et al., 2007).

Hrabalova, Wimmer, Saake, ö Altaner, 2009; Adriana Gregorova, Sedlarik, Pastorek, Jachandra, ö Stelzer, 2011; Haque, Errico, Gentile, Avella, ö Pracella, 2012; Huneault ö Li, 2007; Jariyasakoolroj ö Chirachanchai, 2014; Karagoz ö Ozkoc, 2013; Li ö Huneault, 2011; Lönnberg et al., 2011; Muthuraj et al., 2017; Quiles-Carrillo et al., 2018; Raghu et al., 2018; Schwach et al., 2008; Wu, 2003) consider this characteristic when evaluating the efficiency of various compatibilization strategies. To get a more complete picture on the effect of compatibilization, however, it is worth investigating the mechanical property profile of a material as a whole, including tensile strength, elongation-at-break as well as Young's modulus. In Fig. 9 we present such property profiles of starch- (left column in blue) and lignocellulose-based (right column in green) blends and composites before (▬) and after compatibilization (▬). The relative values listed in the diagrams reflect the change of each mechanical characteristic compared to the non-compatibilized material (100%).

The first three examples in Fig. 9a, b, and c show a rather similar increase in both modulus and strength accompanied by a slight decrease of deformability, indicating that all these materials became more rigid as a result of reactive compatibilization. As discussed above, increased modulus is often related to phenomena not directly related to increased interfacial adhesion which is the main purpose of such modifications. This seems to be the case here as well. In Fig. 9a PCL chains are grafted to granular starch by ROP to improve the properties of PCL/starch blends. However, the relatively short grafted chains have a tendency to crystallize, leading to the observed change in mechanical characteristics. Detyothin et al. (Detyothin et al., 2015) also point out that molar mass of the compatibilizer or that of the macromolecules forming during reactive compatibilization can be a significant factor limiting the efficiency of such modifications. Despite the large number of studies investigating MA-grafted polymers for the compatibilization of polysaccharide-based blends and composites, the molar mass of the reactive polymer is seldom considered, aside from a few exceptions (Mani, Bhattacharya, ö Tang, 1999). Such compatibilizers are typically synthesized by reactive extrusion using peroxide initiators. According to Detyothin et al. (Detyothin et al., 2015), the molar mass of MA-g-PLA, and therefore its intrinsic viscosity, decreases gradually as a function of grafting degree due to chain scission reactions, which phenomenon also affects the macroscopic properties of the materials compatibilized in this manner.

The reason for the similar mechanical behavior presented in Fig. 9b and c, showing the property profile of wood fiber-reinforced plasticized PLA, and PLA/TPS blends, respectively, is somewhat different. The compatibilizer in both cases is an isocyanate, MDI. This latter reacts with any active hydrogen-containing groups in the reaction mixture, such as the −OH moieties of cellulose, starch, and PLA, coupling the phases in order to improve interfacial adhesion. Nevertheless, it also reacts with the respective plasticizers (poly(ethylene glycol) in PLA, and glycerol in TPS) forming polyurethanes and thus increasing the overall stiffness of these heterogeneous materials.

Fig. 9d, e and f, on the other hand, show the effect of successful compatibilization, resulting in both enhanced strength and deformability, while modulus remains largely unaffected in each case. The observed tendencies are rather similar despite the different modification techniques, matrices and dispersed phases. A typical example for the compatibilization of TPS-based blends is the introduction of MA-grafted polymers synthesized in a separate step (Detyothin et al., 2015; Huneault ö Li, 2007) or in-situ during reactive extrusion (Wang et al., 2007). Moderately enhanced mechanical performance compared to the unmodified blend was reported in such cases, as it can be observed in Fig. 9e, due to stronger interfacial adhesion and a more homogeneously dispersed morphology. The increase in strength, however, seems to be much more pronounced in lignocellulose-based composites (Fig. 9d and f). One reason for this might be the different compatibilization approach applied in these cases. MA-g-PLA (Fig. 9e) is essentially assumed to react with one phase (TPS), while its polyester chain promotes stress

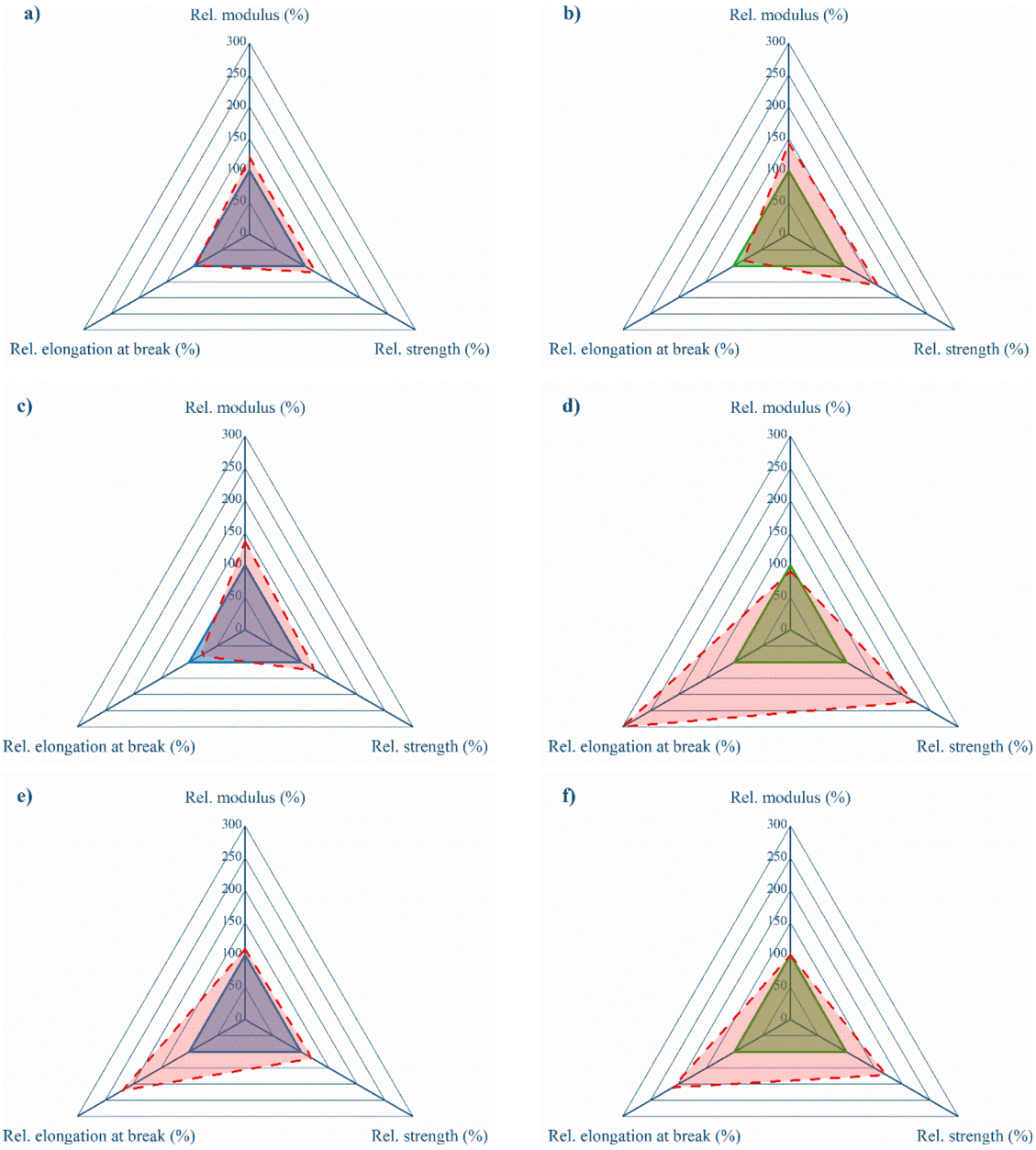

Fig. 9. Mechanical property profile of polysaccharide blends and composites with (▬ and without (▬) compatibilization; **a)** granular starch in PCL, PCL-g-starch compatibilizer (Philippe Dubois & Narayan, 2003), **b)** wood fibers in plasticized PLA, MDI compatibilizer (Adriana Gregorova et al., 2011), **c)** TPS in PLA, MDI compatibilizer (Schwach et al., 2008), **d)** almond shell fibers in PLA, MA-g-linseed oil compatibilizer (Quiles-Carrillo et al., 2018), **e)** TPS in PLA, MA-g-PLA compatibilizer (Detyothin et al., 2015) and **f)** cellulose microfibers in PCL, MAGMA-g-PCL compatibilizer (Haque et al., 2012).

transfer through entanglements by mixing with the matrix polymer. Unlike maleated PLA, MA-g-linseed oil (Fig. 9d) and MA/glycidyl methacrylate-grafted PLA (MAGMA-PCL, Fig. 9f) contain multiple reactive sites, being able to form covalent bonds with both phases. Furthermore, the presence of glycerol as a plasticizer in the TPS/PLA blend possibly leads to side-reactions, further limiting the effectiveness of compatibilization.

As Fig. 10 suggests, there is a general tendency, according to which the mechanical performance of polysaccharide-based composites (○,□,◊) can be enhanced to a far greater extent than that of thermoplastic starch blends (●,■,◆). In the figure we collected the relative tensile strength of various polysaccharide-based heterogeneous materials compared to the respective non-modified system. From each study reviewed (Arbelaiz et al., 2006; Avella et al., 2000; Detyothin et al., 2015; Dubois ö Narayan, 2003; Gregorova et al., 2009; Adriana Gregorova et al., 2011; Haque et al., 2012; Huneault ö Li, 2007; Jariyasakoolroj ö Chirachanchai, 2014; Karagoz ö Ozkoc, 2013; Li ö Huneault, 2011; Lönnberg et al., 2011; Muthuraj et al., 2017; Quiles-Carrillo et al., 2018; Raghu et al., 2018; Schwach et al., 2008; Wu, 2003), we only included the highest values at a certain polysaccharide content, regardless of the type and amount of compatibilizer used. Most available data have been published on compatibilization using reactive polymers (◆,◊), followed by small molecules (□,■), while modification of the polysaccharide fraction by ROP (○,●) is relatively rarely considered. The results seem to justify this tendency: the former two techniques tend to provide better results, especially if one takes into consideration their relative simplicity. As noted earlier, compatibilization tend to affect the strength of composites more than that of blends, and this difference only increases as a function of polysaccharide-content, as the highlighted curves illustrate. The higher the filler content, the higher the tendency of fillers in a composite material to aggregate, thereby deteriorating mechanical properties. Compatibilization can

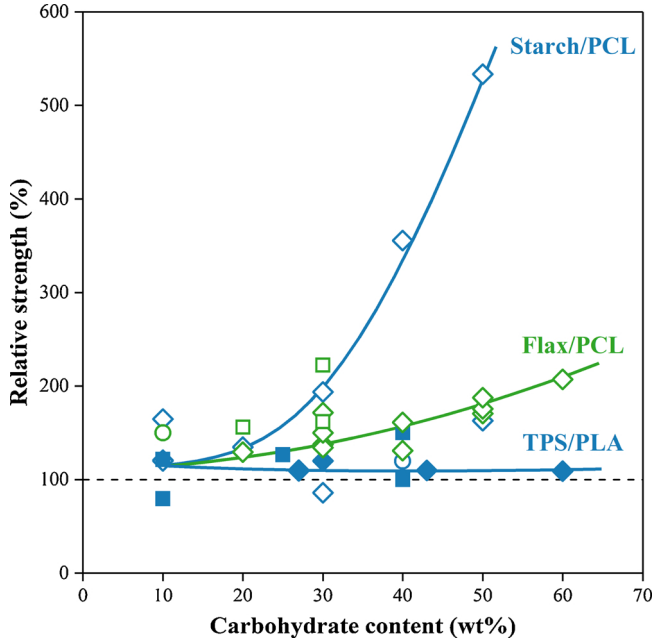

Fig. 10. The relative strength and of compatibilized (blue) starch- and (green) lignocellulose-based (●,■,♦) blends and (○,□,◊) composites; compatibilization technique: (●,○) grafting-to, (■,□) coupling with small molecules, (◊,♦) coupling with reactive polymers; the relative values indicate the change in mechanical characteristics compared to the non-compatibilized material with a similar composition (Arbelaiz et al., 2006; Avella et al., 2000; Detyothin et al., 2015; Dubois & Narayan, 2003; Gregorova et al., 2009, 2011; Haque et al., 2012; Huneault & Li, 2007; Jariyasakoolroj & Chirachanchai, 2014; Karagoz & Ozkoc, 2013; Li & Huneault, 2011; Lönnberg et al., 2011; Muthuraj et al., 2017; Quiles-Carrillo et al., 2018; Raghu et al., 2018; Schwach et al., 2008; Wu, 2003) (For interpretation of the references to colour in this figure legend, the reader is referred to the web version of this article.).

help resolve this issue, resulting in a considerable increase of tensile strength over the unmodified material. In blends such as TPS/PLA, this phenomenon does not play a role. Moreover, strong interfacial interactions due to compatibilization can lead to the break-up of starch granules during processing, leading to smaller dispersed particle size, i.e. more favorable morphology (Starch/PCL). This is not likely to take place in a lignocellulose-reinforced composite (Flax/PCL), due to the much higher inherent strength of the dispersed fibers.

This latter characteristic, however, might limit the performance of plant polysaccharide-based compositions in some cases, as Faludi et al. (Faludi et al., 2014) point out in an elaborate study performed on PLA/lignocellulose composites. As the authors conclude, contrarily to most claims published in the literature, interfacial adhesion between filler and matrix is rather strong in such composites. Therefore, the dominating micromechanical deformation mechanism is the fracture of the dispersed fibers, thus determining also the macroscopic strength such heterogeneous materials. Consequently, enhancing the intrinsic strength of the dispersed phase might be the way to further improve the mechanical properties of polysaccharide-based blends and composites.

The above examples highlight that evaluating the efficiency of compatibilization solely based on mechanical properties is not always sufficient. Although tensile strength is a characteristic of significant importance from a practical point of view, this one value does not reveal the reasons behind the success or failure of a given compatibilization strategy. In order to tailor the properties of polysaccharide blends or composites, detailed analysis of their chemical structure, morphology and mechanical behavior, including micromechanical deformation processes, need to be performed, thus the factors limiting their performance can be identified.

7. Conclusions

Due to their unique properties as well as environmental concerns, plant polysaccharides have been in the focus of research for many decades. Their application for materials purposes, however, is seldom feasible without modification. Thus, polysaccharides are generally used in a derivatized form and/or in combination with other polymers, requiring the compatibilization of such blends and composites. Throughout the paper, reactive compatibilization techniques have been considered due to their efficiency and feasibility in polysaccharide-based compositions. It is difficult to draw general conclusions regarding the most successful strategies currently available. Nonetheless, one can conclude with some certainty that coupling reactions involving either reactive polymers or low molar mass reagents show much promise due to their efficiency and versatility. The substitution of polysaccharide hydroxyls by either monofunctional compounds or longer side-chains through the ROP of cyclic monomers, on the other hand, seems to be more suitable for tailoring the intrinsic properties of polysaccharide substrates rather than for compatibilization purposes. Similarly to other efforts targeting the reactive modification of polymers, melt processing techniques, and most importantly reactive extrusion continue to gain attraction for the compatibilization of polysaccharide blends and composites as well, due to being highly cost-effective, versatile and easily upscalable. Finally, it should be emphasized that the efficiency of compatibilization techniques can be evaluated based on numerous indicators such as processability, morphology and mechanical performance. Nevertheless, the development of successful strategies requires the detailed analysis of the chemical structure, morphology and mechanical behavior of these heterogeneous systems.

Acknowledgements

The authors express their gratitude to the Bio Based Industries Consortium and European Commission for the financial support to the project BARBARA - Biopolymers with advanced functionalities for building and automotive parts processed through additive manufacturing. This project has received funding from the Bio Based Industries Joint Undertaking under the European Union's Horizon 2020 research and innovation programme under grant agreement No 745578.

References

Aburto, J., Alric, I., Thiebaud, S., Borredon, E., Bikiaris, D., Prinos, J., ... Panayiotou, C. (1999). Synthesis, characterization, and biodegradability of fatty-acid esters of amylose and starch. *Journal of Applied Polymer Science, 74*(6), 1440–1451. https://doi.org/10.1002/(sici)1097-4628(19991107)74:6<1440::aid-app17>3.0.co;2-v.

Akrami, M., Ghasemi, I., Azizi, H., Karrabi, M., & Seyedabadi, M. (2016). A new approach in compatibilization of the poly(lactic acid)/thermoplastic starch (PLA/TPS) blends. *Carbohydrate Polymers, 144*, 254–262. https://doi.org/10.1016/j.carbpol.2016.02.035.

Ali Nezamzadeh, S., Ahmadi, Z., & Afshari Taromi, F. (2017). From microstructure to mechanical properties of compatibilized polylactide/thermoplastic starch blends. *Journal of Applied Polymer Science, 134*(16), 1–9. https://doi.org/10.1002/app.44734.

Alissandratos, A., & Halling, P. J. (2012). Enzymatic acylation of starch. *Bioresource Technology, 115*, 41–47. https://doi.org/10.1016/j.biortech.2011.11.030.

Al-Itry, R., Lamnawar, K., & Maazouz, A. (2012). Improvement of thermal stability, rheological and mechanical properties of PLA, PBAT and their blends by reactive extrusion with functionalized epoxy. *Polymer Degradation and Stability, 97*(10), 1898–1914. https://doi.org/10.1016/j.polymdegradstab.2012.06.028.

Alzagameem, A., El Khaldi-Hansen, B., Kamm, B., & Schulze, M. (2018). Lignocellulosic biomass for energy, biofuels, biomaterials, and chemicals. In V. J. Sílvio (Ed.). *Biomass and Green chemistry* (pp. 95–132). Cham: Springer International Publishing. https://doi.org/10.1007/978-3-319-66736-2_5.

Ambrosio-Martín, J., Fabra, M. J., Lopez-Rubio, A., & Lagaron, J. M. (2015). Melt polycondensation to improve the dispersion of bacterial cellulose into polylactide via melt compounding: Enhanced barrier and mechanical properties. *Cellulose, 22*(2), 1201–1226. https://doi.org/10.1007/s10570-014-0523-9.

Arbelaiz, A., Fernández, B., Valea, A., & Mondragon, I. (2006). Mechanical properties of short flax fibre bundle/poly(ε-caprolactone) composites: Influence of matrix modification and fibre content. *Carbohydrate Polymers, 64*(2), 224–232. https://doi.org/

10.1016/j.carbpol.2005.11.030.
Avella, M., Errico, M. E. E., Laurienzo, P., Martuscelli, E., Raimo, M., & Rimedio, R. (2000). Preparation and characterisation of compatibilised polycaprolactone/starch composites. *Polymer, 41*(10), 3875–3881. https://doi.org/10.1016/S0032-3861(99)00663-1.
Balakrishnan, S., Krishnan, M., Narayan, R., & Dubois, P. (2006). Three-arm poly (epsilon-caprolactone) by extrusion polymerization. *Polymer Engineering and Science, 46*(3), 235–240. https://doi.org/10.1002/pen.20344.
Bao, J. S., Xing, J., Phillips, D. L., & Corke, H. (2003). Physical properties of octenyl succinic anhydride modified rice, wheat, and potato starches. *Journal of Agricultural and Food Chemistry, 51*(8), 2283–2287. https://doi.org/10.1021/jf020371u.
Bao, X., Yu, L., Simon, G. P., Shen, S., Xie, F., Liu, H., ... Zhong, L. (2018). Rheokinetics of graft copolymerization of acrylamide in concentrated starch and rheological behaviors and microstructures of reaction products. *Carbohydrate Polymers, 192*, 1–9. https://doi.org/10.1016/j.carbpol.2018.03.040.
Bhosale, R., & Singhal, R. (2006). Process optimization for the synthesis of octenyl succinyl derivative of waxy corn and amaranth starches. *Carbohydrate Polymers, 66*(4), 521–527. https://doi.org/10.1016/j.carbpol.2006.04.007.
Bikiaris, D., & Panayiotou, C. (1998). LDPE/starch blends compatibilized with PE-g-MA copolymers. *Journal of Applied Polymer Science, 70*(8), 1503–1521. https://doi.org/10.1002/(sici)1097-4628(19981121)70:8<1503::aid-app9>3.0.co;2-#.
Bikiaris, D., Prinos, J., Koutsopoulos, K., Vouroutzis, N., Pavlidou, E., Frangis, N., ... Panayiotou, C. (1998). LDPE/plasticized starch blends containing PE-g-MA copolymer as compatibilizer. *Polymer Degradation and Stability, 59*(1–3), 287–291. https://doi.org/10.1016/s0141-3910(97)00126-2.
Biresaw, G., & Carriere, C. J. (2001). Correlation between mechanical adhesion and interfacial properties of starch/biodegradable polyester blends. *Journal of Polymer Science Part B: Polymer Physics, 39*(9), 920–930. https://doi.org/10.1002/polb.1067.
Biswas, A., Shogren, R. L., Selling, G., Salch, J., Willett, J. L., & Buchanan, C. M. (2008). Rapid and environmentally friendly preparation of starch esters. *Carbohydrate Polymers, 74*(1), 137–141. https://doi.org/10.1016/j.carbpol.2008.01.013.
Brown, S. B., & Orlando, C. M. (1998). Reactive extrusion. In H. F. Mark, N. M. Bikales, C. G. Overberger, G. Menges, & J. I. Kroschwitz (Vol. Eds.), *Encyclopedia of polymer science and engineering: Vol. 14*New York: Wiley (p. 169).
Burgert, I., & Keplinger, T. (2013). Plant micro- and nanomechanics: Experimental techniques for plant cell-wall analysis. *Journal of Experimental Botany, 64*(15), 4635–4649. https://doi.org/10.1093/jxb/ert255.
Cai, Q., Wan, Y., Bei, J., & Wang, S. (2003). Synthesis and characterization of biodegradable polylactide-grafted dextran and its application as compatilizer. *Biomaterials, 24*(20), 3555–3562. https://doi.org/10.1016/S0142-9612(03)00199-6.
Casas, J., Persson, P. V., Iversen, T., & Córdova, A. (2004). direct organocatalytic ring-opening polymerizations of lactones. *Advanced Synthesis & Catalysis, 346*(910), 1087–1089. https://doi.org/10.1002/adsc.200404082.
Chen, L., Qiu, X., Deng, M., Hong, Z., Luo, R., Chen, X., ... Jing, X. (2005). The starch grafted poly(l-lactide) and the physical properties of its blending composites. *Polymer, 46*(15), 5723–5729. https://doi.org/10.1016/j.polymer.2005.05.053.
Chen, Q., Yu, H., Wang, L., ul Abdin, Z., Chen, Y., Wang, J., ... Chen, X. (2015). Recent progress in chemical modification of starch and its applications. *RSC Advances, 5*(83), 67459–67474. https://doi.org/10.1039/C5RA10849G.
Cheng, H. N., Dowd, M. K., Selling, G. W., & Biswas, A. (2010). Synthesis of cellulose acetate from cotton byproducts. *Carbohydrate Polymers, 80*(2), 449–452. https://doi.org/10.1016/j.carbpol.2009.11.048.
Chi, H., Xu, K., Wu, X., Chen, Q., Xue, D., Song, C., ... Wang, P. (2008). Effect of acetylation on the properties of corn starch. *Food Chemistry, 106*(3), 923–928. https://doi.org/10.1016/j.foodchem.2007.07.002.
Choi, E. J., Kim, C. H., & Park, J. K. (1999). Synthesis and characterization of starch-g-polycaprolactone copolymer. *Macromolecules, 32*(22), 7402–7408. https://doi.org/10.1021/ma981453f.
Cosgrove, D. J., & Jarvis, M. C. (2012). Comparative structure and biomechanics of plant primary and secondary cell walls. *Frontiers in Plant Science, 3*. https://doi.org/10.3389/fpls.2012.00204.
Danyadi, L., Janecska, T., Szabo, Z., Nagy, G., Moczo, J., & Pukanszky, B. (2007). Wood flour filled PP composites: Compatibilization and adhesion. *Composites Science and Technology, 67*(13), 2838–2846. https://doi.org/10.1016/j.compscitech.2007.01.024.
De Graaf, R. A., & Janssen, L. P. B. M. (2000). The production of a new partially biodegradable starch plastic by reactive extrusion. *Polymer Engineering & Science, 40*(9), 2086–2094. https://doi.org/10.1002/pen.11340.
Della Valle, G., Buleon, A., Carreau, P. J., Lavoie, P.-A., & Vergnes, B. (1998). Relationship between structure and viscoelastic behavior of plasticized starch. *Journal of Rheology, 42*(3), 507–525. https://doi.org/10.1122/1.550900.
Démé, F., Peuvrel-Disdier, E., & Vergnes, B. (2014). Rheology and morphology of polyester/thermoplastic flour blends. *Journal of Applied Polymer Science, 131*(10), https://doi.org/10.1002/app.40222.
Detyothin, S., Selke, S. E. M., Narayan, R., Rubino, M., & Auras, R. (2013). Reactive functionalization of poly(lactic acid), PLA: Effects of the reactive modifier, initiator and processing conditions on the final grafted maleic anhydride content and molecular weight of PLA. *Polymer Degradation and Stability, 98*(12), 2697–2708. https://doi.org/10.1016/j.polymdegradstab.2013.10.001.
Detyothin, S., Selke, S. E. M., Narayan, R., Rubino, M., & Auras, R. A. (2015). Effects of molecular weight and grafted maleic anhydride of functionalized polylactic acid used in reactive compatibilized binary and ternary blends of polylactic acid and thermoplastic cassava starch. *Journal of Applied Polymer Science, 132*(28), 42230. https://doi.org/10.1002/app.42230.
Di Filippo, S., Tupa, M. V. V., Vázquez, A., Foresti, M. L. L., Vazquez, A., & Foresti, M. L. L. (2016). Organocatalytic route for the synthesis of propionylated starch. *Carbohydrate Polymers, 137*, 198–206. https://doi.org/10.1016/j.carbpol.2015.10.039.
Dobrzynski, P., Kasperczyk, J., Janeczek, H., & Bero, M. (2002). Synthesis of biodegradable glycolide/l-lactide copolymers using iron compounds as initiators. *Polymer, 43*(9), 2595–2601. https://doi.org/10.1016/S0032-3861(02)00079-4.
Domínguez de María, P. (2010). Minimal hydrolases: Organocatalytic ring-opening polymerizations catalyzed by naturally occurring carboxylic acids. *ChemCatChem, 2*(5), 487–492. https://doi.org/10.1002/cctc.201000030.
Don, T.-M., Chung, C.-Y., Lai, S.-M., & Chiu, H.-J. (2010). Preparation and properties of blends from poly(3-hydroxybutyrate) with poly(vinyl acetate)-modified starch. *Polymer Engineering & Science, 50*(4), 709–718. https://doi.org/10.1002/pen.21575.
Dubois, P., & Narayan, R. (2003). Biodegradable compositions by reactive processing of aliphatic polyester/polysaccharide blends. *Macromolecular Symposia, 198*(1), 233–244. https://doi.org/10.1002/masy.200350820.
Dubois, P., Krishnan, M., & Narayan, R. (1999). Aliphatic polyester-grafted starch-like polysaccharides by ring-opening polymerization. *Polymer, 40*(11), 3091–3100. https://doi.org/10.1016/s0032-3861(98)00110-4.
Duque, A., Manzanares, P., & Ballesteros, M. (2017). Extrusion as a pretreatment for lignocellulosic biomass: Fundamentals and applications. *Renewable Energy, 114*, 1427–1441. https://doi.org/10.1016/J.RENENE.2017.06.050.
Duquesne, E., Rutot, D., Degee, P., & Dubois, P. (2001). Synthesis and characterization of compatibilized poly(epsilon-caprolactone)/granular starch composites. *Macromolecular Symposia, 175*, 33–43. https://doi.org/10.1002/1521-3900(200110)175:1<33::aid-masy33>3.0.co;2-#.
Erdmenger, R. (1957). *Mixing and kneading machine*.
European Bioplastics, & nova-Institute (2017). *Report - Bioplastics market data*Retrieved fromhttp://docs.european-bioplastics.org/publications/market_data/2017/Report_Bioplastics_Market_Data_2017.pdf.
Faludi, G., Dora, G., Imre, B., Renner, K., Móczó, J., & Pukánszky, B. (2014). PLA/lignocellulosic fiber composites: Particle characteristics, interfacial adhesion, and failure mechanism. *Journal of Applied Polymer Science, 131*(4), https://doi.org/10.1002/app.39902.
Fang, J. M., Fowler, P. A., Sayers, C., & Williams, P. A. (2004). The chemical modification of a range of starches under aqueous reaction conditions. *Carbohydrate Polymers, 55*(3), 283–289. https://doi.org/10.1016/j.carbpol.2003.10.003.
Field, C. B., Behrenfeld, M. J., Randerson, J. T., & Falkowski, P. (1998). Primary production of the biosphere: Integrating terrestrial and oceanic components. *Science, 281*(5374), 237–240. https://doi.org/10.1126/science.281.5374.237.
Galloway, J. A., & Macosko, C. W. (2004). Comparison of methods for the detection of cocontinuity in poly(ethylene oxide)/polystyrene blends. *Polymer Engineering and Science, 44*(4), 714–727. https://doi.org/10.1002/pen.20064.
Gong, Q., Wang, L.-Q., & Tu, K. (2006). In situ polymerization of starch with lactic acid in aqueous solution and the microstructure characterization. *Carbohydrate Polymers, 64*(4), 501–509. https://doi.org/10.1016/j.carbpol.2005.09.005.
Gregorova, A., Hrabalova, M., Wimmer, R., Saake, B., & Altaner, C. (2009). Poly(lactide acid) composites reinforced with fibers obtained from different tissue types of Picea sitchensis. *Journal of Applied Polymer Science, 114*(5), 2616–2623. https://doi.org/10.1002/app.30819.
Gregorova, A., Sedlarik, V., Pastorek, M., Jachandra, H., & Stelzer, F. (2011). Effect of compatibilizing agent on the properties of highly crystalline composites based on poly(lactic acid) and wood flour and/or mica. *Journal of Polymers and the Environment, 19*(2), 372–381. https://doi.org/10.1007/s10924-011-0292-6.
Hafren, J., & Cordova, A. (2007). Direct bronsted acid-catalyzed derivatization of cellulose with poly(L-lactic acid) and d-mandelic acid. *Nordic Pulp & Paper Research Journal, 22*(2), 184–187.
Hafrén, J., & Córdova, A. (2005). Direct organocatalytic polymerization from cellulose fibers. *Macromolecular Rapid Communications, 26*(2), 82–86. https://doi.org/10.1002/marc.200400470.
Hanna, M. A., & Fang, Q. (2002). Starch esterification by reactive extrusion. *Agro Food Industry Hi-Tech, 13*(2), 33–36.
Haque, M. M. U., Errico, M. E., Gentile, G., Avella, M., & Pracella, M. (2012). Functionalization and compatibilization of poly(e-caprolactone) composites with cellulose microfibres: Morphology, thermal and mechanical properties. *Macromolecular Materials and Engineering, 297*(10), 985–993. https://doi.org/10.1002/mame.201100414.
Hatakeyama, H., Yoshida, T., & Hatakeyama, T. (2000). The effect of side chain association on thermal and viscoelastic properties: Cellulose acetate based polycaprolactones. *Journal of Thermal Analysis and Calorimetry, 59*(1/2), 157–168. https://doi.org/10.1023/A:1010140129888.
Hebeish, A., ElRafie, M. H., Higazy, A., & Ramadan, M. (1996). Synthesis, characterization and properties of polyacrylamide-starch composites. *Starch - Stärke, 48*(5), 175–179. https://doi.org/10.1002/star.19960480505.
Hege, C. S., & Schiller, S. M. (2014). Non-toxic catalysts for ring-opening polymerizations of biodegradable polymers at room temperature for biohybrid materials. *Green Chemistry, 16*(3), 1410–1416. https://doi.org/10.1039/C3GC42044B.
Heinze, T., & Liebert, T. (2001). Unconventional methods in cellulose functionalization. *Progress in Polymer Science, 26*(9), 1689–1762. https://doi.org/10.1016/S0079-6700(01)00022-3.
Higazy, A., Bayazeed, A., & Hebeish, A. (1987). Synthesis and applications of reactive carbohydrates part II: Graft polymerization of starch and hydrolyzed starches with acrylamide. *Starch - Stärke, 39*(9), 319–322. https://doi.org/10.1002/star.19870390907.
Hui, R., Qi-he, C., Ming-liang, F., Qiong, X., & Guo-qing, H. (2009). Preparation and properties of octenyl succinic anhydride modified potato starch. *Food Chemistry, 114*(1), 81–86. https://doi.org/10.1016/j.foodchem.2008.09.019.
Huneault, M. A., & Li, H. (2007). Morphology and properties of compatibilized polylactide/thermoplastic starch blends. *Polymer, 48*(1), 270–280. https://doi.org/10.1016/

j.polymer.2006.11.023.
Hwang, S. W., Shim, J. K., Selke, S., Soto-Valdez, H., Rubino, M., & Auras, R. (2013). Effect of maleic-anhydride grafting on the physical and mechanical properties of poly (l-lactic acid)/starch blends. *Macromolecular Materials and Engineering, 298*(6), 624–633. https://doi.org/10.1002/mame.201200111.
Imre, B., & Pukánszky, B. (2013). Compatibilization in bio-based and biodegradable polymer blends. *European Polymer Journal, 49*(6), 1215–1233. https://doi.org/10.1016/j.eurpolymj.2013.01.019.
Imre, B., Renner, K., & Pukanszky, B. (2014). Interactions, structure and properties in poly(lactic acid)/thermoplastic polymer blends. *Express Polymer Letters, 8*(1), 2–14. https://doi.org/10.3144/expresspolymlett.2014.2.
Jacobsen, S., Fritz, H. G., Degee, P., Dubois, P., & Jerome, R. (2000). Continuous reactive extrusion polymerisation of L-lactide - An engineering view. *Macromolecular Symposia, 153*, 261–273. https://doi.org/10.1002/1521-3900(200003)153:1<261::aid-masy261>3.0.co;2-9.
Jacobsen, S., Fritz, H. G., Degée, P., Dubois, P., & Jérôme, R. (2000). Single-step reactive extrusion of PLLA in a corotating twin-screw extruder promoted by 2-ethylhexanoic acid tin(II) salt and triphenylphosphine. *Polymer, 41*(9), 3395–3403. https://doi.org/10.1016/S0032-3861(99)00507-8.
Jang, W. Y., Shin, B. Y., Lee, T. X., & Narayan, R. (2007). Thermal properties and morphology of biodegradable PLA/starch compatibilized blends. *Journal of Industrial and Engineering Chemistry, 13*(3), 457–464.
Janssen, L. P. B. M. (2004). Rheology and rheokinetics. In L. P. B. M. Janssen (Ed.). *Reactive extrusion systems* (pp. 61–74). Boca Raton, FL, USA: CRC Press.
Janssen, J. M. H., & Meijer, H. E. H. (1993). Droplet breakup mechanisms: Stepwise equilibrium versus transient dispersion. *Journal of Rheology, 37*(4), 597–608.
Jariyasakoolroj, P., & Chirachanchai, S. (2014). Silane modified starch for compatible reactive blend with poly(lactic acid). *Carbohydrate Polymers, 106*(1), 255–263. https://doi.org/10.1016/j.carbpol.2014.02.018.
Jiang, W. B., Qiao, X. Y., & Sun, K. (2006). Mechanical and thermal properties of thermoplastic acetylated starch/poly(ethylene-co-vinyl alcohol) blends. *Carbohydrate Polymers, 65*(2), 139–143. https://doi.org/10.1016/j.carbpol.2005.12.038.
Jongbloed, H. A., Kiewiet, J. A., Van Dijk, J. H., & Janssen, L. P. B. M. (1995). The self-wiping co-rotating twin-screw extruder as a polymerization reactor for methacrylates. *Polymer Engineering and Science, 35*(19), 1569–1579. https://doi.org/10.1002/pen.760351911.
Jun, C. L. (2000). Reactive blending of biodegradable polymers: PLA and starch. *Journal of Polymers and the Environment, 8*(1), 33–37. https://doi.org/10.1023/A:1010172112118.
Jyothi, A. N., Sajeev, M. S., & Moorthy, S. N. (2010). Effect of graft-copolymerization with poly(acrylamide) on rheological and thermal properties of cassava starch. *Journal of Applied Polymer Science, 116*(1), 337–346. https://doi.org/10.1002/app.31599.
Karagoz, S., & Ozkoc, G. (2013). Effects of a diisocyanate compatibilizer on the properties of citric acid modified thermoplastic starch/poly(lactic acid) blends. *Polymer Engineering & Science, 53*(10), 2183–2193. https://doi.org/10.1002/pen.23478.
Kim, B. J., & White, J. L. (2003). Continuous polymerization of lactam-lactone block copolymers in a twin-screw extruder. *Journal of Applied Polymer Science, 88*(6), 1429–1437. https://doi.org/10.1002/app.11792.
Kim, I., & White, J. L. (2005). Reactive copolymerization of various monomers based on lactams and lactones in a twin-screw extruder. *Journal of Applied Polymer Science, 96*(5), 1875–1887. https://doi.org/10.1002/app.21494.
Klason, C., Kubat, J., & Gatenholm, P. (1992). Wood fiber reinforced composites. *ACS Symposium Series, 489*, 82–98.
Klemm, D., Philipp, B., Heinze, T., Heinze, U., & Wagenknecht, W. (1998). *Comprehensive cellulose chemistry*, *Vol. 1*Weinheim, FRG: Wiley-VCH Verlag GmbH & Co. KGaAhttps://doi.org/10.1002/3527601929 Verlag GmbH.
Koenig, M. F., & Huang, S. J. (1995). Biodegradable blends and composites of polycaprolactone and starch derivatives. *Polymer, 36*(9), 1877–1882. https://doi.org/10.1016/0032-3861(95)90934-T.
Kohlgrüber, K., & Bierdel, M. (2008). *Co-rotating twin-screw extruders : Fundamentals, technology, and applications.* Munich [Germany]: Carl Hanser Publishers ; Cincinnati, Ohio : Hanser Gardner Publications.
Koning, C., Van Duin, M., Pagnoulle, C., & Jerome, R. (1998). Strategies for compatibilization of polymer blends. *Progress in Polymer Science, 23*(4), 707–757. https://doi.org/10.1016/S0079-6700(97)00054-3.
Kowalski, A., Duda, A., & Penczek, S. (1998). Kinetics and mechanism of cyclic esters polymerization initiated with tin(II) octoate, 1. Polymerization of ε-caprolactone. *Macromolecular Rapid Communications, 19*(11), 567–572. https://doi.org/10.1002/(SICI)1521-3927(19981101)19:11<567::AID-MARC567>3.0.CO;2-T.
Kumar, M., Mohanty, S., Nayak, S. K., & Rahail Parvaiz, M. (2010). Effect of glycidyl methacrylate (GMA) on the thermal, mechanical and morphological property of biodegradable PLA/PBAT blend and its nanocomposites. *Bioresource Technology, 101*(21), 8406–8415. https://doi.org/10.1016/j.biortech.2010.05.075.
Kundys, A., Plichta, A., Florjańczyk, Z., Frydrych, A., & Żurawski, K. (2015). Screening of metal catalysts influence on the synthesis, structure, properties, and biodegradation of PLA-PBA triblock copolymers obtained in melt. *Journal of Polymer Science Part A: Polymer Chemistry, 53*(12), 1444–1456. https://doi.org/10.1002/pola.27576.
Lai, S.-M., Sun, W.-W., & Don, T.-M. (2015). Preparation and characterization of biodegradable polymer blends from poly(3-hydroxybutyrate)/poly(vinyl acetate)-modified corn starch. *Polymer Engineering & Science, 55*(6), 1321–1329. https://doi.org/10.1002/pen.24071.
Landreau, E., Tighzert, L., Bliard, C., Berzin, F., & Lacoste, C. (2009). Morphologies and properties of plasticized starch/polyamide compatibilized blends. *European Polymer Journal, 45*(9), 2609–2618. https://doi.org/10.1016/j.eurpolymj.2009.06.017.
Lecomte, P., & Jérôme, C. (2011). *Recent developments in ring-opening polymerization of lactones. Synthetic biodegradable polymers*173–217. https://doi.org/10.1007/12_2011_144.
Li, H., & Huneault, M. A. (2011). Effect of chain extension on the properties of PLA/TPS blends. *Journal of Applied Polymer Science, 122*(1), 134–141. https://doi.org/10.1002/app.33981.
Lönnberg, H., Larsson, K., Lindström, T., Hult, A., & Malmström, E. (2011). Synthesis of polycaprolactone-grafted microfibrillated cellulose for use in novel bionanocomposites-influence of the graft length on the mechanical properties. *ACS Applied Materials and Interfaces, 3*(5), 1426–1433. https://doi.org/10.1021/am2001828.
Lopez-Rubio, A., Clarke, J. M., Scherer, B., Topping, D. L., & Gilbert, E. P. (2009). Structural modifications of granular starch upon acylation with short-chain fatty acids. *Food Hydrocolloids, 23*(7), 1940–1946. https://doi.org/10.1016/j.foodhyd.2009.01.003.
Ma, P., Hristova-Bogaerds, D. G., Schmit, P., Goossens, J. G. P., & Lemstra, P. J. (2012). Tailoring the morphology and properties of poly(lactic acid)/poly(ethylene)-co-(vinyl acetate)/starch blends via reactive compatibilization. *Polymer International, 61*(8), 1284–1293. https://doi.org/10.1002/pi.4204.
Ma, P., Xu, P., Chen, M., Dong, W., Cai, X., Schmit, P., ... Lemstra, P. J. (2014). Structure–property relationships of reactively compatibilized PHB/EVA/starch blends. *Carbohydrate Polymers, 108*(1), 299–306. https://doi.org/10.1016/j.carbpol.2014.02.058.
Machado, A. V., Bounor-Legare, V., Goncalves, N. D., Melis, F., Cassagnau, P., & Michel, A. (2008). Continuous polymerization of epsilon-caprolactone initiated by titanium phenoxide in a twin-screw extruder. *Journal of Applied Polymer Science, 110*(6), 3480–3487. https://doi.org/10.1002/app.28850.
Maliger, R. B., McGlashan, S. A., Halley, P. J., & Matthew, L. G. (2006). Compatibilization of starch-polyester blends using reactive extrusion. *Polymer Engineering and Science, 46*(3), 248–263. https://doi.org/10.1002/pen.20479.
Mani, R., Bhattacharya, M., & Tang, J. (1999). Functionalization of polyesters with maleic anhydride by reactive extrusion. *Journal of Polymer Science Part A-Polymer Chemistry, 37*(11), 1693–1702. https://doi.org/10.1002/(sici)1099-0518(19990601)37:11<1693::aid-pola15>3.0.co;2-y.
Marques, S., Moreno, A. D., Ballesteros, M., & Gírio, F. (2018). Starch biomass for biofuels, biomaterials, and chemicals. In V. J. Sílvio (Ed.). *Biomass and Green chemistry* (pp. 69–94). Cham: Springer International Publishing. https://doi.org/10.1007/978-3-319-66736-2_4.
Martínez-Abad, A., Ruthes, A. C., & Vilaplana, F. (2016). Enzymatic-assisted extraction and modification of lignocellulosic plant polysaccharides for packaging applications. *Journal of Applied Polymer Science, 133*(2), https://doi.org/10.1002/app.42523.
Martins, A. B., & Santana, R. M. C. (2016). Effect of carboxylic acids as compatibilizer agent on mechanical properties of thermoplastic starch and polypropylene blends. *Carbohydrate Polymers, 135*, 79–85. https://doi.org/10.1016/j.carbpol.2015.08.074.
Miladinov, V. D., & Hanna, M. A. (2000). Starch esterification by reactive extrusion. *Industrial Crops and Products, 11*(1), 51–57. https://doi.org/10.1016/s0926-6690(99)00033-3.
Mittal, V., Akhtar, T., & Matsko, N. (2015). Mechanical, thermal, rheological and morphological properties of binary and ternary blends of PLA, TPS and PCL. *Macromolecular Materials and Engineering, 300*(4), 423–435. https://doi.org/10.1002/mame.201400332.
Müller, P., Bere, J., Fekete, E., Móczó, J., Nagy, B., Kállay, M., ... Pukánszky, B. (2016). Interactions, structure and properties in PLA/plasticized starch blends. *Polymer, 103*, 9–18. https://doi.org/10.1016/j.polymer.2016.09.031.
Muthuraj, R., Misra, M., & Mohanty, A. K. (2017). Biocomposite consisting of miscanthus fiber and biodegradable binary blend matrix: Compatibilization and performance evaluation. *RSC Advances, 7*(44), 27538–27548. https://doi.org/10.1039/c6ra27987b.
Na, Y.-H., He, Y., Shuai, X., Kikkawa, Y., Doi, Y., & Inoue, Y. (2002). Compatibilization effect of poly(ε-caprolactone)-b-poly(ethylene glycol) block copolymers and phase morphology analysis in immiscible poly(lactide)/poly(ε-caprolactone) blends. *Biomacromolecules, 3*(6), 1179–1186.
Nabar, Y., Raquez, J. M., Dubois, P., & Narayan, R. (2005). Production of starch foams by twin-screw extrusion: Effect of maleated poly(butylene adipate-co-terephthalate) as a compatibilizer. *Biomacromolecules, 6*(2), 807–817. https://doi.org/10.1021/bm0494242.
Namazi, H., Fathi, F., & Dadkhah, A. (2011). Hydrophobically modified starch using long-chain fatty acids for preparation of nanosized starch particles. *Scientia Iranica, 18*(3 C), 439–445. https://doi.org/10.1016/j.scient.2011.05.006.
O'Keefe, B. J., Breyfogle, L. E., Hillmyer, M. A., & Tolman, W. B. (2002). Mechanistic comparison of cyclic ester polymerizations by novel iron(III)-alkoxide complexes: Single vs multiple site catalysis. *Journal of the American Chemical Society, 124*(16), 4384–4393. Retrieved from http://www.ncbi.nlm.nih.gov/pubmed/11960467.
Olabisi, O., Robeson, L. M., & Shaw, M. T. (1979). *Polymer-polymer miscibility.* New York: Academic Press.
Olivato, J. B., Grossmann, M. V. E., Bilck, A. P., & Yamashita, F. (2012). Effect of organic acids as additives on the performance of thermoplastic starch/polyester blown films. *Carbohydrate Polymers, 90*(1), 159–164. https://doi.org/10.1016/j.carbpol.2012.05.009.
Olivato, J. B., Müller, C. M. O., Carvalho, G. M., Yamashita, F., & Grossmann, M. V. E. (2014). Physical and structural characterisation of starch/polyester blends with tartaric acid. *Materials Science and Engineering: C, 39*(1), 35–39. https://doi.org/10.1016/j.msec.2014.02.020.
Packaging - Requirements for packaging recoverable through composting and biodegradation - Test scheme and evaluation criteria for the final acceptance of packaging (2000). *Packaging - Requirements for packaging recoverable through composting and biodegradation - Test scheme and evaluation criteria for the final acceptance of packaging.* Retrieved from https://standards.cen.eu/dyn/www/f?p=204:110:0::::FSP_PROJECT,FSP_ORG_ID:13285,6242&

cs=16419E079DF816FA31BA049B6F9169CF8.
Parulekar, Y., & Mohanty, A. K. (2007). Extruded biodegradable cast films from polyhydroxyalkanoate and thermoplastic starch blends: Fabrication and characterization. *Macromolecular Materials and Engineering, 292*(12), 1218–1228. https://doi.org/10.1002/mame.200700125.
Persson, P. V., Schröder, J., Wickholm, K., Hedenström, E., & Iversen, T. (2004). Selective organocatalytic ring-opening polymerization: A versatile route to carbohydrate-functionalized poly(ε-caprolactones). *Macromolecules, 37*(16), 5889–5893. https://doi.org/10.1021/ma049562j.
Plackett, D. (2004). Maleated polylactide as an interfacial compatibilizer in biocomposites. *Journal of Polymers and the Environment, 12*(3), 131–138. https://doi.org/10.1023/B:JOOE.0000038544.75554.0e.
Plastics - Evaluation of compostability - Test scheme and specifications (2006). *Plastics - Evaluation of compostability - Test scheme and specifications.* Retrieved fromhttps://standards.cen.eu/dyn/www/f?p=204:110:0::::FSP_PROJECT,FSP_ORG_ID:21783,6230&cs=12459CCC96FCD875A348D49110FF2D1BF.
Plastics - Recommendation for terminology and characterisation of biopolymers and bioplastics (2010). *Plastics - Recommendation for terminology and characterisation of biopolymers and bioplastics.* Retrieved fromhttps://standards.cen.eu/dyn/www/f?p=204:110:0::::FSP_PROJECT,FSP_ORG_ID:32743,6230&cs=134524C3C3C4D167294D0103298A93304.
Poulesquen, A., Vergnes, B., Cassagnau, P., Gimenez, J., & Michel, A. (2001). Polymerization of ε-caprolactone in a twin screw extruder. *International Polymer Processing, 16*(1), 31–38. https://doi.org/10.3139/217.1626.
Quiles-Carrillo, L., Montanes, N., Sammon, C., Balart, R., & Torres-Giner, S. (2018). Compatibilization of highly sustainable polylactide/almond shell flour composites by reactive extrusion with maleinized linseed oil. *Industrial Crops and Products, 111*, 878–888. https://doi.org/10.1016/j.indcrop.2017.10.062.
Raghu, N., Kale, A., Raj, A., Aggarwal, P., & Chauhan, S. (2018). Mechanical and thermal properties of wood fibers reinforced poly(lactic acid)/thermoplasticized starch composites. *Journal of Applied Polymer Science, 135*(15), 1–10. https://doi.org/10.1002/app.46118.
Raquez, J.-M., Nabar, Y., Narayan, R., & Dubois, P. (2008). In situ compatibilization of maleated thermoplastic starch/polyester melt-blends by reactive extrusion. *Polymer Engineering and Science, 48*(9), 1747–1754. https://doi.org/10.1002/pen.21136.
Raquez, J. M., Nabar, Y., Srinivasan, M., Shin, B. Y., Narayan, R., & Dubois, P. (2008). Maleated thermoplastic starch by reactive extrusion. *Carbohydrate Polymers, 74*(2), 159–169. https://doi.org/10.1016/j.carbpol.2008.01.027.
Raquez, J.-M., Narayan, R., & Dubois, P. (2008). Recent advances in reactive extrusion processing of biodegradable polymer-based compositions. *Macromolecular Materials and Engineering, 293*(6), 447–470. https://doi.org/10.1002/mame.200700395.
Reddy, N., & Yang, Y. (2010). Citric acid cross-linking of starch films. *Food Chemistry, 118*(3), 702–711. https://doi.org/10.1016/j.foodchem.2009.05.050.
Ren, J., Fu, H., Ren, T., & Yuan, W. (2009). Preparation, characterization and properties of binary and ternary blends with thermoplastic starch, poly(lactic acid) and poly (butylene adipate-co-terephthalate). *Carbohydrate Polymers, 77*(3), 576–582. https://doi.org/10.1016/j.carbpol.2009.01.024.
Renner, K., Móczó, J., & Pukánszky, B. (2009). Deformation and failure of PP composites reinforced with lignocellulosic fibers: Effect of inherent strength of the particles. *Composites Science and Technology, 69*(10), 1653–1659. https://doi.org/10.1016/j.compscitech.2009.03.015.
Rodriguez-Gonzalez, F. J., Ramsay, B. A., & Favis, B. D. (2003). High performance LDPE/thermoplastic starch blends: A sustainable alternative to pure polyethylene. *Polymer, 44*(5), 1517–1526. https://doi.org/10.1016/S0032-3861(02)00907-2.
Rudnik, E., Matuschek, G., Milanov, N., & Kettrup, A. (2005). Thermal properties of starch succinates. *Thermochimica Acta, 427*(1–2), 163–166. https://doi.org/10.1016/j.tca.2004.09.006.
Rudnik, E., & Zukowska, E. (2004). Studies on preparation of starch succinate by reactive extrusion. *Polimery, 49*(2), 132–134.
Rutot-Houze, D., Degee, P., Gouttebaron, R., Hecq, M., Narayan, R., & Dubois, P. (2004). In-depth characterization of granular starch-graft-polyester compositions as obtained by in situ polymerization of lactones from the starch surface. *Polymer International, 53*(6), 656–663. https://doi.org/10.1002/pi.1387.
Sailaja, R. R. N., & Seetharamu, S. (2008). Itaconic acid – grafted – LDPE as compatibilizer for LDPE – plasticized Tapioca starch blends. *Reactive and Functional Polymers, 68*(4), 831–841. https://doi.org/10.1016/j.reactfunctpolym.2007.12.003.
Schützenberger, P. (1865). Action de l'acide acétique anhydre sur la cellulose, l'amidon, les sucres, la mannite et ses con-génères, les glucosides et certaines matières colorantes végétales [in French]. *Compt. Rend. Hebd. Séances Acad. Sci. 61*, 484–487.
Schwach, E., & Avérous, L. (2004). Starch-based biodegradable blends: Morphology and interface properties. *Polymer International, 53*(12), 2115–2124. https://doi.org/10.1002/pi.1636.
Schwach, E., Six, J.-L., & Avérous, L. (2008). biodegradable blends based on starch and poly(lactic acid): Comparison of different strategies and estimate of compatibilization. *Journal of Polymers and the Environment, 16*(4), 286–297. https://doi.org/10.1007/s10924-008-0107-6.
Senna, M. M., Hossam, F. M., & El-Naggar, A. W. M. (2008). Compatibilization of low-density polyethylene/plasticized starch blends by reactive compounds and electron beam irradiation. *Polymer Composites, 29*(10), 1137–1144. https://doi.org/10.1002/pc.20393.
Shi, Q., Chen, C., Gao, L., Jiao, L., Xu, H., & Guo, W. (2011). Physical and degradation properties of binary or ternary blends composed of poly (lactic acid), thermoplastic starch and GMA grafted POE. *Polymer Degradation and Stability, 96*(1), 175–182. https://doi.org/10.1016/j.polymdegradstab.2010.10.002.
Shih, F. F., & Daigle, K. W. (2003). Gelatinization and pasting properties of rice starch modified with 2-octen-1-ylsuccinic anhydride. *Nahrung-Food, 47*(1), 64–67. https://doi.org/10.1002/food.200390015.
Shogren, R. (1996). Preparation, thermal properties, and extrusion of high-amylose starch acetates. *Carbohydrate Polymers, 29*(1), 57–62. https://doi.org/10.1016/0144-8617(95)00143-3.
Shogren, R. L. (2003). Rapid preparation of starch esters by high temperature/pressure reaction. *Carbohydrate Polymers, 52*(3), 319–326. https://doi.org/10.1016/s0144-8617(02)00305-3.
Shujun, W., Jiugao, Y., & Jinglin, Y. (2005). Preparation and characterization of compatible thermoplastic starch/polyethylene blends. *Polymer Degradation and Stability, 87*(3), 395–401. https://doi.org/10.1016/j.polymdegradstab.2004.08.012.
Simon, J., Müller, H. P., Koch, R., & Müller, V. (1998). Thermoplastic and biodegradable polymers of cellulose. *Polymer Degradation and Stability, 59*(1–3), 107–115. https://doi.org/10.1016/S0141-3910(97)00151-1.
Söderqvist Lindblad, M., & Albertsson, A.-C. (2004). Chemical modification of hemicelluloses and gums. In S. Dumitriu (Ed.). *Polysaccharides* (pp. 491–508). (2nd ed.). Polymer Technology, Superseded Departments, KTH: CRC Press. https://doi.org/10.1201/9781420030822.ch19.
Stagner, J., Dias Alves, V., Narayan, R., & Beleia, A. (2011). Thermoplasticization of high amylose starch by chemical modification using reactive extrusion. *Journal of Polymers and the Environment, 19*(3), 589–597. https://doi.org/10.1007/s10924-011-0307-3.
Steinmann, S., Gronski, W., & Friedrich, C. (2001). Cocontinuous polymer blends: Influence of viscosity and elasticity ratios of the constituent polymers on phase inversion. *Polymer, 42*(15), 6619–6629. https://doi.org/10.1016/S0032-3861(01)00100-8.
Stolt, M., Krasowska, K., Rutkowska, M., Janik, H., Rosling, A., & Södergård, A. (2005). More on the poly(L-lactide) prepared using ferrous acetate as catalyst. *Polymer International, 54*(2), 362–368. https://doi.org/10.1002/pi.1691.
Sugih, A. K., Picchioni, F., Janssen, L. P. B. M., & Heeres, H. J. (2009). Synthesis of poly-(epsilon)-caprolactone grafted starch co-polymers by ring-opening polymerisation using silylated starch precursors. *Carbohydrate Polymers, 77*(2), 267–275. https://doi.org/10.1016/j.carbpol.2008.12.032.
Számel, G., Domján, A., Klébert, S., & Pukánszky, B. (2008). Molecular structure and properties of cellulose acetate chemically modified with caprolactone. *European Polymer Journal, 44*(2), 357–365. https://doi.org/10.1016/j.eurpolymj.2007.11.006.
Tomasik, P., Wang, Y. J., & Jane, J. L. (1995). Facile route to anionic starches - Succinylation, maleination and phtalation of corn starch on extrusion. *Starch - Stärke, 47*(3), 96–99. https://doi.org/10.1002/star.19950470305.
Tupa, M., Maldonado, L., Vázquez, A., & Foresti, M. L. (2013). Simple organocatalytic route for the synthesis of starch esters. *Carbohydrate Polymers, 98*(1), 349–357. https://doi.org/10.1016/j.carbpol.2013.05.094.
Tupa, M. V., Ávila Ramírez, J. A., Vázquez, A., & Foresti, M. L. (2015). Organocatalytic acetylation of starch: Effect of reaction conditions on DS and characterisation of esterified granules. *Food Chemistry, 170*, 295–302. https://doi.org/10.1016/j.foodchem.2014.08.062.
Tye, Y. Y., Lee, K. T., Wan Abdullah, W. N., & Leh, C. P. (2016). The world availability of non-wood lignocellulosic biomass for the production of cellulosic ethanol and potential pretreatments for the enhancement of enzymatic saccharification. *Renewable and Sustainable Energy Reviews, 60*, 155–172. https://doi.org/10.1016/j.rser.2016.01.072.
Tzoganakis, C. (1989). Reactive extrusion of polymers: A review. *Advances in Polymer Technology, 9*(4), 321–330. https://doi.org/10.1002/adv.1989.060090406 (n.d.).
Uitterhaegen, E., & Evon, P. (2017). Twin-screw extrusion technology for vegetable oil extraction: A review. *Journal of Food Engineering, 212*, 190–200. https://doi.org/10.1016/J.JFOODENG.2017.06.006.
Van Hemelrijck, E., Van Puyvelde, P., & Moldenaers, P. (2006). Rheology and Morphology of Highly Compatibilized Polymer Blends. *Macromolecular Symposia, 233*(1), 51–58. https://doi.org/10.1002/masy.200690028.
Van Puyvelde, P., Velankar, S., & Moldenaers, P. (2001). Rheology and morphology of compatibilized polymer blends. *Current Opinion in Colloid & Interface Science, 6*(5–6), 457–463. https://doi.org/10.1016/S1359-0294(01)00113-3.
Vergnes, B., & Berzin, F. (2006). Modeling of reactive systems in twin-screw extrusion: Challenges and applications. *Comptes Rendus Chimie, 9*(11–12), 1409–1418. https://doi.org/10.1016/j.crci.2006.07.006.
Vidéki, B., Klébert, S., & Pukánszky, B. (2005). Grafting of caprolacton to cellulose acetate by reactive processing. *European Polymer Journal, 41*(8), 1699–1707. https://doi.org/10.1016/j.eurpolymj.2005.03.002.
Vilaplana, F., Zou, W., & Gilbert, R. G. (2018). *Starch and plant storage polysaccharides. Bioinspired materials science and engineering.* Hoboken, NJ, USA: John Wiley & Sons, Inc149–165. https://doi.org/10.1002/9781119390350.ch8.
Vilay, V., Mariatti, M., Ahmad, Z., Pasomsouk, K., & Todo, M. (2010). Improvement of microstructures and properties of biodegradable PLLA and PCL blends compatibilized with a triblock copolymer. *Materials Science and Engineering: A, 527*(26), 6930–6937. https://doi.org/10.1016/j.msea.2010.07.079.
Wang, H., Sun, X., & Seib, P. (2002). Mechanical properties of poly(lactic acid) and wheat starch blends with methylenediphenyl diisocyanate. *Journal of Applied Polymer Science, 84*(6), 1257–1262. https://doi.org/10.1002/app.10457.
Wang, L. F., Shogren, R. L., & Willett, J. L. (1997). Preparation of starch succinates by reactive extrusion. *Starch-Starke, 49*(3), 116–120. https://doi.org/10.1002/star.19970490308.
Wang, N., Yu, J., & Ma, X. (2007). Preparation and characterization of thermoplastic starch/PLA blends by one-step reactive extrusion. *Polymer International, 56*(11), 1440–1447. https://doi.org/10.1002/pi.2302.
Wang, S. J., Yu, J. G., & Yu, J. L. (2005). Compatible thermoplastic starch/polyethylene blends by one-step reactive extrusion. *Polymer International, 54*(2), 279–285. https://doi.org/10.1002/pi.1668.
Wang, S. J., Yu, J. G., & Yu, J. L. (2006). Preparation and characterization of compatible

and degradable thermoplastic starch/polyethylene film. *Journal of Polymers and the Environment, 14*(1), 65–70. https://doi.org/10.1007/s10924-005-8708-9.
Warth, H., Mülhaupt, R., & Schätzle, J. (1997). Thermoplastic cellulose acetate and cellulose acetate compounds prepared by reactive processing. *Journal of Applied Polymer Science, 64*(2), 231–242. https://doi.org/10.1002/(SICI)1097-4628(19970411)64:2<231::AID-APP4>3.0.CO;2-S.
Whistler, R. L. (1945). *Preparation and properties of starch esters. Advances in carbohydrate chemistry*279–307. https://doi.org/10.1016/S0096-5332(08)60412-9.
Wokadala, O. C., Emmambux, N. M., & Ray, S. S. (2014). Inducing PLA/starch compatibility through butyl-etherification of waxy and high amylose starch. *Carbohydrate Polymers, 112*, 216–224. https://doi.org/10.1016/j.carbpol.2014.05.095.
Wu, C.-S. (2003). Physical properties and biodegradability of maleated-polycaprolactone/starch composite. *Polymer Degradation and Stability, 80*(1), 127–134. https://doi.org/10.1016/S0141-3910(02)00393-2.
Wu, S. (1987). Formation of dispersed phase in incompatible polymer blends: Interfacial and rheological effects. *Polymer Engineering & Science, 27*(5), 335–343.
Xie, F., Xue, T., Yu, L., Chen, L., Li, X., & Zhang, X. (2007). rheological properties of starch-based materials and starch/poly(lactic acid) blends. *Macromolecular Symposia, 249–250*(1), 529–534. https://doi.org/10.1002/masy.200750431.
Xie, F., Yu, L., Liu, H., & Dean, K. (2006). Effect of compatibilizer distribution on thermal and rheological properties of gelatinized starch/biodegradable polyesters blends. *International Polymer Processing, 21*(4), 379–385. https://doi.org/10.3139/217.0119.
Xu, J., & Finkenstadt, V. L. (2013). Rheological properties of reactive extrusion modified waxy starch and waxy starch-polyacrylamide copolymer gels. *Starch - Stärke, 65*(11–12), 984–990. https://doi.org/10.1002/star.201200199.
Xu, Q., Kennedy, J. F., & Liu, L. (2008). An ionic liquid as reaction media in the ring opening graft polymerization of epsilon-caprolactone onto starch granules. *Carbohydrate Polymers, 72*(1), 113–121. https://doi.org/10.1016/j.carbpol.2007.07.031.
Xu, Y. X., Miladinov, V., & Hanna, M. A. (2004). Synthesis and characterization of starch acetates with high substitution. *Cereal Chemistry, 81*(6), 735–740. https://doi.org/10.1094/cchem.2004.81.6.735.
Yokesahachart, C., & Yoksan, R. (2011). Effect of amphiphilic molecules on characteristics and tensile properties of thermoplastic starch and its blends with poly (lactic acid). *Carbohydrate Polymers, 83*(1), 22–31. https://doi.org/10.1016/j.carbpol.2010.07.020.
Yu, J., Ai, F., Dufresne, A., Gao, S., Huang, J., & Chang, P. R. (2008). Structure and mechanical properties of poly(lactic acid) filled with (starch nanocrystal)-graft-poly (epsilon-caprolactone). *Macromolecular Materials and Engineering, 293*(9), 763–770. https://doi.org/10.1002/mame.200800134.
Zeng, J.-B., Li, K.-A., & Du, A.-K. (2015). Compatibilization strategies in poly(lactic acid)-based blends. *RSC Advances, 5*(41), 32546–32565. https://doi.org/10.1039/C5RA01655J.
Zeng, J.-B., Jiao, L., Li, Y.-D., Srinivasan, M., Li, T., & Wang, Y.-Z. (2011). Bio-based blends of starch and poly(butylene succinate) with improved miscibility, mechanical properties, and reduced water absorption. *Carbohydrate Polymers, 83*(2), 762–768. https://doi.org/10.1016/j.carbpol.2010.08.051.
Zeng, S., Wang, S., Xiao, M., Han, D., & Meng, Y. (2011). Preparation and properties of biodegradable blend containing poly (propylene carbonate) and starch acetate with different degrees of substitution. *Carbohydrate Polymers, 86*(3), 1260–1265. https://doi.org/10.1016/j.carbpol.2011.06.023.
Zhang, J.-F., & Sun, X. (2004). Mechanical properties of poly(lactic acid)/starch composites compatibilized by maleic anhydride. *Biomacromolecules, 5*(4), 1446–1451. https://doi.org/10.1021/bm0400022.
Zhang, L., Deng, X., Zhao, S., & Huang, Z. (1997). Biodegradable polymer blends of poly (3-hydroxybutyrate) and starch acetate. *Polymer International, 44*(1), 104–110. https://doi.org/10.1002/(SICI)1097-0126(199709)44:1<104::AID-PI812>3.0.CO;2-#.
Zhang, L., Xie, W., Zhao, X., Liu, Y., & Gao, W. (2009). Study on the morphology, crystalline structure and thermal properties of yellow ginger starch acetates with different degrees of substitution. *Thermochimica Acta, 495*(1–2), 57–62. https://doi.org/10.1016/j.tca.2009.05.019.
Zou, W., Yu, L., Liu, X., Chen, L., Zhang, X., Qiao, D., ... Zhang, R. (2012). Effects of amylose/amylopectin ratio on starch-based superabsorbent polymers. *Carbohydrate Polymers, 87*(2), 1583–1588. https://doi.org/10.1016/j.carbpol.2011.09.060.

RESUMEN PUBLICACIONES E INDICADORES DE CALIDAD

A continuación, se resumen la información referente a los artículos publicados y los indicadores de impacto de las revistas:

ARTICULO & DOI	REVISTA	CUARTIL
Sustainable Materials with Enhanced Mechanical Properties Based on Industrial Polyhydroxyalkanoates Reinforced with Organomodified Sepiolite and Montmorillonite **doi.org/10.3390/polym11040696**	Polymers	Impact Factor: **3.426** (2019) ; 5-Year Impact Factor: 3.636 (2019) – **Q1** Citas: 11
Reducing off-Flavour in Commercially Available Polyhydroxyalkanoate Materials by Autooxidation through Compounding with Organoclays **doi.org/10.3390/polym11060945**	Polymers	Impact Factor: **3.426** (2019) ; 5-Year Impact Factor: 3.636 (2019) – **Q1** Citas: 4
Color Fixation Strategies on Sustainable Poly-Butylene Succinate Using Biobased Itaconic Acid **doi.org/10.3390/polym13010079**	Polymers	Impact Factor: **3.426** (2019) ; 5-Year Impact Factor: 3.636 (2019) – **Q1** Citas: 0
Reactive Compatibilization of Plant Polysaccharides and Biobased Polymers: Review on Current Strategies, Expectations and Reality **doi.org/10.1016/j.carbpol.2018.12.082**	Carbohydrate Polymers	Impact Factor: **7.182** (2019), 5-Year Impact Factor: 6.890 – **Q1** Citas: 16

OTROS TRABAJOS DE INTERÉS

Además de los artículos presentados en la presente tesis, la autora reconoce los siguientes trabajos relacionados:

- *Publicación de un póster en congreso internacional (Biopol 2019) con los resultados preliminares de la línea de fijación de color:*

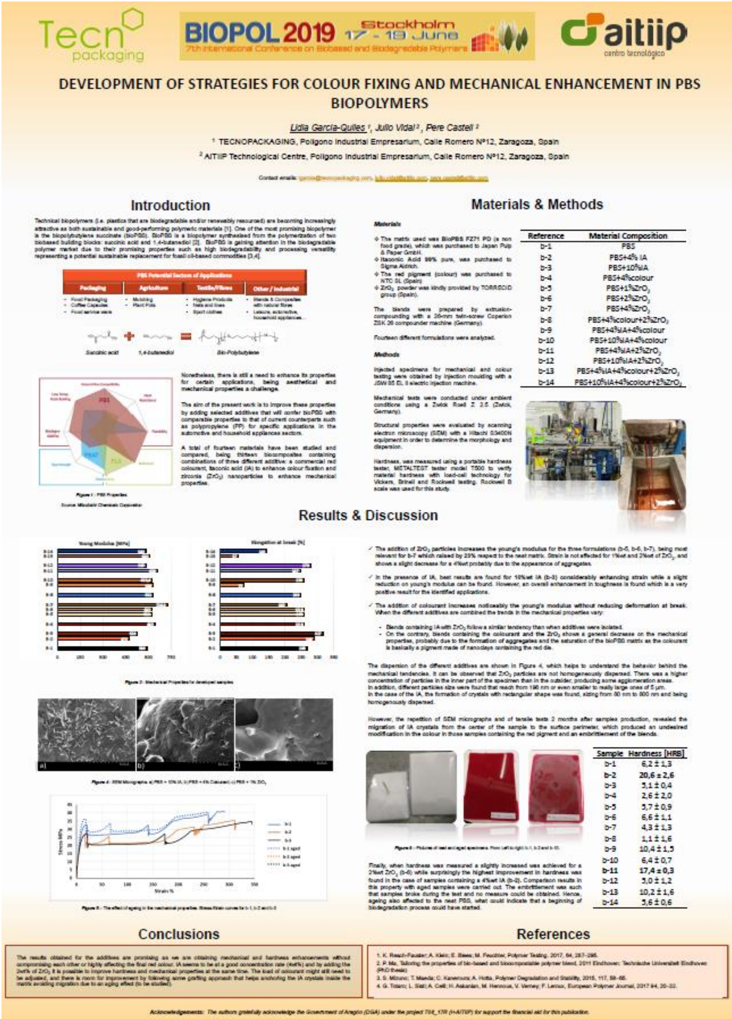

- *Publicación de otros artículos científico-técnicos relacionados con biopolímeros durante el periodo de realización de la tesis:*

  Bordón, P.; Paz, R.; Peñalva, C.; Vega, G.; Monzón, M.; García, L. Biodegradable Polymer Compounds Reinforced with Banana Fiber for the Production of Protective Bags for Banana Fruits in the Context of Circular Economy. Agronomy ***2021****,* 11*, 242.*

  Este artículo surge como resultado del Proyecto europeo Life Baqua *(Ver siguiente apartado para más detalles del proyecto)*

- *Otros proyectos de I+D relacionados con la investigación en biopolímeros. Transferencia de conocimiento a otras aplicaciones industriales apoyadas en proyectos de concurrencia competitiva.*

En el marco de investigación de la tesis (periodo 2016 - 2021), Lidia García ha colaborado en el desarrollo y presentación de proyectos a distintos programas de ámbito regional, nacional y europeo con el fin de conseguir financiación que pueda afianzar y transferir los resultados de la tesis, así como avanzar en otras líneas de interés para la empresa centradas en el desarrollo de biomateriales y sus tecnologías de procesado; nuevas aplicaciones y productos. De este modo la doctoranda participa en la búsqueda activa de fuentes de financiación de las líneas de I+D+i de la empresa Tecnopackaging así como en la creación de relaciones nacionales e internacionales con otros centros de investigación y empresas.

A nivel regional la doctoranda ha participado en convocatorias *InnovAragón & PAIP*; a nivel nacional en programas de *Retos-Colaboración, Misiones y Cien*; y finalmente a nivel europeo en diferentes programas como *H2020-BBI*; *H2020-SC2*; *H2020-Spire*; *Life*; *Eurostars*, *Cosme*…

A continuación se listan algunos de los proyectos más relevantes, incluyendo la principal actividad de I+D desarrollada por Tecnopackaging y dirigida por la doctoranda, que son indicador directo del éxito del desarrollo de la tesis en la empresa y que han servido o bien para realizar transferencia tecnológica o bien para realimentar y abrir nuevas líneas de investigación:

PROYECTO: Código GA & ACTIVIDAD

***BARBARA*: H2020 – BBI- 745578**

Desarrollo y escalado de nuevos materiales técnicos biobasados para tecnologías de impresión 3D - FFF (fabricación por fusión de filamento).

Se ha trabajado en dos líneas:

1. La integración de almidón en matrices termoplásticas con el fin de aumentar el contenido biobasado de las mismas, manteniendo e incrementando las propiedades térmicas y mecánicas del material, dado que se utiliza en una aplicación muy exigente técnicamente: la huella de un molde de RTM (*Resin Transfer Molding*) para la fabricación de piezas de construcción, donde se alcanzan altas presiones y temperaturas. Para lograr una buena compatibilización entre el almidón y la poliamida se utilizó la extrusión reactiva - REX.

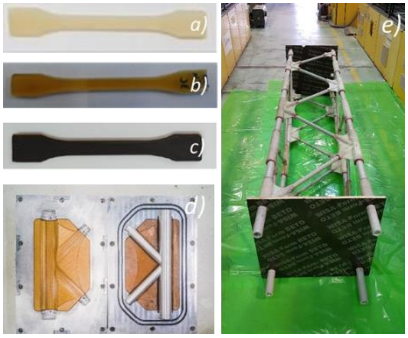

Figura 41: a) muestra de termoplástico con almidón sin modificar; b) muestra laboratorio simulando REX de termoplástico con injerto de almidón modificado; c) muestras escala piloto semi-industrial REX de termoplástico con injerto de almidón modificado; d) Ejemplo de molde híbrido demostrador con huella impresa en 3D; e) Ejemplo de celosía final con nudos fabricados con el molde desarrollado (demostrador de socio industrial).

2. Por otro lado, se trabajó en el desarrollo de blendas en base biopoliester (incorporando polisacáridos) para integrar colorantes naturales, fragancias y texturas obtenidos a partir de residuos agrícolas (limón, brócoli, granada y cáscara de almendra). El conocimiento desarrollado en la tesis ha permitido un mayor control del proceso de extrusión, diseño de la formulación en cuanto a cantidad de los diferentes aditivos a utilizar así como interpretar resultados utilizando las metodologías de caracterización desarrolladas (tanto para evaluar la fijación de color, como para medir y cuantificar la disipación de volátiles de la fragancia utilizada).

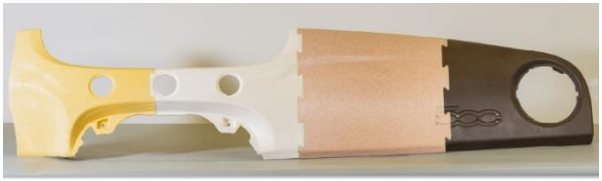

Figura 42: Prototipo de salpicadero elaborado con: colorante extraído del limón, fragancia de limón, cáscara de almendra y colorante extraído de la granada.

***NEWPACK*: H2020 – BBI- 792261**

El objetivo principal de NEWPACK es validar a nivel piloto la producción de 2 nuevos plásticos de base biológica basados en mezclas de PHB-PLA (a partir de residuos agroalimentarios) con un rendimiento de sostenibilidad mejorado y funcionalidades avanzadas gracias a la incorporación de nanoaditivos naturales (para mejorar procesabilidad, barrera a gases y propiedades mecánicas) y otros aditivos antioxidantes y antimicrobianos. Tecnopackaging validad la procesabilidad y transformación de los materiales en films para evaluar potenciales aplicaciones destinadas a envase de alimentos.

Figura 43: Muestras de film, ejemplos de formulaciones (izq) y prueba de soplado de film (dcha)

***INGREEN*: H2020 – BBI- 838120**

El proyecto desarrolla ingredientes funcionales innovadores y biopolímeros (PHAs) a partir de aguas residuales de la industria papelera y otros agroalimentarios (suero de leche, trigo, salvado de centeno…) mediante procesos biotecnológicos para producir alimentos, piensos, productos farmacéuticos, nutracéuticos, cosméticos y envases biodegradables.

Figura 44: Muestras de film, ejemplos de formulaciones

Tecnopackaging participa formulando un material plástico basado en PHA por extrusión-compounding así como su transformación en un producto film super-elástico para aplicaciones de bolsa en caja (“bag-in-box”).

***YPACK*: H2020 – SC2- 773872**

Figura 45: Muestras envases

El proyecto YPACK comprende el escalado y la validación comercial de dos soluciones innovadoras de envasado de alimentos biodegradables (bandeja termoformada y bolsa flow pack) basadas en PHA, con propiedades activas y de barrera pasiva. Estas soluciones se desarrollan para mantener o prolongar la vida útil de los alimentos, reducir el desperdicio de alimentos y minimizar el impacto medioambiental de los envases, pero teniendo en cuenta las tendencias del mercado. Los resultados se han validado con distintos productos como carne, frutas y verduras y pasta fresca, considerados algunos de los más importantes generadores de residuos alimentarios. En este proyecto, Tecnopackaging desarrolla envases tipo flow-pack y bandejas con los materiales desarrollados en el proyecto.

***CIRCPACK*: H2020 – SPIRE- 730423**

En el proyecto se transforman residuos de envases de plástico en materia prima para desarrollar plásticos más sostenibles, de base biológica (biobasados) y reciclables, utilizados para la fabricación de una amplia gama de productos: bandejas, botellas, cápsulas de café, tarros, piezas de automóvil, palés y nuevos tipos de envases multicapa y multimateriales. En CIRC-PACK se desarrollan metodologías de eco-diseño que faciliten la clasificación combinadas con tecnologías de reciclaje que aumenten las tasas de recuperación y garanticen la calidad. Tecnopackaging ha liderado la línea piloto de testeo y validación de los materiales desarrollados y recuperados para el sector del packaging.

Figura 46: Muestras de botellas y bandejas

***FISH4FISH*: COSME-EMFF- 863697**

En el marco de este proyecto se estudian derivados de quitina y quitosano extraídos de residuos de biomasa marina (caparazones de crustáceos) para fabricar nuevos envases para el sector pesquero, que a la vez mejorarán la vida útil del pescado. Además, al final de su vida podrán usarse como fertilizante y agentes antimicrobianos para el cultivo de vegetales. Tecnopackaging lidera el desarrollo de packaging en formato film y termoconformado con los materiales desarrollados.

Figura 47: Ejemplo de film basado en quitosano

***LIFE BAQUA:* LIFE15 ENV/ES/000157**

En colaboración con la Universidad de las Palmas de Gran Canarias en el que se desarrollan bolsas para la protección de piñas de plátano durante su maduración en árbol. Las bolsas se desarrollan con biopolímero compostable (con base PHA), con fibras de los troncos de las palmeras (bananeras) así como ajustes de color (en este caso tonos azulados) para controlar el filtro UV y lograr un amarillo óptimo para que pudiera venderse bajo los estándares de calidad de "Plátano de Canarias". La doctoranda ha dirigido la investigación relacionada tanto en la formulación y mezcla de los biomateriales como en el proceso de soplado de film y diseño de las bolsas.

Se produce trasferencia tecnológica de conocimientos desarrollados durante la tesis en cuanto a la extrusión de PHAs y la integración de colorantes, en este caso necesarios para la funcionalidad de la bolsa más que para propiedades estéticas.

Figura 48: Bolsas para protección de plátanos: convencionales(izq) y desarrolladas en el proyecto (dcha)

BLOQUE 5

CONCLUSIONES

CONCLUSIONES

La presente tesis doctoral surge de una necesidad industrial basada en mejorar las propiedades estéticas de los biopolímeros con el fin de incrementar su aceptación en mercados actualmente dominados por el PP y en aplicaciones diversas como la automoción, electrodomésticos, envases o el mobiliario. Para ello se han definido dos líneas principales de investigación en relación a dichas propiedades estéticas y a la naturaleza de los biopolímeros seleccionados (PHA y bioPBS): una focalizada en disminuir olores desagradables producidos por la autooxidación del material y otra dirigida a mejorar la fijación del color.

Los métodos y resultados de la investigación han sido publicados en 4 artículos científicos, orientando dos para cada línea. En relación a los resultados obtenidos se puede concluir que:

- Se ha desarrollado una metodología para la identificación y cuantificación de volátiles en polímeros, que ha permitido identificar aquellos alcoholes y derivados, causantes del olor a rancio en los polímeros derivados de fermentación bacteriana como es el caso de los PHA. Mediante su aplicación, se ha podido evaluar la capacidad como agentes secuestrantes de las nanoarcillas utilizadas. Se ha demostrado que las nanoarcillas seleccionadas tienen un efecto secuestrante cuya efectividad depende tanto de la naturaleza del volátil (teniendo una gran dependencia con el peso molecular y su estructura – si es lineal o si contiene grupos aromáticos) como de la afinidad de la nanoarcilla con cada matriz. Además, se puede destacar la sepiolita sin modificar - T2 como la nanoarcilla más polivalente y que cubriría un mayor espectro de volátiles (ARTICULO 2[55]).
- Además de ser capaces de evaluar la mejora en propiedades estéticas, se ha podido demostrar la mejora en otras propiedades funcionales como las propiedades mecánicas, destacando el comportamiento de la matriz de P3HB reforzada con T1 (sepiolita modificada superficialmente con aminosilanos), resultado de la excelente afinidad entre el poliéster y la nanoarcilla así como del alto grado de dispersión conseguido para ser un proceso semi-industrial (ARTICULO 1[45]).
- El ácido itacónico actúa inicialmente como agente plastificante en la mezcla, incrementando las propiedades mecánicas (rigidez y tenacidad)

cuando se añade 10wt% aunque ablanda la superficie del material. Además, aparentemente mejora el aspecto del color y brillo. Sin embargo, a las 4 semanas, se observa un envejecimiento de las muestras que las deteriora estéticamente y resulta de la segregación de las fases poliméricas por falta de compatibilidad (ARTICULO 3[86]). Por esta razón, es necesario buscar estrategias de funcionalización adecuadas para usar *entre y para* biopolímeros. Distintas soluciones se presentan en el ARTICULO 4[4], resaltando la extrusión reactiva (REX) como un proceso adecuado para mejorar la compatibilidad entre polímeros y que es industrializable mediante la adaptación del proceso de extrusión convencional.

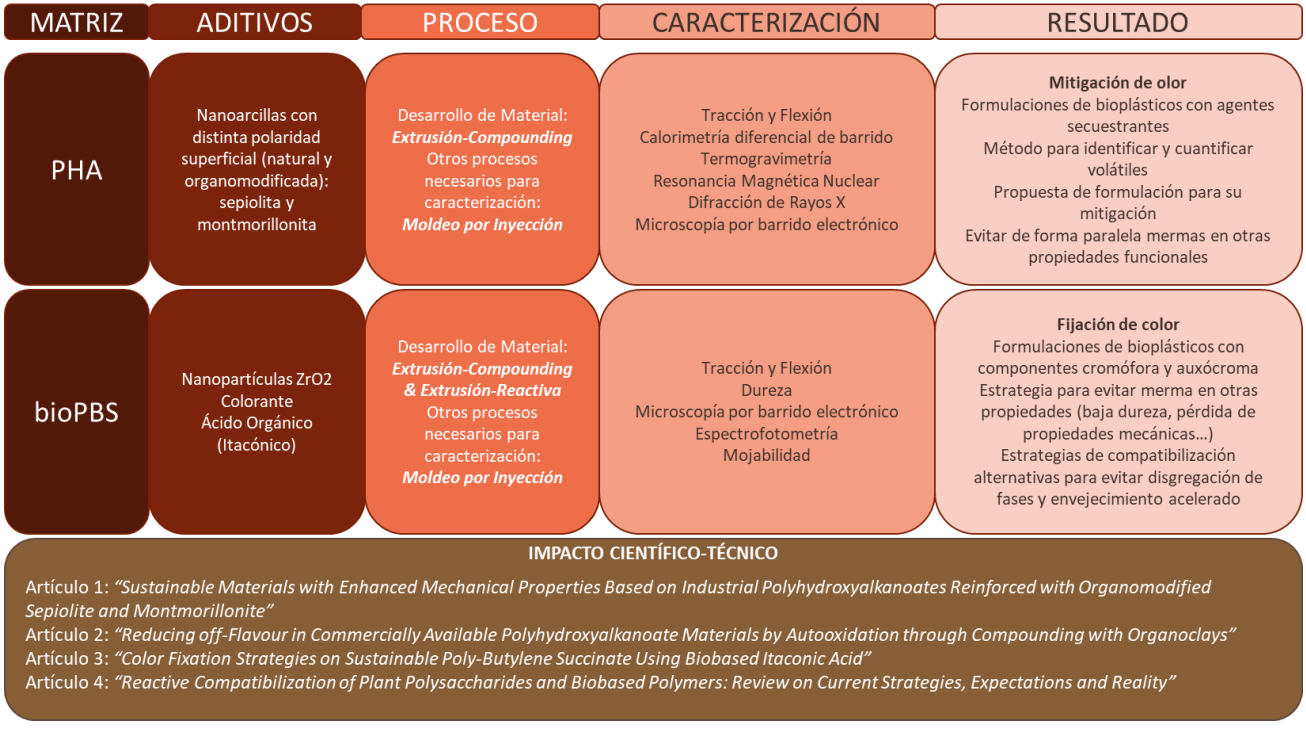

Figura 49: Tabla resumen de las actuaciones y resultados principales de la tesis